RAI: Volume 3, Chapter 2.2.1.1, First Set, Number 1:

Table 2.1-1 should be expanded by adding appropriate columns to provide the following information:

(1) For each feature or component identified in Table 2.1-1, provide a brief qualitative description of how the stated barrier function is attained (e.g., capillary forces at the wall of the emplacement drift limit ingress of water; general corrosion of waste package is very slow, etc.). Ensure that the processes that affect barrier capability (e.g., sorption to stationary corrosion products) are linked to the specific features or components whose capabilities they affect (e.g., corrosion of waste package internal components, etc.).

(2) For each feature or component identified in Table 2.1-1, provide a brief quantitative evaluation of the barrier capability (e.g.; approximately 10% of infiltration enters the drifts as seepage under nominal conditions; the likelihood of waste package failure by general corrosion within 1 million years is less than 15%; packages failed by general corrosion retain the ability to divert up to 50% of the seepage water for up to 100,000 years following the initial breach; etc.). Demonstrate that the evaluation is based on quantitative information from the performance assessment (figures, tables, TSPA intermediate results, TSPA inputs, etc.).

(3) Provide references to portions of the license application (subsections of the SAR, figures and tables) that provide the basis for the information presented in items 1 and 2 or update the SAR accordingly. Ensure that these references point to specific locations within the license application rather than to entire chapters or sections. These references should indicate the location of discussions regarding:

- detailed evaluations of the barrier component/feature capabilities, including information of the effect of specific events or processes
- the uncertainties and variabilities in the capability of the barrier feature or component
- how the capability changes over time

For features or components designated as not important to waste isolation, provide comparable information that illustrates/demonstrates that the performance assessment does not include any significant capability arising from the feature or component.

Basis: Needed for demonstration of compliance with 10 CFR 63.115 (b) and (c). Table 2.1-1 provides information on barrier capability. However, the multiple barrier description provided in the license application is varied in its level of detail. In certain areas, particularly within the discussion of the capability of the engineered barrier system, the discussion does not provide sufficient detail to determine how the component achieves its stated function or how the capability

(or lack of capability) of the features and components identified in Table 2.1-1 are consistent with the performance assessment. The regulation requires consistency between each barrier's capability and its implementation within the performance assessment. The description of barrier capabilities needs to provide sufficient detail to allow for a reasonable comparison of the described capability with the performance assessment model and/or results.

1 RESPONSE

This RAI response contains an attached summary table (Table 2.1-1 Expanded) that derives from SAR Table 2.1-1. For each feature or component, Table 2.1-1 Expanded adds the following information:

- Relevant Features, Events, and Processes (FEPs) Important to Barrier Capability (ITBC) – Tables A-1, A-2, and A-3 from *Postclosure Nuclear Safety Design Bases* (SNL 2008a) (hereafter referred to as the PNSDB report) and SAR Tables 2.1-2, 2.1-3, and 2.1-4 identify ITBC FEPs for each feature. Table 2.1-1 Expanded further associates these ITBC FEPs with components, based on judgement, where appropriate. Some special considerations related to the association of ITBC FEPs with components are identified in Section 1.1.

- Brief Qualitative Description of Barrier Functions – For each feature or component classified as Important to Waste Isolation (ITWI), a brief qualitative discussion of how the barrier function (or functions) is attained is summarized in the table. The basis for the ITWI information is generally SAR Section 2.1. For each non-ITWI feature or component, the rationale for the non-ITWI determination is summarized in the table. The basis for the non-ITWI information is generally Tables A-1, A-2, and A-3 of the PNSDB report (SNL 2008a). In all cases, specific references (e.g., subsections, figures, tables, and/or page numbers) are provided.

- Brief Quantitative Evaluation of Barrier Capability – For each ITWI feature or component, a brief quantitative evaluation of barrier capability is summarized in the table. The basis for the ITWI information is generally model results presented in SAR Section 2.1, supplemented as appropriate by information from *Total System Performance Assessment Model/Analysis for the License Application* (SNL 2008b) (hereafter referred to as the TSPA-LA report), and the other barrier capability RAIs (responses to RAIs 3.2.2.1.1-002 through 3.2.2.1.1-007). In all cases, specific references (e.g., subsections, figures, tables, and/or page numbers) are provided. For each non-ITWI feature or component, no quantitative information is presented; the qualitative information is considered sufficient.

As described above, the additional information provided in Table 2.1-1 Expanded is supported by specific references. In some cases, the additional information requires supporting discussion, which is provided in Section 1.2 of this RAI response. In such cases, the table makes reference to Section 1.2 of this RAI response.

The repository system is composed of three barriers: the Upper Natural Barrier (UNB), the Engineered Barrier System (EBS), and the Lower Natural Barrier (LNB). These three barriers are classified as ITWI as a result of an analysis conducted and documented in the PNSDB report (SNL 2008a, Sections 6.1.2 and 6.1.5). The ITWI classification is based on a barrier's capability to perform one or more of the following barrier functions: (1) prevent or substantially reduce the rate of movement of water from the repository to the accessible environment; (2) prevent the release or substantially reduce the release rate of radionuclides from the waste; (3) prevent or substantially reduce the rate of movement of radionuclides from the repository to the accessible environment (SNL 2008a, Section 6.1.2).

A barrier's features may contribute to the barrier's capability. A barrier's feature is classified as ITWI if it meets two conditions: (1) the feature is associated with one or more processes or characteristics classified as ITBC; and (2) the feature is a significant contributor to the barrier capability relative to the other features of the barrier (SAR Section 2.1.1, pp. 2.1-3 and 2.1-4). The second condition means that some features that are associated with an ITBC process may still not be significant enough contributors to be classified as ITWI. In addition, a feature is classified as ITWI if it is one of the engineered features of the geologic repository whose function is to prevent or mitigate the consequences of potential disruptive events (e.g., criticality) (SAR Section 2.1.1, p. 2.1-4). Some of the features are further divided into components so that the feature as analyzed can be properly classified as ITWI or Non-ITWI. SAR Table 2.1-1 identifies the features and components that comprise each barrier, their contribution to barrier function, and their safety classification (e.g., ITWI or Non-ITWI).

The determination of processes or characteristics that are ITBC was based on an examination of FEPs and their screening justifications (SNL 2008a, Section 1, p. 1-1, and Section 6, p. 6-1). The ITBC classifications of FEPs, and their underlying bases, are presented in Tables A-1 (for the UNB), A-2 (for the EBS), and A-3 (for the LNB) of the PNSDB report (SNL 2008a), and summarized in SAR Tables 2.1-2, 2.1-3, and 2.1-4.

1.1 ASSOCIATING ITBC FEPS WITH EBS COMPONENTS

The following ITBC FEPs are assigned to the EBS Waste Form and Waste Package Internals feature in Table A-2 of the PNSDB report (SNL 2008a) and in SAR Table 2.1-3, but actually apply to multiple EBS features:

- FEP 2.1.09.05.0A – Sorption of dissolved radionuclides in EBS
- FEP 2.1.09.08.0A – Diffusion of dissolved radionuclides in EBS
- FEP 2.1.09.08.0B – Advection of dissolved radionuclides in EBS.

As described in the response to RAI 3.2.2.1.1-005 (Section 1.4), FEP 2.1.09.05.0A, representing sorption onto corrosion products, is associated with several components of the Waste Form and Waste Package Internals feature (consistent with Table A-2 of the PNSDB report (SNL 2008a) and with SAR Table 2.1-3), but is also associated with the inner vessel component of the Waste Package feature. However, only the inner vessel is ITWI for sorption onto corrosion products (Section 1.4 of the response to RAI 3.2.2.1.1-005).

The other two FEPs, representing advection and diffusion, describe transport of radionuclides through the entire EBS and cannot be easily assigned to a single feature or component. Based on the response to RAI 3.2.2.1.1-005 (Section 1.2), the effects of advection and diffusion most directly impact releases from the waste package, and are therefore most closely associated with the Waste Package feature, which is ITWI. Advection and diffusion also occur interior to the waste packages; this region is represented by the CSNF, HLW Glass, and DSNF components of the Waste Form and Waste Package Internals feature (consistent with Table A-2 of the PNSDB report (SNL 2008a) and with SAR Table 2.1-3).

These three FEPs (1) are associated with multiple features, (2) contribute to the ITWI classification of a feature (Waste Package) to which they were not mapped in Table A-2 of the PNSDB report (SNL 2008a) and in SAR Table 2.1-3, and (3) are associated with, but do not contribute to, the ITWI classification of the feature (Waste Form and Waste Package Internals) to which they were mapped in PNSDB Report Table A-2 and SAR Table 2.1-3. As a result, these FEPs are presented in a special category in Table 2.1-1 Expanded (Waste Form and Waste Package Internals – General), and their contribution to the ITWI classification of specific EBS features and components is described on a case-by-case basis.

1.2 INFORMATION SUPPORTING TABLE 2.1-1 EXPANDED

UNB – Topography and Surficial Soils

The following table contains additional information referenced in Table 1.2-1 Expanded for the Topography and Surficial Soils feature of the UNB.

Table 1.2-1. Mean Infiltration as a Percentage of Mean Precipitation

Climate State	Mean Precipitation (mm/yr)	Mean Infiltration (mm/yr)	Ratio of Infiltration to Precipitation (%)
Present Day	173.6	14.3	8.24
Monsoon	275.2	25.5	9.27
Glacial-Transition	283.4	30.0	10.59

Source: SAR Tables 2.3.1-17, 2.3.1-18, and 2.3.1-19.

EBS - Drip Shield

The following tables contain additional information referenced in Table 1.2-1 Expanded for the Drip Shield feature of the EBS.

Quantitative indications of the barrier capability of the Drip Shield feature were developed from cumulative mass releases from the EBS that are presented in Appendix K of the TSPA-LA report (SNL 2008b). The ratio of the cumulative mass releases out of the EBS under dripping conditions for a single early waste package failure (i.e., waste package only fails) to the cumulative releases out of the EBS under dripping conditions for a single early drip shield failure (i.e., waste package and drip shield both fail) gives an indication of the barrier capability of the drip shield.

CDSP Packages

Table 1.2-2. ^{23o7}Np: Ratio of Cumulative Release from 1 CDSP Package with Waste Package Only Failure to Cumulative Release Waste Package and Drip Shield Failure at 1,000, 5,000, 10,000, and 15,000 Years

	Ratio 1,000 Years	Ratio 5,000 Years	Ratio 10,000 Years	Ratio 15,000 Years
Average	0.05	0.17	0.18	0.13

Document: SNL 2008b
Figure K5.3.1-5b and Figure K5.3.3-3b

Table 1.2-3. ^{237}Np: Ratio of Cumulative Release from 1 CDSP Package with Waste Package Only Failure to Cumulative Release Waste Package and Drip Shield Failure at 50,000, 100,000, 200,000, and 500,000 Years

	Ratio 50,000 Years	Ratio 100,000 Years	Ratio 200,000 Years	Ratio 500,000 Years
Average	0.09	0.09	0.09	0.39

Document: SNL 2008b
Figure K5.3.7-1b and Figure K5.3.9-1b

Table 1.2-4. ^{239}Pu: Ratio of Cumulative Release from 1 CDSP Package with Waste Package Only Failure to Cumulative Release Waste Package and Drip Shield Failure at 1,000, 5,000, 10,000, and 15,000 Years

	Ratio 1,000 Years	Ratio 5,000 Years	Ratio 10,000 Years	Ratio 15,000 Years
Average	0.02	0.62	0.58	0.44

Document: SNL 2008b
Figure K5.3.1-7b and Figure K5.3.3-4b

Table 1.2-5. ^{239}Pu: Ratio of Cumulative Release from 1 CDSP Package with Waste Package Only Failure to Cumulative Release Waste Package and Drip Shield Failure at 20,000, 50,000, 100,000, and 200,000 Years

	Ratio 20,000 Years	Ratio 50,000 Years	Ratio 100,000 Years	Ratio 200,000 Years
Average	0.35	0.28	0.25	0.24

Document: SNL 2008b
Figure K5.3.7-2b and Figure K5.3.9-2b

Table 1.2-6. ^{99}Tc: Ratio of Cumulative Release with Waste Package Only Failure to Cumulative Release Waste Package and Drip Shield Failure at 1,000, 5,000, 10,000, and 15,000 Years

	Ratio 1,000 Years	Ratio 5,000 Years	Ratio 10,000 Years	Ratio 15,000 Years
Average	0.15	0.99	0.99	0.99

Document: SNL 2008b
Figure K5.3.1-9b and Figure K5.3.3-5b

CSNF Packages

Table 1.2-7. ^{237}Np: Ratio of Cumulative Release from 1 CSNF Package with Waste Package Only Failure to Cumulative Release Waste Package and Drip Shield Failure at 10,000, 12,000, 14,000, and 16,000 Years

	Ratio 10,000 Years	Ratio 12,000 Years	Ratio 14,000 Years	Ratio 16,000 Years
Average	0.00	3.72*	32.00*	70.99*

Document: SNL 2008b
Figure K5.3.2-3b
Figure K5.3.5-3b

Table 1.2-8. ^{237}Np: Ratio of Cumulative Release from 1 CSNF Package with Waste Package Only Failure to Cumulative Release Waste Package and Drip Shield Failure at 50,000, 100,000, 200,000, and 500,000 Years

	Ratio 50,000 Years	Ratio 100,000 Years	Ratio 200,000 Years	Ratio 500,000 Years
Average	44.82*	17.70*	9.01*	2.76*

Document: SNL 2008b
Figure K5.3.8-1b
Figure K5.3.11-1b

* The ratio is greater than one (i.e., more releases in the waste package failure case than in the waste package and drip shield failure case) because of decay of ^{241}Am to ^{237}Np. ^{241}Am has a very short half-life, 432 years, compared to that of its daughter ^{237}Np, 2,140,000 years. Therefore, the amount of ^{237}Np in the waste package can increase over time. For the waste package and drip shield failure case, releases from the waste package begin early (see SNL 2008b, Figure K5.3.2-3b), while for the waste package only failure case, releases occur much later, after 10,000 years (see SNL 2008b, Figure K5.3.5-3b). Therefore, by the time the releases begin in the waste package only failure case, most of the ^{241}Am has decayed into ^{237}Np, thus providing a larger inventory of ^{237}Np in the waste pacakge available for release.

Table 1.2-9. ^{239}Pu: Ratio of Cumulative Release from 1 CSNF Package with Waste Package Only Failure to Cumulative Release Waste Package and Drip Shield Failure at 10,000, 12,000, 14,000, and 16,000 Years

	Ratio 10,000 Years	Ratio 12,000 Years	Ratio 14,000 Years	Ratio 16,000 Years
Average	0.00	0.13	0.51	0.61

Document: SNL 2008b
Figure K5.3.2-4b
Figure K5.3.5-4b

Table 1.2-10. ^{239}Pu: Ratio of Cumulative Release from 1 CSNF Package with Waste Package Only Failure to Cumulative Release Waste Package and Drip Shield Failure at 20,000, 50,000, 100,000, and 200,000 Years

	Ratio 20,000 Years	Ratio 50,000 Years	Ratio 100,000 Years	Ratio 200,000 Years
Average	0.72	0.68	0.64	0.62

Document: SNL 2008b
Figure K5.3.8-2b
Figure K5.3.11-2b

Table 1.2-11. ^{99}Tc: Ratio of Cumulative Release from 1 CSNF Package with Waste Package Only Failure to Cumulative Release Waste Package and Drip Shield Failure at 10,000, 12,000, 14,000, and 16,000 Years

	Ratio 10,000 Years	Ratio 12,000 Years	Ratio 14,000 Years	Ratio 16,000 Years
Average	0.00	0.63	0.78	0.80

Document: SNL 2008b
Figure K5.3.2-5b
Figure K5.3.5-5b

2 COMMITMENTS TO NRC

None.

3 DESCRIPTION OF PROPOSED LA CHANGE

None.

4 REFERENCES

SNL (Sandia National Laboratories) 2008a. *Postclosure Nuclear Safety Design Bases.* ANL-WIS-MD-000024 REV 01. Las Vegas, Nevada: Sandia National Laboratories. ACC: DOC.20080226.0002; DOC.20080314.0004; LLR.20080507.0018; DOC.20080610.0007.

SNL 2008b. *Total System Performance Assessment Model /Analysis for the License Application.* MDL-WIS-PA-000005 REV 00 AD 01. Las Vegas, Nevada: Sandia National Laboratories. ACC: DOC.20080312.0001; LLR.20080414.0037; LLR.20080507.0002; LLR.20080522.0113; DOC.20080724.0005; DOC.20080106.0001.

5 LIST OF ATTACHMENTS

Attachment A: Table 2.1-1 Expanded.

Table 2.1-1 Expanded. Summary of the Capability of the ITWI Features / Components Supporting Each of the Three Barriers

Barrier, Feature, and Relevant ITBC FEPs	Barrier Function and Qualitative Description of Barrier Functions [*] = *potential for decreased capability*	Safety Classification and Quantitative Evaluation of Barrier Capability
UNB **Topography and Surficial Soils**	**Prevents or substantially reduces the rate of movement of water**	**ITWI**
Precipitation *(Included FEPs are described in SAR Table 2.3.1-1)* 2.3.11.01.0A – Precipitation 1.3.01.00.0A – Climate change 1.4.01.01.0A – Climate modification increases recharge	**Low precipitation prevents or substantially reduces the rate of movement of water** (SAR Section 2.1.2.1.1, pp. 2.1-17 and -18) (SAR Section 2.3.1.1.1, pp. 2.3.1-3 and -4) 1. Arid desert climate (SAR Section 2.1.2.1.1, p. 2.1-18) 2. Low, intermittent precipitation throughout the year (short-duration and/or low-intensity events) (SAR Section 2.1.2.1.1, pp. 2.1-17 and -18)	**Low Precipitation** (SAR Section 2.1.2.1.6.1, pp. 2.1-26 to -27) SAR Tables 2.3.1-17 (Present Day Climate), 2.3.1-18 (Monsoon Climate), and 2.3.1-19 (Glacial-Transition Climate) show that mean annual precipitation ranges from 173.6 to 283.4 mm/yr over the range of expected climate states.
Infiltration *(Included FEPs are described in SAR Table 2.3.1-1)* 2.3.11.03.0A – Infiltration and recharge 2.3.11.02.0A – Surface runoff and evapotranspiration 2.3.01.00.0A – Topography and morphology 2.2.07.08.0A – Fracture flow in the UZ 1.2.02.01.0A – Fractures 2.2.03.02.0A – Rock properties of host rock and other units	**Reduced infiltration prevents or substantially reduces the rate of movement of water** (SAR Sections 2.1.2.1.1, pp. 2.1-17 and -18; and 2.1.2.1.6, p. 2.1-25) (SAR Section 2.3.1.1.1, pp. 2.3.1-5 and -33) 1. High evapotranspiration (arid climate) (SAR Section 2.1.2.1.1, p. 2.1-17) 2. High runoff (isolated high-intensity summer storms and steep topography) (SAR Section 2.1.2.1.1, p. 2.1-17) 3. Limited infiltration (mostly from low-intensity winter storms) (SAR Section 2.1.2.1.1, p. 2.1-17)	**Reduced Infiltration** (SAR Section 2.1.2.1.6.1, pp. 2.1-26 to -27) SAR Tables 2.3.1-17 (Present Day Climate), 2.3.1-18 (Monsoon Climate), and 2.3.1-19 (Glacial-Transition Climate) show that mean annual infiltration ranges from 14.3 to 30.0 mm/yr over the range of expected climate states. The response to RAI 3.2.2.1.1-001 (Table 1.2-1) shows that this corresponds to only from 8% to 11% of the mean annual precipitation, indicating that the topography and surficial soils feature of the UNB reduces the movement of water by 89% to 92%. Over the range of infiltration scenarios (as opposed to just considering the mean infiltration), the net infiltration ranges from less than 3% to about 17% of precipitation over all climate states (SAR Section 2.1.2.1.6.1, p. 2.1-27). Evapotranspiration accounts for most of the reduction, ranging from about 85% to 88% of the precipitation (SAR Section 2.1.2.1.6.1, p. 2.1-27). SAR Figure 2.1-5(a) shows the time histories for precipitation and infiltration. Note that during the post-10,000 year period the mean value of deep percolation is specified by regulation to be 32 mm/yr (SAR Section 2.1.2.1.6.2, p. 2.1-28).

Table 2.1-1 Expanded. Summary of the Capability of the ITWI Features / Components Supporting Each of the Three Barriers (Continued)

Barrier, Feature, and Relevant ITBC FEPs	Barrier Function and Qualitative Description of Barrier Functions [*] = *potential for decreased capability*	Safety Classification and Quantitative Evaluation of Barrier Capability
UNB **Unsaturated Zone above the Repository**	**Prevents or substantially reduces the rate of movement of water**	**ITWI**
Percolation Flux *(Included FEPs are described in SAR Table 2.3.2-1)* 2.2.07.02.0A – Unsaturated groundwater flow in the geosphere 2.2.07.08.0A – Fracture flow in the UZ 2.2.03.01.0A – Stratigraphy 1.3.01.00.0A – Climate change 1.4.01.01.0A – Climate modification increases recharge 1.2.02.01.0A – Fractures 2.2.03.02.0A – Rock properties of host rock and other units	**Attenuated percolation prevents or substantially reduces the rate of movement of water** (SAR Sections 2.1.2.1.2, pp. 2.1-19 to -20; and 2.1.2.1.6.2, p. 2.1-28) (SAR Section 2.3.2.2, pp. 2.3.2-6 to -16) 1. Low percolation rates (arid climate with low infiltration) (SAR Sections 2.1.2.1.1, p. 2.1-17; and 2.1.2.1.6.2, p. 2.1-28) 2. Large depth to repository (greater than 200 m everywhere) (SAR Section 2.1.1.1 p. 2.1-5) 3. Damping of episodic pulses of precipitation and infiltration (SAR Sections 2.1.1.1, p. 2.1-6; and 2.1.2.1.2, p. 2.1-19 to -20)	**Attenuated Percolation** (SAR Sections 2.1.1.1, p. 2.1-6; and 2.1.2.1.6.2, p. 2.1-28) The average percolation flux flowing to the repository is within a few percent of the net infiltration rate (SAR Section 2.1.2.1.6.2, p. 2.1-28). The stratigraphic sequence of both welded and nonwelded tuffs affects the transient propagation of infiltration pulses and tends to spatially redistribute the percolation rates (SAR Section 2.1.2.1, p. 2.1-15). The dominance of matrix flow in the PTn, and the relatively large storage capacity of the matrix within the PTn, resulting from its high porosity and typically low saturation, give the PTn significant capacity to attenuate infiltration pulses (SAR Section 2.1.2.1.2, p. 2.1-19). Damping of episodic flow is shown to have the potential to reduce seepage rates by anywhere from 5 to ~2,200 kg/yr/WP depending on the episodic period, for percolation fluxes ranging from 5 to 100 mm/yr (see response to RAI 3.2.2.1.1-002, Section 1.4 and Table 1-2). The chemical compositions of pore water in different lithologic units provide an understanding regarding the hydrologic relations among the major hydrogeologic units. Chloride concentrations in pore water within the TCw unit support percolation estimates on the order of 7 mm/yr. Dating of fracture coatings in the TSw unit indicate a seepage flux of 2 to 20 mm/yr. ^{14}C data indicate average transport times through the TSw on the order of 5,000 to 10,000 years. Analysis of perched water below the repository horizon yields ^{14}C dates ranging from 3,300 to 11,000 years. The fact that bomb-pulse ^{36}Cl signals were not detected in perched water and modern ^{14}C is absent in perched water suggests that only a small component of younger water results from fast flow paths. (SAR Section 2.3.2.3.4, p. 2.3.2-30)
Seepage *(Included FEPs above are described in SAR Table 2.3.3-1)* 2.1.08.01.0A – Water influx at the repository 2.2.07.20.0A – Flow diversion around repository drifts [1.2.02.01.0A – Fractures] [2.2.03.02.0A – Rock properties of host rock and other units]	**Diversion of seepage prevents or substantially reduces the rate of movement of water** (SAR Sections 2.1.2.1, p. 2.1-16; and 2.1.2.1.2, pp. 2.1-20 to -22) (SAR Section 2.3.3.1, pp. 2.3.3-4 to -6) 1. Capillary forces limit seepage by diverting flow around the drift opening (flow drains between pillars) (SAR Section 2.1.2.1.2, pp. 2.1-19 to -21) 2. Flow focusing limits fraction of waste packages experiencing seepage (SAR Sections 2.1.2.1, p. 2.1-15; and 2.3.3.2.3.5, pp. 2.3.3-38 and -39) 3. Decay heat creates a dry-out zone that vaporizes water and diverts flow away from and around the drift opening (SAR Section 2.1.2.1.2, p. 2.1-21) *(Note: The primary effects of decay heat are discussed under EBS – Emplacement Drift, consistent with the FEP associations in SAR Table 2.1-3. The process is noted, but not further discussed, here because it has a secondary effect on flow diversion)* 4. **[*]** Seismic events tend to fill the drift openings with lithophysal rubble, decreasing the flow diversion effect (SAR Section 2.1.2.1.5, p. 2.1-25) *(Note: The primary effects of drift collapse are discussed under EBS – Emplacement Drift, consistent with the FEP associations in SAR Table 2.1-3. The process is noted, but not further discussed, here because it has a secondary effect on flow diversion)*	**Capillary Diversion** (SAR Section 2.1.2.1.6.2, pp. 2.1-28 to -30) Three mean spatially averaged drift seepage rate (m^3/yr) curves are compared in SAR Figure 2.1-5(b). The ambient seepage rate (labeled as net infiltration in the figure, and calculated as the average net infiltration flux applied to a 5.1 m by 5.5 m area, i.e., the area of a waste package), represents seepage unaffected by capillary or thermal effects. The TSPA-calculated seepage rate from the nominal/early-failure modeling case (labeled as nominal in the figure) is influenced by both capillary and thermal effects. However, thermal effects on seepage (i.e., drift wall temperature above 100°C) are generally only significant in the first 1,000 years or so (SAR Figure 2.3.5-33 and SAR Table 2.3.5-8). Therefore, the effects of capillary diversion can be identified by comparing the ambient and nominal case seepage rate curves at times after 1,000 years. SAR Figure 2.1-5(b) indicates that, after 1,000 years, the nominal case (affected only by capillary diversion) seepage rate is about 11% of the ambient seepage rate (SAR Section 2.1.2.1.6.2, p. 2.1-29). Thermal effects on seepage and the effects of drift collapse on seepage are discussed under EBS – Emplacement Drift.

Table 2.1-1 Expanded. Summary of the Capability of the ITWI Features / Components Supporting Each of the Three Barriers (Continued)

Barrier, Feature, and Relevant ITBC FEPs	Barrier Function and Qualitative Description of Barrier Functions [*] = *potential for decreased capability*	Safety Classification and Quantitative Evaluation of Barrier Capability
EBS **Emplacement Drift**	**Prevents or substantially reduces the rate of movement of water** **Prevents or substantially reduces the rate of movement of radionuclides**	**ITWI**
In-Drift Physical Environment *(Included FEPs are described in SAR Tables 2.3.5-2 and 2.3.4-1)* 2.1.08.07.0A – Unsaturated flow in the EBS 2.1.11.01.0A – Heat generation in EBS 1.2.03.02.0D – Seismic-induced drift collapse alters In-drift thermal-hydrology **Seismic Ground Motion Failure** *(Included FEPs are described in SAR Table 2.3.4-1)* 1.2.03.02.0A – Seismic ground motion damages EBS components 1.2.03.02.0C – Seismic-induced drift collapse damages EBS components 1.2.03.02.0B – Seismic-induced rockfall damages EBS components (EXCLUDED)	**In-drift physical environment prevents or substantially reduces the rate of movement of water** (SAR Sections 2.1.2.2, pp. 2.1-32 and -43 to -44; 2.1.2.2.2, p. 2.1-46; and 2.1.2.2.3 pp. 2.1-47 to -49) (SAR Sections 2.3.2.4.1, pp. 2.3.2-39 to -41; and 2.3.5.4.1, pp. 2.3.5-68 to -96) 1. Location of emplacement drifts above water table (low water saturation) reduces seepage water contact with drip shield and waste package (SAR Section 2.1.2.2, p. 2.1-32) 2. Decay heat in emplacement drift delays seepage water contact with drip shield and waste package (requires T<100°C) (SAR Section 2.1.2.1.2, p. 2.1-21) 3. Stable in-drift physical environment (very slow nominal rate of change of temperature, RH, saturation, and flow pathways) (SAR Section 2.3.5.1, pp. 2.3.5-12 and -13) 4. **[*]** Seismic-induced drift collapse affects temperature, flow pathways, and seepage water contact with drip shield and waste package (SAR Section 2.1.2.2, pp. 2.1-32 and -33)	**In-Drift Physical Environment (**SAR Section 2.1.2.2.6, pp. 2.1-66 to -68 and -74) Drift collapse (rubble starting to fill the drift) generally begins between 1,000 and 10,000 years and the mean of the fraction of the drift filled with rubble reaches 50% by about 200,000 years (SAR Figure 2.1-14). Drift collapse affects the in-drift physical environment (e.g., seepage, temperature, RH). Time-dependent temperatures and relative humidities at the drift wall, waste package, and invert are shown in Figures K4.3-5 and K4.3-6, respectively, of the TSPA-LA report (SNL 2008b) for CSNF and CDSP waste packages in Bin 3 under nominal conditions. Temperatures stabilize at about 25°C after about 100,000 years and relative humidities stabilize at near 1.0 after about 2,000 years. Drift wall temperatures are below 100°C by about 1,000 years. SAR Figure 2.3.5-33 and SAR Table 2.3.5-8 also show that drift wall temperatures are below 100°C by about 1,000 years. Thermal effects on seepage (delayed due to decay heat) are shown schematically in SAR Figures 2.3.3-37, 2.3.3-42, and 2.3.3-43. The combined effects of thermal delay and drift collapse on seepage are quantified in SAR Figure 2.1-5b, which compares three mean spatially averaged drift seepage rate (m^3/yr) curves. The ambient seepage rate (labeled as net infiltration in the figure, and calculated as the average net infiltration flux applied to a 5.1 m by 5.5 m area, i.e., the area of a waste package), represents seepage unaffected by capillary, thermal, or drift collapse effects. The TSPA-calculated seepage rate from the nominal/early-failure modeling case (labeled as nominal in the figure) is influenced by capillary and thermal effects. The TSPA-calculated seepage rate from the seismic ground motion modeling case (labeled as seismic ground motion in the figure) is influenced by capillary, thermal, and drift collapse effects. Thermal effects on seepage are only significant when the drift wall temperature is above 100°C. This is shown by low seepage rates prior to about 700 years in SAR Figure 2.1.5b for the nominal and seismic cases. The effects of drift collapse on seepage are shown in Figure 2.1-5b by comparing the seismic ground motion case seepage rate with the nominal case seepage rate. At 10,000 years, the seepage rates are nearly identical (and both are about 11% of ambient seepage) due to the low volume of rubble, indicating that seepage is not affected by drift collapse. After 10,000 years, the effects of drift collapse become more significant, resulting in a reduction of capillary diversion. By 1,000,000 years, the seismic ground motion case seepage flux is 48% of the ambient seepage flux. (SAR Section 2.1.2.1.6.2, pp. 2.1-29 and 2.1-30)
In-Drift Chemical Environment *(Included FEPs are described in SAR Tables 2.3.5-1, 2.3.5-2, and 2.3.5-3)* 2.1.09.01.0A – Chemical characteristics of water in drifts 2.2.08.12.0A – Chemistry of water flowing into the drift [2.1.11.01.0A – Heat generation in EBS] 2.1.11.08.0A – Thermal effects on chemistry and microbial activity in the EBS	**In-drift chemical environment prevents or substantially reduces the rate of movement of water and prevents or substantially reduces the rate of movement of radionuclides** (SAR Sections 2.1.2.2, pp. 2.1-33 to -34 and -43 to -44; 2.1.2.2.2, p. 2.1-46; and 2.1.2.2.3 pp. 2.1-47 to -49) (SAR Section 2.3.5.3, pp. 2.3.5-20 to -65) 1. Stable in-drift chemical environment (very slow nominal rate of change of pH, ionic strength, and pCO_2) (SAR Section 2.3.5.1, pp. 2.3.5-12 and -13) 2. In-drift chemical environment produces slow drip shield and waste package general corrosion rates (SAR Section 2.1.2.2, pp. 2.1-35 and -37) 3. In-drift chemical environment limits localized corrosion of drip shield and waste package (SAR Section 2.1.2.2, pp. 2.1-35 and -37) *(Note: The effects of localized corrosion of the waste package are discussed under EBS – Waste Package, consistent with the FEP associations in SAR Table 2.1-3)*	**In-Drift Chemical Environment** (SAR Section 2.1.2.2.6, pp. 2.1-66 to -67 and -74) The chemical characteristics of water in the drift are affected by the incoming water chemistry, evaporation, and other thermal-chemical processes in the drift that are a function of the thermal-hydrologic environment (SAR Sections 2.3.5.1 and 2.3.5.5). These chemical characteristics affect the likelihood of potential localized corrosion of the waste package outer barrier (SAR Section 2.3.6.4), as well as the transport characteristics of any radionuclides released from the waste package to the invert. SAR Sections 2.3.7.10, 2.3.7.11, and 2.3.7.12 discuss the transport characteristics affected by the range of in-drift water chemical characteristics, notably radionuclide solubility. (SAR Section 2.1.2.2, pp. 2.1-32) The effects of localized corrosion of the waste package are discussed under EBS – Waste Package. Thermal effects strongly influence the evolution of the water chemistry in the rock and emplacement drifts (SAR Section 2.1.2.2, pp. 2.1-33). SAR Section 2.1.2.2 (p. 2.1-35) states, “General corrosion rates of titanium alloys in a range of expected environmental conditions in the emplacement drifts are sufficiently low.” SAR Section 2.1.2.2 (p. 2.1-37) states, “General corrosion rates of Alloy 22 in a range of expected environmental conditions are sufficiently low.” Time-dependent pCO_2, ionic strength, and pH in the invert are shown in Figures K4.3-7, K4.3-9, K4.3-10, K4.3-12, and K4.3-14 of the TSPA-LA report (SNL 2008b) for CSNF and CDSP waste packages in Bin 3 under nominal conditions. Values of pCO_2 stabilize at about 0.001 bars after about 50,000 years, ionic strength stabilizes at about 0.01 mol/kg after about 2,000 years, and pH stabilizes at between 7 and 9 after about 4,000 years. Although the invert is Non-ITWI, the parameter values listed here are indicative of stable in-drift values.

Table 2.1-1 Expanded. Summary of the Capability of the ITWI Features / Components Supporting Each of the Three Barriers (Continued)

Barrier, Feature, and Relevant ITBC FEPs	Barrier Function and Qualitative Description of Barrier Functions [*] = *potential for decreased capability*	Safety Classification and Quantitative Evaluation of Barrier Capability
EBS Emplacement Drift – Non Emplacement Openings, Closure, Ground Support, and Ventilation System	**None**	**Non-ITWI**
No ITBC FEPs	**Non-Emplacement Openings** **FEP 1.1.01.01.0A (Open Site Investigation Boreholes) Excluded, Non-ITBC** Site investigation boreholes that have been left open, degraded, improperly sealed, or reopened are excluded on the basis that: (1) existing boreholes from site characterization are known, (2) future drilling will be controlled, (3) the regulatory requirements for borehole sealing prior to repository closure will be met, and (4) administrative controls for repository construction and operations will be developed to ensure these outcomes. Accordingly, these features are considered not to be important to barrier capability. (SNL 2008a, Table A-2, p. A-29) **Closure** **FEP 1.1.04.01.0A (Incomplete Closure) Excluded, Non-ITBC** Incomplete closure, sealing, and decommissioning of the disposal vault is excluded by regulation, and is therefore considered not to be important to barrier capability. (SNL 2008a, Table A-2, p. A-32) **FEP 2.1.05.02.0A (Radionuclide transport through seals) Excluded, Non-ITBC** Sealing concepts have been identified for the license application, but the designs of these seals have not been determined. The designs will be supported by evaluations of performance, and the application of construction and operational management and administrative controls to ensure correct implementation. The design addresses seals as closure of the shafts and ramps shall include backfilling for the entire depth of the opening. Site investigation boreholes within or near the footprint of the repository block will be backfilled with material compatible with the host rock and plugged. These design features are intended to meet the intrusion scenarios, and are not performance related. Accordingly, these features are considered not to be important to barrier capability. (SNL 2008a, Table A-2, p. A-42) **Ventilation System** **FEP 1.1.02.02.0A (Preclosure Ventilation) Included, Non-ITBC** Preclosure ventilation removes heat and moisture from the host rock during the ventilation period. The heat removal effect is included explicitly in all postclosure thermal models, while the moisture removal effect is minor compared to postclosure hydrologic processes, and is not significant to postclosure performance. Preclosure removal of heat can be achieved within a wide range of operational parameters, including passive ventilation, and its effects on postclosure conditions are limited. Hence effects are not considered significant to barrier capability. (SNL 2008a, Table A-2, p. A-30)	N/A

Table 2.1-1 Expanded. Summary of the Capability of the ITWI Features / Components Supporting Each of the Three Barriers (Continued)

Barrier, Feature, and Relevant ITBC FEPs	Barrier Function and Qualitative Description of Barrier Functions [*] = *potential for decreased capability*	Safety Classification and Quantitative Evaluation of Barrier Capability
EBS Emplacement Drift – Non Emplacement Openings, Closure, Ground Support, and Ventilation System (continued)		
	Ground Support **FEP 2.1.06.01.0A (Chemical Effects of Rock Reinforcement and Cementitious Materials in EBS) Excluded, Non-ITBC** The effects of seepage water interacting with rock reinforcement and cementitious materials used in repository construction and operation have been evaluated and determined to be insignificant with respect to postclosure performance. In addition, to prevent or limit potentially deleterious effects from rock reinforcement and cementitious materials, construction and operational management and administrative controls will be developed and implemented. Therefore, these effects are considered not to be important to barrier capability. (SNL 2008a, Table A-2, p. A-43) **FEP 2.1.06.02.0A (Mechanical Effects of Rock Reinforcement Materials in EBS) Excluded, Non-ITBC** No postclosure barrier capability is attributed to the rock reinforcement materials used in the EBS. Postclosure models and analyses neglect the potential beneficial effects from rock reinforcement on the rock mass response to thermo-mechanical and seismic stresses. Therefore, these effects are considered not to be important to barrier capability. (SNL 2008a, Table A-2, p. A-43) **FEP 2.1.06.04.0A (Flow Through Rock Reinforcement Materials in EBS) Excluded, Non-ITBC** Groundwater flow and seepage are not significantly affected by the presence of rock reinforcement materials used during repository construction and operations. Therefore, this process has been excluded from the performance assessment. This FEP is not considered ITBC because this does not substantially affect the rate of movement of water and the release or release rate of radionuclides from the Yucca Mountain repository to the accessible environment. This evaluation assumes that the proper controls for operations and design will be in place and that any changes to the controls or the design will be evaluated through an established corrective action program, which will include an evaluation of the impacts. (SNL 2008a, Table A-2, p. A-44)	

Table 2.1-1 Expanded. Summary of the Capability of the ITWI Features / Components Supporting Each of the Three Barriers (Continued)

Barrier, Feature, and Relevant ITBC FEPs	Barrier Function and Qualitative Description of Barrier Functions [*] = *potential for decreased capability*	Safety Classification and Quantitative Evaluation of Barrier Capability
EBS **Drip Shield**	**Prevents or substantially reduces the rate of movement of water** **Prevents or substantially reduces the rate of movement of radionuclides**	**ITWI**
Diversion of Flow by Drip Shield *(Included FEPs are described in SAR Table 2.3.5-2)* 2.1.06.06.0A – Effects of drip shield on flow 2.1.03.11.0A – Physical form of waste package and drip shield	**Diversion of flow by drip shield prevents or substantially reduces the rate of movement of water** (SAR Sections 2.1.2.2, p. 2.1-35; and 2.1.2.2.1, pp. 2.1-44 to -45) (SAR Section 2.3.6.1.1, pp. 2.3.6-6 to -8) 1. Drip shield diverts seepage water and condensate around waste package to invert (SAR Section 2.3.6.8, p. 2.3.6-70) 2. Drip shield protects waste package from deleterious brines during the period of susceptibility to localized corrosion (SAR Section 2.1.2.2, p. 2.1-35). *(Note: The effects of localized corrosion of the waste package are discussed under EBS – Waste Package, consistent with the FEP associations in SAR Table 2.1-3)*	**Diversion of Flow by Drip Shield** (SAR Section 2.1.2.2.6, pp. 2.1-56 to -64, -72 to -74, and -76) The response to RAI 3.2.2.1.1-001 (Section 1.2) quantifies the ratio of cumulative mass releases from the EBS for the waste package early failure case (waste package only fails) and the drip shield early failure case (both waste package and drip shield fail). For CDSP waste packages, the ratios at 15,000 years are 0.13 for ^{237}Np releases, 0.44 for ^{239}Pu releases, and 0.99 for ^{99}Tc releases. The ratios at 200,000 years are 0.09 for ^{237}Np releases and 0.24 for ^{239}Pu releases (the ^{99}Tc ratio was not calculated) (see response to RAI 3.2.2.1.1-001, Tables 1.2-2 through 1.2-6). The ratios less than 1 are indicative of drip shield performance, specifically in reducing advective flow through the system. The ratio for ^{99}Tc releases is close to 1 because it is not solubility limited. Therefore, it can be transported rapidly by diffusion, and is not affected as much by the presence/absence of the drip shield. For CSNF waste packages, the ratios are zero at 10,000 years (i.e., no releases). The ratios at 16,000 years are 71.0 for ^{237}Np releases, 0.61 for ^{239}Pu releases, and 0.80 for ^{99}Tc releases. The ratios at 200,000 years are 9.01 for ^{237}Np releases and 0.62 for ^{239}Pu releases (the ^{99}Tc ratio was not calculated) (see response to RAI 3.2.2.1.1-001, Tables 1.2-7 through 1.2-11). Again, the ratios less than 1 are indicative of drip shield performance. Note that the large ratios for ^{237}Np reflect the ingrowth of ^{237}Np from ^{241}Am, which masks drip shield performance for this case. The low probability of drip shield failure to divert seepage water contributes to the relatively low contribution to mean dose to the RMEI that would result from drip shield failure and subsequent localized corrosion on underlying waste packages. This contribution to mean dose is estimated as described in the TSPA-LA report (SNL 2008b, Section 7.3.2.6.1.3.2), and is less than 5×10^{-3} mrem during 10,000 years.
Drip Shield Degradation *(Included FEPs are described in SAR Table 2.3.6-1)* 2.1.03.01.0B – General corrosion of drip shields 2.1.03.08.0B – Early failure of drip shields 2.1.03.02.0B – Stress corrosion cracking of drip shields (EXCLUDED) 2.1.03.10.0B – Advection of liquids and solids through cracks in the drip shield (EXCLUDED) 2.1.07.05.0B – Creep of metallic materials in the drip shield (EXCLUDED) 2.1.03.03.0B – Localized corrosion of drip shields (EXCLUDED) 2.1.09.28.0B – Localized corrosion on drip shield surfaces due to deliquescence (EXCLUDED)	**Slow drip shield degradation prevents or substantially reduces the rate of movement of water** (SAR Sections 2.3.6.1.1, p. 2.3.6-6; and 2.1.2.2.1, pp. 2.1-44 to -45) (SAR Section 2.3.6.1.1, pp. 2.3.6-6 to -8) 1. Slow drip shield general corrosion rates (SAR Section 2.1.2.2.6, p. 2.1-60 and Section 2.3.6.1.1, p. 2.3.6-6) 2. Minimal drip shield early failures due to manufacturing defects (SAR Section 2.1.3.2, pp. 21-104 and -105) 3. Drip shield SCCs (nominal) do not affect drip shield capability (no advection through cracks) (SAR Section 2.1.2.2, pp. 2.1-35 and -36) 4. Localized corrosion of drip shield does not occur (SAR Section 2.1.2.2, p. 2.1-35) 5. **[*]** Seismic ground motion failures (rupture/tearing or buckling associated with drift collapse) lead to reduction in drip shield lifetime relative to nominal processes (SAR Section 2.1.2.2, pp. 2.1-35 to -37) 6. Drip shield SCCs (from seismic-induced ground motion or rockfall) do not affect drip shield capability (no advection through cracks) (SAR Section 2.1.2.2, pp. 2.1-36 and -37)	**Slow Drip Shield Degradation** (SAR Section 2.1.2.2.6, pp. 2.1-56 to -64, -72 to -74, and -76) <u>Nominal</u> For nominal conditions, the median drip shield failure time is 290,000 years, with a range of 270,000 to 340,000 years (SAR Section 2.1.2.2.6, p. 2.1-57, 4th para.). <u>Early Failure</u> The expected number of early failed drip shields is 0.0181 and the conditional expected number, given that one or more drip shield early failure occurs, is 1.09 (SAR Section 2.4.2.3.2.1.12.1, p. 2.4-191, 3rd para.). <u>Localized Corrosion</u> ΔE, defined as the difference between $E_{critical}$ and E_{corr}, is significantly greater than zero over all ranges of pH, chloride concentration, and temperature, even at the ±4σ confidence level which accounts for data uncertainty. A ΔE of several hundred millivolts is maintained even at very high pH. Localized corrosion of Titanium Grade 7 thus does not initiate in a repository-relevant environment even at pH values as high as 14. (SAR Section 2.3.6.8.2.3, p. 2.3.6-77) <u>Seismic Ground Motion</u> For seismic ground motion conditions, the median drip shield failure time is 255,000 years; 5th percentile 191,000 years; 95th percentile 280,000 years (SAR Section 2.1.2.2.6, p. 2.1-60, 2nd para.).
Seismic Ground Motion Failure *(Included FEPs are described in SAR Table 2.3.4-1)* 1.2.03.02.0C – Seismic-induced drift collapse damages EBS components	**Delayed waste package degradation prevents or substantially reduces the rate of movement of radionuclides** (SAR Section 2.1.2.2, p. 2.1-37) (SAR Section 2.3.6.1.1, pp. 2.3.6-6 to -8) 1. Seismic drift collapse rubble protects waste package from rockfall damage (SAR Section 2.1.2.2, p. 2.1-39)	

Table 2.1-1 Expanded. Summary of the Capability of the ITWI Features / Components Supporting Each of the Three Barriers (Continued)

Barrier, Feature, and Relevant ITBC FEPs	Barrier Function and Qualitative Description of Barrier Functions [*] = *potential for decreased capability*	Safety Classification and Quantitative Evaluation of Barrier Capability
EBS Waste Package	**Prevents or substantially reduces the rate of movement of water Prevents the release of or substantially reduces the release rate of radionuclides Prevents or substantially reduces the rate of movement of radionuclides**	**ITWI**
Diversion of Flow by Waste Package *(Included FEPs are described in SAR Table 2.3.6-1)* 2.1.03.11.0A – Physical form of waste package and drip shield	**Diversion of flow by waste package prevents or substantially reduces the rate of movement of water** (SAR Sections 2.1.2.2, p. 2.1-37; and 2.1.2.2.1, pp. 2.1-44 to -45) (SAR Section 2.3.6.3.4.1, pp. 2.3.6-27 and -28) 1. Waste package delays water contact with waste forms (SAR Section 2.1.2.2, p. 2.1-37) 2. Waste package SCCs limit water contact with waste forms (SAR Section 2.3.7.3.2, p. 2.3.7-14)	**Diversion of Flow by Waste Package** (SAR Section 2.1.2.2.6, pp. 2.1-56 to -65, -72 to -74, and -76 to -77) The response to RAI 3.2.2.1.1-004 (Section 1, p. 5) indicates that the fraction of seepage that can enter a CSNF waste package breached by general corrosion ranges from 0 to 0.11. Therefore, even with significant breaching (e.g., at 1,000,000 years), at least 89% of seepage is still diverted.
Waste Package Degradation *(Included FEPs are described in SAR Table 2.3.6-1)* 2.1.03.01.0A – General corrosion of waste packages 2.1.03.08.0A – Early failure of waste packages 2.1.03.02.0A – Stress corrosion cracking of waste packages 2.1.03.10.0A – Advection of liquids and solids through cracks in the waste package (EXCLUDED) 2.1.03.03.0A – Localized corrosion of waste packages 2.1.09.28.0A – Localized corrosion on waste package outer surface due to deliquescence (EXCLUDED) **Seismic Ground Motion Failure** *(Included FEPs are described in SAR Table 2.3.4-1)* 1.2.03.02.0A – Seismic ground motion damages EBS components	**Slow waste package degradation prevents the release of or substantially reduces the release rate of radionuclides** (SAR Sections 2.1.2.2.1, pp. 2.1-44 to -45; and 2.1.2.2.6, p. 2.1-52) (SAR Sections 2.3.4.1, p. 2.3.4-11, and 2.3.6.2.2, pp. 2.3.6-10 to -15) 1. Slow waste package general corrosion rates (SAR Section 2.1.2.2.1, p. 2.1-45, and Section 2.1.2.2.6, p. 2.1-53) 2. Minimal early failures due to manufacturing defects (SAR Section 2.3.6.6.3.1, pp. 2.3.6-57 and -58) 3. Slow onset of waste package SCC – nominal or seismic-induced (stress-mitigated layer of closure lid welds must be removed) (SAR Section 2.1.2.2, pp. 2.1-37 and -38) 4. Insignificant effects from localized corrosion due to presence of drip shield during the period of susceptibility to localized corrosion (SAR Section 2.1.2.2, p. 2.1-38) 5. Seismic drift collapse rubble protects waste package from rockfall damage (protected by drip shield prior to drip shield failure) (SAR Section 2.1.2.2, p. 2.1-39) 6. Seismic drift collapse rubble reduces damage to waste package from ground motion impacts (SAR Section 2.1.2.2, p. 2.1-39) 7. Seismic failures of CSNF waste packages are limited due to strength of TAD canister (SAR Section 2.1.2.2, p. 2.1-40) 8. **[*]** Seismic failures of CDSP waste packages are mostly SCCs from ground motion (not as significant as patch failures) (SAR Section 2.1.2.2, p. 2.1-40)	**Slow Waste Package Degradation** (SAR Section 2.1.2.2.6, pp. 2.1-56 to -64, -72 to -74, and -76 to -77) Early Failure The expected number of early failed waste packages is 1.09 and the conditional expected number, given that one or more waste package early failure occurs, is 2.5 (SAR Section 2.1.2.2.6, p. 2.1-70). Nominal and Seismic Ground Motion SAR Figure 2.1-10 shows that waste package breaches due to nominal processes are not expected before about 150,000 years. Prior to 170,000 years, radionuclide releases from the EBS in the seismic ground motion modeling case (which includes nominal processes) are determined by waste package failures related to vibratory ground motion (SAR Section 2.1.2.2.6, p. 2.1-75). At 170,000 years, the mean of the expected fraction of waste packages breached is 0.37 for CDSP waste packages (due to seismic cracks) and 0.005 for CSNF waste packages (SAR Figures 2.1-12(c) and 2.1-12(a)). Between 170,000 and 600,000 years, radionuclide releases from the EBS in the seismic ground motion modeling case are determined by waste package failures related to both nominal processes (primarily SCC) and vibratory ground motion (SAR Section 2.1.2.2.6, p. 2.1-75). At 600,000 years, the mean of the expected fraction of waste packages breached is 0.51 for CDSP waste packages (due primarily to seismic and nominal cracks) and 0.25 for CSNF waste packages (due primarily to nominal cracks) (SAR Figures 2.1-12(c) and 2.1-12(a)). After about 600,000 years, radionuclide releases from the EBS in the seismic ground motion modeling case are determined by waste package failures related to nominal processes (both SCC and general corrosion) (SAR Section 2.1.2.2.6, p. 2.1-75). At 1,000,000 years, the mean of the expected fraction of waste packages breached is 0.70 for CDSP waste packages (due to to seismic and nominal cracks and nominal patches) and 0.56 for CSNF waste packages (due to nominal cracks and patches) (SAR Figures 2.1-12(c) and 2.1-12(a)). Based on SAR Figure 2.1-10(b), the mean of the fraction of waste packages breached by nominal patches at 1,000,000 years is approximately 9% (SAR Section 2.1.2.2.6, p. 2.1-59). Localized Corrosion If the drip shield is intact, localized corrosion initiation cannot occur because seepage does not contact the waste package surface. If the drip shield is breached or if the drip shield is assumed to not perform as intended, then the chemistry on the waste package surface may allow localized corrosion to initiate (SNL 2008b, ERD 05, Section O1, p. 3). However, even if the drip shield is breached, the average fraction of waste packages on which localized corrosion may potentially initiate peaks at about 0.34 in the first few hundred years after closure. After a few thousand years, the fraction decreases to below 10^{-3} (SNL 2008b, ERD 05, Section O3, p. 7). The conditions for localized corrosion initiation do not exist anywhere in the repository beyond 12,000 years after closure because temperatures decrease and chemical conditions become less aggressive (SNL 2008b, ERD 05, Section O1, p. 4).
	Limited waste package breach area prevents or substantially reduces the rate of movement of radionuclides (SAR Section 2.1.2.2, pp. 2.1-37 to -38) (SAR Section 2.3.4.5, pp. 2.3.4-108 to -191) 1. Waste package SCCs (nominal, seismic ground motion, early failure) only permit diffusive releases from waste package (SAR Section 2.1.2.2, pp. 2.1-37 and -38)	**Limited Waste Package Breach Area** (SAR Section 2.1.2.2.6, pp. 2.1-56 to -64, -72 to -74, and -76 to -77) Figures K7.7.1-1[a], K7.7.1-2[a], K7.7.2-1[a], and K7.7.2-2[a] of the TSPA-LA report (SNL 2008b) show that, for the seismic ground motion modeling case, stress corrosion cracking of the waste package (indicated by variable SCCTHRP) is the most important uncertain variable controlling dose for the first 250,000 years, and general corrosion of the waste package (indicated by variable WDGCA22) is the most important uncertain variable from 250,000 to 1,000,000 years.

Table 2.1-1 Expanded. Summary of the Capability of the ITWI Features / Components Supporting Each of the Three Barriers (Continued)

Barrier, Feature, and Relevant ITBC FEPs	Barrier Function and Qualitative Description of Barrier Functions [*] = *potential for decreased capability*	Safety Classification and Quantitative Evaluation of Barrier Capability
EBS **Waste Form and Waste Package Internals – General**	**Prevents the release of or substantially reduces the release rate of radionuclides** **Prevents or substantially reduces the rate of movement of radionuclides**	**ITWI –** This "General" category captures ITBC FEPs that contribute to the ITWI classification of the EBS, but are not easily assigned to a single feature or component, as described in response to RAI 3.2.2.1.1-001 (Section 1.1)
Advection and Diffusion in EBS *(Included FEPs are described in SAR Table 2.3.7-1)* 2.1.09.08.0A – Diffusion of dissolved radionuclides in EBS 2.1.09.08.0B – Advection of dissolved radionuclides in EBS (*These ITBC FEPs related to advection and diffusion are assigned to the EBS - Waste Form and Waste Package Internals feature in Table A-2 of the PNSDB report (SNL 2008a) and SAR Table 2.1-3, but also apply to the Waste Package feature, as described in responses to RAIs 3.2.2.1.1-001 (Section 1.1) and 3.2.2.1.1-005 (Section 1.2) and noted in SAR Section 2.1.2.2 (pp. 2.1-37 to -39), under Stress Corrosion Cracking of Waste Packages, Advection of Liquids and Solids through Cracks in the Waste Package, and Seismic Ground Motion Damages EBS Components*)	**Slow advection and diffusion prevents the release of or substantially reduces the release rate of radionuclides and prevents or substantially reduces the rate of movement of radionuclides** (SAR Section 2.1.2.2.2, p. 2.1-46) (SAR Section 2.3.7.1, pp. 2.3.7-10 and -11) 1. Low advection rate and diffusivity in EBS (due to low water saturation) (SAR Sections 2.1.1.2, p. 2.1-7; and 2.1.2.2, p. 2.1-32) 2. Decay heat delays diffusion from waste form and waste package (continuous thin film requires T<100°C, RH>95%) (SAR Section 2.1.2.2.6 , pp. 2.1-66 and -67) 3. Decay heat delays advection from waste form and waste package (requires liquid flux, T<100°C) (SAR Section 2.1.2.2.6 , pp. 2.1-66 and -67) 4. Slow diffusion through thin films of water (low saturation) (SAR Sections 2.1.2.2.2, p. 2.1-46; and 2.3.7.12.3, p. 2.3.7-74) 5. Releases from waste packages are generally only by diffusion until general corrosion occurs (SAR Sections 2.1.2.2.6, pp. 2.1-70 to -74; and 2.3.7.12, pp. 2.3.7-68 and -69) 6. Diffusive releases are typically smaller than advective releases, particularly for solubility-limited radionuclides (SAR Section 2.1.2.2, p. 2.1-42) 7. Insignificant advective transport for several hundreds of thousands of years (SAR Sections 2.1.1.2, p. 2.1-7; and 2.1.2.2.6, pp. 2.1-73 and -74) 8. Advective releases are limited by the low number of patch failures (only from general corrosion, seismic rupture/tearing, some early failures) (SAR Section 2.1.2.2.6, pp. 2.1-58 and -59) 9. Advection from waste package requires both a drip shield and a waste package breach, and seepage (SAR Sections 2.1.2.2.2, pp. 2.1-46 and -66; 2.3.7.1, p. 2.3.7-10)	**Advection and Diffusion** (SAR Section 2.1.2.2.6, pp. 2.1-66 to -67 and -72 to -74) SAR Figure 2.1-20 shows that, for the combined nominal/early-failure modeling case, the mean total activity released from the EBS after 1,000,000 years is only about 7% of the inventory at that time (SAR Section 2.1.2.2.6, p. 2.1-72). SAR Figure 2.1-23 shows that, for the seismic ground motion modeling case, the EBS performance is similar to the combined nominal/early-failure modeling case (SAR Section 2.1.2.2.6, p. 2.1-76). <u>0 to 10,000 Years</u> As described in the response to RAI 3.2.2.1.1-005 (Section 1.2.1.2), for a single realization of the 10,000-year seismic ground motion modeling case (examining only the effects of seismic-induced stress corrosion cracking), Figure 7.3.2-9 of the TSPA-LA report (SNL 2008b) shows the annual dose results for several different crack damage fractions for a seismic event at 100 years. Figure 7.3.2-10 of the TSPA-LA report (SNL 2008b) shows the annual dose history results for a seismic event at 11,200 years. As can be seen from the figures, the shape of the dose history is similar for each of the different damage fractions, and does not significantly change for the 11,200-year event as compared with the 100-year event. More importantly, the magnitude of the annual dose increases proportionally with increasing damage fraction up to a damage fraction of 1×10^{-5}. Figure 7.3.2-12 of the TSPA-LA report (SNL 2008b) more clearly illustrates this effect by comparing the annual doses at 10,000 years for each damage fraction. This figure clearly indicates the strong relationship between damage fraction (i.e., crack area) and annual dose (up to a damage fraction of 1×10^{-5}) for a case with diffusive releases from CDSP waste packages. Beyond a damage fraction of 1×10^{-5}, annual dose does not increase proportionally with increasing damage fraction for this particular modeling case. Generally, annual doses from seismic ground motion are dominated by ^{99}Tc. The lack of increase in annual dose beyond a damage fraction of 1×10^{-5} indicates that, when damage area is sufficiently large, the rate of diffusion through the cracks in the waste package no longer constrains the release of ^{99}Tc from the waste package. <u>10,000 to 1,000,000 Years</u> As described in the response to RAI 3.2.2.1.1-005 (Section 1.2.1.2), for a single realization analysis for the 1,000,000-year seismic ground motion modeling case, SAR Figures 2.4-99 (for CDSP waste packages) and 2.4-101 (for CSNF waste packages) show that for ^{242}Pu (SAR Figures 2.4-99(b) and 2.4-101(b)), the diffusive releases over time mimic the breach areas over time, remaining relatively constant until the onset of general corrosion patch breaches, and then increasing corresponding to the increased breach area due to the patch breaches. The onset of general corrosion patches is typically associated with an increase in advective releases (if seepage is present), but the increased breach area also contributes to increased diffusive releases as shown here. These figures indicate the importance of limited breach area on limiting diffusive releases. For ^{99}Tc (SAR Figures 2.4-99(a) and 2.4-101(a)), the diffusive releases occur over a shorter time. This is reflective of the fact that ^{99}Tc is not solubility limited and does not sorb onto corrosion products, thus leading to faster depletion of the ^{99}Tc inventory, relative to solubility-limited and sorbing radionuclides (i.e., ^{242}Pu). For this reason, ^{99}Tc release rates are more dependent on the time of the first breach than on the breach area evolution over time. As described in the response to RAI 3.2.2.1.1-005 (Section 1.2.1.2), another observation from this seismic ground motion modeling case single realization analysis relates to advective releases from the waste packages. For CSNF, the total release rate of ^{242}Pu (aqueous and colloidal) from all percolation subregions from the EBS is about 3.6 g/yr at 1,000,000 years (SAR Figure 2.4-106), whereas the sum of the diffusive releases from the waste packages for all percolation subregions is about 2.4 g/yr at 1,000,000 years (SAR Figure 2.4-101(b)). The difference, about 1.2 g/yr, which also includes effects of solubility limits and sorption on corrosion products, suggests that, for this realization of the seismic ground motion modeling case, advective release rates are of similar magnitude to diffusive release rates. This is in contrast to circumstances where the waste package outer barrier is completely failed such as in the igneous intrusion modeling case. As described in the response to RAI 3.2.2.1.1-005 (Section 1.2.1.2), Figure 7.7.1-43[a] of the TSPA-LA report (SNL 2008b) indicates that advective releases rates from CSNF waste packages for key radionuclides (^{242}Pu, ^{237}Np, ^{226}Ra, ^{239}Pu, and ^{234}U) are about 2 orders of magnitude greater than the diffusive release rates for a single realization analysis for the 1,000,000-year igneous intrusion modeling case.

Table 2.1-1 Expanded. Summary of the Capability of the ITWI Features / Components Supporting Each of the Three Barriers (Continued)

Barrier, Feature, and Relevant ITBC FEPs	Barrier Function and Qualitative Description of Barrier Functions [*] = *potential for decreased capability*	Safety Classification and Quantitative Evaluation of Barrier Capability
EBS Waste Form and Waste Package Internals – General (continued)	**Prevents the release of or substantially reduces the release rate of radionuclides Prevents or substantially reduces the rate of movement of radionuclides**	**ITWI –** This "General" category captures ITBC FEPs that contribute to the ITWI classification of the EBS, but are not easily assigned to a single feature or component, as described in the response to RAI 3.2.2.1.1-001 (Section 1.1)
Sorption onto Corrosion Products *(Included FEPs are described in SAR Table 2.3.7-1)* 2.1.09.02.0A – Chemical interaction with corrosion products 2.1.09.05.0A – Sorption of dissolved radionuclides in EBS 1.2.03.02.0A – Seismic ground motion damages EBS components (*These ITBC FEPs related to sorption onto corrosion products are assigned to the EBS - Waste Form and Waste Package Internals feature in Table A-2 of the PNSDB report (SNL 2008a) and SAR Table 2.1-3, but also apply to the inner vessel of Waste Package feature, as described in the responses to RAIs 3.2.2.1.1-001 (Section 1.1) and 3.2.2.1.1-005 (Section 1.4) and noted in SAR Section 2.1.2.2 (pp. 2.1-41), under Sorption of Dissolved Radionuclides in the EBS*)	**Sorption onto corrosion products prevents or substantially reduces the rate of movement of radionuclides** (SAR Sections 2.1.2.2, p. 2.1-41; and 2.1.2.2.2, p. 2.1-46) (SAR Section 2.3.7.12, pp. 2.3.7-70 to -73 and -77) 1. Sorption onto corrosion products retards transport of some radionuclides (SAR Sections 2.1.2.2, p. 2.1-41; 2.1.2.2.1 p. 2.1-46; 2.1.2.2.6, p. 2.1-67; and 2.3.7.12, p. 2.3.7-77)	**Sorption onto Corrosion Products** (SAR Section 2.1.2.2.6, pp. 2.1-66 to -67 and -74) For the 10,000-year seismic ground motion modeling case, the radionuclides which constitute most of the mean dose are those without solubility limits, namely ^{99}Tc, ^{14}C, and ^{129}I (SAR Figure 2.4-26). Radionuclides with solubility limits, such as ^{239}Pu, are negligible contributors to the mean dose because the release rate and total mass release from the EBS is also small (SNL 2008b, Figure K7.3-7). The absence of advection through the waste is the dominant factor in limiting the release of these radionuclides. Of the radionuclide mass that is released, sensitivity analysis results (SNL 2008b, Figures K7.3-7 and K.7.3-8) indicate that uncertain variables which affect solubility limits are most influential to the release of ^{239}Pu, with sorption onto corrosion products having less influence within the first 10,000 years. For ^{237}Np releases (SNL 2008b, Figures K7.3-5 and K.7.3-6), sorption onto corrosion products is relatively more influential than are solubility limits. (See response to RAI 3.2.2.1.1-005, Section 1.4.1) For a single realization of the 1,000,000-year seismic ground motion modeling case, SAR Figure 2.4-102 shows that, after the time of initial CSNF waste package breaches (all of which are stress corrosion cracks in this realization) at about 200,000 years, nearly all of the ^{242}Pu mass released from the waste form sorbs onto corrosion products. Subsequent ^{242}Pu mass release rates from the waste package (SAR Figure 2.4-101(b)) are controlled by desorption of ^{242}Pu from the corrosion products, which in turn controls the dissolved concentration in the corrosion products domain (i.e., the waste package) (SAR Figure 2.4-102). Although desorption rates are not presented, SAR Figure 2.4-102 suggests that from 200,000 to 350,000 years, desorption rates are high enough that ^{242}Pu concentrations are controlled by the solubility limits. After 350,000 years, desorption rates are lower, and the available mass of ^{242}Pu is not enough to reach the solubility limits. During this time, ^{242}Pu concentrations are controlled by the desorption rate. (See response to RAI 3.2.2.1.1-005, Section 1.4.2) For the same realization, the CDSP waste packages (SAR Figure 2.4-94) fail much earlier than the CSNF waste packages (SAR Figure 2.4-95) due to seismic ground motion. As with the CSNF waste packages, nearly all of the ^{242}Pu mass released from the waste form sorbs onto corrosion products (SAR Section 2.4.2.2.3.2.2, p. 2.4-102). However, for the CDSP waste packages, the ^{242}Pu dissolved concentrations never reach the solubility limits in this realization (SAR Figure 2.4-100). Therefore, in this realization, the ^{242}Pu concentrations are controlled by the Pu desorption rate for all times. (See response to RAI 3.2.2.1.1-005, Section 1.4.2) For the igneous intrusion modeling case, Figure K6.3.2-3 of the TSPA-LA report (SNL 2008b) shows that, for the first 200,000 years after an igneous event, the uncertain variables that are most influential on the release of ^{237}Np from the EBS are those related to Np solubility (i.e., uncertainty in NpO_2 solubility at ionic strength below 1 molal (EP1NPO2) and uncertainty in pH in CSNF cell 1 under liquid influx conditions (PHCSS)). From 200,000 years after the igneous event, the uncertain variable that is most influential on the release of ^{237}Np from the EBS is the density of sorption sites on goethite (GOESITED), which directly affects the sorptive capability of corrosion products. Figure K6.3.2-4 of the TSPA-LA report (SNL 2008b) shows that, for the first 200,000 years after an igneous intrusion, uncertainty in release of ^{239}Pu is most strongly influenced by uncertainty in plutonium solubility, as indicated by the correlation with uncertainty in Pu solubility at ionic strength below 1 molal (EP1LOWPU). However, sorption onto corrosion products also has an effect, as indicated by the importance of density of sorption sites on goethite (GOESITED). For ^{242}Pu, it is expected that, from 200,000 years after the igneous event and beyond, sorption onto corrosion products will become increasingly influential, as the inventory in the waste form domain is depleted and release from the EBS is increasingly determined by desorption from corrosion products. (See response to RAI 3.2.2.1.1-005, Section 1.4.3) Because the most significant mass of steel is contained in the waste package inner vessel, sorption onto corrosion products only contributes to the ITWI classification of the inner vessel component of the waste package feature. Components of the waste form and waste package internals feature (TAD Canister, DSNF Canister, HLW Canister, TAD Canister Internals, DSNF Canister Internals, and Codisposal Waste Package Internals) are Non-ITWI with respect to sorption onto corrosion products because they do not contain a significant mass of steel that contributes to sorption, relative to the waste package inner vessel. (See response to RAI 3.2.2.1.1-005, Section 1.6)

Table 2.1-1 Expanded. Summary of the Capability of the ITWI Features / Components Supporting Each of the Three Barriers (Continued)

Barrier, Feature, and Relevant ITBC FEPs	Barrier Function and Qualitative Description of Barrier Functions [*] = *potential for decreased capability*	Safety Classification and Quantitative Evaluation of Barrier Capability
EBS Waste Form and Waste Package Internals – TAD Canister	**Prevents the release of or substantially reduces the release rate of radionuclides Prevents or substantially reduces the rate of movement of radionuclides**	**ITWI**
Seismic Ground Motion Failure see Seismic Ground Motion Failure FEPs listed under EBS - Waste Package above	**Delayed CSNF waste package degradation prevents the release of or substantially reduces the release rate of radionuclides and prevents or substantially reduces the rate of movement of radionuclides** (SAR Section 2.1.2.2, p. 2.1-40) (SAR Section 2.3.7.7.3.2, p. 2.3.7-41) 1. Seismic failures of CSNF waste packages are limited due to strength of TAD canister.	**TAD Canister Structural Capability** (SAR Section 2.1.2.2.6, p. 2.1-76) As noted in SAR Section 2.1.2.2.6 (p. 2.1-62), the TAD Canister provides enhanced structural response capability (i.e., damping) to damage from seismic ground motion. SAR Figure 2.1-10 shows that nominal failures do not begin until about 170,000 years. Therefore, all prior failures in the seismic ground motion modeling case are due to damage from seismic events. Comparing SAR Figure 2.1-12(d) for CDSP waste packages and SAR Figure 2.1-12(b) for CSNF waste packages, the mean of the expected fraction of waste packages breached due to seismic ground motion at 170,000 years is 0.37 for CDSP and 0.005 for CSNF (see response to RAI 3.2.2.1.1-005, Section 1.2.2). This result shows that the TAD canister prevents CSNF waste packages from breaching due to seismic ground motion.
EBS Waste Form and Waste Package Internals – Naval Canister	**Prevents the release of or substantially reduces the release rate of radionuclides Prevents or substantially reduces the rate of movement of radionuclides Reduces the probability of criticality**	**ITWI**
See TAD Canister FEPs	**Naval canister prevents the release of or substantially reduces the release rate of radionuclides and prevents or substantially reduces the rate of movement of radionuclides** (SAR Section 2.1.2.2, p. 2.1-40) (SAR Section 2.3.7.3, p. 2.3.7-13) Naval waste packages and naval SNF are included in the model used for the surrogate waste form analysis (SAR Section 2.4.2.3.2.2.4, pp. 2.4-230 to -232). That analysis demonstrates that naval waste packages and naval SNF can be represented by CSNF waste packages and CSNF (SAR Sections 2.1.2.2, p. 2.1-40 and 2.3.7.3, p. 2.3.7-13; SNL 2008a, Section 6.2.2.2, pp. 6-75 and -76). **Naval canister reduces the probability of in-package criticality** Refer to the discussion of in-package criticality under EBS - Waste Form and Waste Package Internals – Naval Canister System Components.	**Reduced Radionuclide Releases** Refer to the discussion under EBS - Waste Form and Waste Package Internals – TAD Canister. **Low Probability of Criticality** Refer to the discussion under EBS - Waste Form and Waste Package Internals – Naval Canister System Components.
EBS Waste Form and Waste Package Internals – DSNF Canister	**None**	**Non-ITWI**
No ITBC FEPs	This component is Non-ITWI because it (1) does not provide additional structural resistance to seismic ground motion damage, and (2) does not contain a significant enough mass of steel that contributes to sorption onto products in the TSPA-LA model (see response to RAI 3.2.2.1.1-005, Section 1.4).	N/A
EBS Waste Form and Waste Package Internals – HLW Canister	**None**	**Non-ITWI**
No ITBC FEPs	This component is Non-ITWI because it (1) does not provide additional structural resistance to seismic ground motion damage, and (2) does not contain a significant enough mass of steel that contributes to sorption onto products in the TSPA-LA model (see response to RAI 3.2.2.1.1-005, Section 1.4).	N/A

Table 2.1-1 Expanded. Summary of the Capability of the ITWI Features / Components Supporting Each of the Three Barriers (Continued)

Barrier, Feature, and Relevant ITBC FEPs	Barrier Function and Qualitative Description of Barrier Functions [*] = *potential for decreased capability*	Safety Classification and Quantitative Evaluation of Barrier Capability
EBS Waste Form and Waste Package Internals – Naval Canister System Components	**Reduces the probability of criticality**	**ITWI**
No ITBC FEPs	**Naval canister system components reduces the probability of criticality** (SAR Section 2.1.2.2, p. 2.1-31) For the postclosure period, criticality control of naval SNF (i.e., assurance of a low probability that criticality involving naval SNF could occur) is provided by controlling one or more of the following characteristics of the loaded naval SNF canister: the amount of fissile material; the materials used for naval SNF canisters, baskets, spacers, naval corrosion-resistant cans, control rods, and installed neutron poison assemblies and their retention hardware; and geometric separation of naval SNF assemblies (SAR Section 1.5.1.4.1.2.2.2, p. 1.5.1-67).	**Low Probability of Criticality** The presence of the naval canister system components contributes to the low probability of in-package criticality. The details of the analysis are in the Classified TSD (Section 2.2.1.4.1) Refer also to the discussion of in-package criticality under EBS – Waste Form and Waste Package Internals – TAD Canister Internals.
EBS Waste Form and Waste Package Internals – Codisposal Waste Package Internals	**None**	**Non-ITWI**
No ITBC FEPs	This component is Non-ITWI because it (1) does not contain a significant enough mass of steel that contributes to sorption onto products in the TSPA-LA model (see response to RAI 3.2.2.1.1-005, Section 1.4), and (2) it does not reduce the probability of criticality associated with CDSP waste packages beyond the criticality control already provided by the DSNF Canister Internals.	N/A
EBS Waste Form and Waste Package Internals – TAD Canister Internals	**Reduces the probability of criticality**	**ITWI**
No ITBC FEPs	**TAD Canister internals reduces the probability of in-package criticality** (SAR Section 2.1.2.2, p. 2.1-31) SAR Section 2.2.1.4.1 (p. 2.2-28) identifies the most significant and effective measures for prevention of criticality in the repository, with the following being specific to the TAD canister internals: inherent geometry of the waste package internals and waste forms; presence of fixed neutron absorbers in the waste package internals; and fuel burnup for CSNF. To ensure that a criticality event does not occur in the repository, the disposal canisters were designed (i.e., canister internal basket, waste package loading, and selected neutron absorber materials) such that the initial emplaced configuration of all of the waste forms remain subcritical, even under flooded conditions (SAR Section 2.2.1.4.1, p. 2.2-29). Details of the specific internals considered in the analysis are described in SAR Section 2.2.1.4.1.1.2.2.	**Low Probability of Criticality** The presence of the TAD canister internals contributes to the low probability of in-package criticality. "The probability of criticality for the in-package location is less than 1 chance in 10,000 of occurrence within 10,000 years after disposal. Therefore, in-package criticality is excluded from the performance assessment" (SNL 2008a, Section 6.2.2.2, p. 6-78). The impact on barrier capability of the in-package criticality FEPs is summarized as follows: "It has been determined that the conditions required to lead to in-package criticality are not likely to occur and the parameter characteristics associated with this process and feature do not substantially effect the release of radionuclides or impact the barrier capability of this feature" (SNL 2008a, Table A-2, pp. A-134 to -141).
EBS Waste Form and Waste Package Internals – DSNF Canister Internals	**Reduces the probability of criticality**	**ITWI**
No ITBC FEPs	**DSNF canister internals reduces the probability of criticality** (SAR Section 2.1.2.2, p. 2.1-31) SAR Section 2.2.1.4.1 (p. 2.2-28) identifies the most significant and effective measures for prevention of criticality in the repository, with the following being specific to the DSNF canister internals: inherent geometry of the waste package internals and waste forms; and presence of fixed neutron absorbers in the waste package internals. To ensure a criticality event does not occur in the repository, the disposal canisters were designed (i.e., canister internal basket, waste package loading, and selected neutron absorber materials) such that the initial emplaced configuration of all of the waste forms remain subcritical, even under flooded conditions (SAR Section 2.2.1.4.1, p. 2.2-29). Details of the specific internals considered in the analysis are described in SAR Section 2.2.1.4.1.1.2.2.	**Low Probability of Criticality** The presence of the DSNF canister internals contributes to the low probability of in-package criticality. "The probability of criticality for the in-package location is less than 1 chance in 10,000 of occurrence within 10,000 years after disposal. Therefore, in-package criticality is excluded from the performance assessment" (SNL 2008a, Section 6.2.2.2, p. 6-78). The impact on barrier capability of the in-package criticality FEPs is summarized as follows: "It has been determined that the conditions required to lead to in-package criticality are not likely to occur and the parameter characteristics associated with this process and feature do not substantially effect the release of radionuclides or impact the barrier capability of this feature" (SNL 2008a, Table A-2, pp. A-134 to -141).

Table 2.1-1 Expanded. Summary of the Capability of the ITWI Features / Components Supporting Each of the Three Barriers (Continued)

Barrier, Feature, and Relevant ITBC FEPs	Barrier Function and Qualitative Description of Barrier Functions [*] = *potential for decreased capability*	Safety Classification and Quantitative Evaluation of Barrier Capability
EBS **Waste Form and Waste Package Internals – CSNF and HLW Glass**	**Prevents the release of or substantially reduces the release rate of radionuclides** **Prevents or substantially reduces the rate of movement of radionuclides**	**ITWI**
Waste Form Degradation *(Included FEPs are described in SAR Table 2.3.7-1)* 2.1.02.02.0A – Commercial SNF degradation (alteration, dissolution, and radionuclide release) 2.1.02.03.0A – HLW glass degradation (alteration, dissolution, and radionuclide release)	**Slow waste form degradation prevents the release of or substantially reduces the release rate of radionuclides** (SAR Section 2.1.2.2.2, p. 2.1-46) (SAR Sections 2.3.7.7 and 2.3.7.9) 1. Slow CSNF degradation rate delays radionuclide release (SAR Sections 2.1.2.2, pp. 2.1-40 and -44; and 2.3.7.7) 2. Slow HLW degradation rate delays radionuclide release (SAR Sections 2.1.2.2, p. 2.1-40 and -44; and 2.3.7.9)	**Waste Form Degradation** (SAR Section 2.1.2.2.6, pp. 2.1-65 to -66) Slow CSNF Degradation For CSNF, the equivalent degradation half-life, based on the degradation equations in SAR Section 2.3.7.7.3.2 (Equations 2.3.7-3 through 2.3.7-5), ranges from 120 to 2,100 years, considering uncertainty in temperature, pH, and specific surface area (see response to RAI 3.2.2.1.1-005, Section 1.1.1). In a single realization analysis of the human intrusion modeling case, SAR Figure 2.4-165 shows the cumulative mass release of Tc and Pu from the waste form inventory following the failure of one CSNF waste package. The waste form starts degrading following the breach at 200,000 years, and due to the relatively slow CSNF degradation rate (about 6.9×10^{-5} yr^{-1}), it requires about 70,000 years to degrade 99% of the waste form (SAR Section 2.4.3.3.5.1, p. 2.4-315). Slow HLW Degradation For HLW, the equivalent degradation half-life, based on the degradation equations in SAR Section 2.3.7.9.3 (Equations 2.3.7-7 through 2.3.7-9), ranges from 180 to 150,000 years, considering uncertainty in temperature, pH, and surface exposure factor (see response to RAI 3.2.2.1.1-005, Section 1.1.1).

Table 2.1-1 Expanded. Summary of the Capability of the ITWI Features / Components Supporting Each of the Three Barriers (Continued)

Barrier, Feature, and Relevant ITBC FEPs	Barrier Function and Qualitative Description of Barrier Functions [*] = *potential for decreased capability*	Safety Classification and Quantitative Evaluation of Barrier Capability
EBS **Waste Form and Waste Package Internals – CSNF and HLW Glass (continued)**	**Prevents the release of or substantially reduces the release rate of radionuclides** **Prevents or substantially reduces the rate of movement of radionuclides**	**ITWI**
In-Package Chemistry and Solubility *(Included FEPs are described in SAR Table 2.3.7-1)* 2.1.09.01.0B – Chemical characteristics of water in waste package 2.1.09.07.0A – Reaction kinetics in waste package 2.1.02.09.0A – Chemical effects of void space in waste package 2.1.09.04.0A – Radionuclide solubility, solubility limits, and speciation in the waste form and EBS	**Low solubility prevents the release of or substantially reduces the release rate of radionuclides and prevents or substantially reduces the rate of movement of radionuclides** (SAR Section 2.1.2.2, p 2.1-41) (SAR Sections 2.3.7.10.3, p. 2.3.7-54) 1. **[*]** In-package chemistry controls radionuclide releases (solubility) (SAR Sections 2.1.2.2, p 2.1-41; and 2.3.7.5) 2. Generally low solubility (SAR Section 2.1.2.2, p. 2.1-41) 3. Solubility limits for some radionuclides delay releases (SAR Section 2.1.2.2, p. 2.1-41)	**Solubility** (SAR Section 2.1.2.2.6, p. 2.1-74) For the 10,000-year seismic ground motion modeling case, the radionuclides which constitute most of the mean dose are those without solubility limits, namely ^{99}Tc, ^{14}C, and ^{129}I (SAR Figure 2.4-26). Radionuclides with solubility limits, such as ^{239}Pu, are negligible contributors to the mean dose because the release rate and total mass release from the EBS is also small (SNL 2008b, Figure K7.3-7). The absence of advection through the waste is the dominant factor in limiting the release of these radionuclides. (See response to RAI 3.2.2.1.1-005, Section 1.3.1.1) For the 10,000-year igneous intrusion modeling case, two radionuclides with solubility limits, ^{239}Pu and ^{240}Pu, are large contributors to the mean dose. Figures K6.3.1-7 and K6.3.1-8 of the TSPA-LA report (SNL 2008b) show that the most influential uncertain variable to the uncertainty in release of ^{239}Pu from the EBS following an igneous intrusion is uncertainty in plutonium solubility at low ionic strength (EP1LOWPU), which directly affects Pu solubility. Other influential uncertain variables control parameters (pH and pCO_2) that influence solubility. (See response to RAI 3.2.2.1.1-005, Section 1.3.1.2) For most of the 1,000,000-year seismic ground motion modeling case,the radionuclides which constitute most of the mean dose are those without solubility limits, namely ^{99}Tc and ^{129}I (SAR Figure 2.4-26). At very late times, both ^{242}Pu and ^{237}Np become relatively large contributors to the mean dose. At later times, the majority of waste package failures in the seismic ground motion modeling case are due to nominal processes (SAR Figure 2.1-12). Thus, the importance of solubility to barrier capability in this case can be observed from the nominal modeling case, which considers only nominal processes. For a single realization of the 1,000,000-year nominal modeling case, SAR Figure 2.4-68 shows that the mass release rate of ^{242}Pu from the waste form is significantly higher than the mass release rate from the waste package. This reduction in release rate between different cells in the EBS transport model indicates the influence of the combined effects of solubility limits and sorption on corrosion products in the waste package. (See response to RAI 3.2.2.1.1-005, Section 1.3.2.1) For the 1,000,000-year igneous intrusion modeling case, the radionuclides which constitute most of the mean dose are ^{239}Pu, ^{242}Pu, and ^{237}Np (SAR Figure 2.4-28). In addition, ^{226}Ra is an important contributor to mean dose, because it results from decay of ^{234}U to ^{230}Th; thus, the influence of uranium solubility may also be important. (See response to RAI 3.2.2.1.1-005, Section 1.3.2.2) For a single realization (Realization 2855) of the 1,000,000-year igneous intrusion modeling case, Figure 7.7.1-40[a] of the TSPA-LA report (SNL 2008b) shows that in the CSNF waste form domain, concentrations of three key radionuclides are solubility limited: U for the entire 1,000,000 years, Pu for the first 200,000 years, and Np for the first 40,000 years. Figure 7.7.1-44[a] of the TSPA-LA report (SNL 2008b) shows that in the CSNF corrosion products domain, concentrations of Pu (270,000 years) and Np (100,000 years) are solubility limited for longer than in the waste form domain, but U never reaches a solubility limit. These solubility limits in the corrosion products domain are directly responsible for the plateau in annual dose (controlled by ^{239}Pu and ^{237}Np) shown in Figure 7.7.1-39[a] of the TSPA-LA report (SNL 2008b). (See response to RAI 3.2.2.1.1-005, Section 1.3.2.2) For a second analyzed realization (Realization 191), the solubility limits and dissolved concentrations for Pu and U in the CSNF waste form domain over time are shown in Figure 7.7.1-51[a] of the TSPA-LA report (SNL 2008b) and described in Section 7.7.1.3[a] (SNL 2008b, pp. 7-59[a] and 7-60[a]). This outlier realization has the highest annual dose from about 50,000 years to about 300,000 years, and the dose is controlled by ^{239}Pu (SNL 2008b, Figure 7.7.1-49[a]). Figure 7.7.1-51[a] indicates that the Pu concentration in the CSNF waste form domain is solubility limited for the first 150,000 years. Therefore, the solubility limit is constraining the annual dose. It should also be noted that the mean annual dose plateaus at a higher value in this realization than in the first realization because the Pu solubility limit, which is determined from sampled parameters, is higher. (See response to RAI 3.2.2.1.1-005, Section 1.3.2.2)

Table 2.1-1 Expanded. Summary of the Capability of the ITWI Features / Components Supporting Each of the Three Barriers (Continued)

Barrier, Feature, and Relevant ITBC FEPs	Barrier Function and Qualitative Description of Barrier Functions [*] = *potential for decreased capability*	Safety Classification and Quantitative Evaluation of Barrier Capability
EBS Waste Form and Waste Package Internals – Naval SNF	**Prevents the release of or substantially reduces the release rate of radionuclides Prevents or substantially reduces the rate of movement of radionuclides**	**ITWI**
Waste Form Degradation see Waste Form Degradation FEPs listed under EBS – Waste Form and Waste Package Internals – CSNF above **Naval SNF Cladding** *(Included FEPs are described in SAR Table 2.3.7-1)* 2.1.02.25.0B – Naval SNF Cladding (*This ITBC FEP related to naval SNF cladding is assigned to the EBS - Cladding feature in Table A-2 of the PNSDB report (SNL 2008a) and SAR Table 2.1-3, but it specifically applies to the EBS – Waste Form and Waste Package Internals – Naval SNF component as noted in Table A-2 of the PNSDB report (SNL 2008a, p. A-107*).	**Naval SNF prevents the release of or substantially reduces the release rate of radionuclides and prevents or substantially reduces the rate of movement of radionuclides** (SAR Section 2.1.2.2, p. 2.1-40) (SAR Section 2.3.7.3, p. 2.3.7-13) The classified TSD (Section 2.3.7) describes the degradation mechanisms of naval SNF and develops a source term. The analyses reflect the structure of naval SNF, the slower dissolution of naval SNF, and smaller radionuclide inventories of naval SNF as compared to CSNF on a per waste package basis (SAR Section 2.4.2.3.2.2.4, pp. 2.4-230 to -232). That source term is used to demonstrate that naval waste packages and naval SNF can be represented by CSNF waste packages and CSNF (SAR Sections 2.1.2.2, p. 2.1-40 and 2.3.7.3, p. 2.3.7-13; SNL 2008a, Section 6.2.2.2, pp. 6-75 and 76). Naval SNF cladding is discussed in the classified TSD (Section 1.5.1.4.1.1).	**Reduced Radionuclide Releases** Refer to the classified TSD (Section 2.3.7). Naval waste packages and naval SNF are represented by CSNF waste packages and CSNF (SAR Sections 2.1.2.2, p. 2.1-40 and 2.3.7.3, p. 2.3.7-13; SNL 2008a, Section 6.2.2.2, pp. 6-75 and 76). Credit is taken for naval SNF cladding in the demonstration that naval SNF can be represented by CSNF (SAR Section 2.4.2.3.2.2.4). However, even when no credit is taken for cladding in the igneous scenario class, naval SNF can still be represented by CSNF (SAR Section 2.4.2.3.2.2.4).
EBS Waste Form and Waste Package Internals – DSNF	**None**	**Non-ITWI**
Waste Form Degradation *(Included FEPs are described in SAR Table 2.3.7-1)* 2.1.02.01.0A – DOE SNF degradation (alteration, dissolution, and radionuclide release)	The degradation of DSNF (except for naval SNF, which is modeled as CSNF) is modeled as degrading instantaneously upon waste package breach (SAR Section 2.3.7.8.1, p. 2.3.7-44). As a result, the DSNF waste form does not directly prevent or reduce radionuclide release or movement. As noted in SAR Section 2.1.2.2 (p. 2.1-43), and described in more detail in SAR Sections 2.3.7.5.1, 2.3.7.5.2, and 2.3.7.5.3, the degradation of DSNF also provides a source of schoepite, which tends to buffer the in-package pH in the near-neutral range. This pH control has an effect on in-package chemistry and therefore has an indirect effect on solubilities. As a result, FEP 2.1.02.01.0A (DOE SNF Degradation) is classified as ITBC (SAR Table 2.1-3, p. 2.1-129).	N/A

Table 2.1-1 Expanded. Summary of the Capability of the ITWI Features / Components Supporting Each of the Three Barriers (Continued)

Barrier, Feature, and Relevant ITBC FEPs	Barrier Function and Qualitative Description of Barrier Functions [*] = *potential for decreased capability*	Safety Classification and Quantitative Evaluation of Barrier Capability
EBS Cladding – CSNF / DSNF	**None**	**Non-ITWI**
No ITBC FEPs	There are a number of cladding FEPs, all of which are Non-ITBC (SNL 2008a, Table A-2, pp. A-93 to -109). The following justification is repeated in most of those FEPs: Cladding has some barrier capability and thus has core and control parameter characteristics that limit its degradation at high temperatures or from mechanical loads. However, the barrier capability of CSNF cladding is not important because cladding can be damaged by seismic activity that does not damage the waste package, and it is destroyed by igneous intrusion. Thus the only opportunity for CSNF cladding to support the barrier function is in the early failure scenario. In addition, except for naval SNF structure, no credit is taken for this capability in the postclosure technical basis.	N/A
EBS Waste Package Emplacement Pallet	**None**	**Non-ITWI**
1.2.03.02.0A – Seismic ground motion damages EBS components	The waste package pallet is not important to waste isolation. While intact, the waste package pallet precludes contact between the waste package and the invert and stabilizes the waste package during seismic events. The invert maintains the pallet, waste package, and drip shield in a nominally horizontal configuration (SNL 2008a, Section 6.2.2.2, p. 6-79). The presence of the pallet can delay diffusive releases of radionuclides from the waste package to the invert, as long as the cradles remain intact and can support the waste package above the invert. The EBS radionuclide transport abstraction model implemented in the TSPA ignores this beneficial characteristic of the pallet and conservatively assumes that the waste package is in direct contact with the invert (SNL 2008a, Section 6.2.2.2, p. 6-79). So, even though there is a relevant ITBC FEP, this component is Non-ITWI.	N/A
EBS Invert	**None**	**Non-ITWI**
No ITBC FEPs	The emplacement drift invert is not important to waste isolation. The invert maintains the pallet, waste package, and drip shield in a nominally horizontal configuration (SNL 2008a, Section 6.2.2.2, p. 6-79). The emplacement drift invert is composed of two parts: a steel invert structure and ballast (or crushed tuff). In the unsaturated repository environment, the crushed tuff in the invert sorbs radionuclides and slows the diffusive movement of radionuclides into the Lower Natural Barrier (SNL 2008a, Section 6.2.2.2, p. 6-79). The following justification is from Non-ITBC FEP 2.2.07.06.0B (Long-Term Release of Radionuclides from the Repository) (SNL 2008a, Table A-2, p. A-166): The release of radionuclides from the repository may occur over a long period of time, as a result of the timing and magnitude of the waste packages and drip shield failures, waste form degradation, and radionuclide transport through the invert. Releases from the waste package and engineered barrier system serve as a time-dependent boundary condition to the mountain-scale radionuclide transport model, regardless of when the release occurs, thus allowing for a general time-dependent radionuclide source term that accounts for long-term releases. As such, this FEP is not considered ITBC because the delay in the invert during the 10,000-year period for non-retarded radionuclides is not significant.	N/A

Table 2.1-1 Expanded. Summary of the Capability of the ITWI Features / Components Supporting Each of the Three Barriers (Continued)

Barrier, Feature, and Relevant ITBC FEPs	Barrier Function and Qualitative Description of Barrier Functions [*] = *potential for decreased capability*	Safety Classification and Quantitative Evaluation of Barrier Capability
LNB **Unsaturated Zone below the Repository**	**Prevents or substantially reduces the rate of movement of radionuclides**	**ITWI**
Advection *(Included FEPs are described in SAR Table 2.3.8-1)* 2.2.07.15.0B – Advection and dispersion in the UZ 2.2.07.02.0A – Unsaturated groundwater flow in the geosphere 2.2.07.08.0A – Fracture flow in the UZ 2.2.07.09.0A – Matrix imbibition in the UZ 1.2.02.01.0A – Fractures 1.2.02.02.0A – Faults 2.2.03.02.0A – Rock properties of host rock and other units 2.2.03.01.0A – Stratigraphy 2.2.07.07.0A – Perched water develops 1.3.01.00.0A – Climate change 1.4.01.01.0A – Climate modification increases recharge	**Slow Advection in unsaturated zone prevents or substantially reduces the rate of movement of radionuclides** (SAR Sections 2.1.2.3, p. 2.1-81; and 2.1.2.3.1, pp. 2.1-84 to -85) (SAR Sections 2.3.8.1, p. 2.3.8-2; and 2.3.8.5.2, p. 2.3.8-59) 1. Low percolation rates (arid climate, unsaturated) (SAR Section 2.1.2.3, pp. 2.1-79 and -80) 2. Large depth to water table (from about 200 to 400m) (SAR Section 2.1.1.3, p. 2.1-9) 3. Matrix flow in CHn vitric below southern half of repository (SAR Section 2.1.2.3.1, p. 2.1-84) 4. **[*]** Climate change increases advection and reduces depth to groundwater by as much as 120 m (SAR Section 2.1.2.3, p. 2.1-79, and Section 2.1.1.3, p. 2.1-9)	**Advection, Matrix Diffusion, and Sorption in Unsaturated Zone** (SAR Section 2.1.2.3.6, pp. 2.1-90 to -101) The response to RAI 3.2.2.1.1-007 (Tables 1-1 through 1-4) summarizes the effects of the unsaturated zone below the repository (UZ below) on barrier capability for the combined nominal/early-failure modeling case and for the seismic ground motion modeling case. These tables identify the relative contributions of the UZ below and the saturated zone to the total reduction of the peak mean activity provided by the LNB as whole (as described in SAR Section 2.1.2.3.6, pp. 2.1-92 to 2.1-101), for 12 key radionuclides. For the combined nominal/early-failure modeling case for 10,000 years (see response to RAI 3.2.2.1.1-007, Table 1-1), the relative contributions of the UZ below are as follows, for selected radionuclides: ^{99}Tc (~70%), ^{237}Np (~40%), ^{242}Pu (~50%), ^{239}Pu (~50%), and ^{240}Pu (~50%). For the combined nominal/early-failure modeling case for post-10,000 years (see response to RAI 3.2.2.1.1-007, Table 1-2), the relative contributions of the UZ below are as follows, for selected radionuclides: ^{99}Tc (~30%), ^{237}Np (~30%), ^{242}Pu (~40%), ^{239}Pu (~50%), and ^{240}Pu (~50%). For the seismic ground motion modeling case for 10,000 years (see response to RAI 3.2.2.1.1-007, Table 1-3), the relative contributions of the UZ below are as follows, for selected radionuclides: ^{99}Tc (~70%), ^{237}Np (~50%), ^{242}Pu (~50%), ^{239}Pu (~50%), and ^{240}Pu (~50%). For the seismic ground motion modeling case for post-10,000 years (see response to RAI 3.2.2.1.1-007, Table 1-4), the relative contributions of the UZ below are as follows, for selected radionuclides: ^{99}Tc (~30%), ^{237}Np (~20%), ^{242}Pu (~40%), ^{239}Pu (~50%), and ^{240}Pu (~50%). The response to RAI 3.2.2.1.1-006 (Tables 1-1 and 1-2) summarizes the relative contributions of advection, matrix diffusion, and sorption in the unsaturated zone below the repository (UZ below) to the barrier capability of the LNB. These tables qualitatively identify the relative contributions for the northern and southern areas of the site for 10,000 years and 1,000,000 years, for 6 key radionuclides. For the northern area for 10,000 years (see response to RAI 3.2.2.1.1-006, Table 1-1a), the relative importance of the various processes is as follows, for selected radionuclides: ^{99}Tc (advection = high, matrix diffusion = low, sorption = none), ^{237}Np (advection = high, matrix diffusion with sorption = low), and ^{240}Pu (advection = high, matrix diffusion with sorption = low to medium). For the northern area for 1,000,000 years (see response to RAI 3.2.2.1.1-006, Table 1-1b), the relative importance of the various processes for the selected radionuclides is the same as for 10,000 years. For the southern area for 10,000 years (see response to RAI 3.2.2.1.1-006, Table 1-2a), the relative importance of the various processes is as follows, for selected radionuclides: ^{99}Tc (advection = high, matrix diffusion = low, sorption = none), ^{237}Np (advection = high, matrix diffusion with sorption = medium), and ^{240}Pu (advection = high, matrix diffusion with sorption = high). For the southern area for 1,000,000 years (see response to RAI 3.2.2.1.1-006, Table 1-2b), the relative importance of the various processes for the selected radionuclides is the same as for 10,000 years, except for ^{237}Np, where matrix diffusion with sorption has changed to low importance).
Matrix Diffusion and Sorption *(Included FEPs are described in SAR Table 2.3.8-1)* 2.2.08.08.0B – Matrix diffusion in the UZ [2.2.03.02.0A – Rock properties of host rock and other units] [1.3.01.00.0A – Climate change] 2.2.08.09.0B – Sorption in the UZ	**Matrix diffusion and sorption in unsaturated zone prevents or substantially reduces the rate of movement of radionuclides** (SAR Sections 2.1.2.3, p. 2.1-81; and 2.1.2.3.1, pp. 2.1-84 to -85) (SAR Section 2.3.8.3.1, p. 2.3.8-18) 1. Matrix diffusion, primarily in TSw, delays transport (SAR Sections 2.1.2.3, p. 2.1-81; and 2.1.2.3.1, pp. 2.1-84 and -85) 2. **[*]** Climate change increases fracture flux and reduces effect of matrix diffusion (SAR Section 2.1.2.3, p. 2.1-79) 3. Sorption in matrix or associated with matrix diffusion delays transport (SAR Section 2.1.2.3.2, p. 2.1-86) 4. Significant sorption in CHn vitric matrix (SAR Section 2.1.2.3.1, p. 2.1-85)	

Table 2.1-1 Expanded. Summary of the Capability of the ITWI Features / Components Supporting Each of the Three Barriers (Continued)

Barrier, Feature, and Relevant ITBC FEPs	Barrier Function and Qualitative Description of Barrier Functions [*] = *potential for decreased capability*	Safety Classification and Quantitative Evaluation of Barrier Capability
LNB Saturated Zone	**Prevents or substantially reduces the rate of movement of radionuclides**	**ITWI**
Advection *(Included FEPs are described in SAR Table 2.3.9-1)* 2.2.07.15.0A – Advection and dispersion in the SZ 2.2.07.12.0A – Saturated groundwater flow in the geosphere 2.2.07.13.0A – Water- conducting features in the SZ 1.2.02.01.0A – Fractures 1.2.02.02.0A – Faults 2.2.03.02.0A – Rock properties of host rock and other units 2.2.03.01.0A – Stratigraphy 1.3.01.00.0A – Climate change 1.4.01.01.0A – Climate modification increases recharge	**Slow advection in saturated zone prevents or substantially reduces the rate of movement of radionuclides** (SAR Sections 2.1.2.3, p. 2.1-83; and 2.1.2.3.1, pp. 2.1-85 to -87) (SAR Section 2.3.9.3.3.1, p. 2.3.9-79) 1. Groundwater transport is faster in volcanics, slower in alluvium (SAR Section 2.3.9.2.1, p. 2.3.9-10) 2. Long transport distance (18 km) from the repository to the accessible environment (location of volcanic–alluvium contact is important) (SAR Section 2.1.1.3, p. 2.1-9 and SAR Section 2.1.2.3.2, p. 2.1-86) 3. **[*]** Climate change increases groundwater flow (SAR Section 2.1.2.1, p. 2.1-12)	**Advection, Matrix Diffusion, and Sorption in Saturated Zone** (SAR Section 2.1.2.3.6, pp. 2.1-90 to -101) The response to RAI 3.2.2.1.1-007 (Tables 1-1 through 1-4) summarizes the effects of the saturated zone on barrier capability for the combined nominal/early-failure modeling case and for the seismic ground motion modeling case. These tables identify the relative contributions of the saturated zone and the unsaturated zone below the repository (UZ below) to the total reduction of the peak mean activity provided by the LNB as whole (as described in SAR Section 2.1.2.3.6, pp. 2.1-92 to 2.1-101), for 12 key radionuclides. For the combined nominal/early-failure modeling case for 10,000 years (see response to RAI 3.2.2.1.1-007, Table 1-1), the relative contributions of the saturated zoneare as follows, for selected radionuclides: ^{99}Tc (~30%), ^{237}Np (~60%), ^{242}Pu (~50%), ^{239}Pu (~50%), and ^{240}Pu (~50%). For the combined nominal/early-failure modeling case for post-10,000 years (see response to RAI 3.2.2.1.1-007, Table 1-2), the relative contributions of the saturated zone are as follows, for selected radionuclides: ^{99}Tc (~70%), ^{237}Np (~70%), ^{242}Pu (~60%), ^{239}Pu (~50%), and ^{240}Pu (~50%). For the seismic ground motion modeling case for 10,000 years (see response to RAI 3.2.2.1.1-007, Table 1-3), the relative contributions of the saturated zone are as follows, for selected radionuclides: ^{99}Tc (~30%), ^{237}Np (~50%), ^{242}Pu (~50%), ^{239}Pu (~50%), and ^{240}Pu (~50%). For the seismic ground motion modeling case for post-10,000 years (see response to RAI 3.2.2.1.1-007, Table 1-4), the relative contributions of the saturated zone are as follows, for selected radionuclides: ^{99}Tc (~70%), ^{237}Np (~80%), ^{242}Pu (~60%), ^{239}Pu (~50%), and ^{240}Pu (~50%).
Matrix Diffusion and Sorption *(Included FEPs are described in SAR Table 2.3.9-1)* 2.2.08.08.0A – Matrix diffusion in the SZ [2.2.03.02.0A – Rock properties of host rock and other units] 2.2.08.09.0A – Sorption in the SZ	**Matrix diffusion and sorption in saturated zone prevents or substantially reduces the rate of movement of radionuclides** (SAR Sections 2.1.2.3, p. 2.1-83; and 2.1.2.3.1, pp. 2.1-85 to -87) (SAR Section 2.3.9.3.3.1, p. 2.3.9-79) 1. Matrix diffusion in volcanics delays transport 2. No matrix diffusion in alluvium (porous medium) (SAR Section 2.1.2.3.2, p. 2.1-86) 3. Sorption associated with matrix diffusion in volcanics delays transport 4. Enhanced sorption in alluvium (location of volcanic–alluvium contact is important)	The response to RAI 3.2.2.1.1-006 (Tables 1-3 through 1-4) summarizes the relative contributions of advection, matrix diffusion and sorption in the saturated zone to the barrier capability of the LNB. These tables qualitatively identify the relative contributions for the volcanic tuff and alluvium for 10,000 years and 1,000,000 years, for 6 key radionuclides. For the volcanic tuff for 10,000 years (see response to RAI 3.2.2.1.1-006, Table 1-3a), the relative importance of the various processes is as follows, for selected radionuclides: ^{99}Tc (advection = high, matrix diffusion = low, sorption = none), ^{237}Np (advection = high, matrix diffusion with sorption = medium), and ^{240}Pu (advection = high, matrix diffusion with sorption = high). For the volcanic tuff for 1,000,000 years (see response to RAI 3.2.2.1.1-006, Table 1-3b), the relative importance of the various processes for the selected radionuclides is the same as for 10,000 years, except for ^{237}Np, where matrix diffusion with sorption has changed to low importance). For the alluvium for 10,000 years (see response to RAI 3.2.2.1.1-006, Table 1-4a), the relative importance of the various processes is as follows, for selected radionuclides: ^{99}Tc (advection = high, matrix diffusion = low, sorption = none), ^{237}Np (advection = high, matrix diffusion with sorption = medium), and ^{240}Pu (advection = high, matrix diffusion with sorption = high). For the alluvium for 1,000,000 years (see response to RAI 3.2.2.1.1-006, Table 1-4b), the relative importance of the various processes for the selected radionuclides is the same as for 10,000 years, except for ^{237}Np, where matrix diffusion with sorption has changed to low importance).

NOTE: Square brackets [ ] in this column indicate FEPs that are associated with more than one process under a single feature or component.

NOTE: References are listed in the response to RAI 3.2.2.1.1-001 (Section 4).

RAI: Volume 3, Chapter 2.2.1.1, First Set, Number 2

Address the effects of damping episodic infiltration pulses within the Paintbrush Tuff and the impact of this damping on the capability of the unsaturated zone above the repository (upper natural barrier) to prevent, or substantially reduce, seepage into the drift.

Basis: Needed for demonstration of compliance with 10 CFR 63.115 (b) and (c). Although there is a discussion of how the episodic infiltration pulses are damped by the Paintbrush Tuff unit, there is no clear description of how this damping affects the barrier capability to prevent or substantially reduce seepage into the drift.

1. RESPONSE

The damping of episodic infiltration is shown in this response to significantly reduce the amount of water expected to enter emplacement drifts.

1.1 Effects of the Paintbrush Nonwelded (PTn) Hydrogeologic Unit on Episodic Flow in the Unsaturated Zone

The net infiltration at the bedrock surface (on top of the Tiva Canyon Welded (TCw) hydrogeologic unit) is conceptualized as episodic, with significant pulses occurring only once every few years (SNL 2008a, Section 6.5.7.5). Spatially and temporally variable pulses of moisture percolate rapidly through the highly fractured tuffs of the TCw. However, at the TCw-PTn interface—where welded tuffs grade sharply into nonwelded tuffs—flow behavior changes from fracture dominated to matrix dominated flow. The highly porous PTn unit attenuates the episodic infiltration flux significantly such that the net episodic percolation flux arriving at the top of the PTn, once crossing the PTn, turns into a percolation flux below the PTn that can be approximated as steady-state (SNL 2007a, Section 6.2.2). Within the repository area, the thickness of the PTn unit ranges from approximately 21 m (70 ft) to over 120 m (400 ft) (SNL 2008b, FEP 2.2.07.05.0A).

The evidence for damping of episodic flow, summarized in SAR Section 2.1.2.1.2, is discussed in more detail in SAR Section 2.3.2.4.2.1.2, in *UZ Flow Models and Submodels* (SNL 2007a, Section 6.9), and in *Features, Events, and Processes for the Total System Performance Assessment: Analyses* (SNL 2008b, FEP 2.2.07.05.0A). This evidence includes 1-D, 2-D, and 3-D modeling results and field test observations from the Exploratory Studies Facility (ESF). The modeling studies considered a wide range of flux boundary conditions and differing PTn thicknesses. These investigations found that matrix imbibition of episodic transient flows in the PTn resulted in substantial damping of the transient flow behavior for all conditions investigated, including future climate conditions. The damping results in approximately steady-flow conditions below the PTn. To demonstrate the importance of flow damping in the PTn on seepage in the following sections, seepage rates from steady-flow conditions below the PTn are compared with the seepage rates expected for flow conditions below the PTn if episodic flow were to penetrate to the repository level.

1.2 Comparison of Seepage into Drifts for Episodic and Steady-Flow Conditions

The damping of episodic flow results in a significant reduction in the mean seepage rate into waste emplacement drifts. Seepage rates into drifts are affected by the percolation flux field (SAR Section 2.3.3.2.1.2). Because episodic flows have been shown to be effectively damped to nearly steady-flow behavior in the PTn hydrogeologic unit above the repository (SAR Sections 2.3.2.4.2.1.2 and 2.2), analyses of seepage into waste emplacement drifts under episodic flow conditions have not been conducted. However, the analysis of seepage has been conducted for a wide range of steady percolation fluxes (SAR Section 2.3.3.4.2).

If seepage into drifts under episodic percolation flux conditions is treated as a quasi-steady process, the variation in seepage behavior for different steady percolation fluxes may be used to evaluate the effects of damping episodic percolation pulses. This is done in this RAI response by comparing the in-drift seepage rates for episodic percolation fluxes with the seepage rates for the equivalent steady percolation fluxes. The "equivalent steady percolation flux" is defined as the time-weighted average of the series of spatially averaged percolation fluxes defining the episodic flow process. This averaging method is used so that, over the averaging time period, the same volume of water passes through a given surface (such as the repository) for the episodic and steady-flow processes. For example, a one-month, spatially averaged, episodic percolation event followed by 11 months of no percolation is averaged to an equivalent, spatially averaged, steady percolation flux that is one-twelfth of the spatially averaged percolation flux that occurred during the event. Similarly, the time-averaged mean seepage rate for the transient process would be one-twelfth of the mean seepage rate that occurred during the transient event. It is shown in this RAI response that the mean seepage rate for the equivalent steady percolation flux is less than the time-averaged mean seepage rate for the transient process. In this response, only the spatially averaged percolation flux over the repository footprint will be discussed. (For brevity, the "spatially averaged percolation flux" will be termed simply the "percolation flux.")

The mean seepage rate as computed in the seepage abstraction model is the total amount of water entering drifts divided by the total number of waste packages (SNL 2007b, Section 6.8). Therefore, changes in the mean seepage rate as a function of percolation flux account for changes in incidents of seepage (seepage fraction) as well as the rate of flow into waste emplacement drifts with seepage. (For brevity, the "mean seepage rate" will be termed simply the "seepage rate.") Because the total number of waste packages is constant, only the seepage rate per waste package needs to be considered as a function of percolation flux. The relationship between the seepage rate and percolation flux is shown in Figure 1-1. The model points (solid squares on Figure 1-1) have been fit using an empirical function (green line on Figure 1-1) that is constrained to be zero for a percolation flux less than 1 mm/yr and is asymptotically proportional to the percolation flux for large values. The seepage rate curve fit is given by:

$$S_{rm} = H(P_a - 1)\left[0.2\exp(-0.003P_a)(P_a - 1)^{1.69} + 28.05\{1 - \exp(-0.001P_a)\}P_a\right]$$

where S_{rm} is the seepage rate in kg/yr/WP, P_a is the percolation flux in mm/yr, and H is a step function which equals 1 for $P_a - 1 \geq 0$ and 0 otherwise. The model points and curve fit show that the seepage rate curve is strictly convex over the range of percolation fluxes displayed in

Figure 1-1. The asymptotic linear behavior of the seepage rate curve occurs at percolation rates in excess of 100 mm/yr.

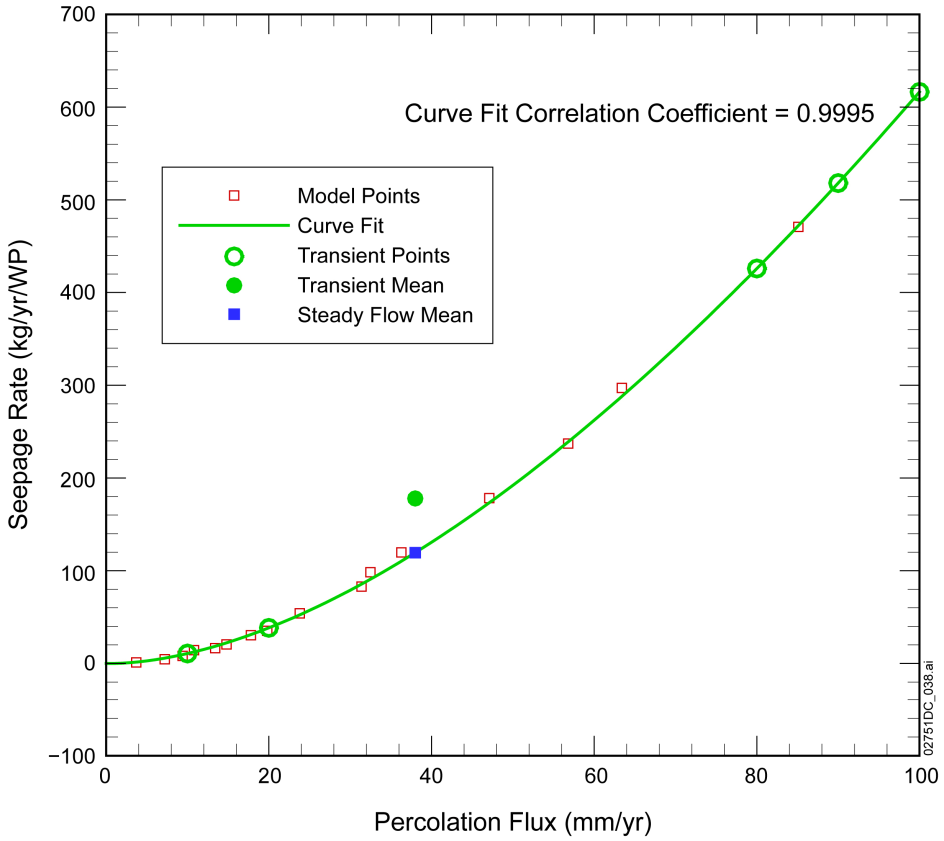

NOTE: Model points from Tables 6-5[a] and 6-6[a] of *Abstraction of Drift Seepage* (SNL 2007b).

Figure 1-1. Seepage Rate as a Function of Percolation Flux

Consider a transient percolation process defined by a series of steady percolation flux conditions over time. The seepage rate for each steady percolation flux condition is plotted on the seepage rate curve, shown as open circles in Figure 1-1. The seepage rate for the equivalent steady percolation flux is shown as the filled square in Figure 1-1.

Because the seepage rate curve is convex, the seepage rate for the equivalent steady percolation flux is always less than the time-weighted average of the transient seepage rates (filled circle in Figure 1-1). This leads to the conclusion that the damping of transient flow by the PTn will always lead to a reduction of water flowing into the drifts.

The seepage rate curve is expected to be linear rather than convex for sufficiently high percolation fluxes. Although the precise level of percolation flux needed to reach this linear regime is not known, it is apparently greater than 100 mm/yr. If all fluxes for the episodic transient process are sufficiently high to be in the linear range of the seepage rate curve, then the time-weighted average seepage into the drifts for the transient process would be equal to the seepage into the drifts for the equivalent steady percolation flux. However, this condition is not

expected because this would require that the time-weighted average percolation flux exceeds 100 mm/yr. The percolation flux is expected to remain at or below 100 mm/yr (SNL 2007b, Table 6-5[a]; NRC 2008). Therefore, the time-weighted average seepage rate into drifts for a transient flow process is expected to be larger than the seepage rate for the equivalent steady percolation flux.

1.3 Example of a Bimodal Transient

An example is shown in Figure 1-2 for a transient process defined by two percolation fluxes, 20 and 80 mm/yr. The seepage rates at these percolation fluxes are identified at points A and B on Figure 1-2. For this example, a time-weighting of 70% and 30% is used for 20 mm/yr and 80 mm/yr, respectively. This leads to a time-weighted average percolation flux of 38 mm/yr, the percolation flux at points C and D in Figure 1-2. The seepage rate for the equivalent steady percolation flux (point D) is about 120 kg/yr/WP. The bimodal transient flow process has a time-weighted average seepage rate (point C) of about 155 kg/yr/WP, which is the time-weighted average of points A and B. Due to the convexity of the seepage curve, point C is always higher than point D, demonstrating the barrier effect attributable to the damping of episodic flow occurring in the PTn.

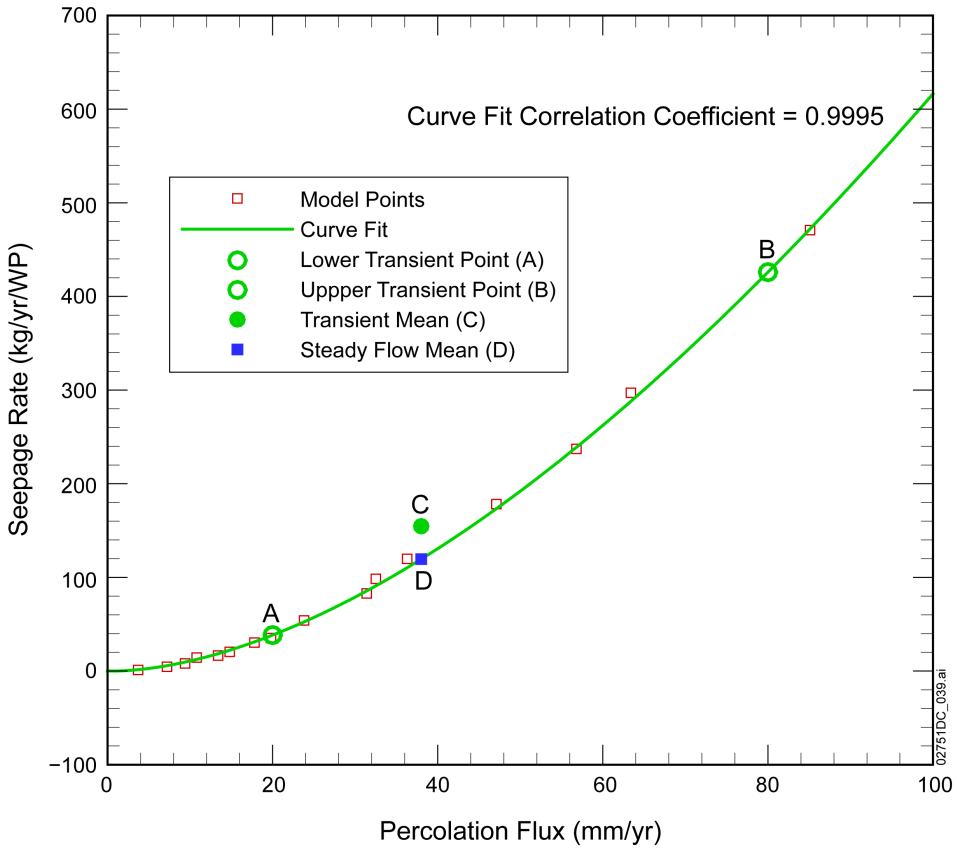

NOTE: Model points from Tables 6-5[a] and 6-6[a] of *Abstraction of Drift Seepage* (SNL 2007b).

Figure 1-2. Example Using a Bimodal Transient

1.4 Episodic Transient Infiltration at Yucca Mountain

The episodic nature of infiltration is more extreme at Yucca Mountain than in the example just presented. Infiltration generally occurs for only a few days per year, with the remainder of the year having zero infiltration (SNL 2008a, Figure 6.5.7.7-6[a]). Precipitation events generally occur 30 to 40 days per year for present-day climate (BSC 2004, Table 6-15). Because some rainfall events are not sufficient to generate infiltration, the number of infiltration days may be less than the number of precipitation days (SNL 2008a, Figures 6.5.7.7-1[a] and 6.5.7.7-6[a]). On the other hand, there may be a slow release from the soil to the bedrock following a precipitation event extending the number of days of infiltration as compared with precipitation. Also, future climates are expected to have more precipitation days per year than the present-day climate.

To evaluate the approximate magnitude of the difference in seepage rate for steady-flow conditions as compared with undamped transient flow, an infiltration rate ranging from 5 mm/yr to 100 mm/yr is uniformly allocated to time periods ranging from 0.2 to 120 days per year. The 0.2 day episodic case is equivalent to an episodic period of one full day every 5 years. The remainder of the year has zero infiltration. The infiltration range roughly corresponds to the range of percolation fluxes expected at the repository for present-day conditions through the post-10,000 year period (SNL 2007b, Table 6-5[a]; NRC 2008). The resulting transient (bimodal) percolation over the repository footprint is assumed to be entirely undamped, and represents the transient percolation flux arriving at the repository. Table 1-1 presents the time-weighted average of the transient seepage rates and the seepage rates for the equivalent steady percolation flux. For example, if an equivalent percolation flux of 100 mm/yr occurred over 20 days, the drift seepage with no damping would amount to 2368 kg/yr/WP, as compared to 616 kg/yr/WP for a steady-flow percolation flux of 100 mm/yr. The time-weighted averages of the transient seepage rates are larger than the seepage rates for the equivalent steady percolation fluxes for all cases. The higher infiltration cases for episodic periods of 0.2 days and 1 day show that the seepage rate has approximately reached the maximum level, i.e., that the seepage rate is equal to percolation flux.

The barrier capability attributed to the damping of episodic flow is related to the difference of the time-weighted average transient seepage rate with the seepage rate for the equivalent steady percolation flux. These differences are shown in Table 1-2. The differences in seepage rates increase as the duration of the episodic event decreases, holding the equivalent steady percolation flux constant, and as the equivalent steady percolation flux increases, holding the duration of the episodic event constant. Note that this analysis uses hypothetical transient conditions and assumes that the PTn does not damp episodic flow; this assumption is applied solely for the purposes of assessing the barrier capability associated with damping of episodic flow. This analysis shows that the amount of water expected to enter waste emplacement drifts is significantly reduced by the damping of episodic flow in the PTn. Therefore, the damping of episodic flow by the PTn is a characteristic that is consistent with the definition of a barrier in 10 CFR 63.2.

Table 1-1. Seepage Rates: Time-Weighted Average Seepage Rates for Bimodal Transient Processes (light blue shading – kg/yr/WP), and Seepage Rates for an Equivalent Steady Percolation Flux (light yellow shading – kg/yr/WP)

	Days of Infiltration/Percolation per Year (episodic flow)						
Equivalent Steady Percolation Flux (mm/yr)	**0.2**	**1**	**5**	**20**	**60**	**120**	**Steady Flow**
5	140	118	62.4	29.0	13.3	7.69	2.75
10	280	273	166	88.4	44.1	26.6	10.7
20	561	561	438	250	139	88.3	38.4
40	1,122	1,122	1,062	666	412	279	131
60	1,683	1,683	1,662	1,176	749	531	262
80	2,244	2,244	2,237	1,753	1,129	824	426
100	2,805	2,805	2,803	2,368	1,546	1,148	616

Table 1-2. Differences in Seepage Rates: Differences between Time-Weighted Average Seepage Rates for Bimodal Transient Process, and Seepage Rates for an Equivalent Steady Percolation Flux (light green shading) (kg/yr/WP)

	Days of Infiltration/Percolation per Year (episodic flow)					
Equivalent Steady Percolation Flux (mm/yr)	**0.2**	**1**	**5**	**20**	**60**	**120**
5	137	116	60	26	11	5
10	270	263	155	78	33	16
20	523	522	400	212	101	50
40	991	991	931	535	281	148
60	1421	1421	1400	914	487	269
80	1818	1818	1811	1327	703	398
100	2189	2189	2187	1752	930	532

Although the damping of episodic flow by the PTn is a barrier capability, FEP 2.2.07.05.0A (Flow in the UZ from Episodic Infiltration) has been identified in *Postclosure Nuclear Safety Design Bases* (SNL 2008c, Table A-1) as not important to barrier capability. This is because FEP 2.2.07.05.0A concerns the existence of episodic flow in the unsaturated zone, which is not important because episodic flow is substantially damped below the PTn. The FEPs that are related to episodic flow damping characteristics of the PTn are FEPs 2.2.03.01.0A (Stratigraphy) and 2.2.03.02.0A (Rock Properties of Host Rock and Other Units). These FEPs are identified in *Postclosure Nuclear Safety Design Bases* (SNL 2008c, Table 7-2) as important to barrier capability because these are the characteristics responsible for damping of episodic flow.

2. COMMITMENTS TO NRC

None

3. DESCRIPTION OF PROPOSED LA CHANGE

None

4. REFERENCES

BSC (Bechtel SAIC Company) 2004. *Yucca Mountain Site Description.* TDR-CRW-GS-000001 REV 02 ICN 01. Two volumes. Las Vegas, Nevada: Bechtel SAIC Company. ACC: DOC.20040504.0008; LLR.20080423.0019; DOC.20080707.0002.

NRC (Nuclear Regulatory Commission) 2008. "Final Rule: 10 CFR Part 63, 'Implementation of a Dose Standard after 10,000 Years'", SECY-08-0170. Washington, D.C.: U.S. Nuclear Regulatory Commission.

SNL (Sandia National Laboratories) 2007a. *UZ Flow Models and Submodels.* MDL-NBS-HS-000006 REV 03 AD 01. Las Vegas, Nevada: Sandia National Laboratories. ACC: DOC.20080108.0003; DOC.20080114.0001; LLR.20080414.0007; LLR.20080414.0033; LLR.20080522.0086.

SNL 2007b. *Abstraction of Drift Seepage.* MDL-NBS-HS-000019 REV 01 ADD 01. Las Vegas, Nevada: Sandia National Laboratories. ACC: DOC.20070807.0001; DOC.20080813.0004; DOC.20081118.0049.

SNL 2008a. *Simulation of Net Infiltration for Present-Day and Potential Future Climates.* MDL-NBS-HS-000023 REV 01 AD 01. Las Vegas, Nevada: Sandia National Laboratories. ACC: DOC.20080201.0002; LLR.20080507.0008; LLR.20080522.0101.

SNL 2008b. *Features, Events, and Processes for the Total System Performance Assessment: Analyses.* ANL-WIS-MD-000027 REV 00. Las Vegas, Nevada: Sandia National Laboratories. ACC: DOC.20080307.0003; DOC.20080407.0009; DOC.20080722.0002.

SNL 2008c. *Postclosure Nuclear Safety Design Bases.* ANL-WIS-MD-000024 REV 01. Las Vegas, Nevada: Sandia National Laboratories. ACC: DOC.20080226.0002; DOC.20080314.0004; LLR.20080507.0018; DOC.20080610.0007.

RAI: Volume 3, Chapter 2.2.1.1, First Set, Number 3:

Identify and describe the barrier capability of the emplacement drift. Describe the capability of the emplacement drift, including uncertainties, consistent with the quantitative analyses in the total system performance assessment (e.g., sensitivity and uncertainty analyses or intermediate results). Provide information on the time period over which the emplacement drift performs its intended function.

Basis: Needed for demonstration of compliance with 10 CFR 63.115 (b) and (c). Although the emplacement drift is identified as important to waste isolation in Table 2.1-1, there does not appear to be any specific discussion of the barrier capability of the emplacement drift in SAR Section 2.1.2.2.1 or 2.1.2.2.2, nor any quantitative supplementation in SAR Section 2.1.2.2.6. Because the capabilities of the emplacement drift are not clearly identified, there does not appear to be any specific discussion of the time over which the emplacement drift performs its function or of the uncertainty in the capabilities of the emplacement drift, nor is it possible to determine whether any capability is consistent with the performance assessment.

There does not appear to be a clear connection between the processes and characteristics affecting the emplacement drift identified in SAR Section 2.1.2.2 and the specific components that contribute to these processes. It is therefore not clear that the barrier capabilities implied by the discussion of these processes are consistent with the safety classification provided in Table 2.1-1. For example, there is no clear explanation of why some components of the emplacement drift identified in Table 2.1-1 are considered to be important to waste isolation and some are not. Although Table 2.1-1 indicates that the emplacement drift is important to waste isolation by virtue of its ability to prevent or substantially reduce the rate of movement of water and radionuclides, there is no clear discussion of how this capability is achieved. Furthermore, the non-emplacement openings, closure, ground support, and ventilation systems are determined to be not important to waste isolation in Table 2.1-1, but there is no clear discussion of why these components do not contribute to the barrier capability of the emplacement drift.

1. RESPONSE

As stated in SAR Table 2.1-1, the emplacement drift contributes to Engineered Barrier System (EBS) barrier capability by (1) preventing or substantially reducing the rate of movement of water to the waste form, and (2) by preventing or substantially reducing the rate of movement of radionuclides from the waste form, as described below.

- Preventing or substantially reducing with the rate of movement of water to the waste form includes seepage diversion by capillary and thermal processes, changes in flow of seepage into or within the EBS resulting from seismically induced drift degradation, unsaturated flow in the EBS, and drift wall condensation.

- Preventing or substantially reducing the rate of movement of radionuclides includes the effects of temperature and water chemistry in the drifts on corrosion of EBS components, the thermal-hydrologic environment for onset of waste form degradation and transport, and the effect of water chemistry on radionuclide transport.

As noted in the following discussion, the barrier capability of the drift with to respect to seepage is largely shared with the Upper Natural Barrier (SAR Section 2.1.2.1). Much of the information required for this response, including quantification of barrier capability, uncertainties in that capability, and the time over which the drift performs its barrier function, is provided in SAR Section 2.1.2.1.

The associated features, events, and processes (FEPs) with important to barrier capability (ITBC) characteristics are identified in the sections below. Many of the core characteristics and control parameter characteristics associated with these FEPs (SNL 2008a, Table A-2) are discussed using available quantitative information on the performance of the emplacement drift and its uncertainties.

1.1 Preventing or Reducing Water Movement to Waste Forms

The emplacement drift contributes to reducing contact of seepage with the waste form in two ways. First, the emplacement drift opening acts in conjunction with the unsaturated zone (Upper Natural Barrier) to limit seepage into the drift. Second, the mechanical integrity of the drift opening affects the function and lifetimes of other EBS components (the drip shield and waste package) which also divert water from the waste form.

Seepage Diversion by Capillary and Thermal Processes

Seepage into drifts is governed by processes that take place at the interface between the Upper Natural Barrier (UNB) and the EBS. The emplacement drift openings are zero-capillarity features embedded in the unsaturated zone; therefore, the drift openings are capillary barriers that have the capability to prevent or substantially reduce seepage. While features of both the UNB and the EBS define the seepage diversion capability, a detailed description of this capability is found in SAR Section 2.1.2.1, pertaining to the UNB, rather than in SAR Section 2.1.2.2, pertaining to the EBS. However, this description applies to both the unsaturated zone and emplacement drift aspects of seepage diversion capability.

As explained in SAR Section 2.1.2.1.2,

> …seepage into the emplacement drifts is less than the percolation flux because capillary forces limit the movement of water into the drift openings. … The effectiveness of capillary forces in limiting water movement into drifts and moving flow around them depends on the characteristics of the rock matrix and fractures, and on the connectivity and permeability of the fracture network. In addition, seepage rates are affected by the characteristics of the drift openings (e.g., asperities on the drift walls, and flow in fractures that may have modified hydrologic properties in the disturbed zone created by drift excavation or heat from emplacement waste). For a period of time, the decay heat of

> the emplaced waste is great enough to heat the rock near the emplacement drifts above boiling. As long as the temperature is above the boiling point of water at the drift wall, the water vapor will be driven away from the emplacement drift wall surfaces. This thermal effect, combined with the capillary effects, further prevents or substantially reduces seepage into the emplacement drifts.

In the ITBC analysis (SNL 2008a, Table A-2), the emplacement drift characteristics that influence capillary diversion of seepage are associated with included FEP 2.1.08.07.0A (Unsaturated Flow in the EBS). Characteristics that influence thermal seepage response have been allocated to included FEP 2.1.11.01.0A (Heat Generation in the EBS), because it deals specifically with how drift wall temperatures constrain the timing of seepage. The related included FEPs 2.1.11.09.0A (Thermal Effects on Flow in the EBS) and 2.1.08.03.0A (Repository Dry-out due to Waste Heat) were not determined to be important to barrier capability because the relevant aspects of the thermal barrier are captured in FEP 2.1.11.01.0A. The excluded FEP 2.2.10.01.0A (Repository-Induced Thermal Effects on Flow in the UZ) was also determined not to be important because it specifically addresses large-scale flow patterns in the unsaturated zone, and does not consider thermal effects on seepage into the drift. Further information on barrier capability with respect to seepage is given in SAR Sections 2.1.2.1.4 (uncertainties), 2.1.2.1.5 (impact of disruptive events), and 2.1.2.1.6 (quantification of barrier capability).

Changes in EBS Flow Resulting from Seismically-Induced Drift Degradation

SAR Section 2.1.2.1.3 discusses long-term changes in the barrier capability with respect to seepage:

> Drift collapse can lead to seepage behavior that is much different from that in intact drifts ([SAR] Section 2.3.3.4). The larger size and possibly different shape of a collapsed drift tends to reduce the potential for flow diversion. In addition, the capillary barrier behavior at the drift wall can be affected by the rubble rock blocks filling the opening, as the capillary strength inside the opening is different from the zero-capillary-strength condition in the initially open drift ([SAR] Section 2.3.3.2.1.4). In the case of full drift collapse in the lithophysal unit, when the original openings have filled with rubble rock material, capillary effects are still expected to cause some flow diversion at the interface between the solid rock and the rubble-filled drift. In the nonlithophysal units, partial drift collapse can result in the loss of capillary diversion. These effects are included in the drift seepage model ([SAR] Section 2.3.3.2.3.4.2).

The partial collapse abstraction for seepage in lithophysal host rock (SAR Sections 2.3.4.5.6.1 and 2.4.2.3.2.1.3) interpolates linearly between the uncollapsed and fully collapsed seepage models, using the accumulated rubble volume interpolated between 5 and 60 m^3/meter of drift. This approach thus represents the change in span of the drift opening during collapse, and simulations have shown that the span reaches its maximum value when approximately 60 m^3/meter of rubble have accumulated. The lower limit of rubble volume represents the stage of collapse at which the increase in span begins to affect seepage. For non-lithophysal rock, a threshold change is implemented when rubble volume accumulates to 0.5 m^3/meter, whereby the

seepage percentage is set to unity—the seepage rate is set equal to the percolation flux (SAR Section 2.4.2.3.2.1.3).

For the abstraction of seismically induced mechanical damage to the waste package and drip shield, the extent of drift collapse is represented by a percentage, calculated from the ratio of accumulated rubble volume, to the epistemic parameter representing the rubble volume for complete collapse (e.g., 30 to 120 m^3/meter of drift; SAR Section 2.3.4.4.8.3.1). This percentage therefore represents the expended portion of the emplacement drift lifetime. For perspective on the timing of drift collapse, estimates are provided for the seismic ground motion case of TSPA (SAR Figure 2.1-14). For these 300 realizations, the earliest complete drift collapse is predicted to occur between 300,000 and 400,000 years. From SAR Figure 2.1-14, the mean time until full collapse in the context of seepage (60 m^3/meter rubble volume) is more than 150,000 years. From SAR Figures 2.3.4-48 and -50, the rubble volume associated with individual seismic events in the non-lithophysal tuff is a smaller fraction of complete collapse as defined for seepage (0.5 m^3/meter) than for the same seismic event in the lithophysal tuff. Thus, the mean time before complete collapse in the context of seepage is greater in the non-lithophysal tuff than in the lithophysal tuff.

As noted above, thermal processes in the host rock near the emplacement drift opening produce a vaporization barrier effect, which acts in addition to capillary diversion, when the temperature of rock at the drift wall is at or above boiling (SAR Section 2.3.3.3.3). In the event of drift collapse during the thermal period, which is unlikely (SAR Section 2.4.2.3.2.1.12.3, p. 2.4-203), vaporization is not effective because temperatures in the intact rock around collapsed openings will not often reach boiling conditions (SAR Section 2.3.3.3.4).

Rubble from drift degradation may accumulate in either lithology due to successive seismic ground motion events, but rubble will accumulate much faster in the lithophysal tuff, given the same exposure to seismic shaking (compare SAR Figures 2.3.4-48 and -50). The emplacement drift opening lifetime will therefore be much greater in the non-lithophysal host rock. Even in the lithophysal tuff, the effects from seismically induced collapse in the first 10,000 years are negligible with respect to seismic damage to the EBS (SAR Section 2.4.2.3.2.1.12.3). Drift collapse rubble contributes to the barrier capability of the EBS with respect to the seismic response by constraining the motions of the drip shield and waste package (and thereby decreasing impact velocities), and by dead-loading the drip shield or waste package, thus increasing dynamic loads in the drip shield crown and sidewalls (SAR Sections 2.3.4.5.3 and 2.3.4.5.4).

In the ITBC analysis (SNL 2008a, Table A-2), the emplacement drift characteristics that influence seepage response in degraded drifts are principally associated with included FEPs 1.2.03.02.0C (Seismic Induced Drift Collapse Damages EBS Components) and 1.2.03.02.0D (Seismic-Induced Drift Collapse Alters In-Drift Thermal-Hydrology). Emplacement drift characteristics that influence mechanical damage to the drip shield and waste package are associated with included FEPs 1.2.03.02.0A (Seismic Ground Motion Damages EBS Components) and 1.2.03.02.0C (Seismic Induced Drift Collapse Damages EBS Components). Emplacement drift characteristics associated with resistance of the drip shield and waste package to seismically induced rockfall damage in the non-lithophysal tuff (rubble block size in the

lithophysal tuff is too small to produce significant damage) are associated with excluded FEP 1.2.03.02.0B (Seismic Induced Rockfall Damages EBS Components). Further information on barrier capability with respect to seepage is given in SAR Sections 2.1.2.1.4 (uncertainties), 2.1.2.1.5 (impact of disruptive events), and 2.1.2.1.6 (quantification of barrier capability). Further information on barrier capability with respect to mechanical damage to EBS components is given in SAR Sections 2.1.2.2.4 (uncertainties), 2.1.2.2.5 (impact of disruptive events), and 2.1.2.2.6 (quantification of barrier capability).

Unsaturated Flow in the EBS

As stated in SAR Section 2.1.2.2, the emplacement drifts are located above the water table and saturated zone. They are expected to remain above the water table in the future (SAR Section 2.3.8.5.3). Therefore, the EBS will remain unsaturated (SNL 2008c, excluded FEP 2.1.08.09.0A (Saturated Flow in the EBS)), thus reducing the effective diffusivity and mobility of radionuclides in a breached waste package and in the invert. The unsaturated environment also means that natural water flow, represented by seepage, will flow downward and will not interact directly with the waste package or waste form, under intact drip shields (SAR Section 2.3.7.12.1). In the ITBC analysis (SNL 2008a, Table A-2), the emplacement drift characteristics that influence unsaturated flow in the EBS are associated with included FEP 2.1.08.07.0A (Unsaturated Flow in the EBS).

Drift Wall Condensation

The in-drift condensation model (SNL 2007a, Section 6.3) was used to estimate the hydrologic effects from axial transport of water vapor and condensation at cooler locations for use as input to the TSPA model (SAR Section 2.3.5.4.2). The in-drift condensation model describes drift wall condensation at discrete waste package locations at successive stages in the repository thermal evolution. Estimates of the drift wall condensation rate are correlated with the rate of percolation in the host rock (SNL 2007a, Section 1). Additional model uncertainties implemented by TSPA are the extent of gas mixing above and below the drip shield and the magnitude of axial transport (SAR Section 2.3.5.4.2.3).

The total volume of seepage into the heated portions of the drifts will be reduced by evaporation, axial transport of water vapor, and condensation at the unheated drift ends (SAR Section 2.3.5.4.1.3.3). However, in TSPA calculations, seepage flux out of the drift at a given waste package location is conservatively assumed to be equivalent to the seepage flux into the drift, plus condensation if it is predicted to occur—no credit is taken for the net evaporative volume reduction of seepage in the heated drift (SNL 2008b, Section 6.3.8.4). If complete drift collapse is realized in TSPA prior to 10,000 years, which is unlikely as discussed above, drift wall condensation ceases (SNL 2008b, Section 6.1.4.12.3).

In the ITBC analysis (SNL 2008a, Table A-2), the emplacement drift characteristics that influence drift wall condensation are principally associated with included FEP 2.1.08.04.0A (Condensation Forms on Roofs of Drifts (drift-scale cold traps)), which, for the reasons described above, has been determined not to be important to barrier capability. Emplacement drift characteristics that influence condensation in collapsed drifts are associated with included

FEP 1.2.03.02.0D (Seismic Induced Drift Collapse Alters In-Drift Thermal-Hydrology), which has been determined to be important to barrier capability. However, the ITBC designation is related to the effects of drift collapse on seepage, not the effects on condensation.

Maximum Allowable Waste Package Temperature Limits

The following information describes some additional contributions from emplacement drift integrity to EBS seepage diversion performance, which are associated with excluded FEPs and are not explicitly identified with EBS barrier capability in SAR Section 2.1.2.2. The integrity of the drift during the first few hundred years of the thermal period contributes to the performance of certain EBS components that can be degraded if maximum temperature limits are exceeded. For example, postclosure temperature limits (SAR Table 1.3.1-2) for the waste package outer surface are 300°C for 500 years, followed by 200°C for 9,500 years (SNL 2008c, FEP 2.1.11.06.0A; SAR Table 2.2-3, Control Parameter 06-03). The waste package surface temperature limit will prevent significant degradation of Alloy 22 from phase changes (SAR Table 2.2-5, FEP 2.1.11.06.0A, Thermal Sensitization of Waste Packages). If full drift collapse occurs within the first 90 years after closure, waste package surface temperatures would exceed 300°C for waste packages in the hottest portions of the emplacement drifts, with low effective thermal conductivity for the collapse rubble (SNL 2008d, Sections 6.4.2.5 and 6.5.1, and Figures 6.4.2-28 and 6.4.2-29). Resistance of the emplacement drift openings to collapse from ground shaking (SNL 2007b, Section 6.7.1) during the peak thermal period will therefore contribute to EBS barrier capability.

Seismic Fault Displacement

The open emplacement drift also provides protection to the waste package in the seismic fault displacement case. Fault displacement can occur along both known and undetected ("generic") faults (SAR Section 2.3.4.5.5.2.3), and can rupture waste packages and drip shields that are co-located with the faults, if the faulting events have sufficient displacement (SAR Section 2.3.4.5.5.1). Waste package damage can occur if the fault displacement exceeds the available clearance around the waste package and the drip shield (SNL 2007b, Section 6.11). Displacements associated with faulting in the emplacement areas are expected to be small (SAR Section 2.3.4.5.5.1; SNL 2007b, Section 6.11), and thus the open spaces in the drift will contribute to EBS performance. In the abstraction of fault displacement consequences for TSPA, drift collapse is assumed to occur at the same time as the faulting event, so the beneficial effect of uncollapsed or partially collapsed drifts is conservatively ignored (SAR Section 2.4.2.3.2.1.12.3; SNL 2007b, Section 6.11.1.1). Fault displacement criteria for EBS damage are given in SAR Section 2.3.4.5.5.2.2 (Tables 2.3.4-52 and -53); displacement in excess of these criteria is considered to rupture the waste package and the overlying drip shield through direct shearing. Combining the allowable displacements (SAR Section 2.3.4.5.5.2.2, Table 2.3.4-53) with the seismic hazard curve (SAR Figure 2.3.4-18) defines the range of exceedance frequencies that can cause waste package failure from fault displacement. Fault displacement hazards and model uncertainty are discussed in SAR Sections 2.3.4.5.5.2.4 and 2.3.4.5.5.3, respectively. It should be noted that damage to naval waste packages by fault displacement is less likely than for other waste packages, as they will not be co-located with known faults that have a measured displacement of greater than 2 meters (SAR Section 1.3.1.1

and SAR Table 1.9-8, Footnote d). However, the naval waste packages are still susceptible to rupture by seismic displacement events along generic faults.

1.2 Preventing or Reducing the Rate of Movement of Radionuclides

Emplacement drift degradation may be either favorable or unfavorable to waste isolation, and the contribution to the barrier capability for the EBS is the net result of effects which may offset each other. Qualitatively, drift collapse early in the thermal period extends the duration of elevated temperatures, which tends to increase the rate of general corrosion of Alloy 22. Drift collapse increases rubble loading on the drip shield, which may lead to sidewall buckling in response to seismic accelerations (SNL 2007b, Section 6.8.3). However, drift collapse may also decrease the incidence of other modes of EBS degradation from seismic ground motion, such as waste package rupture (SNL 2008b, Section 6.6.1.1.2).

Temperature and Water Chemistry Effects on Corrosion of EBS Components

The open drift facilitates radiative heat transfer from the drip shield to the drift wall, limiting waste package and drip shield temperatures, and limiting in-drift relative humidity (SAR Section 2.3.5.4.1.3.2). Cooler waste package temperatures that prevail in open drifts are beneficial for several reasons. The general corrosion rate for the Alloy 22 waste package outer barrier is directly related to temperature (SAR Section 2.3.6.3.3). Partial or complete drift collapse resulting from low-probability seismic events will alter heat transfer, changing EBS temperatures. Heat transfer within drift collapse rubble is discussed in SAR Section 2.3.5.4.1.3.2 (also see SNL 2008e, Section 6.3.17[a]). In the rubble, radiative heat transfer is decreased and conductive transfer is more important (SNL 2008e, Section XI.1[a]), which produces higher waste package temperatures and prolongs the thermal period. However, the seismic ground motion cases of the performance assessment show that complete drift collapse does not occur early enough after repository closure to result in significantly higher waste package temperatures (SAR Figure 2.1-14). Some sensitivity of Alloy 22 corrosion to temperature history is indicated by the sensitivity of total dose to the host-rock thermal conductivity parameter THERMCON (SAR Section 2.4.2.3.3.4). Hence drift integrity, by maintaining cooler waste package temperatures in open drifts, contributes to EBS performance.

The importance of drift integrity with respect to in-drift temperature and relative humidity is addressed in SAR Section 2.3.5.4.1 and in *Multiscale Thermohydrologic Model* (SNL 2008e, Section 6.3.7). In the TSPA, complete drift collapse signifies immediate changes in predicted waste package surface temperature and relative humidity. Complete collapse during the first 10,000 years is unlikely (SAR Figure 2.1-14), but would cause conditions on the waste package surface to become hotter and drier. If complete drift collapse occurs later, then the temperature and relative humidity at the waste package both increase slightly (SNL 2008e, Figures 6.3-82[a] and -83[a]). Waste package temperature and relative humidity are used in the in-drift seepage evaporation abstraction to evaluate the conditions for initiation of localized corrosion on waste packages exposed directly to seepage (SAR Section 2.3.5.5.4.2.1; SNL 2007c, Section 6.9), and in the in-package chemistry abstraction to evaluate water chemistry within the waste package (SAR Section 2.3.7.5.3; SNL 2007d, Section 6.3[a]). Because drift collapse within 10,000 years, which includes the thermal period, is unlikely, and because initiation of localized corrosion in

open drifts will not occur after approximately 12,000 years (SAR Section 2.1.2.2.3), the aspects of drift integrity that are associated with temperature effects on in-drift chemistry are not highly significant to EBS barrier capability.

With respect to in-drift thermal-hydrologic conditions, drifts transition directly from uncollapsed to fully collapsed (SAR Section 2.3.4.5.6.2) when the fraction of drift filled with rubble (defining complete collapse) reaches 100%. This is a reasonable simplification given that significant drift collapse (partial or complete) is unlikely during the first 10,000 years (SAR Section 2.4.1.3), which corresponds to most of the thermal period (SNL 2008e, Section 6.2.12.4[a]). The drift lifetime with respect to temperature effects on corrosion processes is therefore the same as for seismic drift collapse (SAR Figure 2.1-14), and extends beyond 100,000 years.

In the ITBC analysis (SNL 2008a, Table A-2), the emplacement drift characteristics that influence temperature and water chemistry effects on corrosion of EBS components are principally associated with included FEPs 2.1.11.01.0A (Heat Generation in the EBS) and 1.2.03.02.0C (Seismic Induced Drift Collapse Damages EBS Components).

Thermal-Hydrologic Conditions for Onset of Waste Form Degradation and Transport

Degradation of waste forms will commence immediately after waste package breach by seismic damage or rupture, or by corrosion, but transport of radionuclides out of the waste package can occur only when environmental conditions permit (SAR Section 2.4.2.3.2.1.7). Degradation of spent fuel waste forms begins immediately after waste package breach (DOE SNF is assumed to degrade instantaneously), while degradation of high-level waste glass requires waste package relative humidity of at least 44%. Transport of radionuclides out of the waste package can occur if there is advective flow of seepage through the package, or after temperature (less than or equal to 100°C) and relative humidity (greater than or equal to 95%) conditions allow development of water films which support diffusion (SAR Section 2.4.2.3.2.1.7). Cooling of the EBS is fastest in open drifts, which then allow earlier onset of radionuclide transport. However, the impact of this effect on TSPA is low because EBS component failures are unlikely during the thermal period (e.g., 10,000 years). Thus, drift integrity is not highly significant to EBS barrier capability with respect to the onset of waste form degradation and radionuclide transport.

The drift lifetime with respect to thermal-hydrologic conditions for onset of waste form degradation and radionuclide transport is the same as for conditions affecting corrosion discussed above, and extends beyond 100,000 years. Similar drift lifetimes apply to changes in chemistry and radionuclide transport (described above as not highly significant) associated with complete drift collapse. Note that the magnitudes of temperature and humidity changes due to drift collapse become very small after 10,000 years (SNL 2008e, Figures 6.3-82[a] and -83[a]).

In the ITBC analysis (SNL 2008a, Table A-2), the emplacement drift characteristics that influence temperature and water chemistry effects on corrosion of EBS components are principally associated with included FEPs 2.1.11.01.0A (Heat Generation in the EBS) and 1.2.03.02.0D (Seismic Induced Drift Collapse Alters In-Drift Thermal-Hydrology).

Effect of Water Chemistry on Radionuclide Transport

The chemistry of water in the drift environment is affected by elevated temperatures caused by drift collapse. Even if drift collapse occurs hundreds of thousands of years after closure when temperatures have returned nearly to ambient, water chemistry, and particularly ionic strength, may be affected by small changes in relative humidity. For example, in a single realization of the seismic ground motion case for 1,000,000 years (SNL 2008b, Section 7.7.1.4[a]), when complete drift collapse occurred at 380,000 years, the relative humidity at the waste package surface increased from 0.9956 to 0.9984. This small humidity change produced a three-fold decrease in ionic strength (SAR Figure 2.4-103), within the range where changes can stabilize colloids that contribute to radionuclide transport (SNL 2008b, Figure 6.3.7-11). Other aspects of radionuclide transport from breached waste packages and through the invert are also sensitive to changes in temperature and relative humidity caused by drift collapse (SNL 2008b, Sections 6.3.4.1, 6.3.8.1, and 6.6.2). However, drift collapse is only likely to occur after the thermal period, so the impact on water chemistry is limited, and the effect of emplacement drift integrity on chemical transport of radionuclides in the EBS is not highly significant.

In the ITBC analysis (SNL 2008a, Table A-2) the emplacement drift characteristics that influence water chemistry in the context of radionuclide transport are principally associated with included FEPs 2.1.09.01.0A (Chemical Characteristics of Water in Drifts), 2.1.11.08.0A (Thermal Effects on Chemistry and Microbial Activity in the EBS), 2.1.11.01.0A (Heat Generation in the EBS), and 2.2.08.12.0A (Chemistry of Water Flowing into the Drift).

1.3 Contribution of Emplacement Drift Components to Barrier Capability

As noted in SAR Table 2.1-1, several other components of the emplacement drift are not important to waste isolation (ITWI), including the non-emplacement openings, closure, ground support, and ventilation systems. In this section, the rationale for classifying these components as non-ITWI, and non-ITBC, is provided.

- Non-Emplacement Openings—Repository non-emplacement openings are designed to provide a repository grade so overall water drainage and accumulation travels away from the waste package emplacement areas (SNL 2008a, Table 7-5, Parameter 01-12). Although the non-repository openings provide partial support for excluding ponding within the emplacement drifts, high host-rock permeability provides the main basis for screening this process (SNL 2008a, Table A-2, excluded FEP 2.1.08.12.0A, Induced Hydrologic Changes in Invert). Hence, non-emplacement openings are not considered significant to barrier capability.

- Ventilation System—As discussed in *Postclosure Nuclear Safety Design Bases* (SNL 2008a, Table A-2), the effects of preclosure ventilation are associated with included FEP 1.1.02.02.0A (Preclosure Ventilation). Preclosure ventilation removes heat and moisture from the host rock during the ventilation period. The heat removal effect is included explicitly in all postclosure thermal models, while the moisture removal effect is minor compared to postclosure hydrologic processes, and is not significant to postclosure performance. While preclosure ventilation is important in maintaining compliance with

waste package temperature limits (SNL 2008a, Table 7-5, Parameter 06-03), preclosure removal of heat can be achieved within a wide range of operational parameters, including passive ventilation, and its effects on postclosure conditions are limited. Hence, the effects of preclosure ventilation are not considered significant to barrier capability.

- Ground Support—Emplacement drifts include a ground support composed of stainless steel drift liners and rock bolts (SAR Table 1.3.4-5, Parameter 01-15). Interactions with ground support materials have been determined to have a negligible effect on seepage chemistry and in-drift water chemistry (SNL 2008a, Table A-2, excluded FEPs 2.1.06.01.0A, Chemical Effects of Rock Reinforcement and Cementitious Materials in EBS, and 2.2.01.01.0B, Chemical Effects of Excavation and Construction in the Near Field). In addition, no postclosure barrier capability is attributed to the rock reinforcement materials used in the EBS. Postclosure models and analyses neglect the potential beneficial effects from rock reinforcement on the rock mass response to thermo-mechanical and seismic stresses (SNL 2008a, Table A-2, excluded FEP 2.1.06.02.0A, Mechanical Effects of Rock Reinforcement Materials in EBS). Therefore, ground support materials are not considered significant to barrier capability.

- Closure of Ventilation Shafts and Access Ramps—Closure of ventilation shafts and access ramps will be accomplished by backfilling for the entire depth or length of the opening (SNL 2008a, Table 7-5, Parameter 09-01). Fluid flow through the seals is evaluated in excluded FEP 2.1.05.01.0A, Flow Through Seals (Access Ramps and Ventilation Shafts) (SNL 2008c). As described in that FEP, flow through shafts and ramps, which are laterally offset from the emplacement drifts, is not expected to affect the flow and transport of water in the repository in any significant way. Also, long-term changes in the backfill material are not expected to impact repository performance. For these reasons, ventilation shaft and ramp seals are not considered significant to barrier capability (SNL 2008a, Section 6.3). The effectiveness of shaft and ramp backfill placement and compaction procedures will be evaluated as part of the Performance Confirmation Program (SNL 2008f, Section 3.3.3.1).

2. COMMITMENTS TO NRC

None.

3. DESCRIPTION OF PROPOSED LA CHANGE

None.

4. REFERENCES

SNL (Sandia National Laboratories) 2007a. *In-Drift Natural Convection and Condensation.* MDL-EBS-MD-000001 REV 00 AD 01. Las Vegas, Nevada: Sandia National Laboratories. ACC: DOC.20050330.0001; DOC.20051122.0005; DOC.20070907.0004; LLR.20080324.0007.

SNL 2007b. *Seismic Consequence Abstraction.* MDL-WIS-PA-000003 REV 03. Las Vegas, Nevada: Sandia National Laboratories. ACC: DOC.20070928.0011; LLR.20080414.0012.

SNL 2007c. *Engineered Barrier System: Physical and Chemical Environment*. ANL-EBS-MD-000033 REV 06. Las Vegas, Nevada: Sandia National Laboratories. ACC: DOC.20070907.0003; LLR.20080328.0031.

SNL 2007d. *In-Package Chemistry Abstraction*. ANL-EBS-MD-000037 REV 04 ADD 01. Las Vegas, Nevada: Sandia National Laboratories. ACC: DOC.20070816.0004; DOC.20051130.0007; LLR.20080325.0276; DOC.20081120.0004.

SNL 2008a. *Postclosure Nuclear Safety Design Bases.* ANL-WIS-MD-000024 REV 01. Las Vegas, Nevada: Sandia National Laboratories. ACC: DOC.20080226.0002; DOC.20080314.0004; LLR.20080507.0018; DOC.20080610.0007.

SNL 2008b. *Total System Performance Assessment Model /Analysis for the License Application.* MDL-WIS-PA-000005 REV 00 AD 01. Las Vegas, Nevada: Sandia National Laboratories. ACC: DOC.20080312.0001; LLR.20080414.0037; LLR.20080507.0002; LLR.20080522.0113; DOC.20080724.0005; DOC.20080106.0001.

SNL 2008c. *Features, Events, and Processes for the Total System Performance Assessment: Analyses.* ANL-WIS-MD-000027 REV 00. Las Vegas, Nevada: Sandia National Laboratories. ACC: DOC.20080307.0003; DOC.20080407.0009; DOC.20080722.0002.

SNL 2008d. *Postclosure Analysis of the Range of Design Thermal Loadings*. ANL-NBS-HS-000057 REV 00. Las Vegas, Nevada: Sandia National Laboratories. ACC: DOC.20080121.0002; LLR.20080408.0251; DOC.20080828.0006.

SNL 2008e. *Multiscale Thermohydrologic Model*. ANL-EBS-MD-000049 REV 03 AD 02. Las Vegas, Nevada: Sandia National Laboratories. ACC: DOC.20080201.0003; LLR.20080403.0162; LLR.20080617.0077.

SNL 2008f. *Performance Confirmation Plan*. TDR-PCS-SE-000001 REV 05 AD 01. Las Vegas, Nevada: Sandia National Laboratories. ACC: DOC.20080227.0003; DOC.20080324.0002.

RAI: Volume 3, Chapter 2.2.1.1, First Set, Number 4:

Address the capability of a waste package breached by general corrosion to divert seepage water. Describe the capability, including uncertainties arising from the corrosion and EBS flow models, consistent with the quantitative analyses in the total system performance assessment (e.g., sensitivity and uncertainty analyses or intermediate results). Provide information on the time period over which waste package diverts seepage water.

Basis: Needed for demonstration of compliance with 10 CFR 63.115(b) and (c). The SAR identifies the ability of a waste package breached by cracks to prevent water from entering the waste package due to the capillary diversion effect (SAR Section 2.1.2.2.6). However, Section 2.1 of the SAR does not describe or provide performance evidence to support the capability of a waste package breached by general corrosion to divert water. In addition, the effect of corrosion and EBS flow model uncertainties on the waste package capability does not appear to be demonstrated in SAR Section 2.1.2.2.6. This information is needed to confirm the postulated barrier capability.

1. RESPONSE

The capability of a waste package breached by general corrosion to divert seepage water is demonstrated using the flux splitting submodel (SAR Section 2.3.7.12.3.1) to obtain the fraction of drift seepage that enters a waste package having general corrosion breaches, as given by (SNL 2008, Appendix L, Section L.2.13, Equation L-30):

$$F_{WP} = \min\left[\frac{N_p \frac{L_p}{2}}{L_{WP}} f'_{WP}, 1\right], \qquad \text{(Eq. 1)}$$

where

F_{WP} = the fraction of drift seepage that enters a waste package through general corrosion breaches

N_P = the number of general corrosion patch penetrations on a failed waste package

L_P = the length of a waste package general corrosion patch

L_{WP} = the total axial length of a waste package

f'_{WP} = uncertainty factor for the fraction of rivulet flow that enters a breach, uniform distribution, 0-2.41 (SNL 2007, Table 8.2-4).

The average fraction of the waste package surface area damaged by general corrosion patches as a function of time on a waste package failed by general corrosion, $f_{dam,patch,WAPDEG}(t)$, is equal to the fraction of the total number of patches in the TSPA discretized general corrosion model that are penetrated. The TSPA model discretizes the waste package surface into patches, each with an area of 23,150 mm^2, with the total number of patches, N_{pt}, proportional to the surface area of each type of waste package: 1,430 patches for a CSNF waste package and 1,408 patches for the smaller CDSP waste package (SNL 2008, Section 6.3.5.1.2). The patches are assumed to be square, giving a patch length, L_P, equal to 152.15 mm. The total axial length of a CSNF waste package, L_{WP}, is 5.691 m, and the axial length of a CDSP waste package is 5.145 m (SNL 2007, Table 8.2-6).

The number of breaches (or patch penetrations), N_P, can then be expressed as the product of the total number of patches used in the discretization of the waste package surface, N_{pt}, and the fraction of the waste package surface that is breached due to general corrosion:

$$N_p = N_{pt} f_{dam,patch,WAPDEG}(t), \quad \text{(Eq. 2)}$$

and the fraction of seepage flowing through the waste package breached by general corrosion is:

$$F_{WP} = \min\left[\frac{N_{pt} L_p}{2L_{WP}} f_{dam,patch,WAPDEG}(t) f'_{WP}, 1\right]. \quad \text{(Eq. 3)}$$

For a CSNF waste package,

$$F_{WP} = \min[19.1 f_{dam,patch,WAPDEG}(t) f'_{WP}, 1]. \quad \text{(Eq. 4)}$$

For a CDSP waste package,

$$F_{WP} = \min[21.1 f_{dam,patch,WAPDEG}(t) f'_{WP}, 1]. \quad \text{(Eq. 5)}$$

Since the seepage fraction that would flow through a breached waste package is similar for both the CSNF and CDSP waste packages, only the CSNF waste package will be considered in the balance of this response.

Figure 1 shows the fraction of seepage that would flow through a CSNF waste package as a function of the fractional area of the waste package surface degraded (i.e., damaged by general corrosion) for various percentiles of the uniform distribution of the uncertainty factor for rivulet flow, f'_{WP}. It can be seen that a relatively small fraction of the waste package surface needs to be breached by general corrosion to allow all of the drift seepage to enter the waste package; for example, when 4% of the surface is penetrated by general corrosion, the fraction of seepage that flows through a CSNF waste package ranges from 0 to 1.0, with a median fraction of seepage of 0.92 flowing through a waste package. As shown later in this response, the average fractional

area of the waste package surface degraded in 1,000,000 years is smaller than this example, with the result that on average a breached waste package diverts a large fraction of drift seepage.

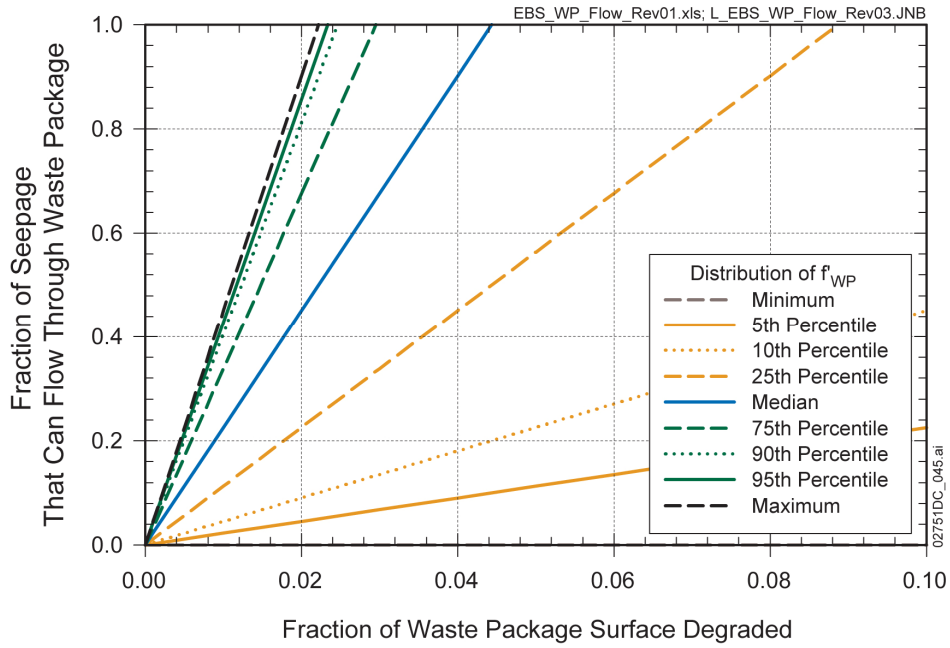

Source: SNL 2008, Figure L-10.

NOTES: Curve for "Minimum" f'_{WP} coincides with horizontal axis (Fraction of Seepage = 0).

This figure has been modified from its original appearance as Figure L-10 in SNL 2008, Appendix L. The range of the *x*-axis has been shortened from 0.5 to 0.1. In addition, to avoid the plotting artifact of curved lines as seepage fractions approach the value 1.0 as seen in SNL 2008, Figure L-10, the dataset was reevaluated without constraints on the fractional values. Although this results in calculated seepage fractions that may rise above 1.0 in the dataset, this reevaluation was done for plotting purposes only and the use of these data is limited to seepage fractional values between 0 and 1 as specified in Equation 4.

Figure 1. Fraction of Seepage that Can Enter a CSNF Waste Package with General Corrosion Breaches at Various Percentiles of the Uniform Distribution of f'_{WP}

As indicated in SAR Figure 2.1-16(a) (reproduced below), the mean curve for the outer barrier average patch-breach area fraction begins abruptly at approximately 240,000 years. The 5th percentile and median are absent from the plots because of the large number of realizations in which no patch breaches occur within 1,000,000 years (SAR Section 2.1.2.2.6). This abrupt increase results from the first occurrence of rupture or puncture in the waste package outer barrier. Once they occur, ruptures and punctures are modeled in the same way as general corrosion patches. Ruptures and punctures can only occur to waste packages that have been weakened by internal corrosion resulting from moisture entering the waste package through previously formed cracks. Therefore, two separate seismic events of sufficient magnitude are required, the first to cause the crack damage and the second to cause the rupture or puncture. Due to the low probability of seismic events that cause crack damage to CSNF waste packages, as well as the low probability of seismic events that subsequently induce ruptures or punctures in the waste package outer barrier, ruptures and punctures occur in only a few realizations (see SAR Section 2.3.4.5 for details regarding the response of the waste package to seismic events).

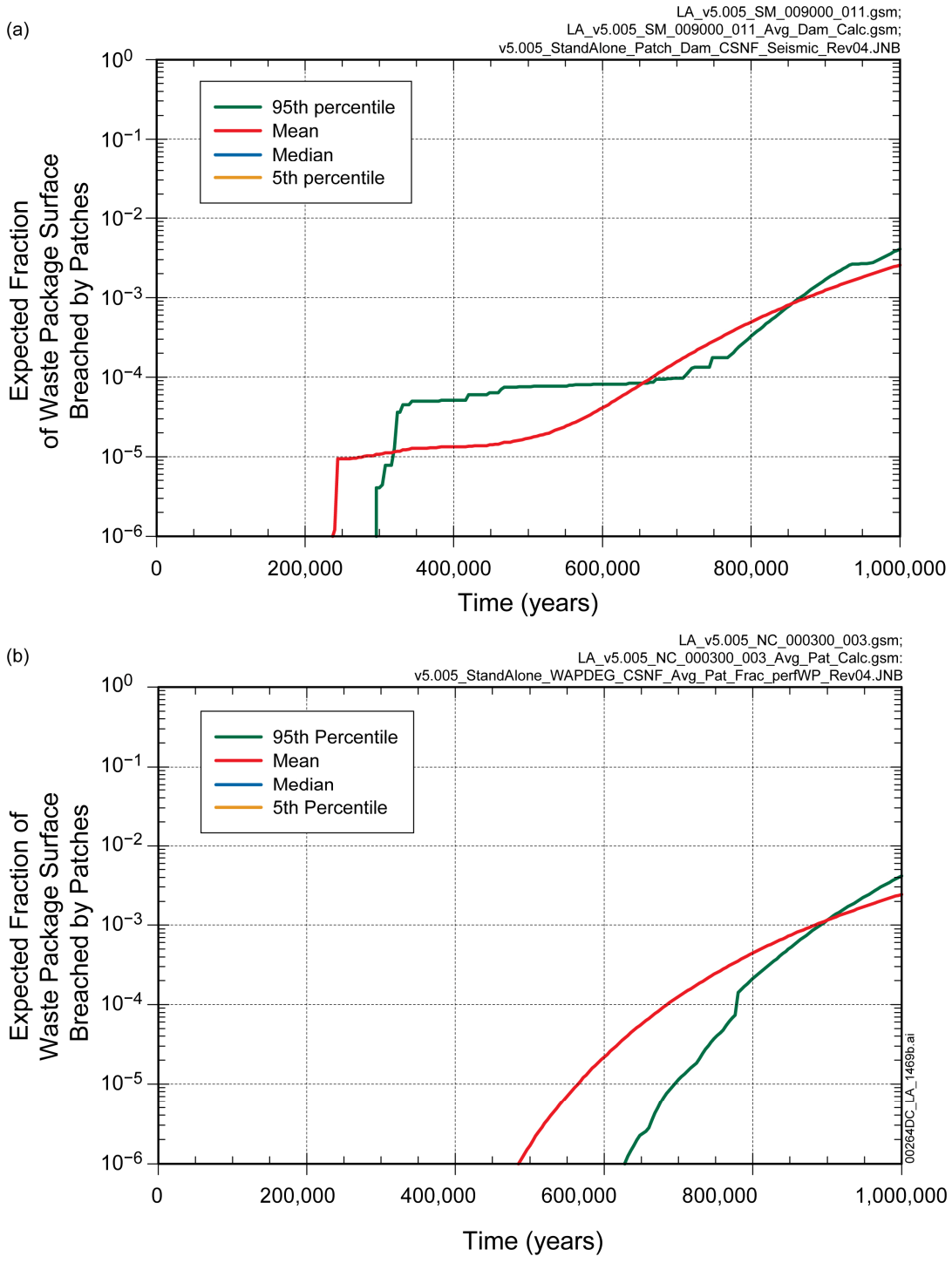

Source: SNL 2008, Figure 8.3-11[a].

SAR Figure 2.1-16. Summary Statistics for Fraction of CSNF Waste Package Surface Breached by Patches per Breached Waste Package for (a) the Seismic Ground Motion Modeling Case and (b) the Nominal Modeling Case, as a Function of Time

Accordingly, until about 480,000 years, the mean curve remains relatively flat, because it is determined by the few realizations in which ruptures or punctures occur. After 480,000 years, the mean curve ascends gradually, corresponding to an increasing likelihood that general corrosion penetrations have occurred. The timing of the initiation of the general corrosion patch penetrations is consistent with the mean curve for the nominal conditions shown on SAR Figure 2.1-16(a). At the end of 1,000,000 years, the mean patch-breach area fraction attributed to seismic conditions, shown in SAR Figure 2.1-16(a), is about 0.26%, whereas for nominal conditions, shown in SAR Figure 2.1-16(b), it is about 0.24%. This small difference between seismic and nominal patch-breach area fractions means that the fraction of surface area breached by patch penetrations on the CSNF waste package outer barrier is dominated by the general corrosion degradation.

Note that the expected fraction of waste package surface breached by patches shown in SAR Figure 2.1-16 is averaged over the entire repository. Not only is the number of realizations with no patch breaches large, as noted above, but also in any given realization the number of waste packages in the repository having no patch breaches is large. By 1,000,000 years, the mean fraction of the CSNF waste packages with at least one patch breach is approximately 9% (SNL 2008, Section 8.3.3.2.1[a]). This indicates that about 90 percent of the CSNF waste packages in the repository would not exhibit general corrosion patch penetrations before 1,000,000 years and would divert all seepage water over that time period.

Using Equation 4 for a CSNF waste package, the fraction of seepage that can enter a waste package breached by general corrosion, based on the mean curve for the nominal conditions, is $0.046 f'_{WP}$. The range in the uncertainty factor for the fraction of flow that enters a breach, f'_{WP} (0-2.41, uniform distribution), provides a measure of the effect of EBS flow uncertainties on the average fraction of seepage that can enter a waste package breached by general corrosion, which will range uniformly from zero to a maximum of 0.11 over the range of f'_{WP}, with a median fraction of seepage that can enter a waste package of 0.055.

The 95th percentile curve in SAR Figure 2.1-16(b) demonstrates the effect of uncertainties in the TSPA model on the fraction of waste package surface that is breached by general corrosion and hence on the capability of a breached waste package to divert seepage water. In the 95th percentile curve, patches begin to appear at about 640,000 years, and the expected fraction of waste package surface breached by patches reaches about 0.41% at 1,000,000 years. At that time, the average fraction of seepage that can enter a waste package breached by general corrosion will range uniformly from zero to a maximum of 0.19, with a median fraction of seepage that can enter a waste package of 0.095, accounting for the range in the uncertainty factor for the fraction of flow that enters a breach, f'_{WP}.

Finally, in addition to the effect accounted for by the EBS flow submodel uncertainty parameter, f'_{WP}, the capability of a waste package breached by general corrosion to divert seepage water is affected by the uncertainty in corrosion model parameters and other TSPA model parameters. As determined by the uncertainty and sensitivity analysis presented in the TSPA report (SNL 2008, Appendix K, Section K4.2 and Figure K4.2-7), uncertainty in the average breached

area on a failed waste package is dominated by the temperature dependence coefficient associated with the general corrosion rate for Alloy 22. The general corrosion rate for Alloy 22, and hence the number of patch breaches in a waste package, decreases as the temperature dependence coefficient increases. The following uncertainty parameters are shown in the TSPA report (SNL 2008, Appendix K) to have smaller effects on the average breached area on a waste package breached by general corrosion:

- Stress corrosion cracking (SCC) parameters; SCC contributes slightly to the total average breached area used in the uncertainty and sensitivity analysis, but not to advective flow through a waste package, since liquid water does not flow through stress corrosion cracks (SAR Table 2.2-1, FEP 2.1.03.10.0A).

- Infiltration level, which, as it increases, tends to lower waste package temperatures and thus reduce the rate of corrosion.

- Host rock thermal conductivity level, which, like infiltration level, tends to lower waste package temperatures and thus reduce the rate of corrosion as it increases.

- Pointer variable used to select from three uncertain general corrosion rate distributions; these distributions derive from both the uncertainty in a base corrosion rate for Alloy 22 at 60°C and the uncertainty that exists in the prediction of small scale variability in chemical and physical conditions across patches used in the modeling of waste package degradation.

Summary

The capability of a waste package breached by general corrosion to divert water is summarized as follows:

- For nominal conditions, the mean patch breach area fraction for a CSNF waste package at the end of 1,000,000 years is about 0.24%, and the average fraction of drift seepage that can enter a waste package breached by general corrosion ranges from zero to 0.11, with a median of 0.055, i.e., 89-100% of drift seepage is diverted; this range is due to uncertainty in the waste package flux splitting submodel.

- The effect of uncertainties in the TSPA model is further demonstrated by the 95th percentile results for the fraction of CSNF waste package surface breached by patches for nominal conditions, for which the average fraction of drift seepage that can enter a waste package breached by general corrosion after 1,000,000 years ranges from zero to 0.19, with a median of 0.095; i.e., 81-100% of drift seepage is diverted, accounting for uncertainty in the waste package flux splitting submodel.

- TSPA uncertainty and sensitivity analyses indicate that the uncertainty in the average breached area on a failed waste package is dominated by the temperature dependence coefficient associated with the general corrosion rate for Alloy 22, with smaller effects due to other parameters that affect the general corrosion rate for Alloy 22.

2. COMMITMENTS TO NRC

None.

3. DESCRIPTION OF PROPOSED LA CHANGE

None.

4. REFERENCES

SNL (Sandia National Laboratories) 2007. *EBS Radionuclide Transport Abstraction.* ANL-WIS-PA-000001 REV 03. Las Vegas, Nevada: Sandia National Laboratories. ACC: DOC.20071004.0001; LLR.20080414.0023.

SNL 2008. *Total System Performance Assessment Model /Analysis for the License Application.* MDL-WIS-PA-000005 REV 00 AD 01. Las Vegas, Nevada: Sandia National Laboratories. ACC: DOC.20080312.0001; LLR.20080414.0037; LLR.20080507.0002; LLR.20080522.0113; DOC.20080724.0005; DOC.20080106.0001.

RAI: Volume 3, Chapter 2.2.1.1, First Set, Number 5:

Address the barrier capability of waste form and waste package internal components. Ensure that this description includes performance assessment inputs or intermediate results demonstrating:

- how various degradation rates of waste forms (e.g., CSNF or HLW glass) at different times affects the EBS barrier capability
- how limited waste package breach area affects the EBS barrier capability
- how solubility affects the EBS barrier capability in the different transport model domains
- how sorption to stationary corrosion products affects the EBS barrier capability
- why colloidal processes do not affect the EBS barrier capability in the nominal and igneous intrusive scenarios

Describe the capability of the waste form and waste package internal components, including uncertainties, consistent with the quantitative analyses in the total system performance assessment (e.g., sensitivity and uncertainty analyses or intermediate results). Provide information on the time period over which the waste form and waste package internal components perform their intended function.

Basis: Needed for demonstration of compliance with 10 CFR 63.115 (b) and (c). There is very limited information on the effectiveness of individual features, events, and processes on the rate of release of radionuclides. It is not clear which processes control the releases from a failed waste package. For example,

- DOE does not provide a detailed description of the degradation rates of the different types of waste forms at different times
- DOE does not provide an indication of how effective the limited breach area associated with cracks is at retaining radionuclides under diffusive release conditions
- DOE does not demonstrate or provide specific descriptions of the effectiveness of solubility limits at limiting the releases from the waste package
- DOE does not demonstrate or provide specific descriptions of the effectiveness of the stationary corrosion products inside the waste package at retaining radionuclides, and in particular, how the desorption rate of radionuclides sorbed to stationary corrosion products affects the rate of radionuclide release from the waste package
- DOE does not describe why colloidal processes are ineffective at transporting radionuclides outside the waste package in the nominal and igneous intrusive scenarios.

Finally, there does not appear to be a clear connection between these processes and the specific components that contribute to these processes. It is therefore not clear that the barrier capabilities implied by the discussion of these processes is consistent with the safety classification provided in Table 2.1-1. For example, corrosion product sorption appears to be a process that is significant in controlling the releases from a failed waste package, and corrosion of the internal canisters appears to be a significant source of these stationary corrosion products; consequently, it is not clear why the codisposal waste canisters are not considered important to waste isolation.

1 RESPONSE

The EBS is classified as a barrier because it provides the following barrier functions: (1) prevents or substantially reduces the rate of movement of water, (2) prevents the release or substantially reduces the release rate of radionuclides, and (3) prevents or substantially reduces the rate of movement of radionuclides (SAR Section 2.1, p. 2.1-1). The EBS is classified as important to waste isolation (ITWI) because it provides a reasonable expectation that SNF and HLW can be disposed of without exceeding the requirements of 10 CFR 63.113(b) and (c) (SAR Section 2.1.1, p. 2.1-3), based on an analysis documented in *Postclosure Nuclear Safety Design Bases* (SNL 2008a, Section 6) (hereafter referred to as the PNSDB report).

The EBS consists of the following features: emplacement drift, drip shield, waste package, cladding, waste form and waste package internals, waste package pallet, and invert (SAR Table 2.1-1; SNL 2008a, Section 6.1.2.1.2, p. 6-11). A barrier's features may contribute to the barrier's capability. This RAI requests additional information describing how five specific processes affect the barrier capability of the waste form and waste package internals feature of the EBS. The barrier capability of the waste form and waste package internals feature is summarized in SAR Table 2.1-1, where specific components of the feature are identified and classified as ITWI or Non-ITWI. The components of the waste form and waste package internals features are: TAD Canister, Naval Canister, DSNF Canister, HLW Canister, Naval SNF Canister System Components, CDSP Waste Package Internals, TAD Canister Internals, DSNF Canister Internals, CSNF, HLW Glass, Naval SNF, and DSNF (SAR Table 2.1-1). Note that, because naval waste packages and naval SNF are represented by CSNF waste packages and CSNF (SAR Section 2.3.7.3, p. 2.3.7-13; SNL 2008a, Section 6.2.2.2, pp. 6-75 and 6-76), the naval components listed above are not addressed separately in this RAI response.

A feature (or component) is classified as ITWI if it meets two conditions: (1) the feature is associated with one or more processes or characteristics classified as important to barrier capability (ITBC); and (2) the feature is a significant contributor to the barrier capability relative to the other features of the barrier (SAR Section 2.1.1, pp. 2.1-3 and 2.1-4). The second condition means that some features or components that are associated with an ITBC process may still not contribute sufficiently to be classified as ITWI. In addition, a feature (or component) is classified as ITWI if it is one of the engineered features of the geologic repository whose function is to prevent or mitigate the consequences of potential disruptive events (e.g., criticality) (SAR Section 2.1.1, p. 2.1-4).

The determination of processes or characteristics that are ITBC was based on an examination of features, events, and processes (FEPs) and their screening justifications, and information from process models and model reports that describe the technical basis for the TSPA-LA (SNL 2008a, Section 1, p. 1-1, and Section 6, p. 6-1). The ITBC classifications of FEPs related to the waste form and waste package internals feature of the EBS, and their underlying bases, are presented in the PNSDB report (SNL 2008a, Table A-2, pp. A-110 to A-143) and summarized in SAR Table 2.1-3 (pp. 2.1-129 to 2.1-131).

The following five subsections provide additional information describing the effects of each of the requested processes on the barrier capability of the waste form and waste package internals feature. The descriptions are based upon performance assessment results presented in SAR Section 2.1, where available, and supplemented by information from other SAR sections (e.g., 2.3.7 and 2.4), from *Total System Performance Assessment Model/Analysis for the License Application* (SNL 2008b) (hereafter referred to as the TSPA-LA report), and from supporting process model reports. Specific references are provided in each of the subsections.

The additional information describes the capability of the components of the waste form and waste package internals feature (qualitatively, and where possible, quantitatively), including uncertainties, consistent with the quantitative analyses in the total system performance assessment (e.g., sensitivity and uncertainty analyses or intermediate results) and provides information on the time period over which the components perform their intended function. The barrier capability of the components of the waste form and waste package internals feature is described with respect to the barrier functions: (1) prevents the release or substantially reduces the release rate of radionuclides; and (2) prevents or substantially reduces the rate of movement of radionuclides.

The additional information also identifies and describes the relationship between each of the five processes and the barrier capabilities of the corresponding components of the waste form and waste package internals, consistent with the safety classification provided in SAR Table 2.1-1. However, while the ITWI classifications in SAR Table 2.1-1 are made at the component level, the ITBC FEP classification in SAR Table 2.1-3 is only mapped to the feature level. Further mapping of ITBC FEPs to components requires some subjectivity because many FEPs apply to multiple components of the feature. As a result, and consistent with the second condition for ITWI classification stated above, there are some components associated with ITBC FEPs that are classified as Non-ITWI.

Where possible, the descriptions directly support the combined nominal/early failure and seismic ground motion cases, as presented in SAR Section 2.1. However, information from other scenarios is also presented, as applicable.

1.1 WASTE FORM DEGRADATION RATES

This subsection describes how the degradation rates of the different types of waste forms (CSNF, HLW, and DSNF) at different times, including uncertainties, affect the capability of the waste form and waste package internals components.

1.1.1 CSNF and HLW Glass

The degradation of CSNF and HLW is represented by ITBC FEPs 2.1.02.02.0A (Commercial SNF Degradation) and 2.1.02.03.0A (HLW Glass Degradation) and is associated with the following ITWI components of the waste form and waste package internals feature listed in SAR Table 2.1-1: Commercial Spent Nuclear Fuel and High Level Glass. Slow degradation of the CSNF and HLW glass waste forms prevents or substantially reduces the release of radionuclides. Although direct TSPA-LA results for CSNF and HLW degradation rates were not compiled, the CSNF degradation model described in SAR Section 2.3.7.7 and the HLW glass dissolution model described in SAR Section 2.3.7.9 provide quantitative support for the capability of the CSNF and HLW Glass components, as implemented in TSPA-LA. In addition, indirect evidence of this barrier effect from TSPA-LA results is provided.

The degradation rates of the CSNF and HLW glass waste forms are represented as fractional rates in the TSPA-LA waste form degradation submodel, i.e., the degradation rates are proportional to the mass remaining. For CSNF, the degradation rate is described in SAR Section 2.3.7.7.3.2 by Equations 2.3.7-3 through 2.3.7-5. The fractional rate is apparent from SAR Equation 2.3.7-3. For HLW glass, the degradation rate is described in SAR Section 2.3.7.9.3 by Equations 2.3.7-7 through 2.3.7-9. The fractional rate is due to the surface area factor (from SAR Equation 2.3.7-7) that decreases proportionally with the mass remaining (SAR Section 2.3.7.9.3, Equation 2.3.7-9). Thus, the degradation rates of each of these waste forms decrease exponentially with time just as the mass remaining decreases exponentially with time. If all other factors remain approximately constant (e.g., pH), then these degradation rates can be described in terms of a half-life.

Using a waste form half-life to quantify the barrier capability of waste form degradation is a simplification because other factors also affect the rate, as explained in SAR Sections 2.3.7.7 and 2.3.7.9. These other factors include pH, total dissolved carbonate (which is linked to the partial pressure of carbon dioxide), temperature, and specific surface area, all of which vary spatially and temporally over the repository lifetime. However, by considering ranges of values for these factors, ranges of values for half-life for each waste form can be calculated.

Degradation of CSNF and HLW waste forms does not begin until the waste package has been breached (SAR Section 2.3.7.7.1, p. 2.3.7-36). The degradation rates are sensitive to temperature, so the calculations presented below use two different values: 90°C, representative of early time (e.g., the first few thousand years after repository closure); and 25°C, representative of later times (e.g., about 50,000 years or more after repository closure) when conditions approach ambient values (SNL 2008b, Figure K4.3-5). The partial pressure of carbon dioxide has only a small effect on the degradation rates and is fixed at 0.001 bar for the illustrative calculations in this RAI response.

For CSNF degradation rates, the major uncertain parameters are pH and specific surface area. The pH range in the CSNF (i.e., in the TSPA-LA EBS transport submodel waste form domain cell 1) under these temperature and CO_2(g) partial pressure conditions is approximately 5 to 9 (SAR Figure 2.3.7-19). The distribution of the log of the specific surface area (m^2/mg) of CSNF is triangular with a minimum of −7.3, maximum of −5.4, and mode of −6.7 (SAR

Tables 2.3.7-13 and 2.3.7-14). Entering these ranges of values into the CSNF degradation rate equations gives fractional rates that convert to conditional half-life values (for the mean specific surface area) ranging from 560 to 2,100 years at 25°C (Table 1.1-1). At 90°C, the conditional half-life values (for the mean specific surface area) range from 120 to 550 years (Table 1.1-1), indicating faster CSNF degradation at higher temperatures.

Table 1.1-1. CSNF Conditional Half-Life (years) at 0.001 bar CO_2(g)

pH	Temperature (°C)	Minimum Specific Surface Area (m^2/mg) (Log A = –7.3)	Mean Specific Surface Area (m^2/mg) (Log A = –6.47)	Maximum Specific Surface Area (m^2/mg) (Log A = –5.4)
5	25	3,800	560	48
6	25	8,400	1,200	110
7	25	14,000	2,100	180
8	25	12,000	1,700	150
5	90	850	120	11
6	90	1,800	270	23
7	90	3,800	550	47
8	90	3,100	450	39

For HLW glass degradation rates, the major uncertain parameters are pH, glass surface exposure factor, and the degradation rate coefficient. The pH range in the HLW glass (i.e., in the TSPA-LA EBS transport submodel waste form domain cell 1a) under these conditions is approximately 5 to 10 (SAR Figure 2.3.7-20). The distribution of the glass surface exposure factor is triangular with a minimum and mode of 4 and a maximum of 17 (SAR Table 2.3.7-21). The distributions of the rate coefficients, k_E, for both acidic and alkaline solutions, are also triangular (SAR Table 2.3.7-21) and are listed in the footer of Table 1.1-2. Entering these ranges of values into the HLW glass degradation rate equations gives fractional rates that convert to conditional half-life values (for the mean k_E and mean surface exposure factor) ranging from 1,700 to 150,000 years at 25°C and 180 to 5,300 years at 90°C (Table 1.1-2).

These waste form half-life values provide a quantitative indication of the delay in radionuclide release after waste package breach provided by the CSNF and HLW Glass components of the waste form and waste package internals feature for a range of temperatures and pH.

The effect of waste form degradation on releases of radionuclides can be observed by examining ^{99}Tc releases from the EBS over time for a single early drip shield failure. Releases of ^{99}Tc from the EBS are indicative of releases from the waste form (and thus waste form degradation) because there is no solubility limit on, or sorption of, ^{99}Tc in the EBS. Figure K5.3.2-5(a) of the TSPA-LA report (SNL 2008b) shows ^{99}Tc releases from the EBS for a CSNF waste package (indicative of CSNF waste form degradation), and Figure K5.3.3-5(a) of the TSPA-LA report (SNL 2008b) shows ^{99}Tc releases from the EBS for a CDSP waste package (indicative of combined DSNF and HLW glass waste form degradation).

Table 1.1-2. HLW Glass Conditional Half-Life (years) at 0.001 bar CO_2(g)

pH	Temperature (°C)	Minimum k_E and Surface Exposure Factor[a]	Mean k_E and Surface Exposure Factor[b]	Maximum k_E and Surface Exposure Factor[c]
5	25	1.6×10^6	1,700	270
7	25	1.5×10^7	1.6×10^4	2,600
8	25	4.7×10^7	4.9×10^4	8,100
9	25	1.4×10^8	1.5×10^5	2.5×10^4
10	25	9.6×10^7	1.1×10^5	1.8×10^4
5	90	1.7×10^5	180	29
7	90	1.6×10^6	1,700	280
8	90	5.0×10^6	5,300	860
9	90	2.0×10^6	2,400	390
10	90	6.6×10^5	770	130

[a] $f_{exposure} = 4$, $k_{E\_acidic} = 8.41 \times 10^3$ g/(m^2 day), $k_{E\_alkaline} = 2.82 \times 10^1$ g/(m^2 day).
[b] $f_{exposure} = 8.33$, $k_{E\_acidic} = 3.84 \times 10^6$ g/(m^2 day), $k_{E\_alkaline} = 1.16 \times 10^4$ g/(m^2 day).
[c] $f_{exposure} = 17$, $k_{E\_acidic} = 1.15 \times 10^7$ g/(m^2 day), $k_{E\_alkaline} = 3.47 \times 10^4$ g/(m^2 day).

For CSNF, after the initial release of radionuclides in the gap and grain boundary (SAR Section 2.3.7.7.3.1), the release rate from the waste form (i.e., degradation rate) decreases approximately exponentially over time (SNL 2008b, Figure K5.3.2-5(a)) and essentially all of the CSNF degrades within 2,000 years of waste package breach (SNL 2008b, Figure K5.3.2-5(b)). For CDSP, there is an instantaneous release of ^{99}Tc from DSNF (see Section 1.1.2), but the continuing release over time is due to HLW glass degradation. The CDSP release rate (i.e., degradation rate) also decreases approximately exponentially over time (SNL 2008b, Figure K5.3.3-5(a)) and most of the glass degrades within 5,000 years of waste package breach (SNL 2008b, Figure K5.3.3-5(b)).

The relatively fast waste form degradation rates apparent in these early failure cases are consistent with the shorter waste form half-lives associated with higher temperatures. In addition, the faster degradation of CSNF as compared with HLW glass is consistent with the shorter waste form half-lives for CSNF. For waste package failures that occur later after repository closure, waste form degradation will be slower because of lower temperatures, and thus waste form degradation effects on radionuclide releases will be more pronounced. However, for radionuclides that have limited solubility or that may sorb to corrosion products, other processes may have greater effects on radionuclide transport than waste form degradation; Sections 1.2 through 1.5 of this response discuss these other processes.

1.1.2 DSNF

DSNF is modeled as degrading instantaneously upon waste package breach (SAR Section 2.3.7.8.1, p. 2.3.7-44). As a result, the DSNF waste form does not directly prevent or reduce radionuclide release or movement and the DOE Spent Nuclear Fuel component of the waste form and waste package internals feature is classified as Non-ITWI in SAR Table 2.1-1. As noted in SAR Section 2.1.2.2 (p. 2.1-43), and described in more detail in SAR

Sections 2.3.7.5.1, 2.3.7.5.2, and 2.3.7.5.3, the degradation of DSNF also provides a source of schoepite, which tends to buffer the in-package pH in the near-neutral range. This pH control has an effect on in-package chemistry and therefore has an indirect effect on solubilities (see Section 1.3 of this RAI response). As a result, FEP 2.1.02.01.0A (DOE SNF Degradation) is classified as ITBC (SAR Table 2.1-3, p. 2.1-129).

1.2 WASTE PACKAGE BREACH AREA

This subsection describes how the occurrence and extent of waste package breaches, including uncertainties, affect the barrier capability of the EBS. Unlike other subsections of this RAI response, FEPs associated with waste package breaches are primarily associated with the waste package feature of the EBS, which is classified as ITWI (SAR Table 2.1-1). Such FEPs also have an indirect association with the TAD Canister component of the waste form and waste package internals feature, which is also classified as ITWI (SAR Table 2.1-1), and the HLW Canister and DSNF Canister components, which are Non-ITWI (SAR Table 2.1-1).

Waste package breaches may occur due to a number of processes and events: general corrosion, localized corrosion, stress corrosion cracking, seismic events, and early failures (SAR Section 2.1.2.2, pp. 2.1-37 to 2.1-39). In the TSPA-LA waste package degradation submodel, these breaches are represented as either through-wall cracks, with a relatively small failure area (maximum opening of about 7.7 mm^2 per crack (SNL 2007, Table 6.3-3)), or failure patches, which have a larger failure area (about 23,150 mm^2 per patch (SNL 2008b, Section 6.3.5.1.2, p. 6.3.5-7)). The presence of patches, which generally result from breaches due to thinning associated with general corrosion or from seismic-induced ruptures or punctures, permits moisture to enter the waste package as liquid water and/or as water vapor. In contrast, the presence of through-wall cracks only permits moisture to enter the waste package as water vapor and only permits diffusive releases of radionuclides from the waste package.

The following statements summarize how the limited waste package breach area affects EBS barrier capability by preventing or substantially reducing the rate of release of radionuclides:

- From the PNSDB report (SNL 2008a, Table A-2, FEP 2.1.03.02.0A – Stress Corrosion Cracking of Waste Packages, p. A-80): "Stress-induced corrosion cracking of Alloy 22 may occur as a result of mechanical degradation following seismic events. Such stress cracks are sufficiently small and tight to allow only the diffusive transport of radionuclides through the cracks. The lack of significant stress corrosion cracking of waste packages, except in the event of seismically-induced damage, is an important characteristic of the waste package."

- From the PNSDB report (SNL 2008a, Table A-2, FEP 2.1.03.10.0A – Advection of Liquids and Solids through Cracks in the Waste Package, p. A-84): "Cracks in the waste package, which may result from mechanical degradation associated with seismic activity, are of insufficient size to allow significant advective flux of water, and therefore this process is excluded from the performance assessment. However, cracks can allow moisture to enter the waste package via diffusion in sufficient amounts to initiate degradation and alteration of the materials and waste forms inside the waste

package. In addition, diffusive transport through these cracks is the dominant transport process for radionuclides released from the waste. The lack of significant advection through cracks in the waste package is an important beneficial characteristic of the waste package feature."

- From the PNSDB report (SNL 2008a, Table A-2, FEP 2.1.09.08.0B – Advection of Dissolved Radionuclides in EBS, p. A-123): "The conditions required for advective transport through a waste package are less likely to occur than those conditions required for diffusion. However, when advective transport through the waste package does occur its consequences are more significant compared to that from diffusion mechanisms because of the amount of water involved. Therefore, advection through the waste package is identified as ITBC."

- From SAR Section 2.1.2.2 (p. 2.1-38 – "Advection of Liquids and Solids through Cracks in the Waste Package"): "…cracks in the waste package are expected to be of insufficient size and morphology to allow for the advection of water into the waste package. As a result, … advective release from the waste package ([SAR] Section 2.3.7.12) is only possible when the degradation mode causing breach is general ([SAR] Section 2.3.6.3) or localized corrosion ([SAR] Section 2.3.6.4), when manufacturing defects result in early failure of waste packages ([SAR] Section 2.3.6.6), or when waste packages rupture due to stresses in the outer barrier exceeding the residual stress threshold as result of seismic vibratory ground motion or fault displacement."

- From SAR Section 2.1.2.2 (p. 2.1-40 – "Seismic Ground Motion Damages EBS Components"): "Vibratory ground motion has the potential to damage the waste package outer corrosion barrier as a result of waste package-to-waste package impacts and waste package-to-pallet impacts that may occur during a seismic event. This damage may result in residual stresses that exceed a tensile threshold for initiation and growth of stress corrosion cracks. The TAD and naval canisters enhance the structural stability of the waste packages prior to waste package breach. Once the outer corrosion barrier is breached by a crack network, corrosion of the waste package internals (specifically TAD and naval canisters) will compromise their capacity to support structural loads and to isolate the waste form during vibratory ground motion."

The remainder of this section presents quantitative results that demonstrate (1) the importance of the limited occurrence and extent of waste package damage area in reducing radionuclide releases from waste packages, and specifically (2) the importance of the TAD canister in reducing seismic-induced damage.

1.2.1 Summary of Waste Package Contribution to Barrier Capability

1.2.1.1 Occurrence and Nature of Waste Package Damage

This section describes the evolution of the waste packages over 1,000,000 years by summarizing results from the TSPA-LA. Four time periods are considered: before 170,000 years; from 170,000 to 300,000 years; from 300,000 years to 600,000 years; and beyond 600,000 years.

SAR Section 2.1.2.2.6 (pp. 2.1-75 and 2.1-76) provides a qualitative summary of these results. Only nominal and seismic events are considered here. Early failures are modeled as complete failure of the affected waste packages and thus do not have a variable effect on EBS capability. An igneous intrusion event, if it occurs, is modeled to cause complete failure of all EBS components, and thus the waste packages no longer act to prevent or slow the rate of movement of radionuclides (SAR Section 2.4.1.2.3, p. 2.4-17). For this reason, igneous events are not addressed in this discussion of waste package contribution to barrier capability.

0 to 170,000 years:

Prior to 170,000 years, mean dose and radionuclide releases from the EBS are determined by processes related to vibratory ground motion-induced waste package failures (SNL 2008b, Section 8.3.3.2.2[a]). These failures consist predominantly of stress corrosion cracks, which occur more frequently on CDSP waste packages than on CSNF waste packages. SAR Figure 2.1-12 demonstrates the relatively higher occurrence of damage to CDSP waste packages before 170,000 years as compared to CSNF waste packages. Comparison of SAR Figure 2.1-15(a) with SAR Figure 2.1-17(a) shows that stress corrosion crack damage is prevalent before 170,000 years as compared to patch damage. SAR Figure 2.1-12(c) for CDSP waste packages and SAR Figure 2.1-12(a) for CSNF waste packages show that the mean of the expected fraction of waste packages breached at 170,000 years is 0.37 for CDSP waste packages, as compared to 0.005 for CSNF waste packages.

170,000 to 300,000 years:

After about 170,000 years, waste package failure by nominal processes becomes more likely. SAR Figure 2.1-9 shows that nominal processes affect CDSP and CSNF waste packages similarly. Initial failure of waste packages by nominal processes consists of stress corrosion cracks of the closure-lid welds (SAR Section 2.4.2.2.1.2.1, p. 2.4-62). Although cracks resulting from nominal processes are more likely to occur than are cracks resulting from seismic events (SAR Figure 2.1-12), the cracks resulting from nominal processes have much less surface area (SAR Figures 2.1-13 and 2.1-15).

Between about 100,000 years and 300,000 years, drip shield failure is observed (SAR Figure 2.1-11). Failure of the drip shield allows accumulated rockfall (SAR Figure 2.1-14) to surround the waste packages, which results in low likelihood of additional damage from seismic events after drip shield failure (SAR Section 2.4.2.2.1.2.2.1, p. 2.4-67).

300,000 to 600,000 years:

From 300,000 to 600,000 years, waste package failures are due primarily to stress corrosion cracks from nominal processes (more common) or seismic events (less common). After 600,000 years, waste package breach by general corrosion (i.e., patches) becomes more likely (SAR Figure 2.1-10 for CSNF waste packages), but SAR Figure 2.1-9 shows that both CSNF and CDSP waste packages have similar responses to nominal processes. Based on SAR Figures 2.1-15(a) and 2.1-17(a), the mean of the expected fraction of CDSP waste package surface breached at 600,000 years is approximately 2×10^{-4} for cracks and approximately 2×10^{-4} for

patches. The crack area remains constant, indicating that new cracks, resulting from nominal processes (see SAR Figure 2.1-15(b)), do not significantly increase the overall crack area, which is largely attributable to prior seismic events. Conversely, the increase in patch area beginning at about 600,000 years (SAR Figure 2.1-17(a)) indicates the onset of general corrosion failures increasing the mean patch damage area beyond the relatively small mean area that results from the relatively infrequent occurrences of ruptures and punctures from seismic events. For CSNF waste packages, the trends in occurrence of damage and damage area between 300,000 and 600,000 years are similar but are smaller in magnitude to those described for CDSP waste packages. SAR Figures 2.1-13(a) and 2.1-16(a) show that the mean of the expected fraction of CSNF waste package surface area breached at 600,000 years is approximately 4×10^{-5} for cracks and approximately 5×10^{-5} for patches. The mean damage areas on CSNF waste packages are smaller than for CDSP waste packages because seismic damage (cracks, ruptures, or punctures) to CSNF waste packages is less likely to occur (see Section 1.2.2 of this RAI response).

600,000 to 1,000,000 years:

After 600,000 years, waste packages breached by general corrosion (i.e., patches) become more likely (SAR Figure 2.1-10), although by 1,000,000 years, the fraction of waste packages with patch breaches is still relatively small (mean of 0.09 at 1,000,000 years). When patches occur, accumulated breach area comprising patches greatly exceeds the breach area consisting of cracks. SAR Figures 2.1-15(a) and 2.1-17(a) show that the mean of the expected fraction of CDSP waste package surface area breached at 1,000,000 years is still approximately 2×10^{-4} for cracks and approximately 4×10^{-3} for patches. SAR Figures 2.1-13(a) and 2.1-16(a) show similar results for CSNF waste packages.

To summarize these results, nearly all waste package failures up to about 600,000 years are due to stress corrosion cracks. Infrequently, seismic events result in ruptures or punctures (SAR Figures 2.1-16(a) and 2.1-17(a)). Breaches by stress corrosion cracks have small failure areas and only permit diffusive releases from the waste packages. After 600,000 years, general corrosion patch failures become increasingly significant. Breaches by patches result in much larger penetration areas than stress corrosion cracks and allow advective releases out of the waste packages if seepage is present.

1.2.1.2 Effects of Waste Package Damage on Barrier Capability

This section describes the effects of waste package damage on the barrier capability of the EBS over 1,000,000 years by summarizing results from the TSPA-LA. Two time periods are considered: before 10,000 years and from 10,000 years to 1,000,000 years. SAR Section 2.1.2.2.6 (pp. 2.1-75 and 2.1-76) provides a qualitative summary of these results. Only nominal and seismic events are considered here for the reasons summarized in Section 1.2.1.1. In addition, the relative importance to repository performance (i.e., mean dose to the RMEI) of ruptures and punctures resulting from seismic events is summarized.

0 to 10,000 years:

The effect of crack breach area on the diffusive release of radionuclides from the waste package, and subsequently on EBS barrier performance, is illustrated by the analysis results documented in Section 7.3.2.6 of the TSPA-LA report (SNL 2008b). This analysis evaluated the numerical accuracy of the calculated expected annual dose for the seismic ground motion modeling case for 10,000 years. The modeling case approximates the consequences of seismic ground motion events by examining only the occurrence of stress corrosion crack (SCC) damage to CDSP waste packages with the drip shield intact and without rockfall, and without considering the effects of corrosion processes. Calculation of expected annual dose involved estimating the annual dose resulting from seismic events at specified times (i.e., 200, 1,000, 3,000, 6,000, 12,000, and 18,000 years) that caused specified surface area damage fractions (consisting of cracks) (i.e., 10^{-7}, 10^{-6}, 10^{-5}, 10^{-4}, and 10^{-3}) (SNL 2008b, Table 7.3.2-3). The modeling case considered that only diffusive releases from the CDSP waste packages can occur. Furthermore, because drift degradation was not considered, the thermal-hydrologic processes in the EBS remained the same as under nominal conditions.

Figure 7.3.2-9 of the TSPA-LA report (SNL 2008b) shows the annual dose results of a single realization (Realization 1) of the seismic ground motion modeling case for several different crack damage fractions for a seismic event at 100 years. Figure 7.3.2-10 of the TSPA-LA report (SNL 2008b) shows the annual dose history results for a seismic event at 11,200 years. As can be seen from the figures, the shape of the dose history is similar for each of different damage fractions, and does not significantly change for the 11,200-year event as compared with the 100-year event. More importantly, the magnitude of the annual dose increases proportionally with increasing damage fraction up to a damage fraction of 1×10^{-5}. Figure 7.3.2-12 of the TSPA-LA report (SNL 2008b) more clearly illustrates this effect by comparing the annual doses at 10,000 years for each damage fraction. This figure clearly indicates the strong relationship between damage fraction (i.e., crack area) and annual dose (up to a damage fraction of 1×10^{-5}) for a case with diffusive releases from CDSP waste packages.

Beyond a damage fraction of 1×10^{-5}, annual dose does not increase proportionally with increasing damage fraction for this particular modeling case. Generally, annual doses from seismic ground motion are dominated by ^{99}Tc (see for example, SAR Figure 2.4-26), and ^{99}Tc releases from the waste packages occur in pulse-like fashion following the initial breach (see for example, Figure K7.3-9(a) of SNL 2008b). The lack of increase in annual dose beyond a damage fraction of 1×10^{-5} indicates that, when damage area is sufficiently large, the rate of diffusion through the cracks in the waste package no longer constrains the release of ^{99}Tc from the waste package. Additional discussions on the effect of waste package breach area limiting ^{99}Tc release rates are provided in SAR Section 2.4.2.2.3.2.1 (pp. 2.4-94 to 2.4-96).

10,000 to 1,000,000 years:

Insight into the relative effects of waste package crack and patch breach areas on radionuclide releases from breached waste packages can be gained from a single realization analysis for the 1,000,000-year seismic ground motion modeling case (Realization 4641), summarized in SAR Section 2.4.2.2.3.2.2 and documented in Section 7.7.1.4[a] of the TSPA-LA report (SNL 2008b).

The breach areas from cracks and patches are shown in SAR Figures 2.4-96 (for a CDSP waste package) and 2.4-97 (for a CSNF waste package). Up to about 600,000 years for CDSP and 700,000 years for CSNF, the breach area is dominated by crack failures, with an area of about 0.01 m^2. After this time, the waste package breach area starts to increase rapidly due to the onset of general corrosion patch breaches.

SAR Figures 2.4-99 (for CDSP waste packages) and 2.4-101 (for CSNF waste packages) show the annual diffusive release rates of ^{99}Tc and ^{242}Pu, corresponding to the breach areas. For ^{242}Pu (SAR Figures 2.4-99(b) and 2.4-101(b)), the diffusive releases over time mimic the breach areas over time, remaining relatively constant until about 600,000 years for CDSP and 700,000 years for CSNF, then increasing corresponding to the increased breach area due to the onset of general corrosion patch breaches. The onset of general corrosion patches is typically associated with an increase in advective releases (if seepage is present), but the increased breach area also contributes to increased diffusive releases as shown in SAR Figures 2.4-99(b) and 2.4-101(b). These figures indicate the importance of limited breach area on limiting diffusive releases.

For ^{99}Tc (SAR Figures 2.4-99(a) and 2.4-101(a)), the diffusive releases occur over a shorter time. This is reflective of the fact that ^{99}Tc is not solubility limited and does not sorb onto corrosion products, thus leading to faster depletion of the ^{99}Tc inventory, relative to solubility-limited and sorbing radionuclides (i.e., ^{242}Pu). For this reason, ^{99}Tc release rates are more dependent on the time of the first breach than on the breach area evolution over time.

Finally, while advective release rates are not shown separately for this single realization analysis of the seismic ground motion modeling case, they can be inferred by comparing SAR Figure 2.4-106 with SAR Figures 2.4-99 and 2.4-101. For CSNF, the total release rate of ^{242}Pu (aqueous and colloidal) from all percolation subregions from the EBS is about 3.6 g/yr at 1,000,000 years (SAR Figure 2.4-106), whereas the sum of the diffusive releases from the waste packages for all percolation subregions is about 2.4 g/yr at 1,000,000 years (SAR Figure 2.4-101(b)). The difference, about 1.2 g/yr, which also reflects effects of solubility-limits and sorption on corrosion products, suggests that, for the waste package damage reflected in this realization of the seismic ground motion modeling case, advective release rates are of similar magnitude to diffusive release rates. This is in contrast to circumstances where the waste package outer barrier is completely failed, such as in the igneous intrusion modeling case. Figure 7.7.1-43[a] of the TSPA-LA report (SNL2008b) shows the annual release rates (advective and diffusive) of key radionuclides from CSNF waste packages in a single realization (Realization 2855) analysis for the 1,000,000-year igneous intrusion modeling case (SNL2008b, Section 7.7.1.3[a]). For each radionuclide, the advective release rate is about two orders of magnitude greater than the diffusive release rate.

1.2.1.3 Importance of Waste Package Rupture and Puncture

Seismic events may result in rupture or puncture of waste packages. Rupture of the waste package is conceptualized to occur when extreme deformation of the waste package outer barrier accumulates as a result of package-to-pallet impacts during seismic events (SNL2008b, Section 6.6.1.2.2.2). Puncture of the waste package may result when a severely deformed outer corrosion barrier is loaded down by rubble from rockfall and thus impinges on the edges or corners of fragments of the degraded internal structure (SNL 2008b, Section 7.3.2.6.1.3.6). Rupture and puncture differ from stress corrosion cracking by permitting advection of seepage through the waste package, and thus would affect EBS barrier capability differently than do stress corrosion cracks. However, analysis provided in TSPA-LA report (SNL 2008b, Sections 7.3.2.6.1.3.5 and 7.3.2.6.1.3.6) shows that the frequency of events resulting in rupture or puncture are small ($<10^{-7}$ per year), and before 10,000 years, the relative importance to mean annual dose of these types of damage is correspondingly negligible. SAR Figures 2.1-16 and 2.1-17 show that rupture and puncture may occur and are considered in the estimated mean dose to the RMEI over the 1,000,000-year period, as reflected by low values of mean damage area prior to the occurrence of patches due to general corrosion around 500,000 years. However, the relatively low contribution to mean dose from solubility-limited radionuclides (e.g., ^{239}Pu in SAR Figure 2.4-26) indicates that waste package rupture and puncture remain of minor importance to mean dose over the 1,000,000-year period.

1.2.2 TAD Canister Enhanced Structural Capability

The discussion presented in Section 1.2.1.1 indicates the effect of the TAD Canister in preventing waste package failures and thereby contributing to the barrier capability of the waste form and waste package internals feature of the EBS. As noted in SAR Section 2.1.2.2.6 (p. 2.1-62), the TAD canister provides enhanced structural response capability (i.e., damping) to damage from seismic ground motion.

As described in Section 1.2.1.1, and shown in SAR Figure 2.1-10, nominal failures do not begin until about 170,000 years. Therefore all prior failures in the seismic ground motion modeling case are due to damage from seismic events. Comparing SAR Figure 2.1-12(d) for CDSP waste packages and SAR Figure 2.1-12(b) for CSNF waste packages, the mean expected fraction of waste packages breached due to seismic ground motion at 170,000 years is 0.37 for CDSP and 0.005 for CSNF. SAR Section 2.4.2.2.1.1.2 provides a value of 5.3×10^{-9} per year for the expected frequency of seismic events which result in damage to intact CSNF waste packages before drift collapse. This compares to a frequency of seismic events that may cause damage to intact CDSP waste packages that is estimated to be as large as 2.2×10^{-5} per year before drift collapse (SNL2008b, Section 7.3.2.1.3.7). The relatively low frequency of damage to CSNF waste packages results from the increased structural strength due to the presence of the TAD canister (SAR Section 2.4.2.2.3.2.2, p. 2.4-99).

1.3 SOLUBILITY LIMITS

This subsection describes how the solubility limits in the different transport model domains, including uncertainties, affect the capability of the components of the waste form and waste package internals.

Solubility limits are represented by ITBC FEP 2.1.09.04.0A (Radionuclide Solubility, Solubility Limits, and Speciation in the Waste Form and EBS) and are associated with the following ITWI waste form and waste package internals components listed in SAR Table 2.1-1: Commercial Spent Nuclear Fuel and High Level Glass. These two components are ITWI because of their slow degradation rates (see Section 1.1). Solubility limits are also associated with DOE Spent Nuclear Fuel, which is classified as Non-ITWI in SAR Table 2.1-1.

In the TSPA-LA submodel for dissolved radionuclide concentration limits (see SAR Section 2.3.7.10), solubilities of Pu, Np, U, Th, Am, Th, Sn, and Pa are modeled as a function of pH and f_{CO2}, which is approximated by pCO_2 (SAR Section 2.3.7.10.3, p. 2.3.7-54). The uncertain variables, pH and f_{CO2}, are outputs of the in-package chemistry submodel. Uncertainties associated with thermodynamic data and water chemistry (e.g., fluoride levels and ionic strength) are accounted for in the solubility models of those eight radionuclides (SAR Sections 2.3.7.10.2 and 2.3.7.10.3).

The solubilities for these elements are shown in SAR Figures 2.3.7-29 through 2.3.7-34. In general, the solubilities have a U-shape (or V-shape) curve with respect to pH. Minimum solubility generally is reached at neutral to mildly basic pH. Solubilities increase as pH moves away from the neutral conditions and becomes more acidic or more alkaline. For a given pH, solubilities increase as f_{CO2} increases (SAR Section 2.3.7.10.3, p. 2.3.7-54). The f_{CO2} dependence is strong under alkaline conditions and becomes negligible under acidic conditions.

For other elements, such as Tc, C, I, Cs, Se, Cl, and Sr, no solubility-limited concentration is defined. Therefore, the release of those elements from the waste form and EBS is not constrained by solubility (SAR Section 2.3.7.10.3, p. 2.3.7-54).

Generally speaking, the solubility-limited elements have low to medium solubilities, depending on pH and f_{CO2}. However, the effectiveness of solubility constraints varies from modeling case to modeling case, from element to element, and from domain to domain. Radionuclides that are affected by solubility limits and also are key contributors to overall dose (SAR Figure 2.4-20) are: ^{239}Pu, ^{240}Pu, and ^{237}Np at 10,000 years; and ^{242}Pu and ^{237}Np at 1,000,000 years.

The effect of these solubility limits to limit releases from the waste form and waste package is demonstrated below using single-realization TSPA-LA results and results from the uncertainty and sensitivity regression analyses in Appendix K of the TSPA-LA report (SNL 2008b).

1.3.1 Effect of Solubility Limits for 10,000 Years Post-Closure

For the first 10,000 years post-closure, the scenarios and modeling cases which make the largest contribution to mean dose to the RMEI are the seismic ground motion and igneous intrusion modeling cases (SAR Figure 2.4-18a). Thus, the extent to which solubility limits prevent radionuclide releases from the waste form and waste package within 10,000 years can be observed from these two modeling cases.

1.3.1.1 Seismic Ground Motion Modeling Case for 10,000 Years

The radionuclides which constitute most of the mean dose to the RMEI from the seismic ground motion modeling case for 10,000 years are those without solubility limits, namely ^{99}Tc, ^{14}C, and ^{129}I (SAR Figure 2.4-26). Radionuclides with solubility limits, such as ^{239}Pu, are negligible contributors to the mean dose because the release rate and total mass release from the EBS is also small (SNL 2008b, Figure K7.3-7). The absence of advection through the waste (Section 1.2 of this RAI response) is the dominant factor in limiting the release of these radionuclides. Of the mass of plutonium that is released, sensitivity analysis results (SNL 2008b, Figures K7.3-7 and K.7.3-8) indicate that uncertain variables which affect solubility limits (uncertainty in plutonium solubility at low ionic strength, EP1LOWPU, uncertainty in partial pressure of CO_2, DELPPCO2, and uncertainty in pH in HLW cell 1a under vapor influx conditions, PH2MCONS) are influential to the uncertainty in ^{239}Pu releases within the first 10,000 years after seismic damage occurs. The first important variable directly affects plutonium solubility, while the other variables control parameters (pH and pCO_2) that influence solubility. Therefore, solubility limits are moderately important (relative to the effect of the limited waste package damage) to barrier capability to prevent the movement of solubility-limited radionuclides for the first 10,000 years, because these solubility limits constrain the movement of radionuclides from the waste form domain to the corrosion products domain. In contrast, for plutonium, sorption onto corrosion products is less influential to ^{239}Pu releases within the first 10,000 years after seismic damage occurs, as indicated by the relatively weak correlation of uncertainty in ^{239}Pu releases with uncertainty in the density of sorption sites on goethite (GOESITED).

For neptunium, Figures K7.3-5 and K7.3-6 of the TSPA-LA report (SNL 2008b) indicate that sorption onto corrosion products is somewhat more influential than solubility limits to releases of ^{237}Np for the first 10,000 years after seismic damage occurs, as indicated by the comparatively stronger correlations of uncertainty in ^{237}Np releases with GOESITED and the appearance of other uncertain variables that influence sorptive capacity (hydrous ferric oxide specific surface area (HFOSA), and goethite specific surface area (GOESA)). In contrast, the analysis shows relatively weaker correlations with uncertain variables that influence neptunium solubility (uncertainty in neptunium solubility in nominal or seismic conditions at ionic strength below 1 molal (EP1LOWNU) and DELPPCO2).

1.3.1.2 Igneous Intrusion Modeling Case for 10,000 Years

The mean dose to the RMEI from the igneous intrusion modeling case for 10,000 years comprises radionuclides with and without solubility limits (SAR Figure 2.4-30). Two radionuclides with solubility limits, ^{239}Pu and ^{240}Pu, are large contributors to the mean dose. Figures K6.3.1-7 and K6.3.1-8 of the TSPA-LA report (SNL 2008b) show that the most influential uncertain variables to the uncertainty in release of ^{239}Pu from the EBS following an igneous intrusion include: uncertainty in plutonium solubility at low ionic strength (EP1LOWPU), uncertainty in partial pressure of CO_2 (DELPPCO2), and uncertainty in pH in CSNF cell 1 under liquid influx conditions (PHCSS). The first important variable directly affects Pu solubility, while the other variables control parameters (pH and pCO_2) that influence solubility. The other influential uncertain variable identified by sensitivity analysis is uncertainty in infiltration scenario (INFIL), which influences the total water moving through the unsaturated zone.

Figures K6.3.1-5 and K6.3.1-6 of the TSPA-LA report (SNL 2008b) show that solubility limits are also important in constraining the release of ^{237}Np from the EBS, although ^{237}Np is a minor contributor to mean dose from this modeling case.

1.3.2 Effect of Solubility Limits for 1,000,000 Years Post-Closure

For 1,000,000 years post-closure, the scenarios and modeling cases which make the largest contribution to mean dose to the RMEI are the seismic ground motion modeling case (which includes nominal processes) and the igneous intrusion modeling case (SAR Figure 2.4-18b). Thus, the extent to which solubility limits prevent radionuclide releases from the waste form and waste package for 1,000,000 years can be observed from these two modeling cases.

1.3.2.1 Seismic Ground Motion Modeling Case for 1,000,000 Years

For most of the 1,000,000-year period, the radionuclides which constitute most of the mean dose to the RMEI from the seismic ground motion modeling case are those without solubility limits, namely ^{99}Tc, and ^{129}I (SAR Figure 2.4-26). At very late times, both ^{242}Pu and ^{237}Np become relatively large contributors to the mean dose. The importance of solubility limits to releases of plutonium and neptunium can be illustrated by results from single realization analyses and from sensitivity analysis.

A single realization analysis for the 1,000,000–year seismic ground motion modeling case (Realization 4641) is summarized in SAR Section 2.4.2.2.3.2.2 and documented in Section 7.7.1.4[a] of the TSPA-LA report (SNL 2008b). The relationship between cumulative mass released from inventory (i.e., waste form degradation), cumulative mass sorbed on corrosion products, solubility limits, and dissolved concentration for ^{242}Pu in failed waste packages over time is discussed in SAR Section 2.4.2.2.3.2.2 (pp. 2.4-102 and 2.4-103). The analysis concludes that the most influential process in reducing releases of ^{242}Pu from failed waste packages is sorption onto corrosion products, although solubility limits also constrain the movement of radionuclides within the waste package. For example, SAR Figure 2.1-102 shows that, from the time of initial CSNF waste package breaches (all of which are stress corrosion

cracks in this realization) at about 200,000 years until about 350,000 years, the ^{242}Pu concentration in the waste package (i.e., in the corrosion products domain) is constrained by the plutonium solubility limit. The combined effects of sorption onto corrosion products and solubility limits on the ^{242}Pu mass release rates from the waste package can be observed by comparing ^{242}Pu mass release rates (SAR Figures 2.4-99(b) and 2.4-101(b)) to the ^{99}Tc mass release rates (SAR Figures 2.4-99(a) and 2.4-101(a)), which are not affected by sorption on corrosion products or solubility limits. The comparison shows that sorption and solubility limits together result in delay and reduction of the release of ^{242}Pu from the waste package after initial waste package breach.

At later times, the majority of CSNF waste package failures in the seismic ground motion modeling case are due to nominal processes (SAR Figure 2.1-12). Thus, the importance of solubility to barrier capability in this case can be observed from the nominal modeling case, which considers only nominal processes. A single realization analysis for the 1,000,000-year nominal modeling case (Realization 286) is summarized in SAR Section 2.4.2.2.3.1 and documented in Section 7.7.1.5[a] of the TSPA-LA report (SNL 2008b). SAR Figure 2.4-68 shows that the mass release rate of ^{242}Pu from the waste form is significantly higher than the mass release rate from the waste package. This reduction in release rate between different cells in the EBS transport model indicates the influence of the combined effects of solubility limits and sorption on corrosion products in the waste package, similar to what was observed in the seismic ground motion modeling case. Sensitivity analyses documented in Appendix K of the TSPA-LA report (SNL 2008b, Figures K4.4-1 and K4.4-2) show that the most influential uncertain variables to uncertainty in the release of ^{237}Np from the EBS are those related to waste package failure (i.e., temperature dependence term in Alloy 22 general corrosion rate (WDGCA22)), followed by several variables related to neptunium solubility (i.e., uncertainty in pH in CSNF cell 1 under vapor influx conditions (PHCSNS) and uncertainty in NpO_2 solubility at ionic strength below 1 molal (EP1NPO2)). EP1NPO2 directly affects Np solubility, while PHCSNS controls pH that in turn influences solubility. The appearance of these two variables in the sensitivity analysis indicates that, after processes influencing waste package failure, solubility limits are the next most important process affecting release of neptunium from the EBS in the seismic ground motion modeling case.

1.3.2.2 Igneous Intrusion Modeling Case for 1,000,000 Years

The radionuclides which constitute most of the mean dose to the RMEI from the igneous intrusion modeling case are ^{239}Pu, ^{242}Pu, and ^{237}Np (SAR Figure 2.4-28). In addition, ^{226}Ra is an important contributor to mean dose, because it results from decay of ^{234}U to ^{230}Th; thus, the influence of uranium solubility may also be important. The importance of solubility limits to releases of plutonium, neptunium, and uranium can be illustrated by results from single realization analyses and from sensitivity analysis.

Two single realization analyses for the 1,000,000-year igneous intrusion modeling case are documented in Section 7.7.1.3[a] of the TSPA-LA report (SNL 2008b). For the first analyzed realization (Realization 2855), the solubility limits and dissolved concentrations for Pu, Np, and U in both the CSNF waste form domain and the CSNF corrosion products domain over time are shown in Figures 7.7.1-40[a] and 7.7.1-44[a], respectively, of the TSPA-LA report (SNL 2008b)

and described in Section 7.7.1.3[a] (SNL 2008b, pp. 7-56[a] to 7-58[a]). For this analyzed realization, the intrusion time is at 10,000 years.

Figure 7.7.1-40[a] shows that in the CSNF waste form domain, concentrations of all three radionuclides are solubility limited: U for the entire 1,000,000 years, Pu for the first 200,000 years, and Np for the first 40,000 years. Figure 7.7.1-44[a] shows that in the CSNF corrosion products domain, concentrations of Pu (270,000 years) and Np (100,000 years) are solubility limited for longer than in the waste form domain, but U never reaches a solubility limit. These solubility limits in the corrosion products domain are directly responsible for the plateau in annual dose (controlled by ^{239}Pu and ^{237}Np) shown in Figure 7.7.1 39[a] of the TSPA-LA report (SNL 2008b).

For the second analyzed realization (Realization 191), the igneous event occurs at 250 years after closure. The solubility limits and dissolved concentrations for Pu and U in the CSNF waste form domain over time are shown in Figure 7.7.1-51[a] of the TSPA-LA report (SNL 2008b) and described in Section 7.7.1.3[a] (SNL 2008b, pp. 7-59[a] and 7-60[a]). This outlier realization has the highest annual dose from about 50,000 years to about 300,000 years, and the dose is controlled by ^{239}Pu (SNL 2008b, Figure 7.7.1-49[a]). Figure 7.7.1-51[a] indicates that the Pu concentration in the CSNF waste form domain is solubility limited for the first 150,000 years. Therefore, the solubility limit is constraining the annual dose. It should also be noted that the mean annual dose plateaus at a higher value in this realization than in the first realization because the Pu solubility limit, which is determined from sampled parameters, is higher.

Additional indicators of the importance of solubility limits are evident in the regression analyses documented in the Appendix K of the TSPA-LA report (SNL 2008b). Figure K6.3.2-4 of the TSPA-LA report (SNL 2008b) shows that the uncertain variable that most influences the release of ^{239}Pu after an igneous event is the uncertainty in plutonium solubility at ionic strength below 1 molal (EP1LOWPU). Other variables which affect solubility are also influential, namely uncertainty in partial pressure of CO_2 (DELPPCO2), and pH in CSNF cell 1 under liquid influx conditions (PHCSS). The influence of these uncertain variables is comparatively stronger than that for the density of sorption sites on goethite (GOESITED), indicating that solubility limits are comparatively more influential than is the process of sorption onto corrosion products. Figure K6.3.2-3 of the TSPA-LA report (SNL 2008b) shows similar influence of solubility limits on ^{237}Np releases (except EP1NPO2, uncertainty in NpO_2 solubility at ionic strength below 1 molal, replaces EP1LOWPU). Finally, Figures K6.3.2-5[a] and K6.3.2-6[a] of the TSPA-LA report (SNL 2008b) show similar influence of solubility limits on ^{234}U releases (with EP1LOWOU, uncertainty in U solubility in other than nominal or seismic conditions at ionic strength below 1 molal, in place of EP1LOWPU).

1.4 SORPTION TO STATIONARY CORROSION PRODUCTS

This subsection describes how sorption to stationary corrosion products and the desorption rate, including uncertainties, affects the capability of the waste form and waste package internals components.

Sorption onto corrosion products is represented by ITBC FEP 2.1.09.05.0A (Sorption of Dissolved Radionuclides in EBS) and is associated with the following ITWI components of the waste form and waste package internals feature listed in SAR Table 2.1-1: TAD Canister. The TAD Canister is ITWI because it provides enhanced structural response capability (i.e., damping) to damage from seismic ground motion (see Section 1.2.2). Corrosion products are also associated with the DSNF Canister and HLW Canister components, which are classified as Non-ITWI in SAR Table 2.1-1 and with several internals components (TAD Canister Internals, DSNF Canister Internals, and Codisposal Waste Package Internals) which are either Non-ITWI or ITWI for reasons unrelated to corrosion products (e.g., criticality control). Finally, corrosion products are associated with the waste package inner vessel, which is an ITWI component of the waste package feature of the EBS.

On average, degradation of steel to corrosion products is complete, as indicated by complete degradation of the inner vessel which is the thickest steel component, by about 95,000 years after initial waste package breach, as discussed in *EBS Radionuclide Transport Abstraction* (SNL 2007, Section 6.3.4.2.1, p. 6-46) (hereafter referred to as the EBS RTA report). The ITWI determination of components affected by sorption onto corrosion products depends on the relative mass of steel in the various components (inner vessel, canisters, and internals) in the CSNF and CDSP waste packages. The relative mass of steel in CSNF and CDSP waste packages in the EBS RTA submodel, implemented in TSPA-LA to model EBS transport, is summarized in Tables 1.4-1 and 1.4-2, respectively. In the EBS RTA submodel, some steel is assigned to the waste form (WF) domain (cell 1) and some steel is assigned to corrosion products (CP) domain (cell 2). Although all of the steel degrades to produce corrosion products, the EBS RTA submodel does not take credit for sorption onto corrosion products in the waste form domain. Therefore, the mass of steel considered for sorption on corrosion products is based on the steel in the CP domain only. It should be noted that, while the steel in the WF domain does not contribute to sorption onto corrosion products, it is considered in the in-package chemistry submodel for that domain.

Table 1.4-1 shows the mass of steel in a CSNF waste package. The mass of steel for each waste package component is based on design values from Table 4.1-22 of the EBS RTA report (SNL 2007). The EBS RTA model domains are identified in the footnotes of Table 6.3-8 of the EBS RTA report (SNL 2007). Table 1.4-2 shows the mass of steel in a CDSP waste package. The mass of steel for each waste package component is based on design values from Table 4.1-22 of the EBS RTA report (SNL 2007) (HLWG Canister and DSNF Canister and Internals masses are from Table 6.3-9 of SNL 2007). The EBS RTA model domains are identified in the footnotes of Table 6.3-9 of the EBS RTA report (SNL 2007). A discussion of the availability of preliminary and final design values for the mass of steel in each waste package component and the values used in the EBS RTA submodel is provided in Section 6.3.4.3.4.1 of the EBS RTA report (SNL 2007).

Table 1.4-1 shows that, for CSNF waste packages, 58.7% of the CP domain corrosion products derive from the waste package inner vessel, 29.7% from the TAD Canister, and 11.6% from the TAD Canister Internals. Table 1.4-2 shows that, for CDSP waste packages, 69.3% of the CP domain corrosion products derive from the waste package inner vessel, 0.0% from the HLW and DSNF Canisters, and 30.7% from the canister and waste package internals. The HLW Canister and the DSNF Canister do not contribute to sorption onto corrosion products because both are assigned to the waste form domain of the CDSP waste package.

Table 1.4-1. Mass of Steel in a CSNF Waste Package

Waste Package Component	EBS Component	EBS RTA Model Domain	Mass (lbm)	% of Mass
Side Guides	Internals	CP	1,690.0	
End Side Guides	Internals	CP	2,520.0	
Corner Guides	Internals	CP	2,070.0	
Fuel Tubes	Internals	Waste Form	13,600.0	
Borated SS A Plates	Internals	Waste Form	2,760.0	
Borated SS B Plates	Internals	Waste Form	2,760.0	
Borated SS C Plates	Internals	Waste Form	2,900.0	
Shield Plug	TAD Canister	N/A [a]	0.0 [a]	
Inner Seal Plugs	TAD Canister	CP	0.5	
Spread Ring	TAD Canister	CP	93.8	
Spread Ring Filler Segment	TAD Canister	CP	2.2	
Outer Seal Plate	TAD Canister	CP	106.0	
Outer Seal Plug	TAD Canister	CP	0.3	
TAD Shell	TAD Canister	CP	15,900.0	
Inner Vessel	WP Inner Vessel	CP	27,093.7	
Inner Vessel Top Lid	WP Inner Vessel	CP	2,120.3	
Inner Vessel Bottom Lid	WP Inner Vessel	CP	2,283.0	
Interface Ring	WP Inner Vessel	CP	85.9	
Spread Ring	WP Inner Vessel	CP	82.1	
Total 316 SS Welds	WP Inner Vessel	CP	91.1	
Total Steel in Waste Form (WF) Domain		Waste Form	22,020.0 [b]	
Total Steel in Corrosion Product (CP) Domain		CP	54,138.9	
Total Steel in CP Domain from Internals	Internals	CP	6280.0	**11.6**
Total Steel in CP Domain from Canister	TAD Canister	CP	16,102.8	**29.7**
Total Steel in CP Domain from WP Inner Vessel	WP Inner Vessel	CP	31,756.1	**58.7**

[a] The mass of steel in the shield plug does not contribute to the mass of corrosion products in the EBS RTA model (SNL 2007, Section 6.5.2.1.1.2, p. 6-165).

[b] The mass of steel in the waste form domain does not contribute to the mass of corrosion products in the EBS RTA model (SNL 2007, Section 6.5.2, p. 6-162).

NOTE: The total steel in the WF domain (10,009 kg based on a conversion factor of 2.2 lbm/kg) is consistent with the value of 9,990 kg shown in Table 6.3-8 of the EBS RTA report (SNL 2007). The total steel in the CP domain (24,609 kg based on a conversion factor of 2.2 lbm/kg) is consistent with the value of 24,600 kg shown in Table 6.3-8 of the EBS RTA report (SNL 2007).

Table 1.4-2. Mass of Steel in a CDSP Waste Package

Waste Package Component	EBS Component	EBS RTA Model Domain	Mass (lbm)	% of Mass
Divider Plate – Plates	Internals	CP	1,107.5	
Divider Plate – Outer Brackets	Internals	CP	4,121.0	
Divider Plate – Inner Brackets	Internals	CP	3,291.6	
Divider Plate – Tube	Internals	CP	4,246.0	
Shield Plug	Canisters	N/A [a]	0.0 [a]	
HLWG Canisters (5)	HLW Canister	Waste Form (HLW)	8,316.0	
DSNF Canister and Internals	DSNF Canister and Internals	Waste Form (DSNF)	2,816.0	
Inner Vessel	WP Inner Vessel	CP	25,884.4	
Inner Vessel Top Lid	WP Inner Vessel	N/A [a]	0.0 [a]	
Inner Vessel Bottom Lid	WP Inner Vessel	CP	2,714.9	
Interface Ring	WP Inner Vessel	CP	93.7	
Spread Ring	WP Inner Vessel	CP	90.0	
Total 316 SS Welds	WP Inner Vessel	CP	100.9	
Total Steel in Waste Form (WF) Domains		Waste Form	11,132.0 [b]	
Total Steel in Corrosion Product (CP) Domain		CP	41,650.0	
Total Steel in CP Domain from Internals	Internals	CP	12,776.1	**30.7**
Total Steel in CP Domain from Canister	Canisters	CP	0.0	**0.0**
Total Steel in CP Domain from WP Inner Vessel	WP Inner Vessel	CP	28,883.9	**69.3**

[a] the mass of steel in the top lid shield plug does not contribute to the mass of corrosion products in the EBS RTA model (EBS RTA Report, Section 6.5.2.1.2, p. 6-167).

[b] the mass of steel in the waste form domain does not contribute to the mass of corrosion products in the EBS RTA model (EBS RTA Report, Section 6.5.2, p. 6-162).

NOTE: The total steel in the WF domain (5,060 kg based on a conversion factor of 2.2 lbm/kg) is consistent with the value of 5,060 kg shown in Table 6.3-9 of the EBS RTA report (SNL 2007). The total steel in the CP domain (18,932 kg based on a conversion factor of 2.2 lbm/kg) is consistent with the value of 18,900 kg shown in Table 6.3-9 of the EBS RTA report (SNL 2007).

Based on the results from Tables 1.4-1 and 1.4-2, only the waste package inner vessel contributes a significant enough mass of steel to be ITWI for sorption onto corrosion products. All of the CSNF components of the waste form and waste package internals feature (TAD Canister and TAD Canister Internals) and all of the CDSP components (HLW Canister, DSNF Canister, DSNF Canister Internals, and Codisposal Waste Package Internals) are Non-ITWI with respect to sorption onto corrosion products because they do not contain a significant enough mass of steel that contributes to sorption onto corrosion products.

In the TSPA-LA submodel for EBS flow and transport (i.e., the EBS RTA model) (see SAR Section 2.3.7.12), a competitive equilibrium sorption-desorption model is implemented for the corrosion products domain (i.e., TSPA-LA EBS transport submodel corrosion products domain (cell 2)). This model considers sorption of U, Np, Pu, Am, Th, and Ni onto the stationary

corrosion products, which are produced from the degradation of steel in the CP domain (cell 2). The model also considers kinetic desorption of Pu and Am that is described by a desorption (backward) rate, based on a sampled forward rate (SAR Section 2.3.7.12.1, pp. 2.3.7-70 and 2.3.7-71). Moreover, the competitive sorption model takes into account the effect of stationary corrosion products on the in-package chemistry (e.g., pH) conditions of the CP domain (SAR Section 2.3.7.12.2, p. 2.3.7-72).

In general, sorption onto stationary corrosion products significantly retards movement of some radionuclides from a breached waste package. Radionuclides that are affected by sorption on corrosion products and also are key contributors to overall dose (SAR Figure 2.4-20) are ^{239}Pu, ^{240}Pu, and ^{237}Np. The effect of sorption on corrosion products to delay and limit releases from the waste package and its relative importance are demonstrated below using TSPA-LA results, including single realization cases and uncertainty and sensitivity analyses.

1.4.1 Seismic Ground Motion Modeling Case for 10,000 Years

The radionuclides which constitute most of the mean dose to the RMEI from the seismic ground motion modeling case for 10,000 years are those without solubility limits, namely ^{99}Tc, ^{14}C, and ^{129}I (SAR Figure 2.4-26). Radionuclides with solubility limits, such as ^{239}Pu, are negligible contributors to the mean dose because the release rate and total mass release from the EBS is also small (SNL 2008b, Figure K7.3-7). The absence of advection through the waste (Section 1.2 of this RAI response) is the dominant factor in limiting the release of these radionuclides. Of the radionuclide mass that is released, as discussed in Section 1.3.1.1, sensitivity analysis results (SNL 2008b, Figures K7.3-7 and K.7.3-8) indicate that uncertain variables which affect solubility limits are most influential to the release of plutonium, with sorption onto corrosion products having less influence within the first 10,000 years. For neptunium releases, sorption onto corrosion products is relatively more influential than are solubility limits.

1.4.2 Seismic Ground Motion Modeling Case for 1,000,000 Years

A single realization analysis for the 1,000,000-year seismic ground motion modeling case (Realization 4641) is summarized in Section 2.4.2.2.3.2.2 of the SAR and documented in Section 7.7.1.4[a] of the TSPA-LA report (SNL 2008b). This is the same analysis referenced in Section 1.3.1 for solubility limits.

The relationship between cumulative mass released from inventory (i.e., waste form degradation), cumulative mass sorbed on corrosion products, solubility limits, and dissolved concentration for ^{242}Pu in CSNF waste packages over time is shown in SAR Figure 2.4-102 and described in SAR Section 2.4.2.2.3.2.2 (pp. 2.4-102 and 2.4-103). The figure shows that, after the time of initial CSNF waste package breaches (all of which are stress corrosion cracks in this realization), at about 200,000 years nearly all of the ^{242}Pu mass released from the waste form sorbs onto corrosion products. Subsequent ^{242}Pu mass release rates from the waste package (SAR Figure 2.4-101(b)) are controlled by desorption of ^{242}Pu from the corrosion products, which in turn controls the dissolved concentration in the corrosion products domain (i.e., the waste package) (SAR Figure 2.4-102). Although desorption rates are not presented, SAR

Figure 2.4-102 suggests that from 200,000 to 350,000 years, desorption rates are high enough that ^{242}Pu concentrations are controlled by the solubility limits. After 350,000 years, desorption rates are lower, and the available mass of ^{242}Pu is not enough to reach the solubility limits. During this time, ^{242}Pu concentrations are controlled by the desorption rate.

As in Section 1.3.1, a comparison of ^{242}Pu mass release rates from the waste package (SAR Figure 2.4-101(b)) with ^{99}Tc mass release rates (SAR Figure 2.4-101(a)), which are not affected by sorption on corrosion products or solubility limits, provides a further indication of the combined effects of solubility limits and sorption on corrosion products in limiting releases from CSNF waste packages.

A similar relationship for ^{242}Pu in CDSP waste packages over time is shown in SAR Figure 2.4-100 and described in SAR Section 2.4.2.2.3.2.2 (p. 2.4-102). The CDSP waste packages (SAR Figure 2.4-94) fail much earlier than the CSNF waste packages (SAR Figure 2.4-94) due to seismic ground motion in this modeling case. As with the CSNF waste packages, nearly all of the ^{242}Pu mass released from the waste form sorbs onto corrosion products (SAR Section 2.4.2.2.3.2.2, p. 2.4-102). However, for the CDSP waste packages, the ^{242}Pu dissolved concentrations never reach the solubility limits in this realization (SAR Figure 2.4-100). Therefore, in this realization, the ^{242}Pu concentrations are controlled by the Pu desorption rate for all times.

1.4.3 Igneous Intrusion Modeling Case

The importance of sorption on corrosion products in the igneous intrusion modeling case is indicated by the regression analyses documented in the Appendix K of the TSPA-LA report (SNL 2008b). Figure K6.3.2-3 of the TSPA-LA report (SNL 2008b) shows that, for the first 200,000 years after an igneous event, the uncertain variables that are most influential on the release of ^{237}Np from the EBS are those related to Np solubility (i.e., uncertainty in NpO_2 solubility at ionic strength below 1 molal (EP1NPO2) and uncertainty in pH in CSNF cell 1 under liquid influx conditions (PHCSS)). From 200,000 years after the igneous event, the uncertain variable that is most influential on the release of ^{237}Np from the EBS is the density of sorption sites on goethite (GOESITED), which directly affects the sorptive capacity of corrosion products.

For plutonium, Figure K6.3.2-4 of the TSPA-LA report (SNL 2008b) shows that, for the first 200,000 years after an igneous intrusion, uncertainty in release of ^{239}Pu is most strongly influenced by uncertainty in plutonium solubility, as indicated by the correlation with uncertainty in Pu solubility at ionic strength below 1 molal (EP1LOWPU). However, sorption onto corrosion products also has an effect because uncertainty in the density of sorption sites on goethite (GOESITED) is also influential on the uncertainty in the release of ^{239}Pu from the EBS. For ^{242}Pu, it is expected that, from 200,000 years after the igneous event and beyond, sorption onto corrosion products will become increasingly influential, as the inventory in the waste form domain is depleted and release from the EBS is increasingly determined by desorption from corrosion products.

1.5 COLLOIDAL PROCESSES

This subsection describes why colloidal processes, including uncertainties, are classified as Non-ITBC. Colloidal processes are associated with the following components of the waste form and waste package internals listed in SAR Table 2.1-1: Commercial Spent Nuclear Fuel and High Level Glass, and DOE Spent Nuclear Fuel. As noted in Section 1, the classification of Non-ITBC does not mean that colloidal radionuclides have no effect on barrier capability, only that they are not a significant contributor to the barrier capability relative to the other processes (i.e., relative to dissolved radionuclides). It should also be noted that this Non-ITBC classification of colloidal processes applies to all scenarios, including nominal, igneous intrusion, and seismic ground motion.

The Non-ITBC classifications of FEPs related to colloidal processes in the EBS, and their underlying bases, are presented in Table A-2 of the PNSDB report (SNL 2008a, pp. A-125 to A-132) and summarized in SAR Table 2.1-3 (p. 2.1-130). Although all of the colloidal process FEPs are Non-ITBC, the following six FEPs are included in the TSPA-LA model:

- 2.1.09.16.0A (Formation of Pseudocolloids (natural) in EBS)
- 2.1.09.17.0A (Formation of Pseudocolloids (corrosion product) in EBS)
- 2.1.09.19.0B (Advection of Colloids in EBS)
- 2.1.09.23.0A (Stability of Colloids in EBS)
- 2.1.09.24.0A (Diffusion of Colloids in EBS)
- 2.1.09.25.0A (Formation of Colloids (waste-form) by Co-Precipitation in EBS).

In the PNSDB report (SNL 2008a, Table A-2, pp. A-125 to A-132), each of these colloid FEPs state, "Although considered and accounted for in the postclosure analyzed basis, the contribution of colloid transport processes is less significant than that associated with the transport of dissolved radionuclides and parameter characteristics associated with the transport of colloids are not considered ITBC."

SAR Figure 2.1-20 shows the mean total activity of all radionuclides released from the EBS for the combined nominal/early failure modeling case for both compliance periods (10,000 years and post-10,000 years). This figure shows that ^{99}Tc dominates the mean total activity released from the EBS over the compliance periods. The second most important radionuclide changes over time. Starting at early time, the second most important radionuclide is ^{137}Cs (up to about 500 years), then ^{241}Am (up to about 2,000 years), then ^{239}Pu (up to about 200,000 years), then ^{237}Np (up to about 300,000 years), and then ^{242}Pu, which is the second most important to mean total activity released from the EBS at 1,000,000 years. ^{242}Pu is also the most important contributor to the overall total mean annual dose at 1,000,000 years (SAR Figure 2.4-20), so ^{242}Pu is examined here. The maximum ^{242}Pu mean activity due to irreversible colloids ($^{242}Pu^{I}$) in SAR Figure 2.1-20 is 30% of the total ^{242}Pu activity ($^{242}Pu^{T}$), occurring at 808,000 years.

SAR Figure 2.1-23 shows the equivalent of SAR Figure 2.1-20 but for the seismic ground motion modeling case. For this case, the maximum ^{242}Pu mean activity due to irreversible colloids is 18%, occurring at 768,000 years.

The TSPA-LA report (SNL 2008b, Section P18.3) describes an impact analysis using the igneous intrusion modeling case. Figure P-13 shows contributions to mean annual dose over time from dissolved and colloidal ^{242}Pu and ^{239}Pu. Associated release rates from the EBS for dissolved and colloidal ^{242}Pu and ^{239}Pu were estimated. Except for a few spikes at early times, the maximum ^{242}Pu release rate due to irreversible colloids is 2.5% of total release rate at 451,000 years. For ^{239}Pu, except for some spikes, the maximum release rate due to irreversible colloids is 4.9% at 122,000 years. The anomalous spikes in the ratio of irreversible colloid release rate to total release result are numerical artifacts (e.g., due to single time steps at early times where there are small total releases) and are not representative of significant colloidal releases.

The results from these three modeling cases show that the contributions from colloidal processes to mean annual dose are not significant (never exceeding 30%), and thus colloidal processes are classified as Non-ITBC. Even in the igneous intrusion case, where colloid suspensions are likely to be stable, the colloidal processes are Non-ITBC.

1.6 SUMMARY

Sections 1.1 through 1.5 provide additional information describing the effects of specific processes on the barrier capability of components of the waste form and waste package internals feature of the EBS. Some processes also affect components of the waste package feature of the EBS.

Section 1.1.1 shows that the slow degradation of the CSNF and HLW glass waste forms, quantified by a range of degradation half-lives that represent uncertainty and cover the relevant time period, contributes to the ITWI classification of the CSNF and HLW Glass components of the waste form and waste package internals feature. Section 1.1.2 shows that the instantaneous degradation of the DSNF waste form supports a Non-ITWI classification of the DSNF component of the waste form and waste package internals feature.

Section 1.2.1 shows that the limited occurrence and extent of waste package damage contributes to EBS capability to limit radionuclide releases from the CSNF and CDSP waste packages. This capability is quantified by a number of TSPA-LA results that cover the 1,000,000-year time period, incorporate uncertainty in input variables, and represent different modeling cases. The limited crack area contributes to the ITWI classification of the Outer Barrier component of the waste package feature. Section 1.2.2 shows that enhanced structural response capability (i.e., damping) to damage from seismic ground motion contributes to the ITWI classification of the TAD Canister component of the waste form and waste package internals feature.

Section 1.3 shows that the solubility limits constrain radionuclide releases from the CSNF, HLW glass, and DSNF waste forms. This capability is quantified by a number of TSPA-LA results that cover the 1,000,000-year time period and incorporate uncertainty in input variables. The solubility limits contribute to the ITWI classification of the CSNF component of the waste form and waste package internals feature, but support a Non-ITWI classification of the HLW Glass and DSNF components of the waste form and waste package internals feature.

Section 1.4 shows that sorption onto stationary corrosion products delays and reduces radionuclide releases from the waste forms and waste packages. This capability is quantified by a number of TSPA-LA results that cover the 1,000,000-year time period and incorporate uncertainty in input variables. Because the most significant mass of steel is contained in the waste package inner vessel, sorption onto corrosion products contributes to the ITWI classification of the inner vessel component of the waste package feature. Accordingly, sorption onto corrosion products also supports Non-ITWI classifications of the components of the waste form and waste package internals feature (TAD Canister, DSNF Canister, HLW Canister, TAD Canister Internals, DSNF Canister Internals, and Codisposal Waste Package Internals) because they do not contain a significant mass of steel, relative to the waste package inner vessel. However, note that some of these components are ITWI for other reasons (e.g., enhanced structural capability, criticality control).

Section 1.5 shows that colloidal processes are not significant relative to dissolved radionuclide transport and, therefore, support a Non-ITWI classification of the CSNF, HLW Glass, and DSNF components of the waste form and waste package internals feature. However, note that CSNF and HLW Glass components are ITWI for other reasons (e.g., slow degradation rates).

These classifications are consistent with the ITWI classifications in SAR Tables 2.1-1 and 1.9-8.

2 COMMITMENTS TO NRC

None.

3 DESCRIPTION OF PROPOSED LA CHANGE

None.

4 REFERENCES

SNL (Sandia National Laboratories) 2007. *EBS Radionuclide Transport Abstraction.* ANL-WIS-PA-000001 REV 03. Las Vegas, Nevada: Sandia National Laboratories. ACC: DOC.20071004.0001; LLR.20080414.0023.

SNL 2008a. *Postclosure Nuclear Safety Design Bases.* ANL-WIS-MD-000024 REV 01. Las Vegas, Nevada: Sandia National Laboratories. ACC: DOC.20080226.0002; DOC.20080314.0004; LLR.20080507.0018; DOC.20080610.0007.

SNL 2008b. *Total System Performance Assessment Model /Analysis for the License Application.* MDL-WIS-PA-000005 REV 00 AD 01. Las Vegas, Nevada: Sandia National Laboratories. ACC: DOC.20080312.0001; LLR.20080414.0037; LLR.20080507.0002; LLR.20080522.0113; DOC.20080724.0005; DOC.20080106.0001.

RAI Volume 3, Chapter 2.2.1.1, First Set, Number 6:

Address the relative contribution of advective transport, matrix diffusion, matrix sorption and colloid filtration to the barrier capability of the lower natural barrier components (unsaturated zone below the repository and saturated zone), and how this is related to relative differences in sorption, solubility, and radioactive decay properties among a set of representative radionuclides.

Describe how these processes affect the capability of the unsaturated zone and saturated zone, including uncertainties, consistent with the quantitative analyses in the total system performance assessment (e.g., sensitivity and uncertainty analyses, model inputs, or intermediate results). Provide information on the time period over which these processes perform their intended function.

Basis: Needed for demonstration of compliance with 10 CFR 63.115 (b) and (c). To demonstrate the capability of the lower natural barrier for a range of releases, using a limited number of calculations, 12 radionuclides were selected for the barrier performance demonstrations. These radionuclides represent a broad range of radioactive decay properties, geochemical behavior, and transport characteristics listed in Section 2.1.2.2.6 (page 2.1-68) of the Safety Analysis Report. Because of their diverse properties, these radionuclides were intended to provide a means of examining the performance characteristics of the lower natural barrier. TSPA results are presented in terms of percentage activity reduction through the lower natural barrier for the representative radionuclides. However, there is no discussion linking the activity reductions and unique properties of the radionuclides to the capability of the lower natural barrier to prevent or substantially reduce the rate of radionuclide movement.

1. RESPONSE

This response consists primarily of a synthesis of information contained within SAR Sections 2.3.8, 2.3.9, and associated supporting documentation. Using a representative set of radionuclides, the response addresses the relative contributions from the unsaturated zone and saturated zone processes (e.g., advective transport, matrix diffusion, matrix sorption and colloid filtration), presented in SAR Sections 2.3.8 and 2.3.9, to the barrier capability of the Lower Natural Barrier unsaturated zone and saturated zone features presented in SAR Section 2.1. The governing mass balance equations used in developing this response are provided in Attachment A. The radionuclides examined in this response represent a broad range of radioactive decay properties, geochemical behaviors, biosphere dose conversion factors, and transport characteristics in geologic media. Consideration of these radionuclides provides a means of examining the overall performance characteristics of the Lower Natural Barrier as discussed in SAR Section 2.1.2.3.6.

The representative set of radionuclides reflects a range of transport properties including: (1) highly soluble, non-sorbing radionuclides, with long half-lives represented by ^{99}Tc; (2) low to moderately soluble, weakly sorbing radionuclides, with long half-lives represented by ^{237}Np; (3) low solubility, very strongly sorbing radionuclides, with long half-lives represented by ^{230}Th; (4) low to moderately soluble, moderate- to strongly sorbing radionuclides, with relatively short half-lives represented by ^{240}Pu; (5) low to moderately soluble, strongly sorbing radionuclides, with very short half-lives represented by ^{137}Cs; and (6) low to moderately soluble, strongly sorbing radionuclides, with very long half-lives represented by ^{135}Cs. Note that the effects of solubility will not be directly considered in the response because the TSPA-LA model conservatively assumes that releases to the unsaturated zone are at concentrations less than solubility limits in the unsaturated zone and solubilities do not need to be considered in the unsaturated zone and saturated zone (SNL 2008e, FEPs 2.2.08.07.0B and 2.2.08.07.0A).

Two metrics are used for the unsaturated zone feature of the Lower Natural Barrier to evaluate the influence of different processes. The first metric is mean particle travel time (the unsaturated zone transport model is a particle tracking model) from the repository to the water table. The second metric is normalized concentration, which is based on the particle travel time distribution to the water table and the radionuclide decay rate. This physically represents the fraction of the radionuclide mass released from the repository that reaches the water table before decaying (see SNL 2008b, Equation 6.8.2-1). In the saturated zone feature of the Lower Natural Barrier, median travel times (50th percentile on the normalized breakthrough curve) are used as one metric and radionuclide half-lives are compared to the travel times as a second metric.

A relative ranking of the contribution of each process is presented in Section 1.1, Tables 1-1 (a) and (b) to 1-4 (a) and (b), which also categorize the influence of each process with respect to the 10,000-year and 1,000,000-year time periods, in order to indicate the time over which a specific process may be important. The tables are also categorized according to the key components of each feature: the northern and southern halves of the repository for the unsaturated zone and the volcanics versus the alluvium for the saturated zone. As described in much greater detail in Section 1.2 of this response, the table rankings for the unsaturated zone are based on results presented in SAR Section 2.3.8, in *Particle Tracking Model and Abstraction of Transport Processes* (SNL 2008b, also referred to herein as the particle tracking report), and in Appendix K of *Total System Performance Assessment Model/Analysis for the License Application* (SNL 2008a, also referred to herein as the TSPA-LA report). The rankings for the saturated zone are based on results presented in SAR Section 2.3.9, in *Saturated Zone Flow and Transport Model Abstraction* (SNL 2008c, also referred to herein as the flow and transport abstraction), in *Site-Scale Saturated Zone Transport* (SNL 2008d, also referred to herein as the site-scale report), and in Appendix K of *Total System Performance Assessment Model/Analysis for the License Application* (SNL 2008a).

As detailed in Section 1.2, this RAI response also includes a demonstration of the effect of uncertainties in both the unsaturated zone and saturated zone features, consistent with the quantitative analyses in Appendix K of *Total System Performance Assessment Model/Analysis for the License Application* (SNL 2008a).

The effectiveness of the Lower Natural Barrier is reflected in its capacity to delay the migration of radionuclides through retarding processes such as matrix diffusion, matrix sorption, and colloid filtration. The only process within the TSPA-LA model that permanently removes radionuclides from the Lower Natural Barrier is radionuclide decay, which is more effective for those radionuclides with short half-lives. Advection within the unsaturated zone and saturated zone controls the migration of radionuclides through the Lower Natural Barrier, and it is the coupling of the aforementioned retarding processes with the advective process that ultimately determines the peak levels of radionuclide releases, the timing of the releases, and the degree to which the mass of radionuclides is reduced by decay. Where applicable (in areas where flow is governed by fracture transport), the influences of matrix diffusion and matrix sorption are presented together because their coupled effects cannot be simply segregated. The effectiveness of matrix diffusion as a process is based on the fact that it diffuses radionuclides into the rock matrix where they can be sorbed. For non-sorbing radionuclides, matrix diffusion is not very effective. Colloid filtration within the Lower Natural Barrier is simulated as reversible using a colloid retardation term in the fractures, which represents chemical filtration or adsorption of the colloids onto the fracture surfaces (SNL 2008c, Section 6.5.2.11). Colloid exclusion, which decreases the probability of colloids diffusing into the rock matrix, is also considered.

1.1 RELATIVE CONTRIBUTIONS OF TRANSPORT PROCESSES IN THE LOWER NATURAL BARRIER

1.1.1 Unsaturated Zone Feature

The relative importance of the processes controlling radionuclide transport in the unsaturated zone is primarily based on a set of sensitivity studies presented in the particle tracking report (SNL 2008b) and, where applicable, uncertainty and sensitivity studies presented in Appendix K of the TSPA-LA report (SNL 2008a). These studies are described in greater detail in Section 1.2. The conclusions are based on results for specific radionuclides considered in the analyses. A summary of the conclusions is presented here and tabulated below in four tables. These four tables are categorized as follows: (1) importance of transport processes in controlling releases from the unsaturated zone over a 10,000-year period for radionuclides released from a northern repository location (Table 1-1a); (2) importance of transport processes in controlling releases from the unsaturated zone over a 1,000,000-year period for radionuclides released from a northern repository location (Table 1-1b); (3) importance of transport processes in controlling releases from the unsaturated zone over a 10,000 year period for radionuclides released from a southern repository location (Table 1-2a); and (4) importance of transport processes in controlling releases from the unsaturated zone over a 1,000,000-year period for radionuclides released from a southern repository location (Table 1-2b).

The tables are categorized by release location to reflect the different processes that are important in the northern and southern halves of the repository region. The time periods were chosen to reflect the time periods of interest in the TSPA-LA simulations. The importance of the processes are ranked as low, medium, and high depending on how much a process will influence the mass reaching the water table by the end of the time period of interest, either by delaying the release or by allowing decay within the unsaturated zone to remove mass from the system. The degree of influence is evaluated based on travel-time data and normalized concentration data that reflect

the influence of decay. It should also be noted that advection is always considered an important process because the degree that the retarding processes such as matrix diffusion, matrix sorption, and colloid filtration offset advection defines the effectiveness of the unsaturated zone as a feature. Also, for dominantly fracture transport, the processes of matrix diffusion and matrix sorption for sorbing species are grouped together because their coupled effects cannot be simply segregated.

As noted in Sections 1.2.1.1 and 1.2.1.3, the nonsorbing, slowly decaying radionuclide ^{99}Tc (half-life = 2.1×10^5 years) is affected by matrix diffusion in the north, but over the course of 10,000 years, the amount of the delay is so small that matrix diffusion is considered to be unimportant (its influence is low) for ^{99}Tc released from a northern location. For releases from a southern location, matrix diffusion shows no influence, reflecting the controlling nature of matrix transport in the CHn vitric facies (Section 1.2.1). Since matrix diffusion is unimportant for a 10,000-year period, it is also unimportant for a 1,000,000-year period.

As discussed in Sections 1.2.1.2 and 1.2.1.3, the weakly sorbing, slowly decaying radionuclide ^{237}Np (half-life = 2.1×10^6 years) is affected by both matrix diffusion and matrix sorption in the north, but over the course of 10,000 years the amount of the delay is so small that matrix diffusion with a small amount of sorption is still considered to be unimportant in the north. For releases from a southern location, where matrix diffusion shows no influence, matrix sorption does have a medium effect on delaying the travel time (over the range of K_d uncertainty), enough that some mass is not released prior to 10,000 years. Over the course of 1,000,000 years, most of the ^{237}Np will be released from the unsaturated zone in both the north and the south.

As discussed in Sections 1.2.1.2 and 1.2.1.3, the travel time of the strongly sorbing, relatively quickly decaying radionuclide ^{240}Pu (half-life = 6.6×10^3 years) is affected by both matrix diffusion and matrix sorption in the north, but over the course of 10,000 years the amount of the delay is small enough (above 1,000 years for only a small number of realizations) that matrix diffusion with a large amount of sorption is still considered to be unimportant in the north. Since matrix diffusion and sorption are unimportant over a 10,000-year period, they are also unimportant over a 1,000,000-year period. For releases from the southern release location, the process of matrix sorption dominates the travel time to the water table and, in conjunction with radionuclide decay, prevents almost all of the ^{240}Pu from reaching the water table. Therefore, the importance of matrix sorption is high for ^{240}Pu for both a 10,000-year and a 1,000,000-year period. Also note that, as discussed in Section 1.2.1.4, reversible colloid transport in the unsaturated zone is not important for ^{240}Pu transport.

As discussed in Sections 1.2.1.3 and 1.2.1.4, the strongly sorbing, moderately decaying (half-life = 75,000 years) radionuclide ^{230}Th is affected by the coupled influence of matrix diffusion and matrix sorption in the north, but over the course of 10,000 years the amount of the delay is relatively small. As shown Figure 6.6.2-7[b] of the particle tracking report (SNL 2008b), for representative values of parameters the ^{230}Th median normalized breakthrough time at the water table is about 1,000 years and over 85% of the mass has reached the water table by 10,000 years. The importance of coupled matrix diffusion and matrix sorption is low for this single run with representative parameters, but would probably be low to medium for the 10,000-year period when uncertainty is considered. The importance of coupled matrix diffusion and matrix sorption

for a northern release would be low for a 1,000,000-year period. For a southern release, matrix sorption ^{230}Th does not reach the water table for the case where a median value of K_d is used. The process of matrix sorption dominates the travel time to the water table and, in conjunction with radionuclide decay, prevents almost all of the ^{230}Th from reaching the water table. Therefore, the importance of matrix sorption is high for ^{230}Th for both a 10,000-year and a 1,000,000-year period. Also note that, as discussed in Section 1.2.1.4, reversible colloid transport in the unsaturated zone may play an effective role in ^{230}Th, but matrix sorption is strong enough for matrix sorption alone to be an effective barrier to ^{230}Th transport in the south.

As discussed in Section 1.2.1.3, the strongly sorbing, very quickly decaying radionuclide ^{137}Cs (half-life = 30 years) is only affected a small amount by matrix diffusion and matrix sorption in the north, but even this short delay helps to reduce the mass released by more than two-thirds due to the very short half-life. In the south, the short half-life in conjunction with matrix diffusion prevents almost all of the ^{137}Cs from reaching the water table. Therefore, the importance of matrix sorption is high for ^{137}Cs for both a 10,000-year and a 1,000,000-year period. For the strongly sorbing, very slowly decaying radionuclide ^{135}Cs (half-life = 2.3×10^6 years), the importance of matrix diffusion and matrix sorption is low in the north with most of the mass reaching the water table after a 1,000-year delay. In the south, the mass release is delayed 10,000 years, making matrix sorption a highly important contributor to the transport processes.

As discussed in Section 1.2.1.4, the transport of radionuclides irreversibly bound to glass colloids is advection-driven, but some retardation occurs due to reversible filtration within the fractures. For ^{240}Pu released from the northern location, the reversible filtration has a large effect on relative travel time, but most of the mass reaches the water table due to the rapid travel times, so the effect is low. In the south, the influence of colloid filtration on relative transport time is less than in the north since the travel time is dominated by matrix flow for which filtration is not simulated. Most of the mass still reaches the water table, so the effect of colloid filtration is still low.

Table 1-1a. Qualitative Summary of the Relative Contributions of the Unsaturated Zone Processes to the Capability of the Lower Natural Barrier for the Unsaturated Zone – Northern Repository Location (10,000 years)

Radionuclide Group	Radionuclide Transport Processes				Radionuclide Half-Life (years)
	Advection	Matrix Diffusion Only[a]	Matrix Diffusion with Sorption[a]	Colloid Filtration[a]	
^{99}Tc - Non-Sorbing	High	Low	—	—	2.1×10^5
^{237}Np – Weakly sorbing	High	—	Low	—	2.1×10^6
^{240}Pu – Moderately to strongly sorbed	High	—	Low to Medium	Low	6.6×10^3
^{230}Th – Strongly Sorbed	High	—	Medium	Medium	7.5×10^4
^{135}Cs – Moderate to strongly sorbing	High	—	Low to Medium	Low	2.3×10^6
^{137}Cs – Moderate to strongly sorbing	High	—	High	Low	30
^{240}Pu – Irreversibly sorbed onto colloids	High	—	—	Medium	6.6×10^3

[a] A "—" symbol means that the process is not applicable (e.g., colloid filtration does not aply to ^{99}Tc) or that the process only works in conjunction with another process (e.g., matrix diffusion alone does not apply to ^{237}Np, but works with matrix sorption).

Table 1-1b. Qualitative Summary of the Relative Contributions of the Unsaturated Zone Processes to the Capability of the Lower Natural Barrier for the Unsaturated Zone – Northern Repository Location (1,000,000 years)

Radionuclide Group	Radionuclide Transport Processes				Radionuclide Half-Life (years)
	Advection	Matrix Diffusion Only[a]	Matrix Diffusion with Sorption[a]	Colloid Filtration[a]	
^{99}Tc – Non-Sorbing	High	Low	—	—	2.1×10^5
^{237}Np – Weakly sorbing	High	—	Low	—	2.1×10^6
^{240}Pu – Moderately to strongly sorbed	High	—	Low to Medium	Low	6.6×10^3
^{230}Th – Strongly Sorbed	High	—	Low to Medium	Medium	7.5×10^4
^{135}Cs – Moderate to strongly sorbing	High	—	Low	Low	2.3×10^6
^{137}Cs – Moderate to strongly sorbing	High	—	High	Low	30
^{240}Pu – Irreversibly sorbed onto colloids	High	—	—	Low	6.6×10^3

[a] A "—" symbol means that the process is not applicable (e.g., colloid filtration does not aply to ^{99}Tc) or that the process only works in conjunction with another process (e.g., matrix diffusion alone does not apply to ^{237}Np, but works with matrix sorption).

Table 1-2a. Qualitative Summary of the Relative Contributions of the Unsaturated Zone Processes to the Capability of the Lower Natural Barrier for the Unsaturated Zone – Southern Repository Locations (10,000 years)

Radionuclide Group	Radionuclide Transport Processes				Radionuclide Half-Life (years)
	Advection	Matrix Diffusion Only[a]	Matrix Sorption[a]	Colloid Filtration[a]	
^{99}Tc - Non-Sorbing	High	Low	—	—	2.1×10^5
^{237}Np - Weakly sorbing	High	—	Medium	—	2.1×10^6
^{240}Pu - Moderately to strongly sorbed	High	—	High	Low	6.6×10^3
^{230}Th - Strongly Sorbed	High	—	High	Moderate	7.5×10^4
^{135}Cs - Moderate to strongly sorbing	High	—	High	Low	2.3×10^6
^{137}Cs - Moderate to strongly sorbing	High	—	High	Low	30
^{240}Pu – Irreversibly sorbed onto colloids	High	—	—	Low	6.6×10^3

[a] A "—" symbol means that the process is not applicable (e.g., colloid filtration does not aply to ^{99}Tc) or that the process only works in conjunction with another process (e.g., matrix diffusion alone does not apply to ^{237}Np, but works with matrix sorption).

Table 1-2b. Qualitative Summary of the Relative Contributions of the Unsaturated Zone Processes to the Capability of the Lower Natural Barrier for the Unsaturated Zone – Southern Repository Locations (1,000,000 years)

Radionuclide Group	Radionuclide Transport Processes				Radionuclide Half-Life (years)
	Advection	Matrix Diffusion Only[a]	Matrix Sorption[a]	Colloid Filtration[a]	
^{99}Tc – Non-Sorbing	High	Low	—	—	2.1×10^5
^{237}Np – Weakly sorbing	High	—	Low	—	2.1×10^6
^{240}Pu – Moderately to strongly sorbed	High	—	High	Low	6.6×10^3
^{230}Th – Strongly Sorbed	High	—	High	Moderate	7.5×10^4
^{135}Cs – Moderate to strongly sorbing	High	—	Low	Low	2.3×10^6
^{137}Cs – Moderate to strongly sorbing	High	—	High	Low	30
^{240}Pu – Irreversibly sorbed onto colloids	High	—	—	Low	6.6×10^3

[a] A "—" symbol means that the process is not applicable (e.g., colloid filtration does not aply to ^{99}Tc) or that the process only works in conjunction with another process (e.g., matrix diffusion alone does not apply to ^{237}Np, but works with matrix sorption).

1.1.2 Saturated Zone Feature

The relative importance of the processes controlling radionuclide transport in the saturated zone is primarily based on a set of sensitivity studies presented in the site-scale report (SNL 2008d), breakthrough curves developed in the flow and transport abstraction (SNL 2008c), and uncertainty and sensitivity studies presented in Appendix K of the TSPA-LA report

(SNL 2008a). The conclusions are based on results for specific radionuclides considered in the analyses. A summary of the conclusions is presented here and tabulated below in four tables. The four tables are broken down as follows: (1) importance of transport processes in the volcanics tuffs, in controlling releases from the saturated zone over a 10,000-year period (Table 1-3a); (2) importance of transport processes in the volcanics tuffs, in controlling releases from the saturated zone over a 1,000,000-year period (Table 1-3b); (3) importance of transport processes in the alluvium, in controlling releases from the saturated zone over a 10,000-year period (Table 1-4a); and (4) importance of transport processes in the alluvium, in controlling releases from the saturated zone over a 1,000,000-year period (Table 1-4b).

The tables are categorized by transport pathway to reflect the different processes that are important in the volcanics versus the alluvium portions of the saturated zone. The time periods were chosen to reflect the time periods of interest in the TSPA-LA simulations. The importance of the processes are ranked as low, medium, and high depending on how much a process will influence the mass reaching the water table by the end of the time period of interest, either by delaying the release or by allowing decay within the saturated zone to remove a large amount of mass from the system. It should also be noted that advection is always considered an important process because the degree that the retarding processes such as matrix diffusion, matrix sorption, and colloid filtration offset advection defines the effectiveness of the saturated zone as a feature. Also, for the volcanic tuffs, the processes of matrix diffusion and matrix sorption for sorbing species are grouped together because their coupled effects cannot be simply segregated. Since matrix sorption in the volcanics and in the alluvium have similar effects, conclusions based on breakthrough cuves where the two pathways are simulated together will be considered the same for each zone (see Section 1.2.2.4 and SNL 2008d, Figures 6.7-4 and 6.7-11).

As discussed in Section 1.2.2.4, the nonsorbing slowly decaying radionuclide ^{99}Tc (half-life = 2.1×10^5 years) is affected by matrix diffusion in the volcanic tuffs, but over the course of 10,000 years, the amount of the delay is so small that matrix diffusion is considered to be unimportant for this time period. Since matrix diffusion is unimportant for a 10,000-year period, it is also unimportant for a 1,000,000-year period.

As discussed in Section 1.2.2.4, the very strongly sorbing, slowly decaying radionuclide ^{230}Th (half-life = 7.5×10^4 years) is substantially affected by matrix diffusion coupled with matrix sorption in the volcanics, and matrix sorption in the alluvium. The travel time for most of the ^{230}Th breakthrough curves in the saturated zone is over 1,000,000 years. Over the course of 10,000 years, the amount of the delay will prevent most of the ^{230}Th released from the repository from reaching the accessible environment at the 18-km boundary in that time period. Because most of the ^{230}Th released from the unsaturated zone will still not reach the 18-km boundary within a 1,000,000-year period, the influence of matrix diffusion coupled with matrix sorption in the volcanics, and matrix sorption in the alluvium, is considered to be high with respect to ^{230}Th for both time periods.

As discussed in Section 1.2.2.4, the strongly sorbing element cesium is substantially affected by matrix diffusion coupled with matrix sorption in the volcanics, and matrix sorption in the alluvium. The travel time for most of the breakthrough curves used to describe cesium transport in the saturated zone is over 1,000,000 years. Over the course of 10,000 years, the amount of the

delay will prevent just about all cesium released from the repository from reaching the 18-km boundary. Over the course of 1,000,000 years, most cesium released from the repository will still not have reached the 18-km boundary. Because of their strong influence with respect to retardation of ^{137}Cs and ^{135}Cs within the saturated zone, the influence of matrix diffusion coupled with matrix sorption in the volcanics, and matrix sorption in the alluvium, is considered high.

As discussed in Section 1.2.2.4, the moderately to strongly sorbing, relatively quickly decaying radionuclide ^{240}Pu (half-life = 6.6×10^3 years) is affected by matrix diffusion coupled with matrix sorption in the volcanics, and matrix sorption in the alluvium. Over the course of 10,000 years, the amount of the delay will prevent just about all ^{240}Pu released from the repository from reaching the 18-km boundary. Over the course of 1,000,000 years, some ^{240}Pu released from the repository will still not have reached the 18-km boundary, but most will. Because little of the ^{240}Pu released from the unsaturated zone will reach the 18-km boundary within a 10,000-year period, the influence of matrix diffusion coupled with matrix sorption in the volcanics, and matrix sorption in the alluvium, is considered to be high with respect to that 10,000-year time period. Although the breakthrough curves indicate that much of the plutonium released from the unsaturated zone would reach the 18-km boundary within a 1,000,000-year period, when the relatively short half-life of ^{240}Pu is considered, most of the released mass will not reach the 18-km boundary in the 1,000,000-year time period. Therefore, the influence of matrix diffusion coupled with matrix sorption in the volcanics, and matrix sorption in the alluvium, is considered to be high in this time period.

As discussed in Section 1.2.2.4, the weakly sorbing, slowly decaying radionuclide ^{237}Np (half-life = 2.1×10^6 years) is affected by matrix diffusion coupled with matrix sorption in the volcanics, and matrix sorption in the alluvium. Over the course of 10,000 years, the amount of the delay will moderately reduce the amount of mass that can reach the accessible environment at the 18-km boundary in that time period, so the influence of matrix diffusion coupled with matrix sorption in the volcanics, and matrix sorption in the alluvium, is considered to be medium with respect to ^{237}Np for this shorter time period. Because most of the ^{237}Np released from the unsaturated zone will reach the 18-km boundary within a 1,000,000-year period, the influence of matrix diffusion coupled with matrix sorption in the volcanics, and matrix sorption in the alluvium, is considered to be low with respect to ^{237}Np for the longer time period.

As discussed in Section 1.2.2.4, it can be seen that colloid filtration in the volcanics and the alluvium plays a large combined role in reducing the amount of ^{240}Pu bound to glass colloids reaching the accessible environment for the 10,000-year time period, so the combined influence of colloid filtration in the volcanics and the alluvium is considered to be high. Over the longer period of 1,000,000 years, most of the ^{240}Pu mass irreversibly sorbed to glass colloids will reach the 18-km boundary, but when the influence of decay (half-life = 6.6×10^3 years) is considered, a large proportion of the mass will decay away before reaching the accessible environment. For this reason, the combined influence of colloid filtration in the volcanics and the alluvium is considered to be high for a 1,000,000-year period. Because the influence of colloid retardation (filtration) in the alluvium is much greater than colloid retardation (filtration) in the volcanics (see SNL 2008d, Figures 6.7-6 and 6.7-12), the influence of colloid retardation (filtration) in the alluvium is considered to be high for either time period. Because the influence of colloid

retardation (filtration) in the volcanics is much less than in the alluvium, the influence of colloid retardation (filtration) in the volcanics is considered medium for either time period.

Table 1-3a. Qualitative Summary of the Relative Contributions of the Volcanic Tuff Saturated Zone Processes to the Capability of the Lower Natural Barrier (10,000 years)

	Radionuclide Transport Processes				
Radionuclide Group	**Advection**	**Matrix Diffusion Only[a]**	**Matrix Diffusion with Sorption[a]**	**Colloid Filtration[a]**	**Radionuclide Half-Life (years)**
^{99}Tc – Non-Sorbing	High	Low	—	—	2.1×10^5
^{237}Np – Weakly sorbing	High	—	Medium	—	2.1×10^6
^{240}Pu – Moderately to strongly sorbed	High	—	High	Low	6.6×10^3
^{230}Th – Strongly Sorbed	High	—	High	Medium	7.5×10^4
^{135}Cs – Moderate to strongly sorbing	High	—	High	Low	2.3×10^6
^{137}Cs – Moderate to strongly sorbing	High	—	High	Low	30
^{240}Pu – Irreversibly sorbed onto colloids	High	—	—	Medium	6.6×10^3

[a] A "—" symbol means that the process is not applicable (e.g., colloid filtration does not aply to ^{99}Tc) or that the process only works in conjunction with another process (e.g., matrix diffusion alone does not apply to ^{237}Np, but works with matrix sorption).

Table 1-3b. Qualitative Summary of the Relative Contributions of the Volcanic Tuff Saturated Zone Processes to the Capability of the Lower Natural Barrier (1,000,000 years)

	Radionuclide Transport Processes				
Radionuclide Group	**Advection**	**Matrix Diffusion Only[a]**	**Matrix Diffusion with Sorption[a]**	**Colloid Filtration[a]**	**Radionuclide Half-Life (years)**
^{99}Tc – Non-Sorbing	High	Low	—	—	2.1×10^5
^{237}Np – Weakly sorbing	High	—	Low	—	2.1×10^6
^{240}Pu – Moderately to strongly sorbed	High	—	High	Low	6.6×10^3
^{230}Th – Strongly Sorbed	High	—	High	Medium	7.5×10^4
^{135}Cs – Moderate to strongly sorbing	High	—	High	Low	2.3×10^6
^{137}Cs – Moderate to strongly sorbing	High	—	High	Low	30
^{240}Pu – Irreversibly sorbed onto colloids	High	—	—	Medium	6.6×10^3

[a] A "—" symbol means that the process is not applicable (e.g., colloid filtration does not aply to ^{99}Tc) or that the process only works in conjunction with another process (e.g., matrix diffusion alone does not apply to ^{237}Np, but works with matrix sorption).

Table 1-4a. Qualitative Summary of the Relative Contributions of the Alluvium Saturated Zone Processes to the Capability of the Lower Natural Barrier (10,000 years)

Radionuclide Group	Radionuclide Transport Processes				Radionuclide Half-Life (years)
	Advection	Matrix Diffusion Only[a]	Matrix Diffusion with Sorption[a]	Colloid Filtration[a]	
^{99}Tc – Non-Sorbing	High	Low	—	—	2.1×10^5
^{237}Np – Weakly sorbing	High	—	Medium	—	2.1×10^6
^{240}Pu – Moderately to strongly sorbed	High	—	High	Low	6.6×10^3
^{230}Th – Strongly Sorbed	High	—	High	Medium	7.5×10^4
^{135}Cs – Moderate to strongly sorbing	High	—	High	Low	2.3×10^6
^{137}Cs – Moderate to strongly sorbing	High	—	High	Low	30
^{240}Pu – Irreversibly sorbed onto colloids	High	—	—	High	6.6×10^3

[a] A "—" symbol means that the process is not applicable (e.g., colloid filtration does not aply to ^{99}Tc) or that the process only works in conjunction with another process (e.g., matrix diffusion alone does not apply to ^{237}Np, but works with matrix sorption).

Table 1-4b. Qualitative Summary of the Relative Contributions of the Alluvium Saturated Zone Processes to the Capability of the Lower Natural Barrier (1,000,000 years)

Radionuclide Group	Radionuclide Transport Processes				Radionuclide Half-Life (years)
	Advection	Matrix Diffusion Only[a]	Matrix Diffusion with Sorption[a]	Colloid Filtration[a]	
^{99}Tc – Non-Sorbing	High	Low	—	—	2.1×10^5
^{237}Np – Weakly sorbing	High	—	Low	—	2.1×10^6
^{240}Pu – Moderately to strongly sorbed	High	—	High	Low	6.6×10^3
^{230}Th – Strongly Sorbed	High	—	High	Medium	7.5×10^4
^{135}Cs – Moderate to strongly sorbing	High	—	High	Low	2.3×10^6
^{137}Cs – Moderate to strongly sorbing	High	—	High	Low	30
^{240}Pu – Irreversibly sorbed onto colloids	High	—	—	High	6.6×10^3

[a] A "—" symbol means that the process is not applicable (e.g., colloid filtration does not aply to ^{99}Tc) or that the process only works in conjunction with another process (e.g., matrix diffusion alone does not apply to ^{237}Np, but works with matrix sorption).

1.2 SYNTHESIS OF EXISTING DOCUMENTATION RELATED TO THE RELATIVE CONTRIBUTION OF TRANSPORT PROCESSES IN THE LOWER NATURAL BARRIER

The Lower Natural Barrier is comprised of the unsaturated zone feature beneath the repository and the saturated zone feature extending from the repository to the accessible environment, 18 km to the south. The transport of radionuclides through the Lower Natural Barrier is a function of various processes, including advective transport, matrix diffusion, sorption, and colloidal filtration, that control the mass travel time and degree of attenuation. The unsaturated zone represents a vertical distance from the repository to the water table that varies with the climate state, being approximately 120 m shorter in the future monsoonal, glacial-transition, and post-10,000-year climate states. As described in SAR Section 2.3.2.5.2: "Future climates are expected to lead to a rise in water table elevation of no more than 120 m (Section 2.3.9.2.4.1). The effect of water table rise on unsaturated zone flow is primarily related to change in the flow path length between the repository and the water table, having little effect otherwise on the unsaturated zone flow fields….Given a present-day water table at 730 m above sea level (Section 2.3.8.5.3), a flat water table at 850 m above sea level is expected to bound the potential effects of water table rise for the purposes of unsaturated zone flow."

The saturated zone feature of the Lower Natural Barrier includes (1) fractured volcanic rocks from below the repository to approximately 11 km south of the southern boundary of the repository footprint (SNL 2008d, Section 6.8.3) and (2) saturated alluvium from the volcanic/alluvium boundary to the accessible environment. Note that the saturated zone represents a much longer pathway of approximately 18,000 m, which allows it to potentially have a greater influence on the attenuation of radionuclides released from the repository.

1.2.1 Unsaturated Zone Feature

To examine the relative importance of different transport processes controlling the migration of radionuclides within the unsaturated zone, the differences between radionuclide transport for releases in the northern and southern halves of the unsaturated zone must be considered. The analyses described below are based on the typical northern and southern release locations shown in SAR Figure 2.3.8-36b.

The following discussion pertaining to radionuclide transport within the unsaturated zone is based on results presented for unsaturated zone transport simulations where mass is applied to fracture nodes Applying the mass to unsaturated zone fracture nodes versus unsaturated zone matrix nodes is an important effect because the Upper Natural Barrier effectively determines the fraction of radionuclide mass released from the EBS that will be released into the unsaturated zone fractures versus the unsaturated zone matrix. This fraction is controlled by the seepage fraction (SAR Tables 2.1-6 to 2.1-9), which will cause most mass to be released into the unsaturated zone fractures for waste packages in seeping zones and most mass to be released into the unsaturated zone rock matrix for waste packages in non-seeping zones. SAR Figure 2.3.8-49 shows the influence of applying mass to matrix nodes versus fracture nodes for a non-sorbing, slowly decaying radionuclide, ^{99}Tc. As can be seen in SAR Figure 2.3.8-49a, for a ^{99}Tc release from the northern release location, the mass release from the repository into the rock matrix

delays the median breakthrough time to the water table by over 4,000 years. On the other hand, as shown in SAR Figure 2.3-49b, for a repository release from a southern location, there is little difference whether the radionuclide mass enters the unsaturated zone through fractures or rock matrix. This is because flow through the CHn vitric rock matrix controls radionuclide transport from the southern release location. In the sections that follow, it is assumed that EBS releases enter the fractures, since the EBS mass that is released into the fractures generally travels much more quickly than the mass released into the matrix, and therefore represents the early part of the mass breakthrough curve (the part for which the Lower Natural Barrier is less effective). For mass released into the fractures, matrix diffusion and matrix sorption both have a delaying effect. However, for releases to the matrix, increased diffusion has the opposite effect of increased sorption—the greater the effective diffusion coefficient, the faster dissolved radionuclides can diffuse out of the matrix and into the fractures and the faster mass can reach the water table. In other words, for a source release to fractures, an increase in diffusion coefficient will retard the transport of radionuclides to the water table, whereas for a source release to the rock matrix, diffusion will have an opposite effect.

Immediately below the repository, radionuclide transport is controlled by fracture flow through the TSw units. Below the northern portion of the repository, at the base of the TSw and through the Calico Hills (CHn), the dominant material is a relatively low-permeability (SNL 2007, Tables B-1 to B-4) zeolitic tuff that supports perched water zones, lateral diversion to faults, and fault dominated vertical flow (SAR Figure 2.1-31; BSC 2004, Figure 6-7). In the southern portion of the repository, at the base of the TSw and through much of the Calico Hills (CHn), the flow process is dominated by matrix flow (SAR Figure 2.1-31; BSC 2004, Figure 6-7) through vitric nonwelded tuff. Although the areal extent of the CHn vitric tuff decreases with depth (BSC 2004, Figure 6-7), the CHn vitric tuff, with its relatively high matrix permeability (SNL 2007c, Tables B-1 to B-4), controls the transport process below the southern portion of the repository, as can be inferred from SAR Figure 2.3.8-36. SAR Figure 2.3.8-36 depicts the spatial distribution of minimum, mean, and maximum travel time for the 10th percentile glacial-transition climate state, based on the release of 10,000 particles (not subject to decay or matrix diffusion) across the repository horizon. As can be discerned from travel time contour maps presented in SAR Figure 2.3.8-36, the mean travel time contour map reflects the generally much shorter travel times in the north where fracture flow, lateral diversion to faults, and transport through faults dominates the advective transport from repository to water table. Note that in the faults, the radionuclides migrate to the water table by advective–dispersive transport (matrix diffusion is not simulated in the fault zones). In the south, SAR Figure 2.3.8-36b shows that the porous matrix flow within the unaltered CHn vitric tuffs generally increases the travel time to the water table.

SAR Figure 2.3.8-37, which compares particle release locations from the repository with the mean exit locations at the water table for a simulation using the glacial-transition flow field based on the 10th percentile infiltration map, is also reflective of the different conceptual models for the north and south. Each dot in the figures is representative of 10,000 particles released from a repository cell (see SAR Figure 2.3.8-37a). The dots in SAR Figure 2.3.8-37a and SAR Figure 2.3.8-37b are color-coded, indicating the infiltration bin they were released from, where percolation flux ranges from lowest for Bin 1 to highest for Bin 5. SAR Figure 2.3.8-37c also presents the mean water table release locations with the color coding indicating the mean travel

times to the location. For releases in the northern section of the repository, the lateral transport of the particles to fault zones such as the Drillhole Wash Fault and the Pagany Wash Fault and transport through the faults can be inferred by comparing SAR Figure 2.3.8-37a and SAR Figure 2.3.8-37b (see SAR Figure 2.3.2-9 for fault locations). This is consistent with the conceptual model of vertical fracture flow to the low-permeability zones where lateral flow to fault zones occurs followed by vertical flow through the faults to the water table. For releases in the southern section of the repository, by comparing SAR Figure 2.3.8-37a and SAR Figure 2.3.8-37b, it can be seen that vertical transport from the repository horizon to the water table is more pervasive than lateral transport. There is some structural control (i.e., lateral flow) in dipping CHn vitric facies (see Figure C-2 of BSC 2004), with a west-to-east component of flow in the central part of the southern region between 231700 m northing and 233200 m northing (see SAR Figure 2.3.8-37 and SNL 2008b, Figure 6.6.2-2), where mass moves eastward to a region where transport to the water table is vertical but does not seem to be fault-controlled.

1.2.1.1 Importance of Matrix Diffusion in the Unsaturated Zone for Non-Sorbing Species

As noted above, the nature of the CHn units beneath the repository controls the effectiveness of the unsaturated zone as a feature of the Lower Natural Barrier. The northern part of the repository below the TSw is underlain by zeolitic CHn tuff and the southern part of the repository below the TSw is underlain by vitric CHn tuff. Below the northern portion of the repository, the flow domain is dominated by vertical fracture flow to the low-permeability zeolitic zones, followed by lateral flow to fault zones then vertical flow through the faults to the water table. Under these conditions, radionuclide transport through the fractured media will control travel times and matrix diffusion will act to retard the advective transport through fractures. The effect of matrix diffusion relative to advective transport is illustrated in SAR Figure 2.3.8-50a for a non-sorbing species, ^{99}Tc, released from the northern part of the repository into the fractures. SAR Figure 2.3.8-50a depicts the mean log travel time in years as a function of the diffusion coefficient. Four curves are presented in the plot representing the four glacial-transition climate flow fields used to describe uncertainty in the percolation fluxes, with GT10 representing the low percolation flux scenario, GT30 the next highest percolation flux scenario, GT50 the next highest percolation flux scenario, and GT90 the highest percolation flux scenario. As shown in SAR Figure 2.3.8-50a, the mean travel time decreases significantly with an increase in infiltration rate. With respect to the influence of diffusion, there is also a significant increase in travel time with increase in diffusion coefficient for each infiltration scenario, especially for GT10 (SAR Figure 2.3.8-50a), which represents the lowest infiltration rate scenario and which occurs 62% of the time (SAR Section 2.4.2.3.2.1.1). The difference between mean travel time at the low end of the diffusion coefficient distribution and high end of the distribution is over an order of magnitude, only slightly less than the change in travel time reflected in the choice of infiltration scenarios. This sensitivity of the system to the diffusion coefficient reflects the influence of the process of matrix diffusion for the radionuclide mass released into the fractures in the northern portion of the repository. Note that in the north, the sensitivity of the travel times to the diffusion coefficient demonstrates the importance of fracture transport and not transport through the fault zones since the fault zones are not subject to matrix diffusion. It should also be noted that even though the results presented here show the influence of matrix diffusion versus infiltration, the travel times are so short that matrix diffusion is not

very important for a non-sorbing species. Its real importance is illustrated in the following section, which describes the coupled effects of matrix diffusion and matrix sorption.

Below the southern portion of the repository, the flow domain is dominated by vertical fracture flow to the vitric base of the TSw and porous media-dominated transport mainly through the rock matrix of the vitric facies at the base of the TSw and the CHn (as reflected in permeabilities presented in Tables B-1 to B-4 of SNL 2007). Under these conditions, radionuclide transport through porous CHn vitric tuff rock matrix will control travel times and matrix diffusion will not be a controlling process, as described in SAR Section 2.3.8.5.5.1. In the overlying fracture-dominated TSw units, matrix diffusion represents an important process, but this effect is masked by the longer travel times within the vitric Calico Hills units. In the vitric Calico Hills units the travel times are a function of the pore velocities in the rock matrix and the fractures do not behave as a short-circuited pathway to the water table, like in the north. As shown in SAR Figure 2.3.8-50b, the mean travel time increases significantly with a decrease in the percolation rates. But unlike in SAR Figure 2.3.8-50a in the north, there is no change in travel time with change in diffusion coefficient, indicating that diffusion has no influence in the CHn vitric units in the south (SAR Figure 2.3.8-50b).

The effect of matrix diffusion with respect to unsaturated zone transport can also be seen in Section K6.4.1 of the TSPA-LA report (SNL 2008a), which presents the results of uncertainty and sensitivity analyses based on a 20,000-year TSPA-LA model igneous intrusion simulation with an event taking place at 10 years. These analyses, which evaluate the effect of input parameter uncertainty on releases of ^{99}Tc from the unsaturated zone, must be considered in the overall context that matrix diffusion is relatively unimportant for non-sorbing species, as described above. In other words, although SAR Figure 2.3.8-50a shows an effect of the matrix diffusion coefficient on ^{99}Tc transport through the unsaturated zone for northern release locations, the range of travel times that span this effect are all quite short; hence, the low rating for matrix diffusion in Table 1-1. However, within this range of short travel times, the uncertainty analyses discussed below will show the importance of matrix diffusion parameters. Also, it should be noted that the igneous case is dominated by mass released from the repository being applied directly into the fractures, but, as discussed above, the influence of matrix diffusion would be the opposite if mass from the repository was released into the matrix of the unsaturated zone.

The partial rank correlation coefficients (PRCCs) for the time dependent release rates (SNL 2008a, Figure K6.4.1-13(e)) and cumulative time dependent release rates (SNL 2008a, Figure K6.4.1-13(f)) of ^{99}Tc from the unsaturated zone presented in this section are used to examine the importance of matrix diffusion to transport of a non-sorbing dissolved radionuclide in the saturated zone. The release rate and cumulative release rate PRCCs indicate that *INFIL* (infiltration scenario), *UZTORRG3* (the logarithm of the tortuosity in rock group 3 of the unsaturated zone), *UZGAM* (exponent gamma in active fracture model (see Equation A-1), dimensionless), and *UZFAG8* (fracture aperture for rock group 8 in unsaturated zone, m) are important parameters in controlling the releases of ^{99}Tc in the unsaturated zone. Note that tortuosity rock group 3 and fracture aperture rock group 8 are parameters controlling matrix diffusion in the devitrified tuff units of the TSw (TSw4 – TSw8). As shown in Figure K6.4.1-13(e) of the TSPA-LA report (SNL 2008a), *INFIL* indicates the infiltration

scenario used in a realization, which controls the flow velocity, but it also influences the EBS release level, so care must be taken in interpreting its relative importance as a unsaturated zone transport process analysis. The higher the value of *INFIL*, the greater the seepage rates and the unsaturated zone flow-field velocities. *INFIL* has a positive correlation on ^{99}Tc transport at early times and a negative correlation at late times, reflecting that the higher flow rates increase the rate of movement of dissolved ^{99}Tc to the water table in early times, which reduces the amount available at later times, creating a negative correlation. *INFIL* in the cumulative time dependent release rates always has a positive correlation, reflecting the cumulative effects.

The other unsaturated zone parameters shown to be of importance in Figure K6.4.1-13(e) of the TSPA-LA report (SNL 2008a), *UZTORRG3, UZGAM*, and *UZFAG8*, are all parameters that affect matrix diffusion (see Equation A-1). Note that the effective diffusion coefficient described in Equation A-1 is the product of the tortuosity and the free-water diffusion coefficient for the species of interest. The larger the tortuosity (*UZTORRG3*) and associated effective diffusion coefficient becomes, the greater the influence of diffusion (Equation A-1). The larger the exponent term (*UZGAM*) of the active fracture model becomes, the smaller the effective diffusive area and the more resistance there is to diffusion into or out of the rock matrix (Equation A-1). Similarly, the larger the fracture aperture, *UZFAG8*, becomes, the smaller the combined diffusion term (Equation A-1) and the more resistance there is to diffusion into or out of the rock matrix. Consistent with the breakthrough curves presented in Figures K6.4.1-13(a) and (c) of the TSPA-LA report (SNL 2008a), and the sharp increase then decline of mass releases during very early times, mass is diffused into and stored up in the rock matrix early and then, during later times, the mass is released from the rock matrix. The very early positive values of *UZGAM* and *UZFAG8*, as seen in Figure K6.4.1-13(e) of the TSPA-LA report (SNL 2008a), represent a positive correlation that is indicative of the retardant effects of diffusion on radionuclide transport while the radionuclide concentrations are higher in the fractures than in the rock matrix. Over time, the mass stored in the rock matrix diffuses back into the fractures and this mass is released from the unsaturated zone, which is reflected in the reversal of the correlation signs. The opposite trend is seen with respect to the tortuosity term for the devitrified tuffs of the TSw.

1.2.1.2 Importance of Matrix Diffusion and Sorption in the Unsaturated Zone

Because matrix diffusion directly influences the effectiveness of matrix sorption, the influence of uncertainty with respect to the matrix diffusion coefficient is examined in conjunction with uncertainty in matrix sorption coefficients, as discussed in SAR Section 2.3.8.5.5.1. Plots showing the relationship of mean travel times to matrix diffusion and matrix sorption coefficients for a weakly sorbing radionuclide, ^{237}Np (SAR Figures 2.3.8-51 and 2.3.8-52), and a moderately strongly sorbing radionuclide, ^{240}Pu (SAR Figures 2.3.8-53 and 2.3.8-54), are presented in the SAR. The travel time distributions for releases from the northern location and southern location are presented for simulations based on the glacial-transition climate state for each of the infiltration scenarios. For each climate scenario, a plot is presented showing contours of mean travel times with respect to the distributions of matrix diffusion and matrix sorption coefficients (SNL 2008b, Tables 6.8.2-1 and 6.8.2-2, respectively).

For the case of ^{237}Np released from the northern location, contours of mean travel times as a function of matrix diffusion and matrix sorption coefficients are presented in SAR Figure 2.3.8-51. As can be seen from this plot, the mean travel times are short and a function of both matrix diffusion and matrix sorption coefficients. The travel times range from less than one year for the high percolation flux infiltration scenario to greater than 100 years for the low percolation flux infiltration scenario. Again, these results are for repository releases into fractures and, as noted in Section 1.2.1, if the releases had been directly applied to the matrix instead, a higher rate of diffusion (i.e., a higher diffusion coefficient) would *increase* the rate of mass transport to the water table, showing an effect opposite of the process of matrix sorption.

For the case of ^{237}Np released from the southern location, contours of mean travel times as a function of matrix diffusion and matrix sorption coefficients are presented in SAR Figure 2.3.8-52. As can be seen from this plot, the mean travel times are much longer in the south, reflecting transport times that are controlled by transport through the CHn vitric matrix and the combined slower porous matrix type flow and sorption within the CHn vitric unit rock matrix. In addition, the influence of matrix diffusion is shown to be negligible in SAR Figure 2.3.8-52, which is consistent with the concept of travel time controlled by flow through the rock matrix of the CHn vitric tuff units, i.e, the travel time spent in the TSw is much lower than that spent in the vitric CHn matrix in the southern half of the repository. Comparing SAR Figures 2.3.8-50b and 2.3.8-52, it can be seen that matrix sorption has a strong influence on transport of ^{237}Np in the south with respect to releases within 10,000 years. The travel times in the southern part of the repository range between less than 500 years for the high percolation flux infiltration scenario to greater than 50,000 years for the low percolation flux infiltration scenario (SAR Figure 2.3.8-52). Note that for releases from the southern location, it is not very important whether the EBS releases are applied to the fractures or the matrix of the TSw because of the much greater travel time spent in the CHn.

For the case of ^{240}Pu released from the northern location, contours of mean travel times as a function of matrix diffusion and matrix sorption coefficients are presented in SAR Figure 2.3.8-53. As can be seen from this plot, the ^{240}Pu mean travel times are longer than for the weakly sorbed ^{237}Np. The contours also reflect that both matrix diffusion and matrix sorption coefficients influence the travel times, with the influence of the sorption coefficient increasing relative to the influence of the diffusion coefficient as the percolation fluxes increase. The travel times range from less than two years for the high percolation flux infiltration scenario to greater than 1,000 years for the low percolation flux infiltration scenario. It is mainly for the high range of diffusion coefficients (80th percentile) for the GT10 and GT30 climate states where matrix diffusion is of importance. The magnitude of the influence of matrix diffusion and matrix sorption in the north can also be seen in Figure 6.8.2-19[b](a) of the particle tracking report (SNL 2008b), where the normalized ^{240}Pu concentration, reflecting the coupled influence of radioactive decay, shows a relatively small decrease in concentration even for a fairly short half-life of 6.6×10^3 years.

For the case of ^{240}Pu release from the southern location, contours of mean travel times as a function of matrix diffusion and matrix sorption coefficients are presented in SAR Figure 2.3.8-54. As can be seen from this plot, the mean travel times range between less than 50,000 years for the high percolation flux infiltration scenario to greater than 500,000 years for

the low percolation flux infiltration scenario. The mean travel times for these southern release locations are controlled by the transport through the CHn vitric matrix, which is reflected in the longer travel times associated with slower porous matrix flow and the strong influence of sorption within the CHn vitric unit rock matrix. In addition, for southern release locations, the influence of matrix diffusion is negligible, which is consistent with mean travel times being controlled by transport through the CHn vitric matrix, as described in SAR Section 2.3.8.5.5.1. The magnitude of the influence of matrix sorption in the south is also reflected in Figure 6.8.2-19[b](b) of the particle tracking report (SNL 2008b), where the normalized ^{240}Pu concentration, reflecting the coupled influence of radioactive decay, shows a large decrease in concentration.

1.2.1.3 The Influence of Radionuclide Decay

As discussed above, the unsaturated zone's capability as a feature of the Lower Natural Barrier differs significantly for radionuclide releases from the northern and southern repository release locations because of the much faster transit time through the northern area compared to the southern area. This difference in travel time also controls the effectiveness of radioactive decay as a process for reducing releases from the unsaturated zone. Transport through the unsaturated zone below the northern section of the repository is rapid enough that most of the mass of slowly decaying radionuclides released from the EBS would reach the water table within 10,000 years (see SAR Figure 2.3.8-43). SAR Figure 2.3.8-43 presents the normalized cumulative breakthrough curves for 14 radionuclides exhibiting a wide range of half-lives and K_ds. Note that the K_ds are representative values that can be found in SAR Table 2.3.8-9. The radionuclides include ^{14}C, ^{135}Cs, ^{137}Cs, ^{129}I, ^{90}Sr, ^{99}Tc, ^{231}Pa, ^{229}Th, ^{232}Th, ^{232}U, ^{226}Ra, ^{36}Cl, ^{79}Se, and ^{126}Sn. For the above species most of the mass reaches the water table beneath the northern part of the repository, with the exception of ^{90}Sr and ^{137}Cs (SAR Figure 2.3.8-43a). ^{90}Sr and ^{137}Cs have short half-lives of 28.8 years and 30.1 years, respectively, and are strongly sorbed (see Table 1-5), which reduces their transport rates. The effectiveness of radioactive decay is much different in the southern area of the repository. Here, over a time span of 1,000,000 years, only species with relatively long half-lives (Table 1-5) and which are weakly or non-sorbing (Table 1-5), such as ^{14}C, ^{135}Cs, ^{129}I, ^{99}Tc, ^{36}Cl, and ^{79}Se, reach the water table. Note that, although the K_d for cesium is high in zeolitic tuffs, it is relatively low in vitric tuffs.

Figure 6.8.2-11[b] of the particle tracking report (SNL 2008b) presents the normalized releases of ^{99}Tc at the water table. Due to ^{99}Tc's long half-life (2.1×10^5 years) and relatively short travel times resulting from its lack of sorption, essentially all ^{99}Tc travelling through the unsaturated zone will eventually reach the water table, whether the release is in the north or south. Even for ^{14}C, with a short half-life of 5,700 years, due to lack of sorption most of the mass released from the EBS will reach the water table as shown in Figure 6.8.2-13[b] of the particle tracking report (SNL 2008b). To see how the combination of matrix diffusion and sorption influences the amount of radionuclide decay of sorbing radionuclides in the unsaturated zone, releases of ^{237}Np and ^{240}Pu can be examined. Figure 6.8.2-15[b] of the particle tracking report (SNL 2008b) presents the normalized cumulative unsaturated zone releases of weakly sorbing ^{237}Np at the water table for a repository release from the northern repository location. The normalized cumulative unsaturated zone releases are plotted as a function of matrix diffusion coefficient and sorption coefficient (see SNL 2008b, Tables 6.8.2-1 and 6.8.2-2, respectively, for the values of

matrix diffusion coefficient and sorption coefficient). Little radionuclide decay occurs in the unsaturated zone over the ranges of the two parameters. This is reflective of the short travel time (SAR Figure 2.3.8-51) and the long half-life (2.1×10^6 years) of ^{237}Np. Figure 6.8.2-16[b] of the particle tracking report (SNL 2008b) presents the normalized releases from the southern release location of weakly sorbing ^{237}Np at the water table as a function of matrix diffusion coefficient and sorption coefficient. Figure 6.8.2-16[b] of the particle tracking report (SNL 2008b) shows that little radionuclide decay occurs over the ranges of the two parameters. This again reflects the influence of the long half-life (2.1×10^6 years) of ^{237}Np.

SAR Figure 2.3.8-55 presents the normalized cumulative unsaturated zone releases from the northern release location of strongly sorbing ^{240}Pu at the water table. The normalized cumulative unsaturated zone releases are plotted as a function of matrix diffusion coefficient and sorption coefficient (see SNL 2008b, Tables 6.8.2-1 and 6.8.2-2, respectively, for the values of matrix diffusion coefficient and sorption coefficient). The normalized cumulative unsaturated zone releases show that little radionuclide decay occurs in the unsaturated zone until the diffusion coefficient reaches the higher end of its distribution ranges. This reflects the relatively short travel time in the north (SAR Figure 2.3.8-53) with respect to the relatively short half-life (6.6×10^3 years) of ^{240}Pu. SAR Figure 2.3.8-56 presents the normalized releases of strongly sorbing ^{240}Pu at the water table for a release from the southern repository location as a function of matrix diffusion coefficient and sorption coefficient. SAR Figure 2.3.8-56 shows that most of the ^{240}Pu has decayed away before reaching the water table. This reflects the long travel time in the region due to matrix transport and strong sorption along with the relatively short half-life (6.6×10^3 years) of ^{240}Pu.

Figure 6.6.2-7[b](a) of the particle tracking report (SNL 2008b) presents the normalized cumulative breakthrough curve for unsaturated zone releases from the northern release location of strongly sorbing ^{230}Th at the water table. A moderate delay of 1,000 years to the 50th percentile breakthrough value is indicated. The normalized cumulative unsaturated zone release breakthrough curve shows that only about 15% of the mass is lost to decay over the 1,000,000-year period. This reflects a small to moderate influence of decay (half-life of ^{230}Th = 7.5×10^4 years) on the particles with longer travel times in the system. The delay of particles is a reflection in the variance of travel times associated with the coupled process of matrix diffusion and matrix sorption. Figure 6.6.2-7[b](b) of the particle tracking report (SNL 2008b) presents the normalized cumulative breakthrough curve for unsaturated zone releases of strongly sorbing ^{230}Th at the water table for a release from the southern repository location. The figure shows that most of the ^{230}Th has decayed away before reaching the water table. This reflects the long travel time in the region due to matrix transport and strong sorption along with the relatively short half-life (7.5×10^4 years) of ^{230}Th.

An example of transport of a strongly sorbing element with both a short-lived and long-lived radionuclide is that of cesium. The strongly sorbing, rapidly decaying radionuclide ^{137}Cs (half-life = 30 years) is only affected to a small degree by matrix diffusion and matrix sorption in the north (see SAR Figure 2.3.8-43a), but even this short delay helps to reduce the mass released by more than two-thirds because of the very short half-life. In the south, the short half-life in conjunction with matrix diffusion prevents almost all of the ^{137}Cs from reaching the water table (see SAR Figure 2.3.8-43b). Therefore, the importance of matrix sorption is high for ^{137}Cs for

both a 10,000-year and a 1,000,000-year period. To evaluate the influence of matrix diffusion and matrix sorption without the effects of decay, the slowly degrading cesium isotope ^{135}Cs (half-life of $^{135}Cs = 2.3 \times 10^6$ years) is also examined. The normalized cumulative unsaturated zone release breakthrough curve for ^{135}Cs shows that 85% of the mass is released early, but after 500,000 years a second release pulse is seen, representing mass that has been held back by the coupled matrix diffusion/matrix sorption process. In the south, the mass release is delayed 10,000 years, making matrix sorption a highly important contributor to the transport processes.

1.2.1.4 Colloid Transport and Filtration

Two processes for colloid-facilitated transport are considered in the unsaturated zone. The first process is irreversible colloidal transport where the radionuclides are assumed to be permanently imbedded in or attached to the colloids and do not interact with the fluid phase or the stationary mineral phases along the fluid path. However, in this case the colloid particles themselves can interact with the stationary phases, which results in retardation of the radionuclide mass transported irreversibly on colloids. The second process is reversible colloidal transport where the radionuclides are simultaneously transported in both the fluid and colloidal phases, and reversible sorption onto the colloid phase is governed by local equilibrium with the fluid phase and the stationary mineral phases.

Irreversible colloid transport is based on permanent attachment of radionuclides to the colloids and advective–dispersive transport of the colloids within the unsaturated zone. Matrix diffusion is not considered in the conceptual model of colloid transport through the unsaturated zone, although advection between matrix and fractures is considered. Migration of colloids between fracture and matrix is controlled by the flow field describing the process of advection in the unsaturated zone. Within the fracture domain, the influence of colloid filtration is incorporated using a colloid retardation factor (SNL 2008b, Table 6-24). The irreversible colloids exiting the EBS enter the unsaturated zone as two phases, a retarded (or slow) phase and non-retarded (or fast) phase. In the TSPA-LA model, the retarded phase represents 99.832% of the release, and the non-retarded phase, 0.168% of the release. SAR Figure 2.3.8-48 presents the normalized cumulative breakthrough curves at the water table for releases of four americium and eight plutonium radionuclides irreversibly attached to colloids ($Ic^{241}Am$, $If^{241}Am$, $Ic^{243}Am$, $Ic^{243}Am$, $Ic^{238}Pu$, $If^{238}Pu$, $Ic^{239}Pu$, $If^{239}Pu$, $Ic^{240}Pu$, $If^{240}Pu$, $Ic^{242}Pu$, and $If^{242}Pu$ where Ic indicates a slow or retarded colloid and If a fast or unretarded colloid). The representative parameters used in the simulations are presented in SAR Table 2.3.8-9. The results are presented for releases of both slow and fast colloids from the northern (SAR Figure 2.3.8-48a) and southern (SAR Figure 2.3.8-48b) release locations. Note that the following discussion will only pertain to five of the radionuclides since ^{239}Pu results are biased by ingrowth as seen in normalized cumulative breakthrough curve values that exceed 1.0. SAR Figure 2.3.8-48a shows the normalized cumulative breakthrough curves at the water table for radionuclides released from the northern release location. The small delaying effect (<100 years) associated with a colloid retardation coefficient of 26 can be seen in the plot. It can be seen that, due to the fast transport time of the colloids (both slow and fast colloids), there is little attenuation due to decay, with only the short half-life radionuclides $Ic^{241}Am$ (half-life = 433 years), $Ic^{238}Pu$ (half-life = 88 years), and $If^{238}Pu$ (half-life = 88 years) demonstrating perceptible effects. In addition, Figure 6.8.2-23[b](a) of the particle tracking report (SNL 2008b), which depicts the relationship between colloid retardation

factor (for slow colloids) and mean log travel time of ^{240}Pu from a northern release location for the four infiltration scenarios, and SAR Figure 2.3.8-57a, which depicts the relationship between colloid retardation factor (for slow colloids) and normalized concentrations of ^{240}Pu from a northern release location for the four infiltration scenarios, indicate that the retardation coefficient can play an important role for species with half lives shorter than that of ^{240}Pu.

SAR Figure 2.3.8-48b shows the normalized cumulative breakthrough curves at the water table for radionuclides released from the southern release location. Although the colloid breakthrough curves in the southern release simulation are much slower than in the northern release simulation, the irreversible colloids tend to reach the water table in less than 10,000 years, so there is little attenuation due to decay with only Ic^{241}Am (half-life = 433 years), If^{241}Am (half-life = 433 years), Ic^{238}Pu (half-life = 88 years), and If^{238}Pu (half-life = 88 years) showing large effects (> 25% decayed). Figure 6.8.2-23[b](b) of the particle tracking report (SNL 2008b), which depicts the relationship between colloid retardation factor (for slow colloids) and mean log travel time of ^{240}Pu from a southern release location for the four infiltration scenarios, and SAR Figure 2.3.8-57b, which depicts the relationship between colloid retardation factor (for slow colloids) and normalized concentrations of ^{240}Pu from a southern release location for the four infiltration scenarios, indicate that the retardation coefficient can play an important role for the species with half-lives shorter than that of ^{240}Pu. However, the influence of colloid retardation in fractures on the slow colloids is less apparent in the southern release location results for most of the breakthrough curves. This is because much of the transport time in the south is through the vitric CHn matrix where the colloids are not subject to retardation in the model.

Reversible colloidal transport in the unsaturated zone includes the migration of radionuclides in the fractures in both the dissolved and colloidal phases, assuming local equilibrium. The governing equation for transport of the radionuclides in the two different phases can be summed and rewritten in terms of the dissolved phase as noted in Section 6.4.5 of the particle tracking report (SNL 2008b) and presented in Equation A-1. This creates an effective storage term (see Equation A-1) which considers the storage in both the dissolved and colloidal phase and reflects the influence of filtration on the transport velocity in the fractures. It also creates a term that effectively decreases the matrix diffusion term. Based on the latter term the reversible sorption of radionuclides onto colloids in the fractures effectively reduces the rate of the diffusion into the matrix (see Equation A-1) since mass in the fracture is partitioned into two phases and diffusion is only applicable to the fluid phase. In the TSPA-LA model, radionuclides subject to reversible colloid transport include ^{241}Am, ^{243}Am, ^{238}Pu, ^{239}Pu, ^{240}Pu, ^{242}Pu, ^{135}Cs, ^{137}Cs, ^{231}Pa, ^{229}Th, ^{232}Th, and ^{126}Sn.

Sensitivity to colloid filtration (based on the colloid retardation term) for reversible colloids is not examined in the particle tracking report (SNL 2008b). Therefore, only a qualitative assessment of importance is considered. To evaluate the importance of reversible colloid sorption as a process in the TSPA-LA model, results from Appendix K and Appendix K[a] of the TSPA-LA report (SNL 2008a) are examined. Two uncertainty and sensitivity analyses performed for the igneous intrusion modeling case give some insight into the influence of reversible colloid transport with respect to the transport of ^{239}Pu and ^{230}Th. Both ^{239}Pu and ^{230}Th are modeled as dissolved species subject to reversible sorption onto colloids transported through

the unsaturated zone. The transport of ^{239}Pu was simulated for a 20,000-year time period and the uncertainty and sensitivity analyses for unsaturated zone releases at the water table are presented in Section K6.4.1 of the TSPA-LA report (SNL2008a). Uncertainty and sensitivity analyses for unsaturated zone releases of ^{230}Th at the water table for a 1,000,000-year time period were also presented in Section K6.4.2[a] of the TSPA-LA report (SNL 2008a). Note that because the unsaturated zone releases are highly reflective of the EBS releases, the important unsaturated zone properties may be masked in the uncertainty analyses or may appear as less important. The two parameters that control the influence of reversible sorption on radionuclide transport (see Equation A-1) are the colloid retardation factor (SNL 2008b, Section 6.5-13 and Table 6-24) and the colloid K_c, which is the product of radionuclide sorption coefficient onto colloids (SNL 2008b, Section 6.5-12 and Table 6-22) and colloid concentration (SNL 2008b, Section 6.5-12 and Table 6-21). Figures K6.4.1-10 and K6.4.1-11 of the TSPA-LA report (SNL 2008a) present the PRCCs and the stepwise rank regression analyses for the unsaturated zone releases of ^{239}Pu for a 20,000-year igneous intrusion simulation with an igneous event occurring at 10 years. These figures show that, even for a strongly sorbing species such as ^{239}Pu, neither colloid parameter (*UZCOKDPU*, which is the analysis variable name for the plutonium K_c, and *UZRCOL*, which is the analysis variable name for the colloid retardation coefficient in fractures) shows up in the PRCCs or stepwise rank regression analyses for the unsaturated zone releases or the unsaturated zone cumulative releases of ^{239}Pu. Figures K6.4.2-4[a] and K6.4.2-5[a] of the TSPA-LA report (SNL 2008a) present the PRCCs and stepwise rank regression analyses for the unsaturated zone releases and the unsaturated zone cumulative releases of ^{230}Th for a 1,000,000-year stochastic igneous intrusion simulation with an igneous event occurring at 250 years. The figure shows that for ^{230}Th, which has a K_c range that is higher than that of plutonium (SNL 2008b, Section 6.5-12 and Table 6-22), the parameter *UZCOKDAM*, which is the analysis variable name for the americium, thorium, and protactinium K_cs, and *UZRCOL*, which is the analysis variable name for the colloid retardation coefficient in fractures, appear in the PRCC plots for unsaturated zone releases of ^{230}Th, but with very small correlation values. Again note that there are other parameters, especially those controlling the release from the EBS, that show a stronger correlation with the results, but the occurrence of parameters associated with reversible sorption in the PRCC indicates that the process of reversible sorption onto colloids and associated chemical filtration (SNL 2008c, Section 6.5.2-11) has some influence on highly sorbing species such as thorium (SNL 2008b, Table 6-22) in the unsaturated zone.

1.2.2 Saturated Zone Feature

The saturated zone flow and transport submodel can be divided into two segments, reflecting the processes controlling transport within them. The first segment, involving fractured volcanic rocks, is based on a dual porosity conceptual model and the second segment, representing transport through the alluvium, is based on a single porosity conceptual model. The volcanic units of the model extend southward approximately 11 km from the southern boundary of the repository footprint (SNL 2008d, Section 6.8.3). South of the volcanics, the radionuclide transport in alluvium is simulated up to the location of the accessible environment (approximately 18 km south of the repository). Advective–dispersive transport with diffusion into a non-mobile rock matrix is simulated in the first segment. The dominant transport processes within the volcanic units for dissolved species are advection in the fractures, matrix

diffusion between fractures and the rock matrix, and sorption within the rock matrix. The dominant transport processes within the volcanic units for colloidal-bound species include advection and colloid filtration within fractures (as approximated using a retardation factor, which is discussed in SNL 2008c, Section 6.5.2-11). The dominant transport processes within the alluvium are advection and sorption for dissolved species and advection, dispersion, and colloid filtration (as approximated using a retardation factor) for colloidal-bound radionuclides.

A series of sensitivity analyses are presented in *Site-Scale Saturated Zone Transport* (SNL 2008d), which demonstrate the importance of some of these transport processes. Two figures (SNL 2008d, Figures 6.8-2b and 6.8-2a) from those sensitivity analyses present breakthrough curves at the volcanics/alluvium contact and at the 18-km boundary, respectively, for conservative (non-sorbing) species transported with and without matrix diffusion. The simulation parameters (see SNL 2008d, Table 6.7-1) are representative parameters for the TSPA-LA model. As can be seen by comparing the times associated with the median values of the no-diffusion breakthrough curves on the two figures, purely advective–dispersive transport in the shorter alluvium transport leg would take about four times as long as in the volcanics leg.

Figure 6.7-1 of the site-scale report (SNL 2008d) presents breakthrough curves at the 18-km boundary for a conservative (non-sorbing) species that show the sensitivity of transport in the saturated zone to the uncertainty in the specific discharge multiplier for the saturated zone. Except for specific discharge multiplier values, the simulation parameters (see SNL 2008d, Table 6.7-1) are representative parameters for the TSPA-LA model. The specific discharge multiplier values for the three curves are the minimum value of the distribution used in the TSPA-LA model, 0.112, the base-case value of 1.0 and the maximum value of the distribution used in the TSPA-LA model, 8.933. The median (or 50%) breakthrough times for the minimum specific discharge multiplier value and maximum value are 31 and 52,840 years, respectively. The broad range of breakthroughs is indicative of the potentially strong influence of advective transport in the saturated zone.

1.2.2.1 Importance of Matrix Diffusion in the Saturated Zone for Non-Sorbing Species

The two sensitivity analyses figures (SNL 2008d, Figures 6.8-2b and 6.8-2a), present the advective–dispersive breakthrough curves at the volcanic/alluvium interface and at the 18-km boundary for the case of zero matrix diffusion versus the case based on a representative value for the matrix diffusion coefficient. Comparing these breakthrough curves for the simulations including matrix diffusion with those for no matrix diffusion shows the importance of matrix diffusion as a delaying factor. The no-diffusion breakthrough curves in these two figures show that matrix diffusion is only important in the fractured volcanics, which must be true since the alluvium is a single-porosity medium. Considering the arrival time of the 50% concentration level, the arrival time for no matrix diffusion is about 30 years at the volcanic/alluvium boundary 11 km downgradient from the southern boundary of the repository footprint (SNL 2008d, Section 6.8.3). For the combined travel through the volcanics and alluvium to the 18-km point downgradient, the 50% arrival time is about 150 years. Thus, the alluvium provides a travel time delay of about 120 years based on just the travel distance through the single porosity medium, whereas the fractures in the volcanic unit provide only a 30-year delay. Since the arrival time is about 800 years for the case with matrix diffusion, this diffusion process is adding about

650 years of delay to the saturated zone feature of the Lower Natural Barrier. Note that these results are for present-day flow, which means that the delay time would be much smaller over most of the simulation time. This change is a relatively small change with respect to time periods of interest (10,000 years and 1,000,000 years), so matrix diffusion alone (without matrix sorption) is not an effective delaying process in the saturated zone.

Section K6.5.1 of the TSPA-LA report (SNL 2008a) presents the results of uncertainty and sensitivity analyses based on a 20,000-year igneous intrusion modeling case with an event taking place at 10 years. The PRCCs for the time dependent release rates (SNL 2008a, Figure K6.5.1-13(e)) and cumulative time-dependent releases (SNL 2008a, Figure K6.5.1-13(f)) of ^{99}Tc from the saturated zone presented in this section can be used to examine the importance of advection and matrix diffusion in the transport of non-sorbing dissolved radionuclides in the saturated zone. The release rate PRCCs indicate that *SZGWSPDM* (the logarithm of the groundwater specific discharge multiplier) has a positive correlation with ^{99}Tc release rate at early times and a negative correlation at late times. Since the groundwater flow rates are proportional to the groundwater specific discharge multiplier, and because ^{99}Tc exhibits rapid transport through the saturated zone, most of the mass is released at early times. The more mass released at early times, the less mass remaining in the tail of the breakthrough curve to be released at late times. This is the cause of the positive correlation early and the negative correlation late. *SZGWSPDM* in the cumulative time-dependent releases is always positive reflecting the cumulative effects. *SZFIPOVO* (flowing interval porosity in the volcanic unit of the saturated zone) shows an opposite effect on release rates with a negative correlation to ^{99}Tc release at early times and a positive correlation at late times. This reflects the tendency for increasing flowing interval porosity values to reduce the transport velocity, as can be discerned from Equations A-5 and A-10. Note that at later times flowing interval porosity does not exert the degree of influence shown by *SZGWSPDM*. This is because the flowing interval porosity also influences matrix diffusion as shown in Equation A-5. The effect of flowing interval porosity on diffusion would be the opposite of its effect on advection. The other saturated zone parameter shown to be of importance in Figure K6.5.1-13(e) of the TSPA-LA report (SNL 2008a) is *SZFISPVO* (flowing interval spacing in volcanic units of saturated zone, m). The parameter shows a positive correlation with ^{99}Tc release at early times and a negative correlation at later times. The flowing interval spacing has an inverse relationship with matrix diffusion as can be seen in Equation A-6. The higher the value, the less effective matrix diffusion becomes. This is consistent with diffusion into the matrix at early times and out of the matrix at later times when most of the mass has passed through and concentrations are higher in the matrix than in the fractures. The importance of matrix diffusion as reflected in the PRCC results for flowing interval spacing are consistent with observations seen in Figures 6.8-2a and 6.8-2b of the site-scale report (SNL 2008d), discussed above.

1.2.2.2 Importance of Matrix Diffusion and Sorption in the Saturated Zone

The importance of sorption, in conjunction with matrix diffusion in the volcanic component of the saturated zone, to the transport of a weakly sorbing radionuclide such as ^{237}Np is seen by examining SAR Figure 2.3.9-48. The sensitivity analysis plot depicts the breakthrough curves of a conservative (non-sorbing) base-case species and a weakly sorbing species with a K_d of 1.3 mL/g, which is representative of neptunium in volcanic rock (see Table 6-8 of SNL 2008c).

The breakthrough curves show that, in conjunction with matrix diffusion, even a small matrix K_d increases the travel time by an order of magnitude. This is indicative of the importance of the sorption process in the saturated zone feature of the Lower Natural Barrier.

The uncertainty and sensitivity analyses presented in Appendix K of the TSPA-LA report (SNL 2008a) are not as definitive about the importance of sorption, in conjunction with matrix diffusion, in the volcanics. This is because for neptunium there are many parameters controlling the source input to the saturated zone, so that the importance of sensitive parameters within the saturated zone is partially obscured. For a weakly sorbing species, Section K6.5.1 of the TSPA-LA report (SNL 2008a) presents the results of uncertainty and sensitivity analyses for ^{237}Np, based on a 20,000-year igneous intrusion modeling case with an event taking place at 10 years (see SNL 2008a, Figures K6.5.1-7 and K6.5.1-8). The PRCCs (SNL 2008a, Figures K6.5.1-7(e) and K6.5.1-7(f)) indicate that the saturated zone parameters *SZGWSPDM* (the logarithm of the groundwater specific discharge multiplier) and *SZFIPOVO* (flowing interval porosity in the volcanic unit of the saturated zone) are important parameters at early times, with their influence decreasing with time. At early times, *SZGWSPDM* shows a strong positive correlation with the saturated zone releases of ^{237}Np and at later times a weaker positive correlation. At early times, *SZFIPOVO* shows a strong negative correlation with the saturated zone releases of ^{237}Np and at later times a weak positive correlation. At early times the negative correlation reflects the influence of *SZFIPOVO* on fracture flow—the higher the flowing interval porosity, the slower the fracture velocity. It should be noted that the flowing interval porosity affects two processes involved in radionuclide transport. First it influences the transport flow rate as shown in Equation A-10. It also influences the effectiveness of matrix diffusion as shown in the last term of Equation A-5. The greater the flowing interval porosity, the slower the fracture flow rate and the less effective matrix diffusion is. These influences have opposite effects on the transport of dissolved species. At later times, the positive correlation of *SZFIPOVO* to the saturated zone releases seems to reflect the parameter's influence on matrix diffusion (see Equation A-5).

For a strongly sorbing species, ^{239}Pu, Section K6.5.2 of the TSPA-LA report (SNL 2008a) presents the results of uncertainty and sensitivity analyses based on a 200,000-year igneous intrusion modeling case simulation with an event taking place at 250 years. The longer time period used for this analysis is necessary because of the later breakthrough times and associated zero values for the saturated zone releases of ^{239}Pu in the 20,000-year analysis. The three saturated zone parameters shown to be important in the PRCCs presented in Figure K6.5.2-4 of the TSPA-LA report (SNL 2008a) are *SZGWSPDM* (the logarithm of the groundwater specific discharge multiplier), *SZFISPVO* (flowing interval spacing in volcanic unit of saturated zone, m), and *SZDIFCVO* (diffusion coefficient for volcanic unit of saturated zone, m^2/s). *SZGWSPDM* is shown to be the most influential parameter in the transport with a positive correlation reflecting how the faster flow velocities increase the releases. The flowing interval spacing and diffusion coefficient both influence the effectiveness of matrix diffusion. The wider the flowing interval spacing, the less effective matrix diffusion is (see Equation A-5). This means that the correlation between *SZFISPVO* and the saturated zone releases is positive when the concentrations in the fractures exceed the concentrations in the matrix. For the time period presented in Figure K6.5.2-4 of the TSPA-LA report (SNL 2008a), this is the case. After most of the mass is out of the system and the release of ^{239}Pu is dependent on diffusion out of the

matrix, the correlation sign will reverse. The diffusion coefficient has the opposite effect on saturated zone releases. The lower the diffusion coefficient, the less effective matrix diffusion is (see Equation A-5). This means that the correlation between *SZDIFCVO* and the saturated zone releases is negative when the concentrations in the fractures exceed the concentrations in the matrix. For the time period presented in Figure K6.5.2-4 of the TSPA-LA report (SNL 2008a), this is the case. After most of the mass is out of the system and the release of ^{239}Pu is dependent on diffusion out of the matrix, the correlation sign will reverse.

The importance of sorption in the alluvium to the transport of a weakly sorbing radionuclide such as ^{237}Np in the saturated zone can be seen by examining Figure 6.7-4 of the site-scale report (SNL 2008d). The plot of the sensitivity analysis depicts the breakthrough curves of a base-case conservative (non-sorbing) species, a weakly sorbing species with a K_d of 6.3 mL/g, which is representative of neptunium in alluvium (see Table 6-8 of SNL 2008c), and a very strongly sorbing species with a K_d of 10,000, which is a high-end value for thorium, americium, or protactinium (see Table 6-8 of SNL 2008c). The breakthrough curves show that even a small alluvium K_d increases the travel time by an order of magnitude. A third breakthrough curve shows that for extremely high alluvium K_ds, mass will not reach the 18-km boundary in less than 1,000,000 years.

1.2.2.3 Colloid Transport and Filtration

As with the unsaturated zone, two processes simulating colloid-facilitated transport are considered in the saturated zone. The first process is irreversible colloidal transport where the radionuclides are assumed to be permanently imbedded in or attached to the colloids and do not interact with the fluid phase or the stationary mineral phases along the fluid path. However, in this case the colloid particles themselves can interact with the stationary phases, which results in retardation of the radionuclide mass transported irreversibly on colloids. The second process is reversible colloidal transport where the radionuclides are simultaneously transported in both the fluid and colloidal phases and reversible sorption onto the colloid phase is governed by local equilibrium with the fluid phase and the stationary mineral phases.

The importance of colloid filtration on irreversible colloid transport is demonstrated using the sensitivity analyses presented in Section K6.5.1 of the TSPA-LA report (SNL 2008a) and in Section 6.7 of the site-scale report (SNL 2008d). The importance of colloid filtration in conjunction with sorption on reversible colloid transport is demonstrated using the sensitivity analyses for ^{230}Th presented in Section K6.5.2[a] of the TSPA-LA report (SNL 2008a).

For ^{239}Pu irreversibly attached to slow colloids, which are affected by filtration, Section K6.5.1 of the TSPA-LA report (SNL 2008a) presents the results of uncertainty and sensitivity analyses based on a 20,000-year igneous intrusion modeling case with an event taking place at 10 years. The three saturated zone parameters shown to be important in the PRCCs presented in Figure K6.5.1-1 of the TSPA-LA report (SNL 2008a) are *SZCOLRAL* (logarithm of the colloid retardation factor in the alluvial unit of the saturated zone), *SZGWSPDM* (the logarithm of the groundwater specific discharge multiplier), and *SZFIPOVO* (flowing interval porosity in the volcanic unit of the saturated zone). The broad uncertainty range for *SZCOLRAL* (SNL 2008c, Table 6-8) causes a strong negative correlation between *SZCOLRAL* and saturated zone release

rate, since a higher *SZCOLRAL* causes a lower release rate as a result of retardation. The importance of *SZGWSPDM* and *SZFIPOVO* is a function of how they affect the flow velocities. When *SZGWSPDM* is increased, the flow rate in both the fractures and alluvium increases. *SZGWSPDM* shows a positive correlation because larger values are increasing the rate of mass release from the saturated zone. *SZFIPOVO* influences the rate of flow in fractures—the higher the value, the slower the flow (see Equations A-5 and A-10). *SZFIPOVO* shows a negative correlation because the higher the value the lower the rate of mass release from the saturated zone (a higher *SZFIPOVO* means a higher storativity in the saturated zone fractures).

Figure 6.7-12 of the site-scale report (SNL 2008d) presents breakthrough curves at the 18-km boundary for radionuclides irreversibly sorbed onto colloids for two different values of the colloid retardation (filtration) factor in the fractures of the volcanic pathway. Except for the volcanic colloid retardation factors, the other simulation parameters (see SNL 2008d, Table 6.7-1) are assigned representative values from the TSPA parameter distributions. The volcanic colloid retardation factors for the two colloid transport breakthrough curves (the base-case curve on the plot is for a dissolved species and includes diffusion) are the minimum value (6) of the distribution used in the TSPA-LA model and the maximum value (794) of the distribution used in the TSPA-LA model. The median (or 50%) breakthrough times for the minimum and maximum values are 4,600 and 28,599 years, respectively. This broad range of breakthrough times is indicative of the importance of colloid filtration in the volcanics for that portion of the plutonium mass transported irreversibly on colloids. However, more of the plutonium mass is transported as dissolved than as irreversibly sorbed on colloids (SNL 2008a, Figures K6.5.2-1, K6.5.2-4, K7.5-1, and K7.5-4), which is why colloid transport is considered to be not important to Lower Natural Barrier capability in SAR Table 2.1-4.

Figure 6.7-6 of the site-scale report (SNL 2008d) presents breakthrough curves at the 18-km boundary for radionuclides irreversibly sorbed onto colloids for two different values of the colloid retardation (filtration) factor for the alluvium. Except for the alluvium colloid retardation factors, the other simulation parameters (see SNL 2008d, Table 6.7-1) are assigned representative values from the TSPA parameter distributions. The alluvium colloid retardation factors for the three colloid transport breakthrough curves (the base-case curve on the plot is for a dissolved species and includes diffusion) are the fast-fraction colloid value of zero (labeled as "Diffusion, 1×10^{-50}"), the minimum value (8) of the distribution used in the TSPA-LA model (labeled as "alluvium-Low"), and the maximum value (5188) of the distribution used in the TSPA-LA model (labeled as "alluvium-Hi"). The median (or 50%) breakthrough times for the minimum and maximum values are 1,859 and 688,357 years, respectively. The unretarded ("fast") colloid breakthrough time is over an order of magnitude less than the minimum distribution value (8) breakthrough time. This broad range of breakthroughs is indicative of the importance of colloid retardation in the alluvium for that portion of the plutonium mass transported irreversibly on colloids. However, more of the plutonium mass is transported as dissolved than as irreversibly sorbed on colloids (SNL 2008a, Figures K6.5.2-1, K6.5.2-4, K7.5-1, and K7.5-4), which is why colloid transport is considered to be not important to Lower Natural Barrier capability in SAR Table 2.1-4. Finally, it can be seen by comparing Figure 6.7-6 of the site-scale report (SNL 2008d) with Figure 6.7-12 (SNL 2008d) that colloid filtration (retardation) in the alluvium is greater than colloid filtration (retardation) in the volcanics.

Reversible colloidal transport in the saturated zone simulates the migration of radionuclides in the fractures in both the dissolved and colloidal phases. The governing equation for transport of the radionuclides in the two phases can then be summed and rewritten in terms of the dissolved phase as noted in Section 6.4.5 of the particle tracking report (SNL 2008b) and presented in Equation A-5. In the TSPA-LA model, radionuclides subject to reversible colloid transport include ^{241}Am, ^{243}Am, ^{238}Pu, ^{239}Pu, ^{240}Pu, ^{242}Pu, ^{135}Cs, ^{137}Cs, ^{231}Pa, ^{229}Th, ^{232}Th, and ^{126}Sn. Reversible colloid transport is mainly important in radionuclides with very high sorption onto colloids, such as ^{241}Am, ^{243}Am, ^{231}Pa, ^{229}Th, ^{232}Th, and ^{126}Sn. To evaluate the importance of reversible colloid sorption as a process in the saturated zone, results from Section K6.5.2[a] of the TSPA-LA report (SNL 2008a) are examined. The uncertainty and sensitivity analyses for the igneous intrusion modeling case presented there give some insight into the influence of reversible colloid transport in the saturated zone with respect to the transport of ^{230}Th. The two parameters that control the influence of reversible sorption on radionuclide transport (see Equation A-5) are the colloid retardation factor (SNL 2008c, Section 6.5.2-11) and colloid K_c. The latter is the product of the radionuclide sorption coefficient onto colloids (SNL 2008c, Section 6.5.2-12) and the colloid concentration (SNL 2008c, Section 6.5.2-12) in the aqueous phase. Figures K6.5.2-8[a] and Figures K6.5.2-9[a] of the TSPA-LA report (SNL 2008a) present the PRCCs and stepwise rank regression analyses for the saturated zone releases and the saturated zone cumulative releases of ^{230}Th for a 1,000,000-year igneous intrusion simulation with an igneous event occurring at 250 years. The PRCC plots (SNL 2008a, Figure K6.5.2-8[a]) show that for ^{230}Th, the releases are most strongly correlated with the parameter *SZCONCOL* (logarithm of the concentration of colloids in ground water, g/mL), which exerts a strong control over reversible sorption in both the fractures (Equation A-5) and alluvium (Equation A-11). This is reflective of the importance of reversible sorption in the transport of highly sorbing radionuclides. In addition, the stepwise rank regression analyses, presented in Figure K6.5.2-9[a] of the TSPA-LA report (SNL 2008a), shows that *SZCONCOL* shows the highest correlation with the releases through most of the simulation. The stepwise rank regression analyses also show that *SZKDAMCO* (sorption coefficient for reversible sorption of americium, thorium, and protactinium onto groundwater colloids, mL/g) is also an important parameter. In all the analyses, the two parameters show positive correlations because the higher they are, the more radionuclide mass is transported in the colloid phase, which is not subject to matrix diffusion.

1.2.2.4 Influence of Decay

The breakthrough curves used to evaluate three-dimensional saturated zone transport in the TSPA model (SNL 2008c, Section 6.6[a]) will be used to evaluate how the transport processes of advection, matrix diffusion, matrix sorption, and colloid filtration can have varying effects based on relative differences in the decay rate of radionuclides. These breakthrough curves include one or more of the aforementioned transport processes but in the absence of radioactive decay. By comparing the distribution of saturated zone travel times without decay to the half-life of the radionuclide, it is possible to draw various conclusions about how the effectiveness of each process, or a combination of processes, is influenced by radioactive decay. Seven different sets of breakthrough curves are considered for seven different radioactive species that are affected to varying degrees by one or more of the transport processes: (1) a non-sorbing dissolved species (SNL 2008c, Figure 6-6[a]), (2) a very highly sorbing dissolved species subject to reversible

sorption onto colloids (SNL 2008c, Figure 6-7[a]), (3) a strongly sorbing dissolved species subject to reversible sorption onto colloids (SNL 2008c, Figure 6-8[a]), (4) moderately to strongly sorbing dissolved species subject to sorption onto smectite colloids (SNL 2008c, Figure 6-9[a]) (5) a weakly sorbing dissolved species (SNL 2008c, Figure 6-11[a]), (6) a species irreversibly bound to glass colloids which can be filtered (SNL 2008c, Figure 6-12[a]), and (7) a species irreversibly bound to glass colloids which cannot be filtered (SNL 2008c, Figure 6-13[a]). Table 6-10[a] of the flow and transport abstraction (SNL 2008c) presents a summary of simulated transport times for the above radionuclides in the saturated zone for the glacial-transition climate state. Note that these plots from Section 6.6.1[a] of the flow and transport abstraction (SNL 2008c) are for the northwest saturated zone source region. This means that the travel times discussed will be slightly longer than a release in a southern region.

The breakthrough curves discussed here represent the results of sampling all uncertain parameters, including those from the volcanic tuffs and those from alluvium. Therefore, the influence of processes such as matrix diffusion (and matrix sorption) in the volcanics cannot be separated from matrix sorption in the alluvium. However, a comparison of these curves provides insight into the effectiveness of the whole of the saturated zone as a feature of the Lower Natural Barrier for specific radionuclides, and the relative influence of transport processes in the saturated zone can be discerned by comparing sets of breakthrough curves representing radionuclides with different half-lives and different transport properties (e.g., sorption coefficients). The effectiveness of the saturated zone as a feature of the Lower Natural Barrier for specific radionuclides can be broken down into the degree that radionuclides are delayed in the saturated zone (which controls the timing of releases to the accessible environment) and how much radionuclide decay reduces the amount of mass reaching the accessible environment.

An examination of Figure 6-6[a] of the flow and transport abstraction (SNL 2008c) shows that the median travel time for all breakthrough curves for non-sorbing dissolved species such as ^{99}Tc (based on the time value for the median or 50th percentile relative mass value on the curve) is about 230 years. It can also be seen that most of the 50th percentile relative mass values on the breakthrough curves reach the 18-km boundary before 10,000 years. This indicates that, because of its long half-life (2.1×10^5 years), matrix diffusion in the volcanics will not be an important factor in decreasing the mass of ^{99}Tc, since matrix diffusion alone cannot result in enough delay time in the unsaturated zone to begin to cause significant decay.

Figure 6-7[a] of the flow and transport abstraction (SNL 2008c) shows that the median travel time for all breakthrough curves for a very highly sorbing dissolved species subject to reversible sorption onto smectite colloids, such as ^{230}Th, is greater than 1,000,000 years. It can also be seen that most of the 50th percentile relative mass values on the breakthrough curves will not reach the 18-km boundary before 1,000,000 years. When the breakthrough times are considered in conjunction with ^{230}Th's half-life of 7.5×10^4 years, it can be concluded that very little ^{230}Th will reach the 18-km boundary except as a daughter product of ^{234}U. With respect to the transport processes controlling the attenuation of ^{230}Th in the saturated zone, a comparison of Figure 6-7[a] and Figure 6-6[a] of the flow and transport abstraction (SNL 2008c) shows that the combination of matrix diffusion coupled with matrix sorption in the volcanics, as well as matrix sorption in the alluvium (and to some extent colloid filtration), are important factors in reducing the amount of ^{230}Th reaching the accessible environment.

Figure 6-8[a] of the flow and transport abstraction (SNL 2008c) shows that the median travel time for all breakthrough curves for a strongly sorbing dissolved element subject to reversible sorption onto smectite colloids, such as cesium, is over 1,000,000 years. It can also be seen that most of the 50th percentile relative mass values on the breakthrough curves will not reach the 18-km boundary before 1,000,000 years. When considering the breakthrough times in conjunction with ^{137}Cs's half-life of 30 years, ^{137}Cs will not reach the accessible environment. On the other hand, the much longer half-life of ^{135}Cs (2.3×10^6 years) will dictate that decay is not important with respect to transport processes. With respect to the transport processes controlling the attenuation of cesium in the saturated zone, a comparison of Figure 6-8[a] and Figure 6-6[a] of the flow and transport abstraction (SNL 2008c) shows that the combination of matrix diffusion coupled with matrix sorption in the volcanics, as well as matrix sorption in the alluvium, will keep most ^{137}Cs and ^{135}Cs from reaching the accessible environment.

Figure 6-9[a] of the flow and transport abstraction (SNL 2008c) shows that the median travel time for all breakthrough curves for moderately to strongly sorbing dissolved species subject to reversible sorption onto smectite colloids, such as ^{240}Pu is 95,000 years. It can also be seen that some of the 50th percentile relative mass values on the breakthrough curves won't reach the 18-km boundary before 1,000,000 years, which will cause a moderate reduction in mass reaching the accessible environment. When considering the breakthrough times in conjunction with ^{240}Pu's half-life of 6.6×10^3 years, very little ^{240}Pu will reach the 18-km boundary. With respect to the transport processes controlling the attenuation of ^{240}Pu in the saturated zone, a comparison of Figure 6-9[a] and Figure 6-6[a] of the flow and transport abstraction (SNL 2008c) shows that the combination of matrix diffusion coupled with matrix sorption in the volcanics, as well as matrix sorption in the alluvium, are important factors in reducing the amount of ^{240}Pu reaching the accessible environment.

Figure 6-11[a] of the flow and transport abstraction (SNL 2008c) shows that the median travel time for all breakthrough curves for a weakly sorbing dissolved species, such as ^{237}Np, is 3,700 years. It can also be seen that some of the 50th percentile relative mass values on the breakthrough curves will not reach the 18-km boundary before 10,000 years, which will cause a moderate reduction in mass reaching the accessible environment for that time period. Most of the mass will reach the accessible environment by 1,000,000 years. When considering the breakthrough times in conjunction with ^{237}Np's long half-life (2.1×10^6 years), decay will not factor into the release amounts. With respect to the transport processes controlling the attenuation of ^{237}Np in the saturated zone, a comparison of Figure 6-11[a] and Figure 6-6[a] of the flow and transport abstraction (SNL 2008c) shows that the combination of matrix diffusion coupled with matrix sorption in the volcanics, as well as matrix sorption in the alluvium, are important factors in reducing the amount of ^{237}Np reaching the accessible environment, especially over a 10,000-year period.

Figure 6-13[a] of the flow and transport abstraction (SNL 2008c) shows that the median travel time for all breakthrough curves for radionuclides irreversibly attached to glass colloids and not subject to colloid filtration, such as ^{240}Pu, is 60 years. It can also be seen that all of the 50th percentile relative mass values on the breakthrough curves will reach the 18-km boundary before 2,000 years. When considering the breakthrough times in conjunction with ^{240}Pu's half-life of 6.6×10^3 years, very little loss of mass to decay will take place, so the saturated zone barrier effectiveness will be low. Figure 6-12[a] of the flow and transport abstraction (SNL 2008c)

shows that the median travel time for all breakthrough curves for radionuclides irreversibly attached to glass colloids and subject to colloid filtration, such as ^{240}Pu, is 4,500 years. When considering the large range of times over which the breakthrough curves are spread, 100 years to about 500,000 years (SNL 2008c, Table 6-10[a]), in conjunction with ^{240}Pu's half-life of 6.6×10^3 years, there will be a substantial loss of mass to decay for some realizations but not much for others. Comparing Figure 6-13[a] and Figure 6-12[a] of the flow and transport abstraction (SNL 2008c), it can be seen that colloid filtration in the volcanics and the alluvium can play a large role in reducing the amount of irreversibly attached ^{240}Pu that reaches the accessible environment.

Table 1-5. Radionuclide Half-Lives and Sorption-Coefficient Distributions for the Unsaturated Zone

Species	Half-Life[a] (years)	Rock Type	Type of Uncertainty Distribution	Coefficients Describing Distribution[b] (K_d: mL/g)
^{14}C	5.7×10^3	Zeolitic	Uniform	0.0
		Devitrified	Uniform	0.0
		Vitric	Uniform	0.0
^{36}Cl	3.0×10^5	Zeolitic	Uniform	0.0
		Devitrified	Uniform	0.0
		Vitric	Uniform	0.0
^{135}Cs	2.3×10^6	Zeolitic	Cumulative	(K_d value, probability) (425., 0) (5000., 0.5) (20000., 1.0)
		Devitrified	Uniform	Range = 1 – 15
		Vitric	Cumulative	(K_d value, probability) (0., 0) (2., 0.5) (100., 1.0)
^{137}Cs	30	Zeolitic	Cumulative	(K_d value, probability) (425., 0) (5000., 0.5) (20000., 1.0)
		Devitrified	Uniform	Range = 1 – 15
		Vitric	Cumulative	(K_d value, probability) (0., 0) (2., 0.5) (100., 1.0)
^{129}I	1.6×10^7	Zeolitic	Uniform	0.0
		Devitrified	Uniform	0.0
		Vitric	Uniform	0.0
^{237}Np	2.1×10^6	Zeolitic	Cumulative	(K_d value, probability) (0., 0) (0.5, 0.5) (6., 1.0)
		Devitrified	Cumulative	(K_d value, probability) (0., 0) (0.5, 0.5) (6., 1.0)
		Vitric	Cumulative	(K_d value, probability) (0., 0) (1.0, 0.5) (3., 1.0)
^{231}Pa	3.3×10^4	Zeolitic	Truncated Normal	Range = 1000 – 10000 Mean=5500 Std Dev=1500
		Devitrified	Truncated Normal	Range = 1000 – 10000 Mean=5500 Std Dev=1500
		Vitric	Truncated Normal	Range = 1000 – 10000 Mean=5500 Std Dev=1500

Table 1-5. Radionuclide Half-Lives and Sorption-Coefficient Distributions for the Unsaturated Zone (Continued)

Species	Half-Life[a] (years)	Rock Type	Type of Uncertainty Distribution	Coefficients Describing Distribution[b] (K_d: mL/g)
^{239}Pu	2.4×10^4	Zeolitic	Cumulative	(K_d value, probability) (10., 0) (100., 0.5) (200., 1.0)
		Devitrified	Cumulative	K_d value, probability) (10., 0) (70., 0.5) (200., 1.0)
		Vitric	Cumulative	K_d value, probability) (10., 0) (100., 0.5) (200., 1.0)
^{240}Pu	6.6×10^3	Zeolitic	Cumulative	(K_d value, probability) (10., 0) (100., 0.5) (200., 1.0)
		Devitrified	Cumulative	K_d value, probability) (10., 0) (70., 0.5) (200., 1.0)
		Vitric	Cumulative	K_d value, probability) (10., 0) (100., 0.5) (200., 1.0)
^{242}Pu	3.8×10^5	Zeolitic	Cumulative	(K_d value, probability) (10., 0) (100., 0.5) (200., 1.0)
		Devitrified	Cumulative	K_d value, probability) (10., 0) (70., 0.5) (200., 1.0)
		Vitric	Cumulative	K_d value, probability) (10., 0) (100., 0.5) (200., 1.0)
^{226}Ra	1.6×10^3	Zeolitic	Uniform	Range = 1000 – 5000
		Devitrified	Uniform	Range = 100 – 1000
		Vitric	Uniform	Range = 50 – 600
^{79}Se[c]	2.9×10^5	Zeolitic	Truncated Log Normal	Range = 1 – 35 Mean=14.3 Std Dev=7.9
		Devitrified	Truncated Log Normal	Range = 1 – 50 Mean=14 Std Dev=11.2
		Vitric	Truncated Log Normal	Range = 0 – 25 Mean=8.6 Std Dev=7.9
^{126}Sn[c]	2.3×10^5	Zeolitic	Log Uniform	Range = 100 – 5000
		Devitrified	Log Uniform	Range = 100 – 100000
		Vitric	Log Uniform	Range = 100 – 5000
^{90}Sr	2.9×10^1	Zeolitic	Uniform	Range = 50 – 2000
		Devitrified	Uniform	Range = 10 – 70
		Vitric	Uniform	Range = 0 – 50
^{99}Tc	2.1×10^5	Zeolitic	Uniform	0.0
		Devitrified	Uniform	0.0
		Vitric	Uniform	0.0
^{229}Th	7.3×10^3	Zeolitic	Uniform	Range = 1000 - 30000
		Devitrified	Uniform	Range = 1000 - 10000
		Vitric	Uniform	Range = 1000 - 10000
^{230}Th	7.5×10^4	Zeolitic	Uniform	Range = 1000 - 30000
		Devitrified	Uniform	Range = 1000 - 10000
		Vitric	Uniform	Range = 1000 - 10000

Table 1-5. Radionuclide Half-Lives and Sorption-Coefficient Distributions for the Unsaturated Zone (Continued)

Species	Half-Life[a] (years)	Rock Type	Type of Uncertainty Distribution	Coefficients Describing Distribution[b] (K_d: mL/g)
^{232}Th	1.4×10^{10}	Zeolitic	Uniform	Range = 1000 - 30000
		Devitrified	Uniform	Range = 1000 - 10000
		Vitric	Uniform	Range = 1000 - 10000
^{232}U	7.0×10^{1}	Zeolitic	Cumulative	(K_d value, probability) (0, 0) (0.5, 0.5) (30, 1.0)
		Devitrified	Cumulative	(K_d value, probability) (0, 0) (0.2, 0.5) (4., 1.0)
		Vitric	Cumulative	(K_d value, probability) (0, 0) (0.2, 0.5) (3., 1.0)

NOTE: The radioisotopes of carbon, iodine, technetium, and chlorine are treated as nonsorbing and are assigned 0.0 K_d values for all three rock types. The values used for the base-case model are median values of these distributions and are listed in Section 6.6.1 of *Particle Tracking Model and Abstraction of Transport Processes* (SNL 2008b).

2. COMMITMENTS TO NRC

None.

3. DESCRIPTION OF PROPOSED LA CHANGE

None.

4. REFERENCES

BSC (Bechtel SAIC Company) 2004. *Development of Numerical Grids for UZ Flow and Transport Modeling.* ANL-NBS-HS-000015 REV 02. Las Vegas, Nevada: Bechtel SAIC Company. ACC: DOC.20040901.0001; LLR.20080522.0082

SNL 2007. *UZ Flow Models and Submodels.* MDL-NBS-HS-000006 REV 03 AD 01. Las Vegas, Nevada: Sandia National Laboratories. ACC: DOC.20080108.0003; DOC.20080114.0001; LLR.20080414.0007; LLR.20080414.0033; LLR.20080522.0086.

SNL 2008a. *Total System Performance Assessment Model /Analysis for the License Application.* MDL-WIS-PA-000005 REV 00 AD 01. Las Vegas, Nevada: Sandia National Laboratories. ACC: DOC.20080312.0001; LLR.20080414.0037; LLR.20080507.0002; LLR.20080522.0113; DOC.20080724.0005.

SNL 2008b. *Particle Tracking Model and Abstraction of Transport Processes.* MDL-NBS-HS-000020 REV 02 AD 02. Las Vegas, Nevada: Sandia National Laboratories. ACC: DOC.20080129.0008; DOC.20070920.0003; LLR.20080325.0287; LLR.20080522.0170; LLR.20080603.0082; DOC.20090113.0002.

SNL 2008c. *Saturated Zone Flow and Transport Model Abstraction.* MDL-NBS-HS-000021 REV 03 AD 02. Las Vegas, Nevada: Sandia National Laboratories. ACC: DOC.20080107.0006; LLR.20080408.0256.

SNL 2008d. *Site-Scale Saturated Zone Transport.* MDL-NBS-HS-000010 REV 03 AD 01. Las Vegas, Nevada: Sandia National Laboratories. ACC: DOC.20080121.0003; DOC.20080117.0002; DOC.20090115.0001.

SNL 2008e. *Features, Events, and Processes for the Total System Performance Assessment: Analyses.* ANL-WIS-MD-000027 REV 00. Las Vegas, Nevada: Sandia National Laboratories. ACC: DOC.20080307.0003; DOC.20080407.0009; DOC.20080722.0002.

5. LIST OF ATTACHMENTS

Attachment A: GOVERNING MASS BALANCE EQUATIONS

ATTACHMENT A: GOVERNING MASS BALANCE EQUATIONS

A.1 Governing Equations for Mass Transport in the Unsaturated Zone

The governing equations for radionuclide transport, as implemented in the unsaturated zone transport model, are presented here. Note that decay is not considered in the equations below. In the unsaturated zone particle tracking model, decay is separately implemented by permanently removing a calculated number of particles (see SNL 2008b, Section 6.4.4) from the simulation for each group of particles, where each group represents the mass of a specific radionuclide released over a specific time step. The governing equations for radionuclide transport in the unsaturated zone (SNL 2008b, Equations 6-16, C-5, C-6, C-39 and C-40) can be expressed as follows:

$$\left[\frac{R_f + K_c R_{coll}}{1 + K_c}\right]\frac{\partial C_f}{\partial t} = D\frac{\partial^2 C_f}{\partial z^2} - v_f\frac{\partial C_f}{\partial z} + \left.\frac{S_{eff}^{1+\gamma} D_m \theta_m}{\theta_f b(1 + K_c)}\frac{\partial C_m}{\partial x}\right|_{x=b} \quad \text{(Eq. A-1)}$$

$$R_m\frac{\partial C_m}{\partial t} = S_{eff}^{2\gamma} D_m\frac{\partial^2 C_m}{\partial x^2} - v_m\frac{\partial C_m}{\partial z}, \quad \text{(Eq. A-2)}$$

$$K_c = K_{dc} C_{coll} \quad \text{(Eq. A-3)}$$

$$R_m = 1 + \frac{\rho_{bm} K_{dm}}{\theta_m} \quad \text{(Eq. A-4)}$$

where:

C_f = dissolved species concentration in the fracture (m/L^3)

R_{coll} = colloid retardation coefficient (dimensionless)

R_f = fracture retardation coefficient (dimensionless)

K_c = colloid distribution parameter (dimensionless)

K_{dc} = radionuclide sorption coefficient onto colloids (L^3/m)

C_{coll} = colloid concentration (m/L^3)

v_f = fracture interstitial pore water velocity (L/t)

D = fracture dispersion coefficient (L^2/t)

D_m = matrix diffusion coefficient (L^2/t)

S_{eff} = effective fracture saturation (dimensionless)

γ = active fracture model exponent (dimensionless)

b = half-aperture (L)

θ_f = fracture water content (dimensionless)

θ_m = matrix water content (dimensionless)

C_m = dissolved species concentration in the matrix (m/L^3)

K_{dm} = radionuclide sorption coefficient onto rock matrix (L^3/m)

ρ_{bm} = bulk density of the rock matrix (m/L^3)

R_m = matrix retardation coefficient (dimensionless)

v_m = matrix interstitial pore water velocity (L/t).

A.2 Governing Equations for Mass Transport in the Saturated Zone

The governing equations for radionuclide transport, as implemented in the saturated zone transport model, are presented here. Note that decay is not considered in the equations. The governing equations for radionuclide transport in the saturated-zone volcanics (SNL 2008c, Equations 6-8 and 6-12) are as follows:

$$\left[\frac{R_f^{'}+K_{dc}C_{coll}R_{coll}}{1+K_{dc}C_{coll}}\right]\frac{\partial C_f}{\partial t}=D\frac{\partial^2 C_f}{\partial z^2}-V_f\frac{\partial C_f}{\partial z}+\frac{2D_m\phi_m}{\phi_{fi}S_{fi}\left(1+K_{dc}C_{coll}\right)}\frac{\partial C_m}{\partial x}\bigg|_{x=b} \quad \text{(Eq. A-5)}$$

$$R_m\frac{\partial C_m}{\partial t}=D_m\frac{\partial^2 C_m}{\partial x^2}, \quad \text{(Eq. A-6)}$$

$$R_f^{'}=1+\frac{(\phi_{fi}-\phi_{fi}^{avg})}{(\phi_m-\phi_{fi}^{avg})}\frac{\rho_{bm}K_{dm}}{\phi_m}\bigg|_{\phi_{fi}>\phi_{fi}^{avg}} \quad \text{(Eq. A-7)}$$

$$R_f^{'}=1\big|_{\phi_{fi}\le\phi_{fi}^{avg}} \quad \text{(Eq. A-8)}$$

$$R_m=1+\frac{\rho_{bm}K_{dm}}{\phi_m} \quad \text{(Eq. A-9)}$$

$$V_f=\frac{(1+\phi_{fi})S_{fi}V_d}{\phi_{fi}S_{fi}}\cong\frac{S_{fi}V_d}{\phi_{fi}S_{fi}}=\frac{V_d}{\phi_{fi}} \quad \text{(Eq. A-10)}$$

The governing equation for radionuclide transport in the saturated zone alluvium is similar to that in the volcanics, except with no term representing matrix diffusion:

$$\left[\frac{R_a + K_{dc} C_{coll} R_{coll}}{1 + K_{dc} C_{coll}}\right] \frac{\partial C_a}{\partial t} = D \frac{\partial^2 C_a}{\partial z^2} - V_a \frac{\partial C_a}{\partial z} \qquad \text{(Eq. A-11)}$$

where:

C_f = dissolved species concentration in the fracture (m/L^3)

R_{coll} = colloid retardation coefficient (dimensionless)

$R_f^{'}$ = fracture retardation coefficient (dimensionless)

K_{dc} = radionuclide sorption coefficient onto colloids (L^3/m)

C_{coll} = colloid concentration (m/L^3)

V_d = Darcy velocity (L/t)

V_f = Fracture velocity (L/t)

D = fracture dispersion coefficient (L^2/t)

D_m = matrix diffusion coefficient (L^2/t)

b = half-aperture (L)

S_{fi} = Flowing interval fracture spacing (L)

φ_{fi} = Flowing interval fracture porosity (dimensionless)

φ_m = matrix porosity (dimensionless)

C_m = dissolved species concentration in the matrix (m/L^3)

R_m = matrix retardation coefficient (dimensionless)

V_m = matrix interstitial pore water velocity (L/t)

K_{dm} = radionuclide sorption coefficient in rock matrix (L^3/m)

ρ_{bm} = Bulk density of the rock matrix (m/L^3)

C_a = dissolved species concentration in the alluvium (m/L^3)

R_a = alluvium retardation coefficient (dimensionless)

V_a = alluvium interstitial pore water velocity (L/t).

RAI: Volume 3, Chapter 2.2.1.1, First Set, Number 7:

Address the relative capabilities of the unsaturated zone below the repository and the saturated zone. Include uncertainties, consistent with the quantitative analyses in the total system performance assessment (e.g., sensitivity and uncertainty analyses or intermediate results). Provide information on the time period over which these components perform their intended function.

Basis: Needed for demonstration of compliance with 10 CFR 63.115 (b) and (c). Section 2.1.2.3.6 of the Safety Analysis Report compares activity releases from the engineered barrier system with activity releases to the accessible environment as the means of quantifying the barrier performance of the lower natural barrier. These TSPA-derived activity results combine the capabilities of the two component features of the lower natural barrier features, namely the unsaturated zone below the repository and the saturated zone. Examination of the TSPA GoldSim code indicates that calculations of activity releases from the unsaturated zone to the saturated zone (i.e. though the water table) can be saved from the simulation outputs. However, these intermediate results are not presented nor discussed in support of the capability of the lower natural barrier to prevent or substantially reduce the rate of radionuclide movement

1. RESPONSE

This response provides a tabular summary of the relative contributions from the unsaturated zone (UZ) and saturated zone (SZ) features on the performance of the Lower Natural Barrier when they are functioning concurrently or redundantly (see Tables 1-1 through 1-4) and when acting alone or non-redundantly (see Tables 1-5 through 1-8). The radionuclides examined in this response are those used to demonstrate the performance of the Lower Natural Barrier as discussed in SAR Section 2.1.2.3.6. These 12 radionuclides represent a broad range of radioactive decay properties, geochemical behaviors, biosphere dose conversion factors, and transport characteristics in geologic media. Thus, consideration of these 12 radionuclides provides a means of examining the overall performance characteristics of the natural and engineered barriers (SAR Section 2.1.2.2.6). This response also discusses the uncertainties, consistent with the quantitative analyses in the TSPA results presented in *Total System Performance Assessment Model/Analysis for the License Application (TSPA-LA)*, (SNL 2008) appendix Sections K5.4, K5.5, K6.4, K6.5, K7.4, and K7.5 (SNL 2008). This response also discusses the time period over which the unsaturated zone and saturated zone features of the Lower Natural Barrier function relative to each of the radionuclides presented, consistent with the discussion presented in SAR Section 2.1.2.3.3.

In SAR Section 2.1 the quantification of barrier capabilities for the Upper Natural Barrier, Engineered Barrier System and Lower Natural Barrier are discussed in the context of two demonstration modeling cases, the combined nominal / early failure modeling case and the seismic ground motion modeling case. As discussed in SAR Section 2.1.2, the combined nominal / early failure modeling case is selected as a representation of repository futures in which disruptive events do not occur and the seismic ground motion modeling case is selected as

a representation of repository futures that include disruptive events and have been shown to be important to demonstration of compliance with the regulatory standards (SAR Section 2.4.2.2). To maintain consistency with the quantitative discussion of the barrier capability of the Lower Natural Barrier presented in SAR Section 2.1.2.3.6, this response addresses the same demonstration modeling cases.

1.1 RELATIVE CAPABILITIES OF THE UNSATURATED ZONE AND SATURATED ZONE FEATURES OF THE LOWER NATURAL BARRIER

The information listed in the tables provided in this response was compiled from the discussions in SAR Section 2.1.2.3.6, from Section 8.3.3.3.1[a] of *Total System Performance Assessment Model/Analysis for the License Application* (SNL 2008), and from DTN: MO0710PLOTSFIG.000.

1.1.1 Relative Capability of the Unsaturated Zone Feature of the Lower Natural Barrier

As can be seen from Tables 1-1 and 1-3, for three of the radionuclides characterized in SAR Section 2.1.2.2.6 as having a large initial inventory and short half-life (e.g., ^{137}Cs, ^{90}Sr, ^{241}Am), the unsaturated zone prevents the release of nearly all of the activity released from the engineered barrier system over the 10,000-year period (SAR Section 2.1.2.3.6, pp. 2.1-94 and 2.1-98; SNL 2008, Section 8.3.3.3.1[a]). Since the inventories of ^{137}Cs and ^{90}Sr are essentially depleted by radioactive decay by 1,000 years after closure, Tables 1-2 and 1-4 do not show relative capabilities for these radionuclides (SAR Section 2.1.2.3.6, pp.2.1-96 and 2.1-99). Over the post-10,000-year period, the unsaturated zone accounts for the majority of ^{241}Am reduction. For ^{240}Pu, however, the unsaturated zone accounts for approximately half of the Lower Natural Barrier reduction in ^{240}Pu released from the engineered barrier system over the post-10,000-year period (Tables 1-2 and 1-4) (SAR Section 2.1.2.3.6, pp. 2.1-96 and 2.1-99; SNL 2008, Section 8.3.3.3.1[a]).

For radionuclides that are highly soluble, non-sorbing, and have a long half-life (e.g., ^{99}Tc), the unsaturated zone accounts for the majority of the containment of releases through the Lower Natural Barrier over the 10,000-year period. As demonstrated by ^{99}Tc, over 70% of the activity reduction in the Lower Natural Barrier is within the unsaturated zone over the 10,000-year period (Tables 1-1 and 1-3) (SAR Section 2.1.2.3.6, pp.2.1-95 and 2.1-98; SNL 2008, Section 8.3.3.3.1[a]). Over the post-10,000-year period, the unsaturated zone accounts for approximately one third of the Lower Natural Barrier reduction in the ^{99}Tc activity released from the engineered barrier system (Tables 1-2 and 1-4) (SAR Section 2.1.2.3.6, pp.2.1-96 and 2.1-99). Differences between these two time periods can mainly be attributed to the effect of travel time. In particular, most of the ^{99}Tc has exited the unsaturated zone in the post-10,000-year time frame (because it is a conservative tracer and is only delayed in the unsaturated zone via matrix diffusion), so the unsaturated zone barrier contribution decreases through time.

Regarding radionuclides that have moderate to low solubility, low sorption, and a long half-life, such as ^{239}Pu, ^{242}Pu, ^{237}Np, and ^{234}U, the unsaturated zone accounts for about half of the Lower Natural Barrier reduction in activity released from the engineered barrier system over the

10,000-year period (Tables 1-1 and 1-3). However, in the 10,000-year seismic ground motion case, the unsaturated zone has a slightly greater contribution to the Lower Natural Barrier capability than the nominal/early-failure case because of differences in the timing of the releases and degradation of the engineered barrier system components. For the post-10,000-year period, the unsaturated zone provides less than half of the Lower Natural Barrier's reduction in the activity released from the engineered barrier system, simply because there is more time for radionuclides to transport out of the unsaturated zone (Tables 1-2 and 1-4) (SAR Section 2.1.2.3.6, pp. 2.1-97 and 2.1-100; SNL 2008, Section 8.3.3.3.1[a], pp.8-74[a] and 8.76[a]). Furthermore, for ^{237}Np, and ^{234}U, the seismic ground motion case shows less relative capability for the unsaturated zone compared to the nominal/early-failure case. Drift degradation reduces flow diversion by the capillary barrier at the drift wall (SAR Section 2.3.3.2.4) and significantly increases drift seepage (SAR Sections 2.4.2.2.1.2.2.1 and 2.4.2.3.2.1.3). An increase in the seepage rate and seepage fraction increases the fraction of radionuclides that enter the unsaturated zone feature in its fracture component rather than its matrix component (a discussion of this behavior is presented in SAR Section 2.4.2.2.3.2.2, specifically p. 2.4-104). Travel through fractures is much more rapid, which would thus cause the unsaturated zone to show less capability at long time frames in the seismic ground motion case.

For ^{243}Am, ^{230}Th, and ^{226}Ra, which are strongly sorbed, or in the case of ^{226}Ra produced by decay chain ingrowth, the unsaturated zone accounts for the majority of the relative reduction in activity released from the engineered barrier system over both the 10,000-year period and the post-10,000-year period (Tables 1-1 through 1-4) (SAR Section 2.1.2.3.6, pp. 2.1-96, 2.1-97, 2.1-99, and 2.1-100). However, for ^{230}Th releases over the post-10,000-year period, the unsaturated zone provides about half of the Lower Natural Barrier's reduction in the activity released from the engineered barrier system.

1.1.2 Relative Capability of the Saturated Zone Feature of the Lower Natural Barrier

Tables 1-1 and 1-3 show that, for radionuclides with a large initial inventory and short half-life (e.g., ^{137}Cs, ^{90}Sr, ^{241}Am), the saturated zone prevents the release of essentially all of the activity released from the engineered barrier system that passes through the unsaturated zone over the 10,000-year period (SAR Section 2.1.2.3.6, pp. 2.1-94 and 2.1-98; SNL 2008, Section 8.3.3.3.1[a]). The inventories of ^{137}Cs and ^{90}Sr are essentially depleted by radioactive decay by 1,000 years after closure (Tables 1-2 and 1-4) (SAR Section 2.1.2.3.6, pp.2.1-96 and 2.1-99). Over the post-10,000-year period, the saturated zone accounts for the small remainder of ^{241}Am and approximately half of the Lower Natural Barrier's nearly 100% activity reduction in ^{240}Pu released from the engineered barrier system (Tables 1-2 and 1-4) (SAR Section 2.1.2.3.6, pp. 2.1-96 and 2.1-99; SNL 2008, Section 8.3.3.3.1[a]).

For radionuclides that are highly soluble, non-sorbing, and have a long half-life (e.g., ^{99}Tc), the saturated zone accounts for approximately 30% of the relative activity reduction in the Lower Natural Barrier over the 10,000-year period (Tables 1-1 and 1-3). In contrast, over the post-10,000-year period, the saturated zone accounts for the majority of the Lower Natural Barrier's activity reduction in ^{99}Tc (Tables 1-2 and 1-4) (SAR Section 2.1.2.3.6, pp. 2.1-96 and 2.1-98). The saturated zone accounts for approximately 70% of the relative reduction in the ^{99}Tc activity released from the engineered barrier system (Tables 1-2 and 1-4).

Regarding radionuclides that have low to moderate solubility, low sorption, and a long half-life, such as ^{239}Pu, ^{242}Pu, ^{237}Np, and ^{234}U, the saturated zone accounts for about half of the Lower Natural Barrier reduction in activity released from the engineered barrier system over the 10,000-year period (Tables 1-1 and 1-3). For the post-10,000-year period, the saturated zone provides more than half of the Lower Natural Barrier's reduction in the activity released from the engineered barrier system (Tables 1-2 and 1-4) (SAR Section 2.1.2.3.6, pp. 2.1-97 and p.2.1-100; SNL 2008, Section 8.3.3.3.1[a], pp.8-74[a] and 8.76[a]). As discussed in the previous section, differences between the two time periods can be attributed to relative radionuclide travel times for each feature. Furthermore, the unsaturated zone transport is dependent upon the fraction of the releases going through the unsaturated zone rock matrix, which is higher on average over the 10,000-year period. The post-10,000-year period has a higher seepage fraction, based upon the post-10,000-year percolation rates, and thus a high fraction of the radionuclide releases go into the unsaturated zone fracture pathways, which reduces the radionuclide travel time through the unsaturated zone. The foregoing is true for both the nominal/early-failure and seismic cases and, in addition, the seismic case has higher seepage at late times because of drift collapse.

For ^{243}Am, ^{230}Th, and ^{226}Ra, which are strongly sorbed, or in the case of ^{226}Ra produced by decay chain ingrowth, the unsaturated zone accounts for the majority of the relative reduction in activity released from the engineered barrier system over both the 10,000-year period and the post-10,000-year period (Tables 1-1 through 1-4) (SAR Section 2.1.2.3.6, pp. 2.1-96, 2.1-97, 2.1-99, and 2.1-100). The saturated zone accounts for less than half of the Lower Natural Barrier's reduction. However, for ^{230}Th releases over the post-10,000-year period, the saturated zone provides about half of the Lower Natural Barrier's reduction in the activity released from the engineered barrier.

Table 1-1. Summary Table for Relative Capabilities of the Features of the Lower Natural Barrier for the Combined Nominal/Early-Failure Modeling Case for 10,000 Years after Closure

Radionuclide (half-life)	Relative Capability of Lower Natural Barrier Features		Total Reduction of the Peak Mean Activity for the Lower Natural Barrier (LNB)[c]
	Unsaturated Zone [a]	Saturated Zone [b]	
^{137}Cs (30.1 years)	~90%	~10%	~100% reduction (from ~40 µCi to ~0 µCi)
^{90}Sr (28.8 years)	~90%	~10%	~100% reduction (from ~7 µCi to ~0 µCi)
^{241}Am (433 years)	~90%	~10%	~99.9% reduction (from ~3 mCi to ~4 µCi)
^{240}Pu (6,560 years)	~50%	~50%	~99.5% reduction (from ~17 mCi to ~80 µCi)
^{99}Tc (2.13×10^5 years)	~70%	~30%	~62% reduction (from ~14 Ci to ~ 5.3 Ci)
^{239}Pu (2.41×10^4 years)	~50%	~50%	~99.6% reduction (from ~60 mCi to ~0.3 mCi)
^{242}Pu (3.75×10^5 years)	~50%	~50%	~99.1% reduction (from ~62 µCi to ~0.5 µCi)
^{237}Np (2.14×10^6 years)	~40%	~60%	~78% reduction (from ~0.3 mCi to ~77 µCi)
^{234}U (2.46×10^5 years)	~30 %	~70%	~89% reduction (from ~0.1 mCi to ~16 µCi)
^{243}Am (7,370 years)	~60%	~40%	~99.8% reduction (from ~2 mCi to ~4 µCi)
^{230}Th (7.54×10^4 years)	~60%	~40%	~99.4% reduction (from ~76 µCi to ~0.5 µCi)
^{226}Ra (1,600 years)	~60%	~40%	~99.9% reduction (from ~0.6 mCi to ~0.3 µCi)

Data Source: SAR Section 2.1.2.3.6; SNL 2008, Section 8.3.3.3.1[a]; and DTN: MO0710PLOTSFIG.000, files: *Nominal-EF_EBS_Releases.xls*, *Nominal-EF_UZ_Releases.xls*, and *Nominal-EF_SZ_Releases.xls*.

NOTE: The relative capability is calculated: [a] [1 – (UZ activity released / EBS activity released)] / [1 – (SZ activity released / EBS activity released)] * 100 = UZ Feature; [b] [100 – UZ Feature] = SZ Feature; and [c] SAR Section 2.1.2.3.6 (as calculated per Equation 2.1-5 in SAR Section 2.1).

Table 1-2. Summary Table for Relative Capabilities of the Features of the Lower Natural Barrier for the Combined Nominal/Early-Failure Modeling Case for Post-10,000 Years

Radionuclide (half-life)	Relative Capability of Lower Natural Barrier Features		Total Reduction of the Peak Mean Activity for the Lower Natural Barrier (LNB) [c]
	Unsaturated Zone [a]	Saturated Zone [b]	
^{137}Cs (30.1 years)	—	—	Depleted by radioactive decay by 10,000 years
^{90}Sr (28.8 years)	—	—	Depleted by radioactive decay by 10,000 years
^{241}Am (433 years)	~98%	~2%	~100% reduction (from ~0.2 mCi to ~0 mCi)
^{240}Pu (6,560 years)	~50%	~50%	~98% reduction (from ~60 mCi to ~1 mCi)
^{99}Tc (2.13 × 10^5 years)	~30%	~70%	~5% reduction (from ~2.8 × 10^4 Ci to ~2.6 × 10^4 Ci)
^{239}Pu (2.41 × 10^4 years)	~50%	~50%	~90% reduction (from ~0.8 Ci to ~0.08 Ci)
^{242}Pu (3.75 × 10^5 years)	~40%	~60%	~66% reduction (from ~44 Ci to ~15 Ci)
^{237}Np (2.14 × 10^6 years)	~30%	~70%	~23% reduction (from ~16 Ci to ~13 Ci)
^{234}U (2.46 × 10^5 years)	~40%	~60%	~32% reduction (from ~1.5 Ci to ~1 Ci)
^{243}Am (7,370 years)	~70%	~30%	~99.6% reduction (from ~0.2 Ci to ~0.7 mCi)
^{230}Th (7.54 × 10^4 years)	~50%	~50%	~85% reduction (from ~4.5 Ci to ~0.7 Ci)
^{226}Ra (1,600 years)	~80%	~20%	~97.6% reduction (from ~28 Ci to ~0.7 Ci)

Data Source: SAR Section 2.1.2.3.6; SNL 2008, Section 8.3.3.3.1[a]; and DTN: MO0710PLOTSFIG.000, files: *Nominal-EF_EBS_Releases.xls*, *Nominal-EF_UZ_Releases.xls*, and *Nominal-EF_SZ_Releases.xls*.

NOTE: The relative capability is calculated: [a] [1 – (UZ activity released / EBS activity released)] / [1 – (SZ activity released / EBS activity released)] * 100 = UZ Feature; [b] [100 – UZ Feature] = SZ Feature; and [c] SAR Section 2.1.2.3.6 (as calculated per Equation 2.1-5 in SAR Section 2.1).

Table 1-3. Summary Table for Relative Capabilities of the Features of the Lower Natural Barrier for the Seismic Ground Motion Modeling Case for 10,000 Years after Closure

Radionuclide (half-life)	Relative Capability of Lower Natural Barrier Features		Total Reduction of the Peak Mean Activity for the Lower Natural Barrier (LNB) [c]
	Unsaturated Zone [a]	Saturated Zone [b]	
^{137}Cs (30.1 years)	~90%	~10%	~100% reduction (from ~0.6 µCi to ~0 µCi)
^{90}Sr (28.8 years)	~80%	~20%	~100% reduction (from ~0.03 µCi to ~0 µCi)
^{241}Am (433 years)	~90%	~10%	~100% reduction (from ~73 µCi to ~0 µCi)
^{240}Pu (6,560 years)	~50%	~50%	~99.6% reduction (from ~15 mCi to ~ 55 µCi)
^{99}Tc (2.13×10^5 years)	~70%	~30%	~55% reduction (from ~941 Ci to ~ 427 Ci)
^{239}Pu (2.41×10^4 years)	~50%	~50%	~99.6% reduction (from ~48 mCi to ~0.2 mCi)
^{242}Pu (3.75×10^5 years)	~50%	~50%	~99.6% reduction (from ~49 µCi to ~0.2 µCi)
^{237}Np (2.14×10^6 years)	~50%	~50%	~81% reduction (from ~0.1 mCi to ~20 µCi)
^{234}U (2.46×10^5 years)	~60%	~40%	~93% reduction (from ~0.3 mCi to ~22 µCi)
^{243}Am (7,370 years)	~60%	~40%	~100% reduction (from ~10 µCi to ~0 µCi)
^{230}Th (7.54×10^4 years)	~70%	~30%	~96.2% reduction (from ~11 µCi to ~0.4 µCi)
^{226}Ra (1,600 years)	~60%	~40%	~100% reduction (from ~30 mCi to ~0.6 µCi)

Data Source: SAR Section 2.1.2.3.6; SNL 2008, Section 8.3.3.3.1[a]; and DTN: MO0710PLOTSFIG.000: files: *SeismicGM_EBS_Releases.xls*, *SeismicGM_UZ_Releases.xls*, and *SeismicGM_SZ_Releases.xls*.

NOTE: The relative capability is calculated: [a] [1 – (UZ activity released / EBS activity released)] / [1 – (SZ activity released / EBS activity released)] * 100 = UZ Feature; [b] [100 – UZ Feature] = SZ Feature; and [c] SAR Section 2.1.2.3.6 (as calculated per Equation 2.1-5 in SAR Section 2.1).

Table 1-4. Summary Table for Relative Capabilities of the Features of the Lower Natural Barrier for the Seismic Ground Motion Modeling Case for Post-10,000 Years

Radionuclide (half-life)	Relative Capability of Lower Natural Barrier Features		Total Reduction of the Peak Mean Activity for the Lower Natural Barrier (LNB) [c]
	Unsaturated Zone [a]	Saturated Zone [b]	
^{137}Cs (30.1 years)	—	—	Depleted by radioactive decay by 10,000 years
^{90}Sr (28.8 years)	—	—	Depleted by radioactive decay by 10,000 years
^{241}Am (433 years)	~98%	~ 2%	~100% reduction (from ~3 µCi to ~0 µCi)
^{240}Pu (6,560 years)	~50%	~50%	~97% reduction (from ~0.1 Ci to ~4 mCi)
^{99}Tc (2.13 × 10^5 years)	~30%	~70%	~5% reduction (from ~3.3 × 10^4 Ci to ~ 3.1 × 10^4 Ci)
^{239}Pu (2.41 × 10^4 years)	~50%	~50%	~88% reduction (from ~11 Ci to ~1.4 Ci)
^{242}Pu (3.75 × 10^5 years)	~40%	~60%	~70% reduction (from ~200 Ci to ~62 Ci)
^{237}Np (2.14 × 10^6 years)	~20%	~80%	~20% reduction (from ~100 Ci to ~81 Ci)
^{234}U (2.46 × 10^5 years)	~20%	~80%	~25% reduction (from ~14 Ci to ~10 Ci)
^{243}Am (7,370 years)	~60%	~40%	~99.8% reduction (from ~3 mCi to ~8 µCi)
^{230}Th (7.54 × 10^4 years)	~50%	~50%	~89% reduction (from ~71 Ci to ~8 Ci)
^{226}Ra (1,600 years)	~75%	~25%	~97% reduction (from ~260 Ci to ~8 Ci)

Data Source: SAR Section 2.1.2.3.6; SNL 2008, Section 8.3.3.3.1[a]; and DTN: MO0710PLOTSFIG.000, files: *SeismicGM_EBS_Releases.xls*, *SeismicGM_UZ_Releases.xls*, *SeismicGM_SZ_Releases.xls*.

NOTE: The relative capability is calculated: [a] [1 – (UZ activity released / EBS activity released)] / [1 – (SZ activity released / EBS activity released)] * 100 = UZ Feature; [b] [100 – UZ Feature] = SZ Feature; and [c] SAR Section 2.1.2.3.6 (as calculated per Equation 2.1-5 in SAR Section 2.1).

1.1.3 Percent Reduction of the Peak Activity in the Features of the Lower Natural Barrier

As described in SAR Section 2.1.2.3.6, to provide a quantitative metric of barrier effectiveness, the radionuclide activity released from the Lower Natural Barrier was computed using the TSPA model and the balance equations (SAR Section 2.1.2.3.6, Equations 2.1-2 and 2.1-3; SNL 2008, Section 8.3.3.3[a]). The arithmetic means of these quantities are compared with the mean EBS releases to provide an indication of the barrier capability. For radionuclide, denoted by the subscript k, the mean percent reduction in the activity achieved by the unsaturated zone feature ($PR_{UZ,k}$) and the Lower Natural Barrier as a whole ($PR_{LNB,k}$) (i.e., the unsaturated zone and saturated zone features) is calculated using Equations 2.1-4 and 2.1-5 (SAR Section 2.1.2.3.6; SNL 2008, Section 8.3.3.3[a]). The percent reductions in the peak values of the mean activity release of each radionuclide within the time period under consideration (i.e., 0 to 10,000-year period or post-10,000-year period) was examined in SAR Section 2.1.2.3.6. The cumulative releases are decayed through time; thus, for short-lived radionuclides (e.g., ^{90}Sr, ^{137}Cs, ^{241}Am) the peak of the mean activity released in the 10,000-year period may be higher than the post-10,000-year values. These results are compiled and presented in Tables 1-5 through 1-8. In addition, for completeness, the percent reduction in the saturated zone is included in the tables provided in this response.

The relative capability percentages shown in Tables 1-1 to 1-4 emphasize the capability of the unsaturated zone feature because it is first in the sequence of the two redundant features. Thus, the capability of the saturated zone feature is not readily apparent in the information presented in these tables. In contrast, the capability (percent reduction) attributable to the saturated zone ($PR_{SZ,k}$) feature regardless of the presence of the unsaturated zone feature is readily apparent by examining the information presented in Tables 1-5 through 1-8. As an illustration of the two different methods of portraying the capability or effectiveness of each feature, consider ^{239}Pu for the nominal/early-failure case for the 10,000-year period. In Table 1-1, the relative contribution of the unsaturated zone and saturated zone is 50% each, whereas in Table 1-5 the percent reduction of the unsaturated zone is 53% (about the same as Table 1-1), but the percent reduction of the saturated zone is 99% (instead of 50%) because the saturated zone feature by itself reduces any ^{239}Pu activity it receives by 99%.

Table 1-5. Summary Table for Percent Reduction (Barrier Effectiveness) of the Features of the Lower Natural Barrier for the Combined Nominal/Early-Failure Modeling Case, 10,000-Year Period

Radionuclide (half-life)	Peak of the Mean Activity Released			Percent Reduction		
	EBS	UZ	SZ	$PR_{UZ,k}$	$PR_{SZ,k}$	$PR_{LNB,k}$
^{137}Cs (30.1 years)	~43 µCi	~4 µCi	~0 µCi	~91%	~100%	~100%
^{90}Sr (28.8 years)	~7 µCi	~0.9 µCi	~0 µCi)	~87%	~100%	~100%
^{241}Am (433 years)	~3 mCi	~0.3 mCi	~4 µCi	~89%	~99%	~99.9%
^{240}Pu (6,560 years)	~17 mCi	~8 mCi	~80 µCi	~53%	~99%	~99.5%
^{99}Tc (2.13×10^5 years)	~14 Ci	~8 Ci	~5.3 Ci	~45%	~30%	~62%
^{239}Pu (2.41×10^4 years)	~60 mCi	~28 mCi	~0.3 mCi	~53%	~99%	~99.6%
^{242}Pu (3.75×10^5 years)	~62 µCi	~29 µCi	~0.5 µCi	~52%	~98%	~99.1%
^{237}Np (2.14×10^6 years)	~0.3 mCi	~0.2 mCi	~77 µCi	~31%	~68%	~78%
^{234}U (2.46×10^5 years)	~0.1 mCi	~0.1 mCi	~16 µCi	~29%	~84%	~89%
^{243}Am (7,370 years)	~2 mCi	~1 mCi	~4 µCi	~57%	~99%	~99.8%
^{230}Th (7.54×10^4 years)	~76 µCi	~30 µCi	~0.5 µCi	~60%	~98%	~99.4%
^{226}Ra (1,600 years)	~0.6 mCi	~0.2 mCi	~0.3 µCi	~60%	~99%	~99.9%

Data Source: SAR Section 2.1.2.3.6, Equations 2.1-4 ($PR_{UZ,k}$) and 2.1-5 ($PR_{LNB,k}$); DTN: MO0710PLOTSFIG.000, files: *Nominal-EF_EBS_Releases.xls*, *Nominal-EF _UZ_Releases.xls*, and *Nominal-EF_SZ_ Releases.xls*.

NOTE: $PR_{SZ,k}$ is calculated: [1 – (SZ Activity Released / UZ Activity Released)] * 100.

Table 1-6. Summary Table for Percent Reduction (Barrier Effectiveness) of the Features of the Lower Natural Barrier for the Combined Nominal/Early Failure Modeling Case, Post-10,000 Years

Radionuclide (half-life)	Peak of the Mean Activity Released			Percent Reduction		
	EBS	UZ	SZ	$PR_{UZ,k}$	$PR_{SZ,k}$	$PR_{LNB,k}$
^{137}Cs (30.1 years)	—	—	—	—	—	—
^{90}Sr (28.8 years)	—	—	—	—	—	—
^{241}Am (433 years)	~0.2 mCi	~3 µCi	~0 µCi	~98%	~100%	~100%
^{240}Pu (6,560 years)	~60 mCi	~29 mCi	~1 mCi	~52%	~95%	~98%
^{99}Tc (2.13×10^5 years)	~27,552 Ci	~27,030 Ci	~26,029 Ci	~2%	~4%	~5%
^{239}Pu (2.41×10^4 years)	~800 mCi	~400 mCi	~78 mCi	~45%	~82%	~90%
^{242}Pu (3.75×10^5 years)	~44 Ci	~32 Ci	~15 Ci	~27%	~54%	~66%
^{237}Np (2.14×10^6 years)	~16 Ci	~15 Ci	~13 Ci	~7%	~17%	~23%
^{234}U (2.46×10^5 years)	~1.5 Ci	~1.4 Ci	~1 Ci	~11%	~23%	~32%
^{243}Am (7,370 years)	~178 mCi	~51mCi	~0.7 mCi	~71%	~99%	~99.6%
^{230}Th (7.54×10^4 years)	~4.5 Ci	~2.5 Ci	~0.7 Ci	~43%	~73%	~85%
^{226}Ra (1,600 years)	~28 Ci	~5.9 Ci	~0.7 Ci	~79%	~88%	~98%

Data Source: SAR Section 2.1.2.3.6, Equations 2.1-4 ($PR_{UZ,k}$) and 2.1-5 ($PR_{LNB,k}$); DTN: MO0710PLOTSFIG.000, files: *Nominal-EF _EBS_Releases.xls*, *Nominal-EF _UZ_Releases.xls*, and *Nominal-EF_SZ_ Releases.xls*.

NOTE: $PR_{SZ,K}$ is calculated: [1 – (SZ Activity Released / UZ Activity Released)] * 100.

Table 1-7. Summary Table for Percent Reduction (Barrier Effectiveness) of the Features of the Lower Natural Barrier for the Seismic Ground Motion Modeling Case, 10,000-Year Period

Radionuclide (half-life)	Peak of the Mean Activity Released			Percent Reduction		
	EBS	UZ	SZ	$PR_{UZ,k}$	$PR_{SZ,k}$	$PR_{LNB,k}$
^{137}Cs (30.1 years)	~0.6 µCi	~0.07 µCi	~0 µCi	~87%	~100%	~100%
^{90}Sr (28.8 years)	~0.03 µCi	~0.005 µCi	~0 µCi)	~81%	~100%	~100%
^{241}Am (433 years)	~73 µCi	~8 µCi	~0 µCi	~89%	~100%	~100%
^{240}Pu (6,560 years)	~15 mCi	~7 mCi	~55 µCi	~53%	~99%	~99.6%
^{99}Tc (2.13 × 10^5 years)	~941 Ci	~589 Ci	~427 Ci	~37%	~28%	~55%
^{239}Pu (2.41 × 10^4 years)	~48 mCi	~22 mCi	~0.2 mCi	~53%	~99%	~99.6%
^{242}Pu (3.75 × 10^5 years)	~49 µCi	~23 µCi	~0.2 µCi	~53%	~99%	~99.6%
^{237}Np (2.14 × 10^6 years)	~0.1 mCi	~59 µCi	~20 µCi	~43%	~66%	~81%
^{234}U (2.46 × 10^5 years)	~0.3 mCi	~0.1 mCi	~22 µCi	~56%	~84%	~93%
^{243}Am (7,370 years)	~10 µCi	~4 µCi	~0 µCi	~59%	~100%	~100%
^{230}Th (7.54 × 10^4 years)	~11 µCi	~4 µCi	~0.4 µCi	~64%	~89%	~96.2%
^{226}Ra (1,600 years)	~30 mCi	~13 mCi	~0.6 µCi	~57%	~100%	~100%

Data Source: SAR Section 2.1.2.3.6, Equations 2.1-4 ($PR_{UZ,k}$) and 2.1-5 ($PR_{LNB,k}$); DTN: MO0710PLOTSFIG.000, files: *SeismicGM_EBS_Releases.xls*, *SeismicGM_UZ_Releases.xls*, and *SeismicGM_SZ_ Releases.xls*.

NOTE: $PR_{SZ,K}$ is calculated: [1 – (SZ Activity Released / UZ Activity Released)] * 100.

Table 1-8. Summary Table for Percent Reduction (Barrier Effectiveness) of the Features of the Lower Natural Barrier for the Seismic Ground Motion Modeling Case for Post-10,000 Years

Radionuclide (half-life)	Peak of the Mean Activity Released)			Percent Reduction		
	EBS	UZ	SZ	UZ ($PR_{UZ,k}$)	SZ ($PR_{SZ,k}$)	LNB ($PR_{LNB,k}$)
^{137}Cs (30.1 years)	—	—	—	—	—	—
^{90}Sr (28.8 years)	—	—	—	—	—	—
^{241}Am (433 years)	~3 µCi	~ 0.06 µCi	~0 µCi	~98%	~100%	~100%
^{240}Pu (6,560 years)	~137 mCi	~67 mCi	~4 mCi	~51%	~94%	~97%
^{99}Tc (2.13 × 10^5 years)	~3.3 × 10^4 Ci	~3.2 × 10^4 Ci	~3.1 × 10^4 Ci	~1%	~4%	~5%
^{239}Pu (2.41 × 10^4 years)	~11 Ci	~6.5 Ci	~1.4 Ci	~44%	~78%	~88%
^{242}Pu (3.75 × 10^5 years)	~200 Ci	~144 Ci	~62 Ci	~29%	~57%	~70%
^{237}Np (2.14 × 10^6 years)	~100 Ci	~97 Ci	~81 Ci	~4%	~16%	~20%
^{234}U (2.46 × 10^5 years)	~14 Ci	~13 Ci	~10 Ci	~6%	~20%	~25%
^{243}Am (7,370 yrs)	~3 mCi	~1 mCi	~8 µCi	~63%	~99%	~99.8%
^{230}Th (7.54 × 10^4 years)	~71 Ci	~40 Ci	~8 Ci	~44 %	~81 %	~89 %
^{226}Ra (1,600 years)	~260 Ci	~70 Ci	~8 Ci	~72 %	~89 %	~97 %

Data Source: SAR Section 2.1.2.3.6, Equations 2.1-4 ($PR_{UZ,k}$) and 2.1-5 ($PR_{LNB,k}$); DTN: MO0710PLOTSFIG.000, files: *SeismicGM_EBS_Releases.xls*, *SeismicGM_UZ_Releases.xls*, and *SeismicGM_SZ_ Releases.xls*.

NOTE: $PR_{SZ,K}$ is calculated: [1 – (SZ Activity Released/ UZ Activity Released)]*100.

1.2 UNCERTAINTY AND SENSITVITY ANALYSES OF THE UNSATURATED ZONE AND SATURATED ZONE FEATURES OF THE LOWER NATURAL BARRIER

The key uncertain parameters of the Lower Natural Barrier are identified and discussed in SAR Section 2.1.2.3.4. The key uncertain input parameters (i.e., groundwater flux, sorption coefficients, and matrix diffusion transport parameters) are subject to uncertain distributions based on the available data and observations, and these uncertainties are reflected in the model results. A quantitative demonstration of the parameter sensitivity analyses of the unsaturated zone and saturated zone releases are documented in Appendices K and K[a] of *Total System Performance Assessment Model/Analysis for the License Application* (SNL 2008). Tables 1-9 and 1-10 list the relevant sections.

Uncertainty in the unsaturated zone and saturated zone features of the Lower Natural Barrier is evaluated using a subset of the 12 radionuclides presented in the demonstration of Lower Natural Barrier performance documented in SAR Section 2.1.2.3.6. Three radionuclides were selected for the 10,000-year period: ^{239}Pu, ^{237}Np, and ^{99}Tc. ^{239}Pu and ^{237}Np have low to moderate solubility, low sorption, and a long half-life. On the other hand, ^{99}Tc is highly soluble, non-sorbing, and has a long half-life. Over the post-10,000-year period, ^{234}U, ^{230}Th, and ^{226}Ra are analyzed. ^{234}U has low to moderate solubility, low sorption, and a long half-life, whereas ^{230}Th is strongly sorbed and ^{226}Ra is produced by decay chain ingrowth. These results are documented in Appendices K and K[a] of *Total System Performance Assessment Model/Analysis for the License Application* (SNL 2008).

1.2.1 Uncertainty in the Unsaturated Zone Releases

The effect of uncertainty on radionuclide transport through the unsaturated zone feature of the Lower Natural Barrier over the 10,000-year period is evaluated by examining the results presented in (1) Section K5.4.1 (SNL 2008) for the early failure of one drip shield above a CDSP waste package in percolation bin 3 under dripping conditions; (2) Section K7.4 for a seismic ground motion induced fractional damaged area of 10^{-6} at 200 years to all CDSP waste packages in the repository; and (3) Section K6.4.1 for an igneous intrusive event at 10 years. The effect of uncertainty on radionuclide transport through the unsaturated zone feature of the Lower Natural Barrier for the post-10,000-year period is evaluated using the Igneous Intrusion Modeling Case for three radionuclides, ^{234}U, ^{230}Th, and ^{226}Ra, as documented in Section K6.4.2[a] (SNL 2008).

The quantitative evaluation of the uncertainty in the unsaturated zone feature reveals that this analysis is dominated by the uncertainty in the releases from the engineered barrier system (SNL 2008, Sections K5.4.1, K6.4.1, K6.4.2[a], and K7.4). However, for certain radionuclides, these sensitivity analyses revealed key parameters in the unsaturated zone that are important to the uncertainty in the results. For example, over the 10,000-year time period, *UZKDPUDT* (sorption coefficient for plutonium in devitrified tuff units of unsaturated zone, mL/g) has an influence on the uncertainty in the unsaturated zone plutonium release rate and cumulative release, *UZPU239* and *UZPU239C*, as shown by a negative Partial Rank Correlation Coefficient (PRCC) (SNL 2008, Figures K5.4.1-10e,f and 6.4.1-11a,b). Also, *UZTORRG3* (tortuosity in rock group 3 of the unsaturated zone, dimensionless; as sampled, *UZTORRG3* is actually the logarithm of the indicated tortuosity) appears in the analysis for *UZPU239C* with a negative

PRCC (SNL 2008, Figures K5.4.1-10f, 6.4.1-13e,f, and 6.4.1-14a,b). In addition, over the 10,000-year time period, as indicated by the PRCCs in Figure K6.4.1-13e (SNL 2008), variables such as *UZTORRG3*, *UZGAM* (gamma exponent in the active fracture model, dimensionless), *UZFAG8* (fracture aperture for rock group 8 in unsaturated zone, m) and *UZFAG3* (fracture aperture for rock group 3 in unsaturated zone, m) tend to have temporally dependent effects on *UZTC99* that derive from the role that the particular parameter plays on speeding up or slowing down the movement of ^{99}Tc in the unsaturated zone. However, as previously noted, these effects tend to diminish with time as a result of the essentially complete movement of ^{99}Tc through the unsaturated zone (SNL 2008, Section K6.4.1).

For the post-10,000-year period, for highly sorbing radionuclides (as demonstrated by ^{226}Ra), the unsaturated zone feature of the Lower Natural Barrier is important relative to the Lower Natural Barrier's ability to retain or reduce the activity released. The uncertainty analysis reveals that the dominant parameters affecting the uncertainty in unsaturated zone radium release rate and cumulative release, *UZRA226* and *UZRA226C,* are *UZKDCSDT* (sorption coefficient for cesium and radium in devitrified tuff units of unsaturated zone, mL/g; also used as sorption coefficient for cesium and radium in ballast in EBS), *INFIL* (infiltration scenario), *UZFAG8* (fracture aperture for Group 8 rock unit in unsaturated zone, m), and *UZTORRG3* (tortuosity for Group 3 rock unit in unsaturated zone) (SNL 2008, Figures K6.4.2-7e,f[a] and K6.4.2-8a,b[a]). The negative effects associated with *UZKDCSDT* and *UZTORRG3* result because (1) increasing *UZKDCSDT* increases the retardation of ^{226}Ra in the EBS and the unsaturated zone and (2) increasing *UZTORRG3* increases the transport time in the unsaturated zone. The positive effects associated with *INFIL* and *UZFAG8* result because (1) increasing *INFIL* increases the seepage fraction in the EBS and water flow in both the EBS and unsaturated zone and (2) increasing *UZFAG8* increases the amount of ^{226}Ra transported by flow in fractures.

These observations of the key uncertainties in the unsaturated zone are consistent with the unsaturated zone feature's relative contribution to the barrier capability of the Lower Natural Barrier presented in SAR Section 2.1.2.3.6 and highlighted in this response. The features of the unsaturated zone important to the Lower Natural Barrier capability are detailed in SAR Section 2.3.8 and in the response to RAI 3.2.2.1.1-006.

1.2.2 Uncertainty in the Saturated Zone Releases

Uncertainty in the saturated zone releases over the 10,000-year period is demonstrated using the results from the Drip Shield Early Failure, Seismic Ground Motion, and Igneous Intrusion Modeling Cases for three radionuclides, ^{239}Pu, ^{237}Np, and ^{99}Tc, as documented in Sections K5.5.1, K6.5.1, and K7.5 (SNL 2008) and associated figures (see Table 1-10). Specifically, the effect of uncertainty on radionuclide transport through the unsaturated zone is demonstrated by examining the results presented in (1) Section K5.5.1 (SNL 2008) for the early failure of one drip shield above a CDSP waste package in percolation bin 3 under dripping conditions; (2) Section K7.5 for a seismic ground motion induced fractional damaged area of 10^{-6} at 200 years to all CDSP waste packages in the repository; and (3) Section K6.5.1 for an igneous intrusive event at 10 years. For the post-10,000-year period, saturated zone uncertainty is presented using the Igneous Intrusion Modeling Case for ^{239}Pu and ^{237}Np, documented in

Section K6.5.2 (SNL 2008) and three additional radionuclides, ^{234}U, ^{230}Th, and ^{226}Ra, documented in Section K6.4.2[a] (SNL 2008).

A quantitative evaluation of the uncertainty in the saturated zone releases, documented in Appendices K and K[a] (SNL 2008), reveals that like the unsaturated zone feature of the Lower Natural Barrier, this analysis is highly influenced by the uncertainty in the releases from the engineered barrier system (SNL 2008, Sections K5.5.1, K6.5.1, K6.5.2, and K6.5.2[a]).

As indicated by the PRCCs in Figure K6.5.1-7e,f and the regression analyses in Figure K6.5.1-8a,b (SNL 2008), the uncertainty in saturated zone neptunium release rate and cumulative release, *SZNP237*and *SZNP237C*, over the 10,000-year period is primarily affected by uncertainty in *SZGWSPDM* (groundwater specific discharge multiplier*;* as sampled, *SZGWSPDM* is actually the logarithm of the indicated multiplier). Additionally, the saturated zone uncertain parameters, *SZKDCSVO* (sorption coefficient for cesium in volcanic unit of saturated zone, mL/g) and *SZKDNPVO* (sorption coefficient for neptunium in volcanic unit of saturated zone, mL/g), have small effects on *SZNP237C* (SNL 2008, Section K6.5.1). Overall, the uncertainty in *SZNP237*and *SZNP237C* is determined by small effects associated with a large number of variables (SNL 2008, Section K6.5.1).

The uncertainty analysis for ^{239}Pu reveals that for many sample elements, there is no significant movement of ^{239}Pu through the saturated zone to the location of the RMEI over the 10,000-year period (Tables 1-1 and 1-3) (SNL 2008, Figure K6.5.1-12). However, the uncertainty in whether or not significant movement of ^{239}Pu through the saturated zone to the location of the RMEI occurs is dominated by *SZGWSPDM* (groundwater specific discharge multiplier), with no significant movement occurring when *SZGWSPDM* is less than 0 and often no significant movement occurring when *SZGWSPDM* is less than 0.5 (SNL 2008, Figure K6.5.1-11f).

The uncertainty analysis results of saturated zone transport of ^{99}Tc are displayed in both the PRCCs in Figure K6.5.1-13e and the regression analyses in Figure K6.5.1-14a (SNL 2008). The most important variable with respect to the uncertainty in saturated zone technetium release rate, *SZTC99,* is *INFIL* (infiltration level), with the saturated zone uncertainty parameters *SZGWSPDM* (groundwater specific discharge multiplier) and *SZFIPOVO* (flowing interval porosity in the volcanic unit) having smaller effects (SNL 2008, Section K6.5.1). Increasing *INFIL*, which increases the seepage fraction in the EBS (and water flow rates through the EBS and unsaturated zone), increases the mass of ^{99}Tc released from the unsaturated zone to the saturated zone. Increasing *SZGWSPDM* increases the rate of ^{99}Tc movement through the saturated zone (SNL 2008, Section K6.5.1). An increase in *SZFIPOVO*, however, reduces the release of ^{99}Tc at early times (due to greater storativity) and thus results in larger values for *SZTC99* at later times (SNL 2008, Section K6.5.1).

For the post-10,000-year period, as shown by the results in Figure K6.5.2-7[a], the saturated zone has a noticeable effect on the movement of ^{234}U in the Lower Natural Barrier over the 50,000-year time period (SNL 2008, Figure K6.5.2-7a[a]). The most important saturated zone variable with respect to the uncertainty in saturated zone uranium release rate and cumulative release, *SZU234* and *SZU234C*, is *SZGWSPDM* (groundwater specific discharge multiplier). Post-10,000-year uncertainty analysis of ^{230}Th reveals that the dominant saturated zone variables

affecting saturated zone thorium release rate and cumulative release, *SZTH230* and *SZTH230C*, are *SZCONCOL* (concentration of colloids in ground water, g/mL; as sampled, *SZCONCOL* is actually the logarithm of the indicated concentration), *SZKDAMCO* (sorption coefficient for reversible sorption of americium, thorium, and protactinium onto ground water colloids, mL/g), *INFIL* (infiltration level), and *SZGWSPDM* (groundwater specific discharge multiplier) (SNL 2008, Figures K6.5.2-8e,f[a] and K6.5.2-9a,b[a]). Additionally, for strongly sorbing radionuclides, as shown by the results of the ^{226}Ra uncertainty analysis (Figure K6.5.2-13[a]), the saturated zone has a large effect on the radionuclide movement from the unsaturated zone to the location of the RMEI (SNL 2008, Section K6.5.2[a]).

These observations of the key uncertain input variables for the saturated zone are consistent with the saturated zone features' relative contribution to the barrier capability of the Lower Natural Barrier presented in SAR Section 2.1.2.3.6 and highlighted in this response. The features of the saturated zone important to the Lower Natural Barrier capability are detailed in SAR Section 2.3.9 and in the response to RAI 3.2.2.1.1-006.

Table 1-9. Parameter Sensitivity and Uncertainty Analyses for Unsaturated Zone Releases

Scenario Class	Document Location	Figures
Early Failure	Section K5.4.1 (10K)	K5.4.1-7, K5.4.1-8, K5.4.1-9, K5.4.1-10, K5.4.1-11, K5.4.1-12, K5.4.1-13, K5.4.1-14, K5.4.1-15,
Seismic Ground Motion	Section K7.4 (10K)	K7.4-3, K7.4-4, K7.4-5
Igneous Intrusion	Section K6.4.1 (10K)	K6.4.1-7, K6.4.1-8, K6.4.1-9, K6.4.1-10, K6.4.1-11, K6.4.1-12, K6.4.1-13, K6.4.1-14, K6.4.1-15
	Section K6.4.2[a] (1M)	K6.4.2-1[a], K6.4.2-2[a], K6.4.2-3[a], K6.4.2-4[a], K6.4.2-5[a], K6.4.2-6[a], K6.4.2-7[a], K6.4.2-8[a], K6.4.2-9[a]

Source: SNL 2008, Appendix K and Appendix K[a].

Table 1-10. Parameter Sensitivity and Uncertainty Analyses for Saturated Zone Releases

Scenario Class	Document Location	Figures
Early Failure	Section K5.5.1(10K)	K5.5.1-3, K5.5.1-4, K5.5.1-5
Seismic Ground Motion	Section K7.5 (10K)	K7.5-3, K7.5 -4, K7.5-5
Igneous Intrusion	Section K6.5.1(10K)	K6.5.1-7, K6.5.1-8, K6.5.1-9, K6.5.1-10, K6.5.1-11, K6.5.1-12, K6.5.1-13, K6.5.1-14, K6.5.1-15
	Section K6.5.2 (1M)	K6.5.2-3, K6.5.2-4
	Section K6.5.2[a] (1M)	K6.5.2-5[a], K6.5.2-6[a], K6.5.2-7[a], K6.5.2-8[a], K6.5.2-9[a], K6.5.2-10[a], K6.5.2-11[a], K6.5.2-12[a], K6.5.2-13[a]

Source: SNL 2008, Appendix K and Appendix K[a].

1.3 TIME PERIOD OVER WHICH THE UNSATURATED ZONE AND SATURATED ZONE FEATURES OF THE LOWER NATURAL BARRIER FUNCTION

As discussed in SAR Section 2.1.2.3.3, the Lower Natural Barrier is a durable feature of the geologic setting at Yucca Mountain. Comparison of the relative contribution of the unsaturated zone and saturated zone features of the Lower Natural Barrier (Tables 1-1 to 1-4) shows that the relative performance of the unsaturated zone and saturated zone features of the Lower Natural Barrier remains essentially constant over time and modeling cases. Processes acting during the first 10,000-year assessment continue throughout the period of geologic stability (SAR Section 2.1.2.3.3). A slight decrease in the relative contribution of the unsaturated zone feature and an increase in the saturated zone feature contribution to the Lower Natural Barrier capability to reduce or retain radionuclide releases is primarily due to the shorter radionuclide travel time through the unsaturated zone feature than the travel time through the saturated zone feature (SAR Sections 2.3.8 and 2.3.9, Figures 2.3.8-40 and 2.3.9-42). The unsaturated zone feature tends to be the dominant feature of the Lower Natural Barrier over the 10,000-year period (Tables 1-1 and 1-3), when considering relative capability. However, the much longer saturated zone transport distances and the sorption characteristics of the alluvium component of the saturated zone transport pathway result in a larger relative contribution from the saturated zone feature to the overall Lower Natural Barrier performance over longer time periods (Tables 1-2 and 1-4).

For the radionuclide group with a large initial inventory and short half-life (e.g., ^{137}Cs, ^{90}Sr, ^{241}Am), the unsaturated zone prevents the release of nearly all of the activity released from the engineered barrier system over all time periods. In the case of highly soluble radionuclides with long half-life, like ^{99}Tc, the reduction in the unsaturated zone is mainly a transient condition (SAR Section 2.1.4, p. 2.1-111). However, the combined effects of both the unsaturated zone and saturated zone features of the Lower Natural Barrier result in a delay in the ^{99}Tc releases that accounts for an approximately 5% reduction in the total ^{99}Tc activity released from the engineered barrier system. Radionuclides included in Tables 1-1 through 1-4 that have moderate to low solubility, low sorption, and a long half-life (such as ^{239}Pu, ^{242}Pu, ^{237}Np, and ^{234}U), and radionuclides which are strongly sorbed (e.g., ^{243}Am, ^{230}Th, and ^{226}Ra), demonstrate that the relative performance of the unsaturated zone and saturated zone features of the Lower Natural Barrier remains fairly constant over time, but with a slight trend over time toward a decrease in the relative contribution of the unsaturated zone and an increase in the saturated zone contribution to the Lower Natural Barrier capability. Part of this increase is a result of the relative length of transit time during the two time periods considered (10,000 versus 1,000,000 years), and part is a result of an increased seepage fraction in the Upper Natural Barrier (resulting from climate change and/or drift collapse), which increases radionuclide releases into the fractures of the unsaturated zone, thereby reducing its effectiveness because of the resulting shorter transit time. The processes acting in both the unsaturated and saturated zone features of the Lower Natural Barrier during the first 10,000-year assessment continue throughout the period of geologic stability ending at 1,000,000 years after closure (SAR Section 2.1.2.3.3).

The summary tables of barrier (or feature) effectiveness (Tables 1-5 to 1-8) confirm the results of the relative capability tables (Tables 1-1 to 1-4) with respect to the time period over which the features perform their function. With the exception of the increase in percolation, increase in saturated zone flux, and water table rise as a result of future climate states, the hydrogeology and

physical characteristics of the Lower Natural Barrier are not expected to change in any significant way in the 10,000 years after closure (SAR Section 2.1.2.3.3, p. 2.1-87). However, as time progresses, the Lower Natural Barrier features provide less percentage reduction in activity because of the increasing time available for the radionuclide mass to transport across the finite distance to the RMEI. Yet, even over the 1,000,000-year time frame, the unsaturated zone and saturated zone features provide a significant percent activity reduction for sorbing and/or shorter half-life radionuclides.

2. COMMITMENTS TO NRC

None.

3. DESCRIPTION OF PROPOSED LA CHANGE

None.

4. REFERENCES

MO0710PLOTSFIG.000. Plots and Figures for TSPA-LA Addendum (V5.005). Submittal date: 03/07/2008. (Files: *Nominal-EF_EBS_Releases.xls*, *Nominal-EF_UZ_Releases.xls*, *Nominal-EF_SZ_Releases.xls*, *SeismicGM_EBS_Releases.xls*, *SeismicGM_UZ_Releases.xls*, and *SeismicGM_SZ_Releases.xls*.)

SNL (Sandia National Laboratories) 2008. *Total System Performance Assessment Model /Analysis for the License Application.* MDL-WIS-PA-000005 REV 00 AD 01. Las Vegas, Nevada: Sandia National Laboratories. ACC: DOC.20080312.0001; LLR.20080414.0037; LLR.20080507.0002; LLR.20080522.0113; DOC.20080724.0005.